Synthesis and reactivity studies of Group 5 imido and hydrazido complexes

Karen Yazmín Gamero Vega



Thesis submitted to the University of Oxford for the degree of Doctor of Philosophy in Inorganic Chemistry, August 2018.

The work described in this Thesis was carried out in the Chemistry Research Laboratory, University of Oxford from October 2014 to August 2018 under the supervision of Professor Philip Mountford. All work is my own unless stated to the contrary, and has not previously been submitted for any degree at this or any other university.



Karen Yazmín Gamero Vega

August 2018

Abstract

Karen Yazmín Gamero Vega Trinity 2018
St Edmund Hall D.Phil. Thesis

This Thesis describes the synthesis and reactivity of Group 5 imido and hydrazido complexes with tridentate, trianionic ligands. Various synthetic routes towards these hydrazido compounds were explored and in which several intermediates were synthesised and their chemistry was explored. The reactivity of the imido and hydrazido complexes with unsaturated and other small molecules was also studied.

Chapter One provides a general introduction to tridentate pincer and tripodal ligands. The structure, synthesis and reactivity of Group 4 and 5 imido and hydrazido complexes is also reviewed.

Chapter Two describes three different synthetic routes towards tantalum hydrazido complexes with tridentate, trianionic ligands. Synthesis, characterization and bonding analysis of the precursor dichloride species $Ta(NN_2^{SiMe3})Cl_2$, which is used as starting material for two of the synthetic routes, is also described. The synthesis, characterization and bonding analysis of the tantalum dialkyl and alkyl-amido precursors prepared in the multistep route is also explored.

Chapter Three describes the synthesis and characterisation of Group 5 imido complexes with tridentate, trianionic ligands of the type $Li_3(NN_2^{R})$ and $Li_3(NNN^{SiMe3})$. Reactivity studies of the imido complex $Nb(NN_2^{iPr})(N^tBu)(py)_2$ with unsaturated and other small molecules are also explored.

Chapter Four describes the synthesis and characterisation of Group 5 hydrazido complexes with tridentate, trianionic ligands by two different synthetic routes, alongside a bonding analysis of the imido compounds $M(NN_2^{R})(N^tBu)(py)_2$ and their hydrazido analogues $M(NN_2^{R})(NNPh_2)(L)_x$. Reactivity studies of the hydrazido complex $Nb(NN_2^{iPr})(NNPh_2)(py)_2$ with unsaturated and other small substrates are also described.

Chapter Five presents full experimental procedures and characterising data for the new methodologies and complexes reported in this Thesis.

CD Appendix contains CIF files for all new crystallographically characterised complexes.

Acknowledgements

Writing this Thesis would not have been possible without the guidance and encouragement of some people over the last four years. First and foremost, my sincere thanks to Prof. Philip Mountford for his support, advice and encourage to continue with a challenging project. It has been an honour being part of his research group.

I would like to express my gratitude to the Mexican Council of Science and Technology (CONACYT, grant reference 383661) for the financial support, without which my DPhil studies would not have been possible.

I thank all my colleagues in the Mountford group, in particular to Dr. Richard Collins for introducing Group 5 chemistry to me with a big smile and lots of ideas. Massive thanks to Dr. Benjamin Clough for his help with X-ray crystallography, proof-reading of this Thesis, continuing support and also for great advice when it comes to beer. Adan Reyes, Nichabhat Diteepeng, Simona Mellino, Theresa Scharbert and Natalia Reis for their amazing friendship and supporting conversations. Thanks to Dr Andrey Protchenko for his advice and Bowen Xie and Prof. Richard Cooper for assistance with X-ray crystallography.

I would like to thank my family for their love and support (moral and financial), I love you all so much. Lastly, to Tim Stöβer for sharing his happiness and love with me, Ich liebe dich.

Contents

	Declaration	ii
	Abstract	iii
	Acknowledgements	iv
	Contents	v
	Abbreviations	viii
	Notes	xii

Chapter One: Introduction

1.1	General introduction	2
1.2	Tridentate, trianionic ligands	3
1.3	The imido ligand	5
1.3.1	Group 4 imido complexes	6
1.3.2	Group 5 imido complexes	11
1.4	The hydrazido ligand	16
1.4.1	Group 4 hydrazido complexes	17
1.4.2	Group 5 hydrazido complexes	20
1.5	Summary and Objectives	23
1.6	References	24

Chapter Two: Routes towards the synthesis of tantalum hydrazido complexes with tridentate, trianionic ligands: synthesis, structure and bonding of dialkyl, bis(amido) and alkyl-amido precursors

2.1	Overview	33
2.2	Introduction	33
2.3	Selection and synthesis of tridentate, trianionic pincer ligands	35
2.4	Synthesis of $Ta(NN_2^{SiMe3})Cl_2$ (**3**)	37
2.5	Electronic structure analysis of $Ta(NN_2^{SiR3})Me_2$	39
2.6	Route A: Reactions $Ta(NN_2^{SiMe3})Cl_2$ (**3**) with hydrazines or *via* bis(amido) and dimethyl precursors	43
2.7	Route B: Reaction of the hydrazide precursor $Ta(NNPh_2)Cl_3(DME)$ (**1.80**) with the $Li_3(NNN^R)$ ligand	45

2.8	Route C: Multistep synthetic route *via* dialkyl and alkyl-amido precursors with NN_2^{SiMe3} ligand	48
2.8.1	Reactions of $Ta(NN_2^{SiMe3})Cl_2$ (**3**) with metal alkyls	49
2.8.2	Reactions of tantalum alkyls with *tert*-butylamine	58
2.8.3	Reactions of tantalum alkyl-amide complexes with Lewis bases	64
2.9	Conclusions and Outlook	65
2.10	References	66

Chapter Three: Group 5 imido complexes with tridentate, trianionic ligands: synthesis, structure and reactivity

3.1	Overview	74
3.2	Introduction	74
3.3	Pyridine substitution reactions of $M(N^tBu)Cl_3(py)_2$ (M = Nb, Ta or V)	76
3.4	Installation of tridentate, trianionic supporting ligands	79
3.4.1	Installation of NN_2^R supporting ligand	80
3.4.2	Installation of NNN^{SiMe3} supporting ligand	95
3.5	Reactivity of $Nb(NN_2^{iPr})(N^tBu)(py)_2$ (**21**) with unsaturated small molecules	98
3.6	Conclusions and Outlook	100
3.7	References	103

Chapter Four: Group 5 hydrazido complexes with tridentate, trianionic ligands: synthesis, structure, bonding and reactivity

4.1	Overview	109
4.2	Introduction	109
4.3	Synthesis of hydrazido synthons	110
4.3.1	Synthesis of $M(NNPh_2)Cl_3(L)$	111
4.4	Installation of tridentate, trianionic supporting ligands NN_2^R	116
4.5	Synthesis of hydrazido complexes *via* hydrazine/*tert*-butylimide exchange reactions	117
4.6	Bonding in $Ta(NN_2^R)(NNPh_2)(py)_2$	130
4.7	Reactivity of $Nb(NN_2^{iPr})(NNPh_2)(py)_2$ (**48**) with unsaturated small molecules	
4.8	Conclusions and Outlook	140
4.9	References	144

Chapter Five: Experimental details and characterising data

5.1	General methods and implementation	149
5.2	Literature preparations	149
5.3	X-ray data collection and processing parameters	153
5.4	Computational details	153
5.5	Experimental details and characterising data for Chapter Two	154
5.6	Experimental details and characterising data for Chapter Three	159
5.7	Experimental details and characterising data for Chapter Five	169
5.8	References	179

CD Appendix

Abbreviations

General

Å	Ångstrom
atm	atmosphere(s)
Avg.	average
ca	*circa*, about
cf.	*confer*, compared to
^{o}	degrees
^{o}C	degrees Celsius
d	day(s)
e	elementary charge
Fac	facially coordinating
g	grams
h	hour(s)
η	hapticity
K	Kelvin
kcal mol^{-1}	kilocalorie(s) per mole
M	molarity, mol dm^{-3}
Mer	Meridonally coordinating
min	minute(s)
mL	millilitre(s)
mmol	millimole(s)
MOCVD	Metal-Organic Chemical Vapour Deposition
RT	room temperature
s	second(s)
μ	bridging
μmol	micromole(s)
vs	versus

Chemical

9-BBN	9-borabicyclo[3.3.1]nonane
Ar	aryl group

Ar'	2,6-$C_6H_3{}^iPr_2$
Ar^F	C_6F_5
bipy	2,2'-bipyridyl
^nBu	*n*-butyl
$CN_2^{Ar'}$	1,3-$C_6H_4(CH_2N^{Ar'})_2$
Cp	C_5H_5
Cp*	C_5Me_5
Cp'	C_5H_4Me
Cy	Cyclohexyl
di-^{t}Bu-bipy	di-*tert*-butyl pyridyl
DMAP	4-dimethylaminopyridine
DME	1,2-dimethoxyethane
E	generic chalcogen atom
Et	Ethyl
H_2Me_4taa	tetramethyl dibenzotetraaza[14]annulene
^{i}Pr	*iso*-propyl
L	a supporting ligand (set)
Me	methyl
$Me_3[6]aneN_3$	1,3,5-trimethyltriazacyclohexane
$Me_3[9]aneN_3$	1,4,7-trimethyltriazacyclononane
Np	*neo*-pentyl, $-CH_2{}^tBu$
NN_2^{Me}	N(MeN-*o*-$C_6H_4)_2$
NN_2^{iPr}	N(^{i}PrN-*o*-$C_6H_4)_2$
NN_2^{SiMe3}	N($SiMe_3$N-*o*-$C_6H_4)_2$
NNN^{iPr}	$MeC(CH_2N^iPr)_3$
NNN^{SiMe3}	$MeC(CH_2NSiMe_3)_3$
N_2NN'	(2-$C_5H_4N)CH_2N(CH_2CH_2NSiMe_3)_2$
N_2N^R	generic diamide-amine ligand
N_2N^{py}	$MeC(2\text{-}C_5H_4N)(CH_2NSiMe_3)_2$
$N_2N^{SiMe_3}$	$Me_3SiN(CH_2CH_2NSiMe_3)_2$
$N_2{}^{iPr}N^{Me}$	$MeN(CH_2CH_2N^iPr)_2$
N_2ArO	O-(2-C6H4NSiMe3)2
ONO	2,6-(OC_6H_2-$^tBu_2)_2$-C_5H_3N
Ph	phenyl
py	pyridine

R	generic aryl or alkyl
^{t}Bu	*tert*-butyl
THF	tetrahydrofuran
TMEDA	N,N,N',N'-tetramethylethylenediamine
Tol	4-C_6H_4Me
X	generic anionic ligand
Xyl	2,6-$C_6H_3Me_2$

Calculations

DFT	density functional theory
HOMO	highest occupied molecular orbital
LUMO	lowest unoccupied molecular orbital
MO	molecular orbital
SALCs	Symmetry adapted linear combinations
WBIs	Selected Wiberg Bond Indices

Mass Spectrometry

EI	electron impact
FI	field impact
HR	high-resolution
m/z	mass to charge ratio
MS	mass spectrometry

Nuclear Magnetic Resonance Spectroscopy

$^{13}C\{^{1}H\}$	proton-decoupled ^{13}C
br.	broad
COSY	correlation spectrocopy
d	doublet
HMBC	heteronuclear multiple-bond correlation
HSQC	heteronuclear single quantum correlation
Hz	Hertz
i	*ipso*

J	coupling constant
m	*meta*
m	multiplet
MHz	Megahertz
NMR	nuclear magnetic resonance
o	*ortho*
p	*para*
ppm	parts per million
q	quartet
ROESY	Rotating-frame nuclear Overhauser Effect spectroscopy
s	singlet
sept.	septet
t	triplet
VT	variable temperature
δ	chemical shift in ppm

Infrared Spectroscopy

br.	broad
FT-IR	fourier transform infrared
IR	infrared
cm^{-1}	wavenumber
m	medium
s	strong
w	weak
ν	frequency

Notes

Literature compounds described in this Thesis are numbered **1.x**, **2.x**, **3.x**, **4.x**, **5.x** according to the Chapter in which they first occur. The new compounds described in this Thesis are numbered **1** – **53**. Density functional theory (DFT) calculated compounds are clearly stated in the text.

X-ray crystallography data was collected and solved by Dr. Benjamin Clough, Dr. Bowen Xie and Dr. Richard Collins. Molecular structures were refined by the Author with the help and guidance of Dr. Benjamin A. Clough, Dr. Bowen Xie, Dr. Richard Collins, Prof. Philip Mountford and Prof. Richard Cooper. Molecular drawings were produced by Prof. Philip Mountford.

DFT calculations were performed by Prof. Philip Mountford of the University of Oxford.

Chapter One

Introduction

1.1 General introduction

The chemistry of the transition metal−nitrogen multiple bond is an ongoing area of extensive interest, wherein the study of imido and hydrazido complexes of Group 4 and 6 metals is well established and various applications have been reported, such as catalytic reduction of dinitrogen,[1-6] MOCVD (Metal-organic Chemical Vapour Deposition),[7-11] olefin polymerisation[12-15] and hydrohydrazination.[16-20] Our research group has been particularly interested in the chemistry of Group 4 imido and hydrazido complexes of the type (L)Ti=NR or (L)Ti=NNR_2 (R = alkyl, aryl; L = ancillary ligand set), with a wide variety of ancillary ligand sets. More recently, the reactivity of these complexes has been explored and a range of reactions with unsaturated organic substrates was found.[19,21-29]

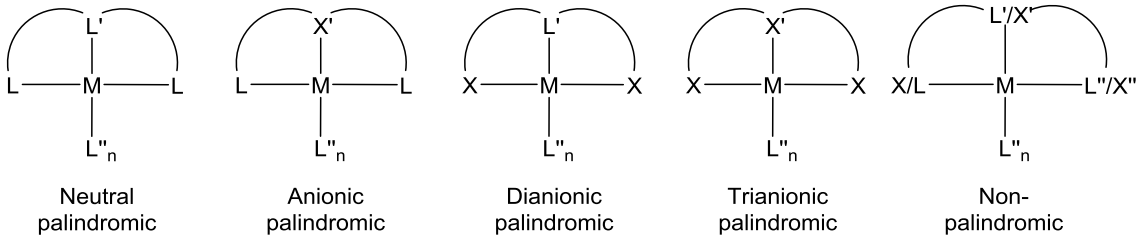
Although there exist examples of vanadium hydrazido(2-) complexes,[30-36] the number of tantalum and niobium compounds is relatively smaller. It was found that these tantalum and niobium complexes containing chloride or pyridine (cationic complex) ligands showed negligible reactivity, in contrast to their Group 4 counterparts. [34,37-41] Thus, this Thesis describes new approaches towards the synthesis of neutral Group 5 complexes of the type M(N_3)($NNPh_2$)($L)_x$ species (N_3 = a trianionic, tridentate ligand, L = Lewis base, x = 0 or 1), in which the replacement of the chloride ligand by a labile Lewis base would hopefully allow access to reactive compounds.

Chapter Two details various synthetic routes towards tantalum hydrazido complexes with tridentate, trianionic ligands in which several intermediates were synthesised and their chemistry was explored, including the tantalum dichloride species Ta(NN_2^{SiMe3})Cl_2, along with a series of tantalum dialkyl and alkyl-amido complexes. Group 5 imido complexes with two different tridentate pincer ligands were also synthesised, as precursors of the analogous hydrazido compounds, and their reactivity was explored (Chapter Three). Finally, the synthesis, structure and reactivity of Group 5 hydrazido complexes with tridentate, trianionic ligands will be described in Chapter Four.

1.2 Tridentate, trianionic ligands

Tridentate pincer ligands have been known since the late 1970s.[42,43] Historically, the concept "pincer movement" is a military manoeuvre use to surround an enemy unit; in the same way a pincer ligand (nowadays referring to any three-coordinate ligand) binds to a metal ion through a central and two flanking donor groups usually adopting a meridional geometry. The use of pincer ligands is emerging as variation in their design allows modification of the electronic and steric properties.[44,45]

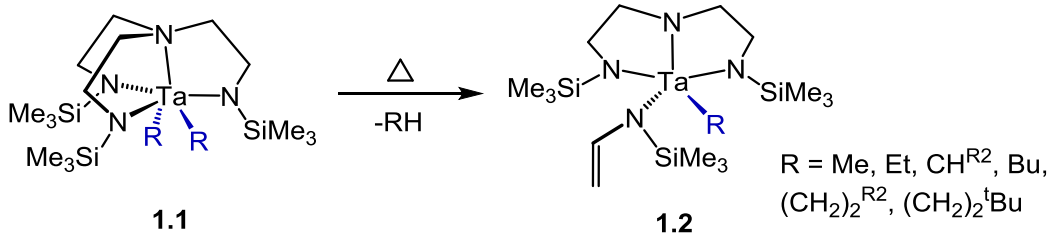
Peris and Crabtree suggested a classification of pincer ligands according to their symmetry (palindromic or non-palindromic) and the nature of the flanking donor groups (neutral or ionic) (Figure 1.1).[45] The electronic stabilization provided by the trianionic charge in tridentate pincer ligands makes these well-suited to study with high-valent metal ions (M^{n+}; $n \geq 3$).[44] These type of pincer ligands, particularly the NNN^{3-} ligand family, are of relevance to this Thesis.



L = flanking neutral donor = PR_2, NR_2, OR, SC, C (from NHC)
L'R_2 = central neutral donor = pyridine, PR_3, NR_3, C (from NHC)
X = flanking anionic donor = O, NR, C (from phenyl)
X' = central anionic donor = C (from phenyl), SiR, N (imide), etc.

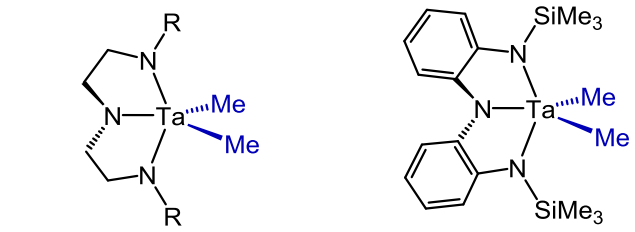
Figure 1.1. Classification of pincer ligands.[45]

Schrock and co-workers' research on the NNN^{3-} trianionic pincer ligand was the first of this type, which was obtained from degradation of the triamido-tripodal ligand N_3N^{3-} ($\{N(CH_2CH_2NSiMe_3)_3\}^{3-}$) from thermolysis of the tantalum complex **1.1** yielding **1.2** supported by the trianionic NNN^{3-} pincer ligand (Equation 1.1).[46,47]



Equation 1.1.

This and other NNN^{3-} trianionic ligands have been metalated using $TaMe_5$[48] to give, for example, $Ta\{(Me_3SiNCH_2CH_2)_2N\}Me_2$ (**1.3**), the relatively unstable $Ta\{(C_6F_5NCH_2CH_2)_2NH\}Me_3$, which evolves one equiv. of methane to give $Ta\{(C_6F_5NCH_2CH_2)_2N\}Me_2$ (**1.4**), and $Ta\{(Me_3SiN\text{-}o\text{-}C_6H_4)_2N\}Me_2$ (**1.5**) (Figure 1.2).[49]

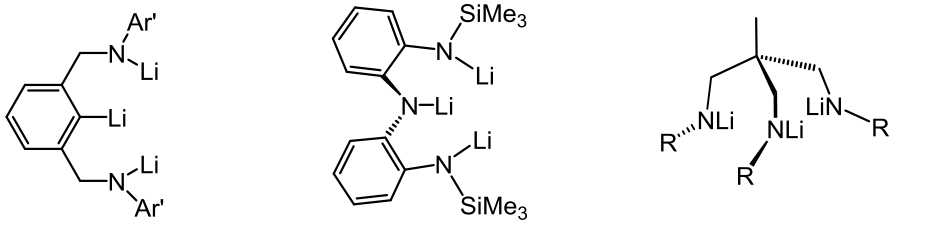


R = $SiMe_3$ (**1.3**) or C_6F_5 (**1.4**) **1.5**

Figure 1.2. Dimethyl tantalum complexes with tridentate, trianionic ligands.[49]

Veige and co-workers took a different approach for the metalation of the NCN^{3-} trianionic pincer ligands, which involved first the lithiation of 1,3-$C_6H_4(CH_2N^{Ar'})_2$ ($H_3CN_2^{Ar'}$, Ar' = 2,6-$C_6H_3{}^iPr_2$) with 3.5 equiv. of methyllithium yielding the trilithiated salt $Li_3(CN_2^{Ar'})$ (**1.6**) (Figure 1.3).[44,50] In a similar manner, our group reported the reaction of $H_3\{N(SiMe_3N\text{-}o\text{-}C_6H_4)_2\}$ with 3.5 equiv. of *n*-butyllithium producing the salt $Li_3(NN_2^{SiMe3})$ (**1.7**) (Figure 1.3).[51]

Tridentate tripodal ligands are not considered pincer-type ligands as the facial mode of coordination is preferred or dictated by their structure.[45] However, polydentate alkyl- or silylamide tripodal ligands can also be tuneable to meet the electronic requirements for early transition metals in high oxidation states. The lithiated face-capping ligands $Li_3\{MeC(CH_2NR)_3\}$ (R = Me, CH_2Me, ^iPr (**1.8**), $SiHMe_2$ or $SiMe_3$ (**1.9**)) were introduced by Gade and co-workers in 1993 (Figure 1.3).[52]



Ar' = 2,6-$C_6H_3{}^iPr_2$ (**1.6**) **1.7** R = ^iPr (**1.8**) or $SiMe_3$ (**1.9**)

Figure 1.3. Selected lithiated tridentate pincer ligands.[50-52]

1.3 The imido ligand

Transition metal imido complexes have been known since 1956 with the first osmium imido complex $Os(N^tBu)O_3$ reported by Clifford and Kobayashi.[53,54] Since then, numerous imido complexes with transition metals have been reported. In general, there are six different metal–imido bonding modes possible for transition metal imides.[55] However, the discussion in this Thesis will be limited to the bonded units shown in Figure 1.4.

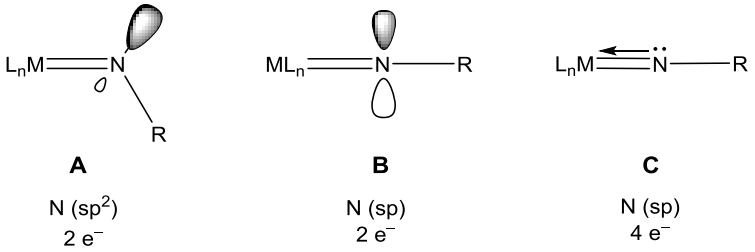


Figure 1.4. Common bonding modes of terminal imido ligands in early transition metal complexes, shown with the N atom orbital hybridisation and the neutral valence electron count of the imido ligand.[55,56]

Early transition metal imido complexes commonly feature a metal–nitrogen triple (or double) bond with a nucleophilic imido nitrogen (Figure 1.4). The bent M−N−R arrangement (structure A) arises when the nitrogen atom is unable to donate its lone pair to the metal. The metal-nitrogen bond is formally described as M═N double bond ($\sigma^2\pi^2$) containing an sp^2-hybridised nitrogen atom. For instance, the complex $Mn(N^tBu)_3Cl$ in which there is delocalisation from the three imido ligands (formally two 4-electron and one 2-electron donation) and with M−N−R angles in the range 138.5(3) – 141.8(3) º.[57] Most of the imido complexes fall in the bonding mode "C" with a near-linear imido ligand arrangement (sp hybridised N-atom) where there is an effective donation of the lone pair to the metal centre. This is formally seen as a M≡N triple bond ($\sigma^2\pi^4$) and acts as a four-electron donor. The bonding mode "B" (Figure 1.4) is an intermediate structure between bent (A) and linear (C) where the N-atom is sp hybridised but not all of the π electrons are donated to the metal centre ($\sigma^2\pi^2$). This situation is observed in complexes where there is a severe competition for the available dπ-orbitals of the metal (π-loaded systems). For instance, complex $Cp^*_2Ta(NPh)H$[58] (Cp^* = η-C_5Me_5) has a ligand-based non-bonding MO which contains two electrons, thus effectively reducing the electron count to eighteen.[59]

1.3.1 Group 4 imido complexes

The chemistry of Group 4 complexes containing imido ligands has been extensively studied since 1960 when Bradley and Thomas reported the first titanium and zirconium complexes of the type $M(NR_2)_4$ (R = Me, Et, ^{n}Pr or ^{t}Bu).[60] These complexes were used later in reactions with H_2N^tBu to form polynuclear materials containing bridging imido ligands with a proposed structure of the type **1.10** (Figure 1.5, left).[61] Terminal imido compounds $Cp_2Zr(NR)$ (R = ^{t}Bu (**1.11**), Xyl or 4-$C_6H_4{}^t$Bu) were prepared by Bergman and co-workers in 1988.[62] These complexes are transient species formed by the thermolysis of the respective complex $Cp_2Zr(Me)(NHR)$ and resulted in bridging imido dimeric species when isolated in the solid state. However, when the thermolysis of **1.11** is performed in THF the monomeric imide species $Cp_2Zr(N^tBu)(THF)$ (**1.12**) was isolated (Figure 1.5, right).[62]

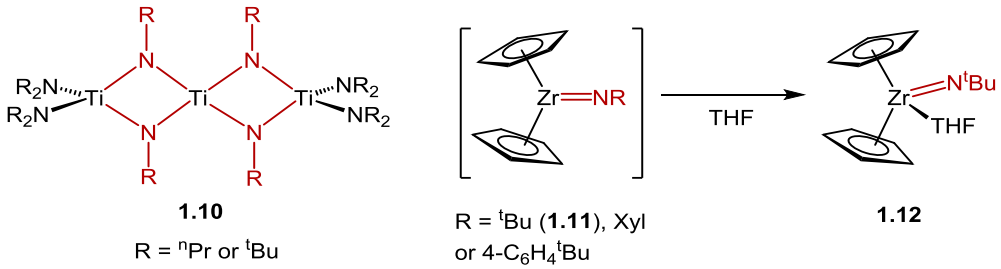
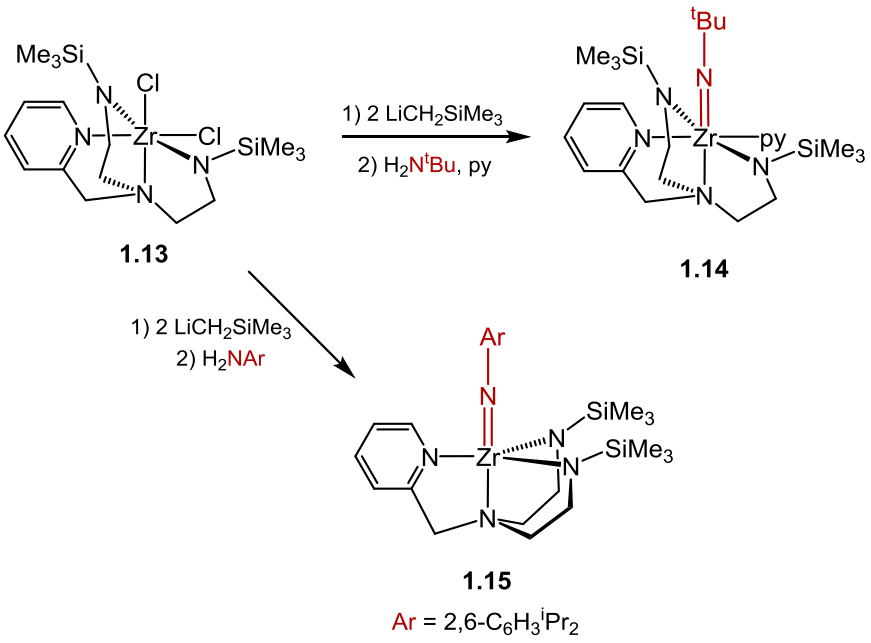


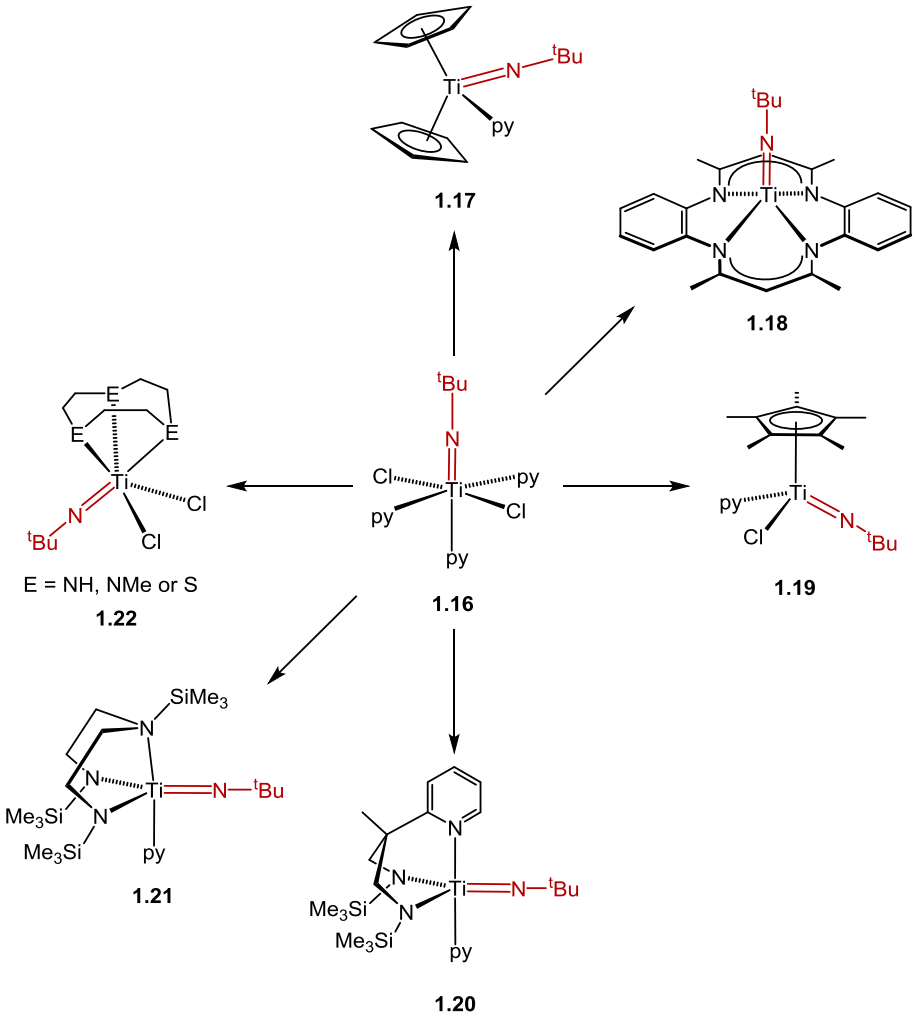
Figure 1.5. Early examples of Group 4 imido complexes. [61,62]

Various synthetic routes to Group 4 imido complexes have been used, for example by addition of primary amines. Our research group reported the reaction of the dichloride species $Zr(N_2NN')Cl_2$ (**1.13**) with $LiCH_2SiMe_3$, H_2N^tBu and pyridine to give the imido complex $Zr(N_2NN')(N^tBu)(py)$ (**1.14**, N_2NN' = $(2\text{-}C_5H_4N)CH_2N(CH_2CH_2NSiMe_3)_2$) (Scheme 1.1).[63] In a similar manner, the analogous zirconium imido complex $Zr(N_2NN')(NAr)$ (**1.15**, Ar = 2,6-$C_6H_3{}^iPr_2$) can be obtained from the *in situ*-generated $Zr(N_2NN')(CH_2SiMe_3)_2$, from the reaction of **1.13** with $LiCH_2SiMe_3$, with H_2NAr' (Scheme 1.1).[63]



Scheme 1.1. Synthesis of $Zr(N_2NN')(N^tBu)(py)$ (**1.14**) and $Zr(N_2NN')(NAr)$ (**1.15**).[63]

Imido synthons of the type $M(NR)_xCl_y(L)_z$ (M = Group 4 metal, R = alkyl or aryl substituents, L = Lewis base)[64-68] have been useful for reactions with a variety of lithiated ligands simplifying the synthesis of imido complexes. In 1997, Mountford and co-workers reported various titanium synthons of that type, for instance the complex $Ti(N^tBu)Cl_2(py)_3$ (**1.16**) prepared from $TiCl_4$, H_2N^tBu and pyridine.[65] Analogous arylimido complexes of the type $Ti(NAr)Cl_2(py)_3$ have also been synthesised from **1.16** by aniline/*tert*-butylimide exchange reactions.[65] Salt metathesis reactions between the synthon **1.16** and various lithiated ligands has been reported (Scheme 1.2),[69,70] giving complexes such as $Ti(N_2N^{py})(N^tBu)(py)$ (**1.20**, N_2N^{py} = $(2\text{-}C_5H_4N)CMe(CH_2NSiMe_3)_2$) and $Ti(N_2N^{SiMe3})(N^tBu)(py)$ (**1.21**, N_2N^{SiMe3} = $Me_3SiN\{(CH_2)_2NSiMe_3\}_2$) from reaction with the corresponding lithiated diamide-donor ligands $Li_2N_2N^{py}$ and $Li_2N_2N^{SiMe3}$ (Scheme 1.22).[71,72]

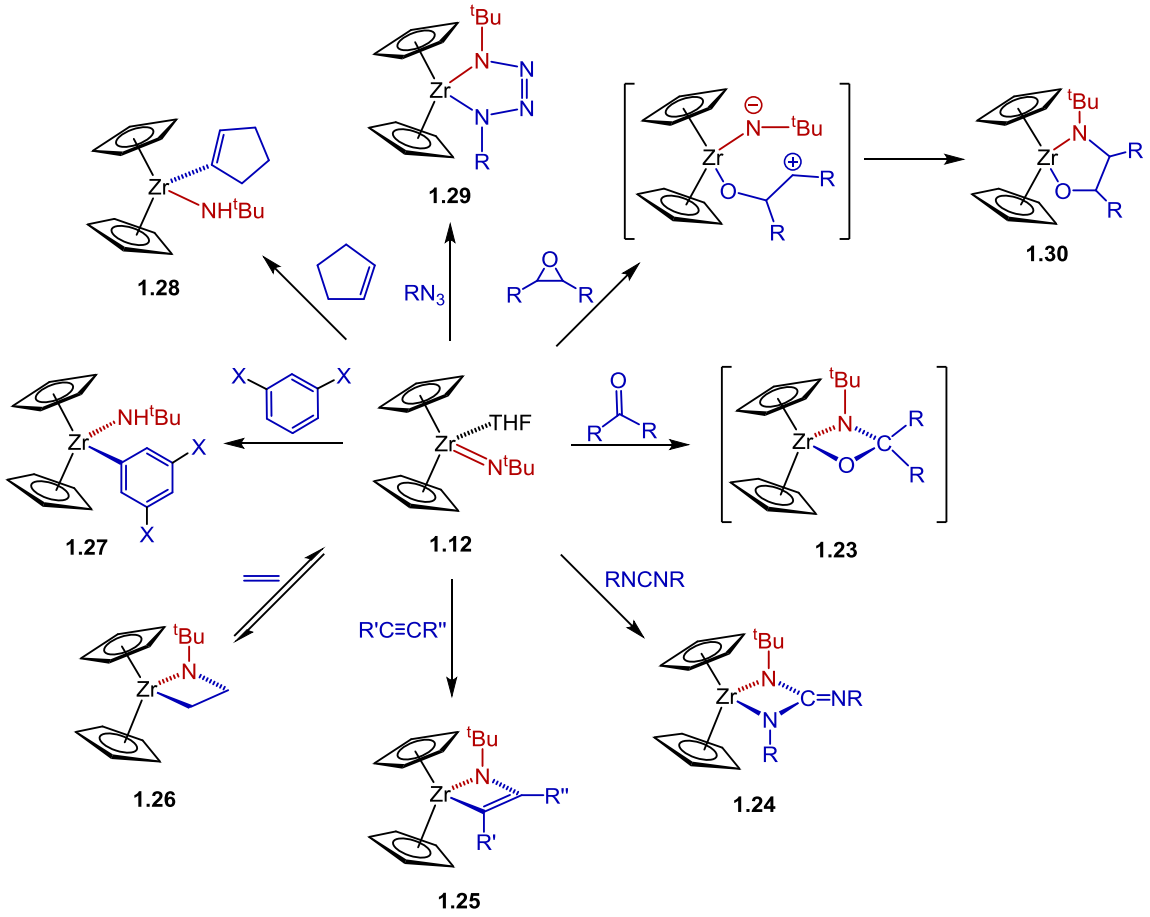


Scheme (1.2). Examples of various titanium *tert*-butylimido complexes synthesised from $Ti(N^tBu)Cl_2(py)_3$ (**1.16**).[69,70]

Various reactivity studies of Group 4 imido compounds (L)M=N−R (R = alkyl or aryl) with small unsaturated molecules have been published in the last decades. Two remarkable examples are the zirconocene imido complex $Cp_2Zr(N^tBu)(THF)$ (**1.12**)[62] and the diamide-amine complex $Ti(N_2N^{py})(N^tBu)(py)$ (**1.20**)[73], both of which showed a rich reaction chemistry.[70,74-78]

For instance, [2+2] cycloaddition reactions of $Cp_2Zr(N^tBu)(THF)$ (**1.12**) with carbonyls and carbodiimides take place to afford the complexes $Cp_2Zr\{N(^tBu)C(R)(R)O\}$ (**1.23**) and $Cp_2Zr\{N(^tBu)C(NR)N(R)\}$ (**1.24**) (Scheme 1.3).[74] Reactions of $Cp_2Zr(NR)(THF)$ (R = ^{t}Bu (**1.12**) or Xyl), with both internal and terminal alkynes R'CCR" (R', R" = H, Me or Ar) also gave the [2+2] cycloaddition products $Cp_2Zr\{N(R)C(R")C(R')\}$ (R = ^{t}Bu (**1.25**, Scheme 1.4) or Xyl). This behaviour was also observed in reactions with alkenes, such as

ethylene (**1.26**, Scheme 1.4) and norbornene, in equilibrium with the starting material.[74] Early observations by Bergman and co-workers that imidozirconocene complexes activated the C−H bonds of benzene led them to study the reactivity of complex **1.12** with substrates containing sp^2 C−H bonds. Clean reactions with disubstituted arenes with electron-withdrawing groups (Cl or CF_3) gave the products of C−H activation *meta* to both substituents (**1.27**, Scheme 1.3). C−H bond activation was also observed in reactions with cyclopentane (**1.28**, Scheme 1.3), norbornene and other Cp-supported transition metal complexes yielding in this case bimetallic complexes.[74]

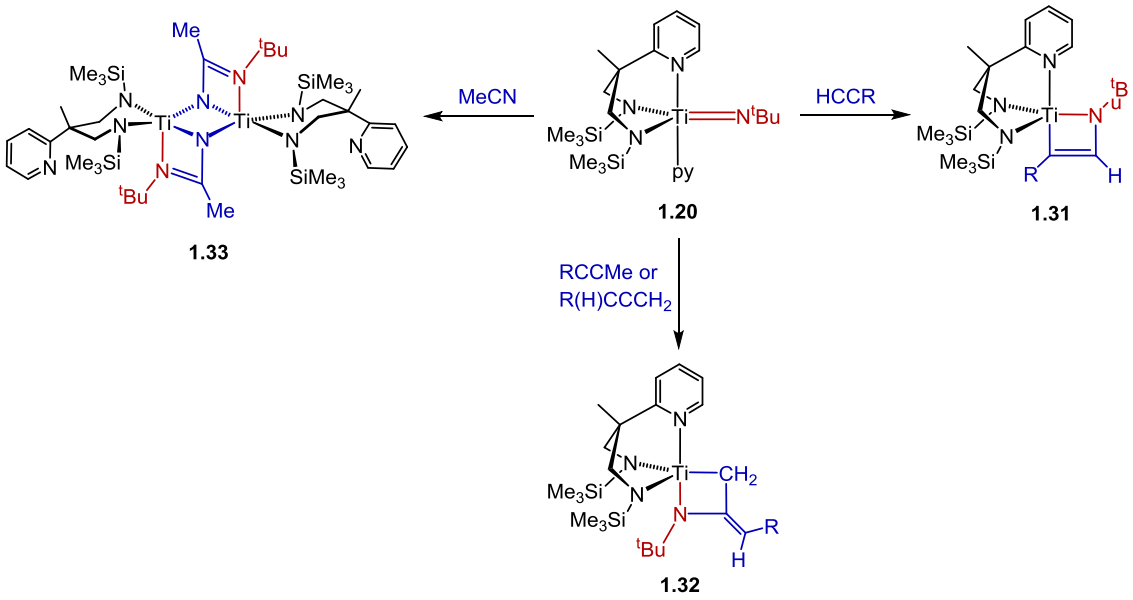


Scheme 1.3. Reactions of $Cp_2Zr(N^tBu)(THF)$ (**1.12**) with unsaturated substrates.[56,74,75]

Reactions of the zirconium imido complex $Cp_2Zr(N^tBu)(THF)$ (**1.12**) with organic azides such as *tert*-butyl, phenyl and *p*-tolyl azides are known to proceed through [3+2] cycloaddition reactions resulting in metallatetrazene-type complexes (**1.29**, Scheme 1.3). These reactions proceeded further *via* extrusion of *tert*-butyl azide to give $Cp_2Zr{=}NPh$ and form tetrazene-type compounds with additional azide.[79] Reactions of the zirconium imido complex $Cp_2Zr(N^tBu)(THF)$ (**1.12**) with epoxides have also been investigated.

Coordination of either styrene oxide, stilbene oxide or *exo*-norbornene oxide to the metal centre occurred, and proceeded with ring-opening promoted by the imido moiety followed by the formation of the metallacycle complexes **1.30**, Scheme 1.3.[80]

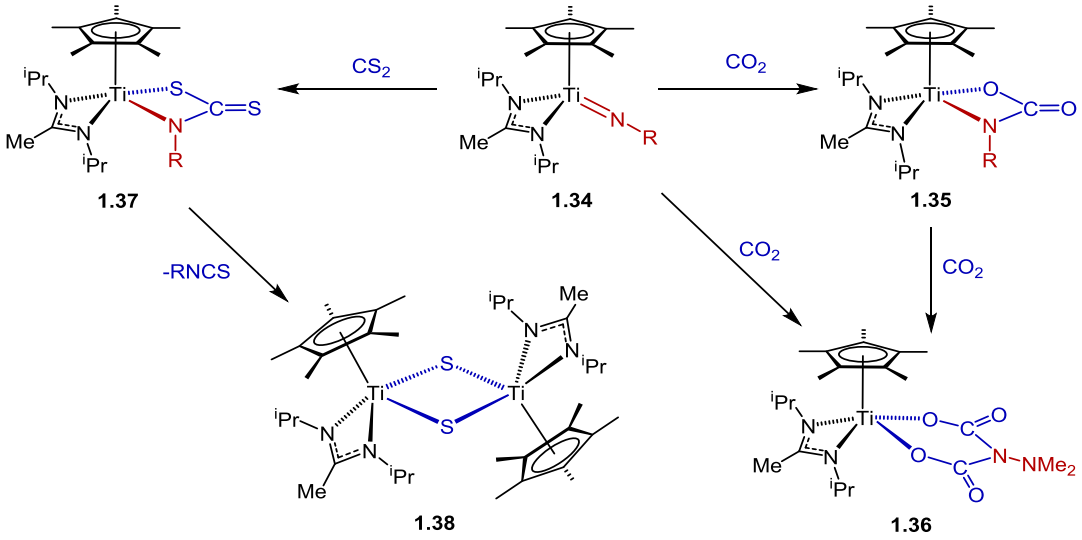
Similarly to complex **1.12**, [2+2] cycloaddition reactions were reported with the diamide-amine-supported complex Ti(N_2N^{py})(N^tBu)(py) (**1.20**) reacting with terminal (**1.31**) and internal alkynes or allenes (**1.32**),[78,81,82] and dimerisation reactions with nitriles (MeCN) afforded the complex [$Ti_2\{\mu$-η^2-NC(Me)$N^tBu\}_2(L)_2$] (1.33) (Scheme 1.4).[83]



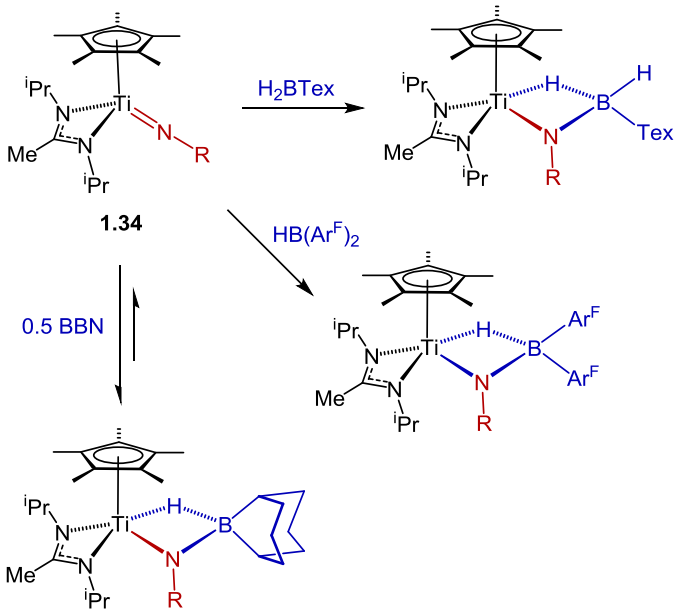
Scheme 1.4. Selected reactions of Ti(N_2N^{py})(N^tBu)(py) (**1.20**) with unsaturated substrates.[78,81-83]

Mountford and co-workers have observed cycloaddition of CO_2 to the Ti=NR bond in the complexes Ti(NR)(Me_4taa) (Me_4taa = dianion of tetramethyldibenzotetraaza[14]annulene),[84] Ti(NR)(Me_2calix) (Me_2calix = the dianion of 1,3-dimethyl ether *p-tert*-butylcalix[4]-arene),[85] Ti(NR)(O_2NN') (H_2O_2NN' = (2-C_5H_4N)CH_2N-(2-HO-3,5-$C_6H_2{}^tBu_2$)$_2$),[86] and Cp*Ti(NR)$\{MeC(N^iPr)_2\}$ (**1.34**, R = ^{t}Bu or Ar, Scheme 1.5)[87] giving a carbamate product of the type [$(L)_nTi\{OC(O)N(R)\}$] (e.g. Cp*Ti$\{MeC(N^iPr)_2\}\{O(CO)NR\}$ (**1.35**)[87,88]). Similarly, the cyclopentadienyl-amidinate imido complexes Cp*Ti(NR)$\{MeC(N^iPr)_2\}$ (**1.34**, R = ^{t}Bu, Ar or Tol) gave cycloaddition-elimination reactions with CS_2 forming the dimeric sulfido-bridged complexes **1.38** (Scheme 1.6).[88] More recently, our research group communicated the reactivity of titanium imido and hydrazido complexes with boranes. The imide Cp*Ti(NTol)$\{MeC(N^iPr)_2\}$ (**1.34**) reacted cleanly with the hydroboranes H_2BTex (Tex =

tert-hexyl), 9-BBN and $HBAr^F_2$ forming the hydride-bridged adducts Cp*Ti{N(Tol)HBRR′}{$MeC(N^iPr_2)_2$} (Scheme 1.6).[29]



Scheme 1.5. Reactions of Cp*Ti(NR){$MeC(N^iPr)_2$} (**1.34**, R = ^{t}Bu, Ar or Tol) with CO_2 and CS_2.[87,88]

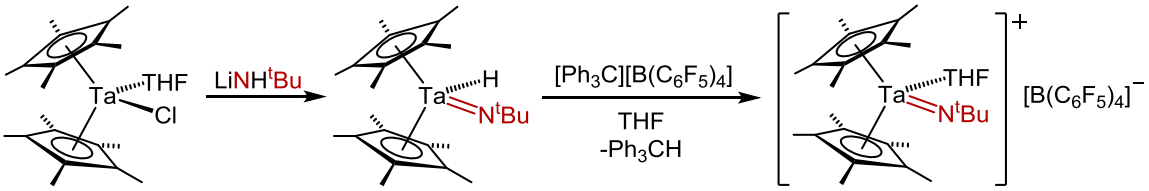


Scheme 1.6. Reactions of Cp*Ti(NR){$MeC(N^iPr)_2$} (**1.34**, R = Tol) with boranes.[29]

1.3.2 Group 5 imido complexes

The first tantalum and niobium imido complexes $M(N^tBu)(NMe_2)_3$ were observed by Bradley and Thomas in 1962.[89] However, it wasn't until 1978 that Nugent and Harlow reported the isolated products from the reaction of MCl_5 (M = Ta or Nb) with $LiNMe_2$

and LiNH^{t}Bu.[90] Subsequently, other Group 5 compounds containing imido ligands were reported,[91-97] for instance the permethyl tantalocene complex Cp*$_2$Ta(N^{t}Bu)H (**1.39**, Scheme 1.7) synthesised from *in situ* prepared THF adduct Cp*$_2$TaCl(THF) with LiNH^{t}Bu.[98] The tantalocene complex **1.39** was later used as a precursor to cationic imido complexes (**1.40**, Scheme 1.7).[91] However, it wasn't until the synthesis of imido synthons of the type M(NR)$_x$Cl$_y$(L)$_z$ (R = alkyl or aryl substituents; L = Lewis base)[99-106] when numerous examples of imido complexes were synthesised.

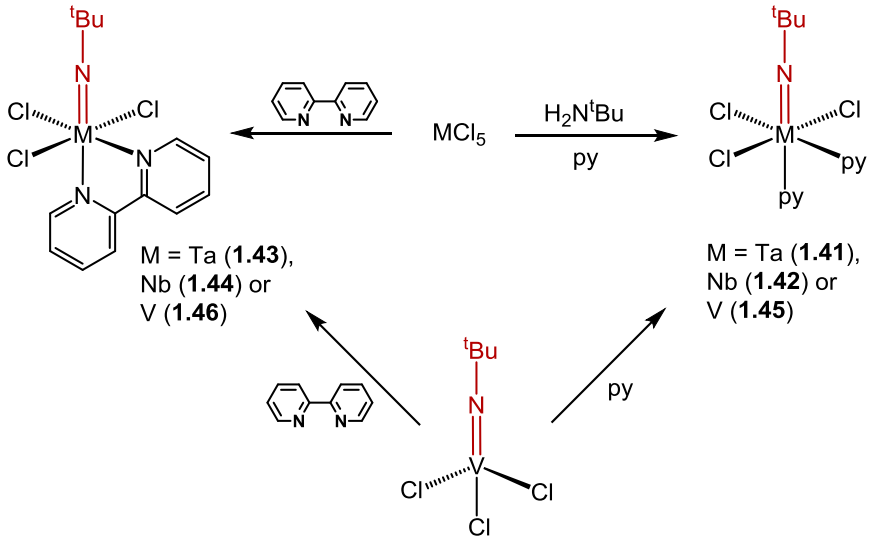


1.39 **1.40**

Scheme 1.7. Synthesis of the precursor Cp*$_2$Ta(N^{t}Bu)H (**1.39**) to cationic imido complex (**1.40**).[91,98]

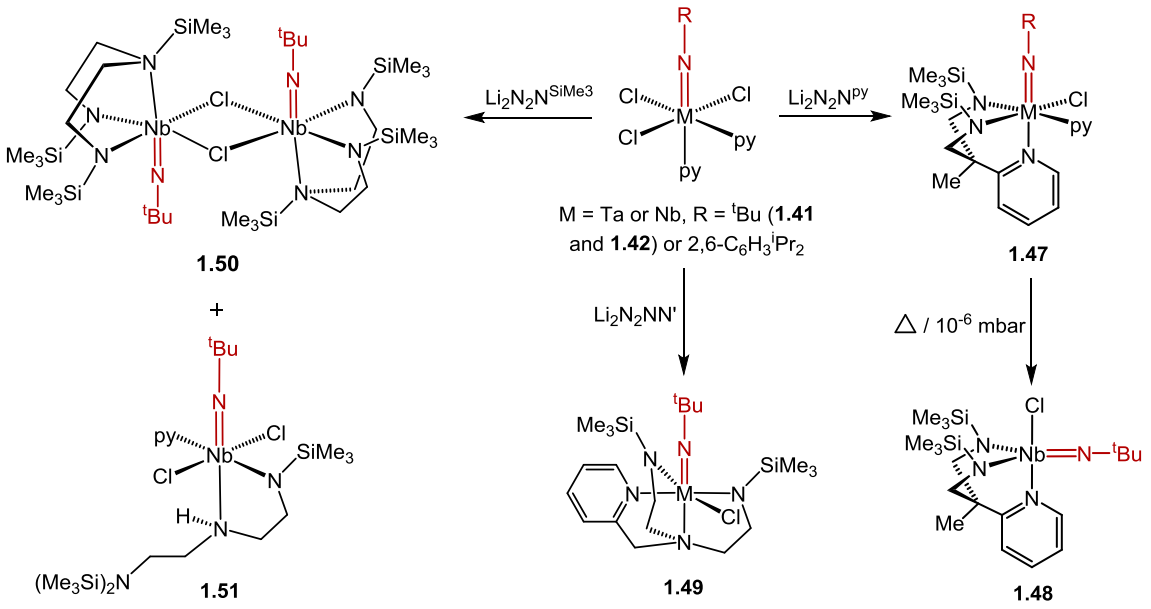
The first Group 5 imido synthons of this type were the tantalum and niobium imides M(NR)Cl$_3$(THF)$_2$ (M = Ta or Nb, R = Ph, Me or ^{t}Bu) reported by Schrock and co-workers in 1980.[107] These complexes were obtained from the reaction of M(CH^{t}Bu)Cl$_3$(THF) and RN=CHPh in THF, which yielded *cis*- and *trans*-^{t}BuCH=CHPh and the corresponding imido complexes.[107] Later, these compounds gave access to olefin complexes of the type Ta(NPh)(olefin)L$_3$Cl.[108] The imido complexes M(N^{t}Bu)Cl$_3$(py)$_2$ (M = Ta (**1.41**) or Nb (**1.42**)) were obtained by the reaction of the metal pentachloride and three equiv. of *tert*-butylamine, followed by the addition of 2 equiv. of pyridine to afford the microcrystalline yellow imido complexes (Scheme 1.8). These compounds were first reported by Sundermeyer and co-workers along with a series of hydridotris(pyrazolyl)borate complexes of Group 5–7 metals.[103] More recently, a slightly different methodology for the synthesis of these two complexes, along with a multinuclear NMR spectroscopy analysis and the investigation of their reactivity with isocyanides and ketones, was published by Gómez and co-workers.[101] The analogous compounds M(N^{t}Bu)Cl$_3$(bipy) (M = Ta (**1.43**) or Nb (**1.44**), bipy = 2,2'-bipyridyl) were prepared by a similar synthetic route in 1988 by Nielson (Scheme 1.8).[109] Preuss and co-workers synthesised the complexes V(N^{t}Bu)Cl$_3$(py)$_2$ (**1.45**)[104] and V(N^{t}Bu)Cl$_3$(bipy) (**1.46**)[110] by ligand exchange reaction between VOCl$_3$ and V(N^{t}Bu)(OSiMe$_3$)$_3$ yielding the

trichloride complex V(N^{t}Bu)Cl$_3$. Further reaction with either pyridine or bipy formed complexes **1.45** and **1.46**, respectively (Scheme 1.8).



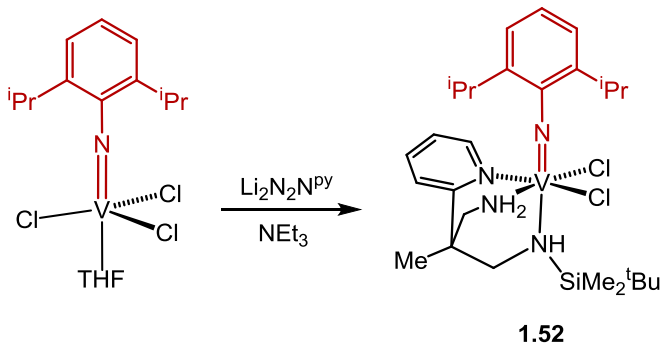
Scheme 1.8. Synthesis of Group 5 imido synthons of the type M(N^{t}Bu)Cl$_3$(L)$_2$ (M = Ta, Nb or V, L = py or bipy). [101,103,104,109,110]

Studies by Mountford and Gade and their co-workers have shown convenient access to imido compounds from M(N^{t}Bu)Cl$_3$(py)$_2$ (M = Ta (**1.41**) or Nb (**1.42**)) with diamido-pyridine N$_2$N^{py}, diamido-amine-pyridine N$_2$NN′ ((2-NC$_5$H$_4$)CH$_2$N(CH$_2$CH$_2$NSiMe$_3$)$_2$) and diamido-amine ligands N$_2$N^{SiMe3}, analogous to the previously reported Group 4 imido complexes (Scheme 1.9).[77] Incorporating these lithiated ligands by salt metathesis reactions with the tantalum and niobium precursors resulted in six-coordinated neutral complexes such as the diamido-pyridine-supported compounds M(N$_2$N^{py})(NR)Cl(py) (**1.47**, M = Ta or Nb, R = ^{t}Bu or 2,6-C$_6$H$_3$^{i}Pr$_2$) and the diamido-amine-pyridine-supported complexes M(N$_2$NN′)(N^{t}Bu)Cl (**1.49**, M = Ta or Nb) (Scheme 1.9).[77] Interestingly, a fluxional process in complexes **1.47** suggest two enantiomeric forms, which was proved with the isolation of the complex Nb(N$_2$N^{py})(N^{t}Bu)Cl (**1.48**, Scheme 1.9). This complex was obtained by sublimation of M(NR)Cl(N$_2$N^{py})(py) (**1.47**, M = Nb, R = ^{t}Bu) at high-vacuum (10^{-6} mbar), showing that the imido group is positioned *cis* to the pyridine ligand, although this complex is unstable in solution over 24 h.[77] When the niobium trichloride synthon **1.42** reacted via salt metathesis with LiN$_2$N^{SiMe3}, a mixture of the dimer [Nb(μ-N^{t}Bu)(N$_2$N^{SiMe3})(μ-Cl)]$_2$ (**1.50**) and complex Nb(N^{t}Bu)Cl$_2${Me$_3$SiN(CH$_2$)$_2$NH(CH$_2$)$_2$N(SiMe$_3$)$_2$}(py) (**1.51**) was formed (Scheme 1.9).



Scheme 1.9. Examples of Group 5 imido complexes supported by diamido-amine-pyridine and diamido-pyridine ligands.[77]

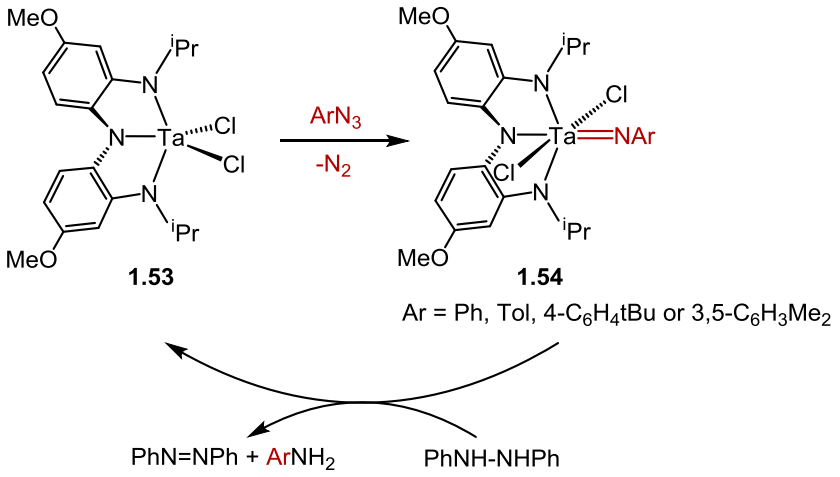
In general, the chemical properties of vanadium differ significantly from those of niobium and tantalum, the chemistry of which are dominated by the +5 oxidation state and are more resistant to redox processes than vanadium.[111] The relative stability of lower oxidation states (vanadium (IV), (III) and (II)) makes studies of vanadium (V) more challenging. This was exemplified by Mountford and co-workers, when efforts to obtain vanadium complexes with the diamido-pyridine ligands N_2N^{py} or N'_2NN' using the synthon $V(NAr)Cl_3(THF)$ (Ar′ = 2,6- $C_6H_3{}^iPr_2$) resulted in product mixtures. Nonetheless, the isolation of $V(NAr)Cl_2(H_3N'N'N_{py})$ (**1.52**, $H_3N'N'N_{py}$ = MeC(2-C_5H_4N)($CH_2NHSiMe_2{}^tBu$)(CH_2NH_2))[112] was achieved (Equation 1.2).[77]



Equation 1.2.

Ligand exchange reactions of the the diamido-pyridine-supported compounds $M(N_2N^{py})(NR)Cl(py)$ (**1.47**, M = Ta or Nb, R = ^{t}Bu or Ar′) showed the formation of aryloxide, amide and benzamidinate derivatives by displacement of the pyridine and the chloride ligands with the respective co-ligand.[77] Reaction of the same complexes with $MgClCH_2Ph$, LiCp' (Cp' = C_5H_4Me) and $LiCHR(SiMe_3)$ (R = H or $SiMe_3$) resulted in the first Group 5 alkyl complexes incorporating both imido and diamido ligands.[77] However, in all these cases the imido ligand acted as a "spectator" or "ancillary" ligand.

Bercaw and co-workers studied a series of tantalum imido and amido compounds supported by the bis(phenolate)pyridine ligand (ONO^{cat}) ((2,6-OC_6H_2-2,4-$^t Bu_2)_2NC_5H_3$) that exhibit either C_s- or C_2-symmetric binding which is determined by the degree of Ta−O π-bonding required to complete the 18-electron count. They found that the bis(phenolate)pyridine ligand is not a strong enough π-donor to provide control over the electronic and geometric properties of the complexes.[113] The particular design of the redox-active bis(2-isopropylamino-4-methoxyphenyl)amine (NNN^{cat}) ligand in contrast to the well-known (ONO^{cat}) first offers three amides acting as strong π-donors towards the metal centre. This allows the ligand to have one- and two-electron oxidations to retain the formal Ta(V) metal centre. Heyduk and co-workers synthesised $Ta(NNN^{cat})Cl_2$ (**1.53**) by direct coordination of the ligand $(NNN^{cat})H_3$ with the previously reported $TaCl_2Me_3$.[114] Two-electron oxidation is observed when **1.53** reacts with PhN_3 and *p*-$^t BuC_6H_4N_3$ by releasing N_2 to afford the tantalum imido complexes $Ta(NNN^{cat})(NR)Cl_2$ (**1.54**, R = Ph, Tol, 4-$C_6H_4{}^t$Bu or 3,5-$C_6H_3Me_2$) (Scheme 1.10).[115] Nitrogen transfer to olefins, alkynes, SMe_2, H_2 and PPh3 cannot be achieved with these imido complexes. However, they can be reduced with 1,2-diphenylhydrazine to form aniline and azobenzene or fully reduced to the dichloride complex **1.53** when reactions are carried out in THF (Scheme 1.10).[44,116]



Scheme 1.10. Synthesis of $Ta(NNN^{cat})(NR)Cl_2$ (**1.54**, R = Ph, Tol, 4-$C_6H_4{}^tBu$ or 3,5-$C_6H_3Me_2$) and its nitrene transfer reactions. [44,116]

1.4 The hydrazido ligand

Since imido and hydrazido functional groups (M=NH, $M=NNH_2$) were proposed as intermediates in the Chatt-type[1] cycle of N_2 reduction, the chemistry of transition metal–ligand multiple bonding has been an active area of investigation. Much of the early work focussed on molybdenum and tungsten hydrazido complexes[2,117-119] and many other nitrogen-containing products from the reactions of the $M{=}NNR_2$ functional group have also been studied in detail.

Hydrazido ligands present several bonding modes to transition metal centres. Relevant bonding modes of the 1,1-dialkylhydrazido ligand are shown in Figure 1.6.[120] The formal charge on the $N_\alpha N_\beta R_2$ hydrazido ligand (−1 or −2) is determined by the N_β substituents. The metal may also be bound to one (η^1) or both (η^2) nitrogen atoms of the hydrazido ligand and hydrazido (2−) ligands may be coordinated to a single metal or bridging to two (μ_2) metal centres. In some complexes it is possible that the η^1-hydrazido(2−) unit could be described as a formally neutral diazene, which is a resonance form arising from the participation of the lone pair on the N_β. Strong donation will form a $N_\alpha{=}N_\beta$ double and a weak π-bond interaction between the ligand and the metal. This resonance form can be identified through geometric parameters ($M{-}N_\alpha$ and $N_\alpha{-}N_\beta$ bond lengths, and $M{-}N_\alpha{-}N_\beta$ angles).

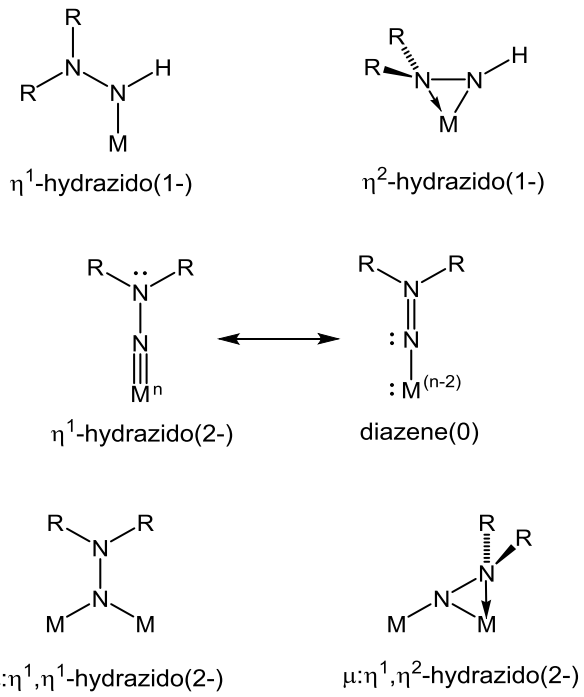


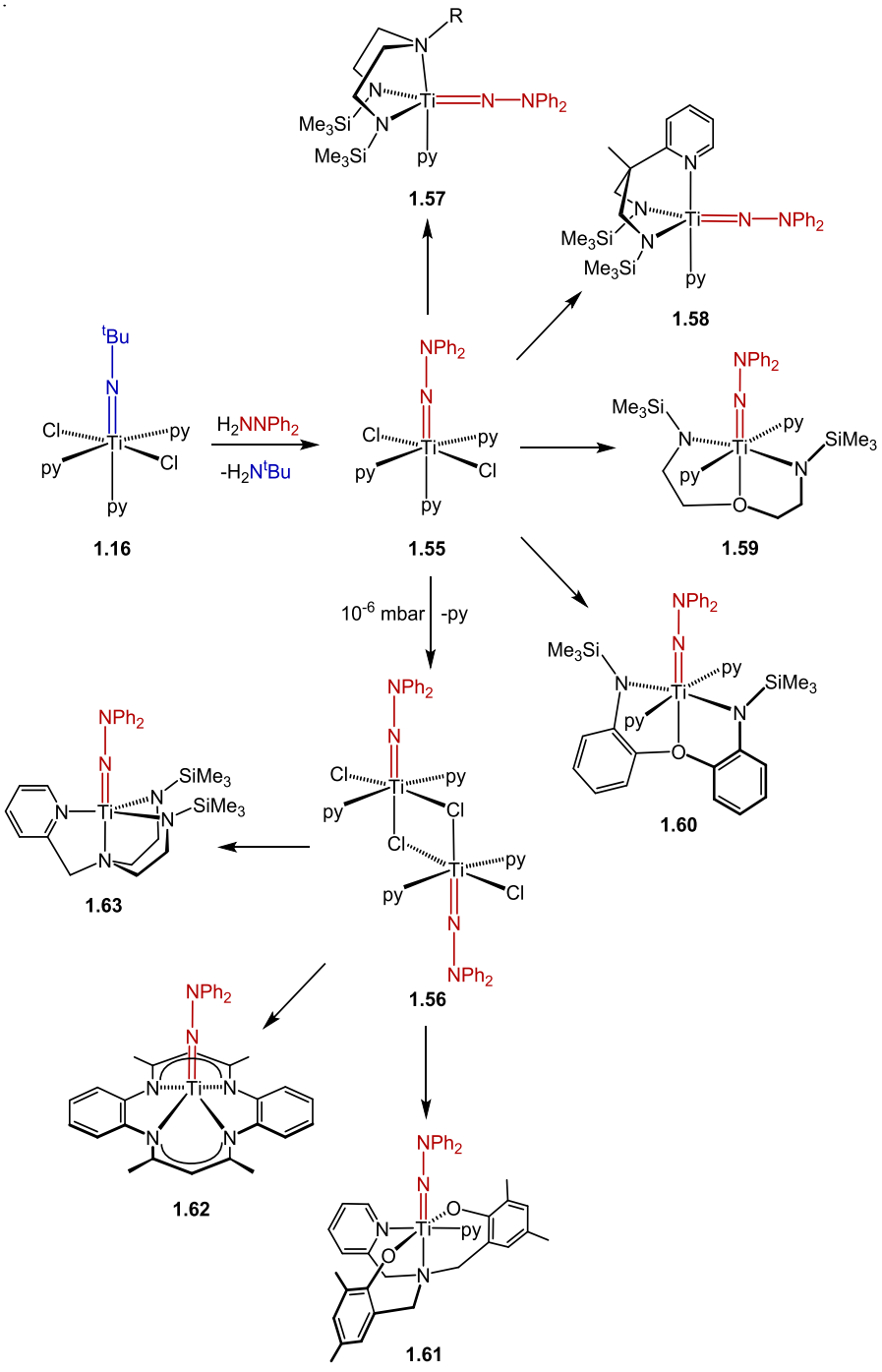
Figure 1.6. Relevant bonding modes for dialkylhydrazido ligands and neutral diazene resonance form, and associated nomenclature.[40,120]

1.4.1 Group 4 hydrazido complexes

Wiberg *et al*. and Bergman *et al*. were the pioneers of Group 4 hydrazido chemistry, reporting the first titanium ($Cp_2Ti\{NN(SiMe_3)_2\}$)[121] and zirconium ($Cp_2Zr(NNPh_2)(DMAP)$)[122] hydrazido complexes, respectively. However, it was not until the hydrazido synthons were synthesised that complexes of the type $(L)M{=}NNR_2$ (M = Group 4 metals, R = alkyl, aryl; L = ancillary ligand set) with a wide variety of ancillary ligand sets escalated.

The titanium diphenylhydrazido synthon $Ti(NNPh_2)Cl_2(py)_3$ (**1.55**) was synthesised by Mountford and co-workers in 2008 from *tert*-butylimido synthon $Ti(N^tBu)Cl_2(py)_3$ (**1.16**)[65] (which can be prepared on the multigram scale) by hydrazine/*tert*-butylimide exchange reaction (Scheme 1.11).[123] The strong labilizing effect of the hydrazido ligand on the *trans* pyridine leads to loss of this pyridine ligand when **1.55** is exposed to dynamic vacuum affording the bis(pyridine) dimer $[Ti(NNPh_2)Cl_2(py)_2]_2$ (**1.56**). These complexes (**1.55** and **1.56**) were used as starting materials in salt metathesis reactions with various lithiated ligands affording hydrazido complexes supported by ligands like the diamide-donor ligands N_2N^R (**1.57**) and N_2N^{py} (**1.58**), diamido-ether ligands N_2O (**1.59**, $N_2O = O(CH_2CH_2NSiMe_3)_2$) and $N_2{}^{Ar}O$ (**1.60**, $N_2{}^{Ar}O = O(2\text{-}C_6H_4NSiMe_3)_2$),

bis(phenolate)-diamine O_2NN' (**1.61**, O_2NN' = (2-C_5H_4N)CH_2N-(2-O-3,5-$C_6H_2{}^tBu_2$)$_2$), macrocycle Me_4taa (**1.62**), and diamido-amine-pyridine ligand N_2NN' (**1.63**) (Scheme 1.11).[27,123]

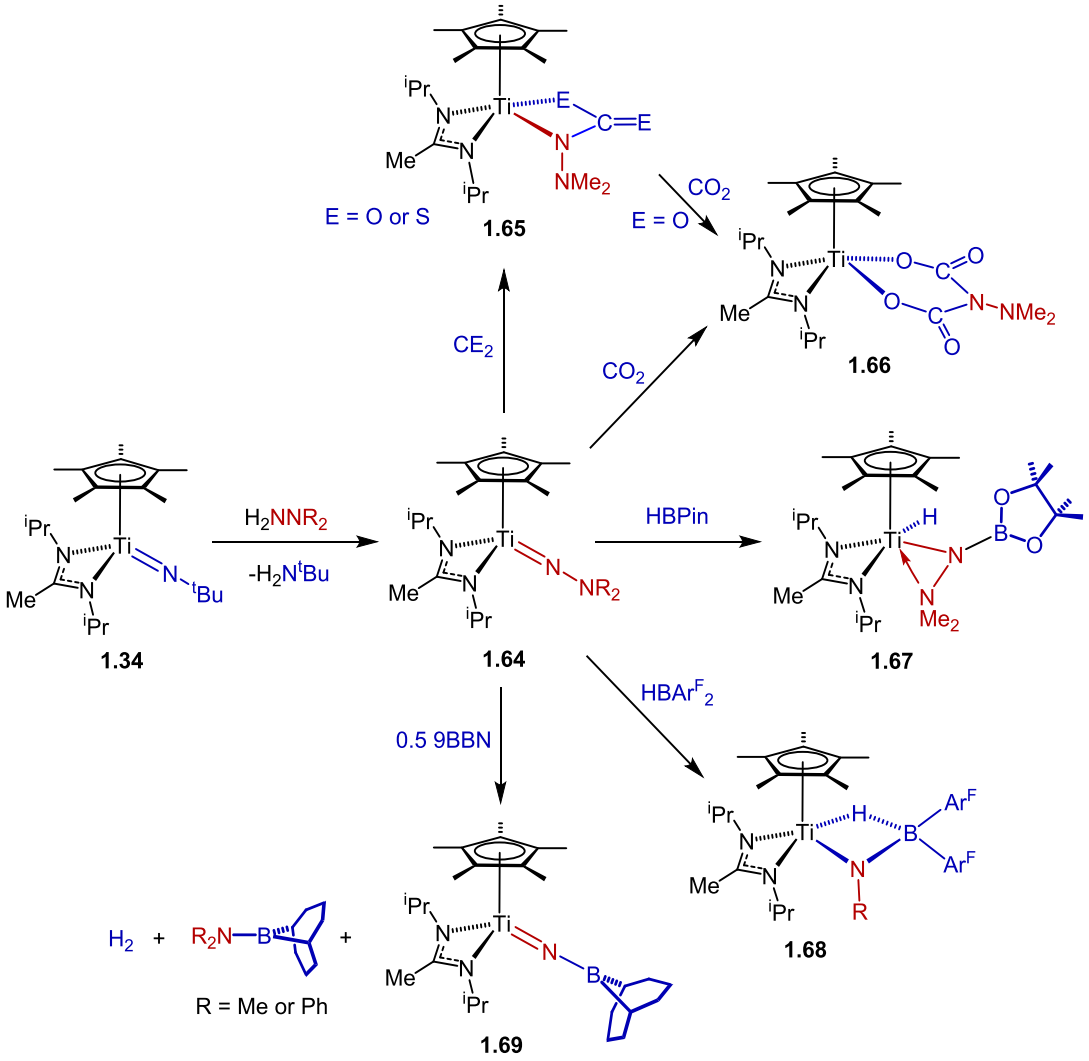


Scheme 1.11. Examples of various titanium hydrazido complexes synthesised from $Ti(NNPh_2)Cl_2(py)_3$ (**1.55**) and $[Ti(NNPh_2)Cl_2(py)_2]_2$ (**1.56**).[27,123]

Several of these titanium hydrazido complexes (Scheme 1.11) exhibit rich reactivity with small molecules at the M−N_α multiple bond *via* [2+2] cycloaddition reactions,[17,23,25-27,124-

[128] N_α–N_β bond cleavage[19,23,28,29,122,125,129-131] and catalytic hydrohydrazination[16-20]. For instance, the hydrazido complexes Ti(N_2N^R)($NNPh_2$)(py) (**1.57**)[21] and their analogues with other dianionic N_3-donor ligands (**1.58**) and/or with zirconium or hafnium,[22,24,127,132] and their reactive intermediates of the type M(N_2N^R)($NNPh_2$) from the dissociation of pyridine, have shown interesting reactivity, for example cycloaddition reactions with terminal and internal alkynes.[19]

The titanium hydrazido complex Cp*Ti{MeC(N^iPr_2)$_2$}(NNR_2) (**1.64**, R = Me or Ph) has been extensively studied in reactions with small substrates. In a similar manner, complex **1.64** is synthesised *via* hydrazine/*tert*-butylimide exchange, however in this case from the analogous imido compound Cp*Ti{MeC(N^iPr_2)$_2$}(N^tBu) (**1.34**) rather than titanium hydrazido synthons (Scheme 1.12).[25]



Scheme 1.12. Synthesis of Cp*Ti{MeC(N^iPr_2)$_2$}(NNR_2) (**1.64**) and reactions with small substrates.[25,133]

Some examples from reactivity studies of the titanium hydrazido complexes Cp*Ti{MeC(N^{i}Pr)$_2$}(NNR$_2$) (**1.64**, R = Me or Ph) are the [2+2] cycloaddition, cycloaddition−insertion and cycloaddition−elimination reactions at the Ti−N$_\alpha$ multiple bond with CO$_2$ (**1.65** and **1.66**, Scheme 1.12), CS$_2$ (**1.65**, Scheme 1.12) and isocyanates depending on the N$_\beta$ substituents.[25] More recently, our research group communicated the reactivity of **1.64** with boranes giving in all cases different final products. The reaction with HBPin resulted in κ^2-borylhydrazide(1−)hydride compound Cp*Ti{MeC(N^{i}Pr)$_2$}(H){N(BPin)NMe$_2$} (**1.67**). In contrast, reaction with HBAr$^F{}_2$ gave a hydride-bridged complex Cp*Ti{MeC(N^{i}Pr)$_2$}{N(NMe$_2$)HBAr$^F{}_2$} (**1.68**) and the reaction with 9-BBN resulted in a 1:1 mixture of Cp*Ti{MeC(N^{i}Pr)$_2$}(NBC$_8$H$_{14}$) (**1.69**) and the corresponding aminoborane R$_2$NBC$_8$H$_{14}$ and elimination of H$_2$ (Scheme 1.12).[29]

Reductive N$_\alpha$−N$_\beta$ bond cleavage is an interesting reaction that has been observed for example with the transient zirconium hydrazido intermediate Cp$_2$Zr(NNPh$_2$) with CO$_2$ and alkynes.[122] The titanium diamide-donor-supported complex Ti(N$_2$N^{py})(NNPh$_2$)(py) (**1.58**) with alkynes, nitriles and isonitriles gave a product from the insertion of the substrate into the N$_\alpha$−N$_\beta$ bond.[19,23]

1.4.2 Group 5 hydrazido complexes

Although there exist examples of vanadium hydrazido(2-) complexes[30-36], the number of niobium and tantalum compounds is comparatively smaller. The complex CpNb(NNMe$_2$)Cl$_2$, reported by Green in 1997, was the first niobium hydrazido complex.[38] The solid state structure of this complex showed it to be a dimer with two hydrazido ligands with different coordination modes: η^1 and an unusual μ-η^2 bonding. Reaction of the hydrazido compound CpNb(NNMe$_2$)Cl$_2$ with LiCp gave the niobocene hydrazido complex Cp$_2$Nb(NNMe$_2$)Cl (**1.70**, Figure 1.7) and the solid state structure of the analogous compound Cp'$_2$Nb(NNMe$_2$)Cl proved to be monomeric.[37]

In the case of tantalum hydrazide chemistry, Wilkinson and co-workers reported in 1997 the anionic complex [Ta{NN(2,6-C$_5$H$_6$Me$_4$)}$_2$Cl$_4$]$^-$ alongside the niobium analogue.[34] Metrical data for the two hydrazido moieties suggested a weak π-bond interaction between the ligand and the metal; this resonance form is better described as isodiazene(0) rather than hydrazido(2-). A decade later, Winter and co-workers synthesised tantalum and niobium cationic complexes of the formula [M(NNR$_2$)Cl$_2$(NH$_2$NR$_2$)(TMEDA)]Cl (**1.71**) and [M{NN(CH$_2$}$_5$)Cl$_2${NH$_2$N(CH$_2$)$_5$}]Cl (**1.72**) in which different hydrazido

ligand coordination modes are present, with η^1 and η^2 bonding (Figure 1.8).[39] More recently, Sita and co-workers prepared the complex Cp*Ta{N(^{i}Pr)C(NMe$_2$)N(^{i}Pr)}(NNMe$_2$)Cl (**1.73**, Figure 1.7) through the reaction of Cp*Ta{N(^{i}Pr)C(NMe$_2$)N(^{i}Pr)}Cl$_3$ with 2 equiv. of lithium 1,1-dimethylhydrazide (LiNHNMe$_2$).[134]

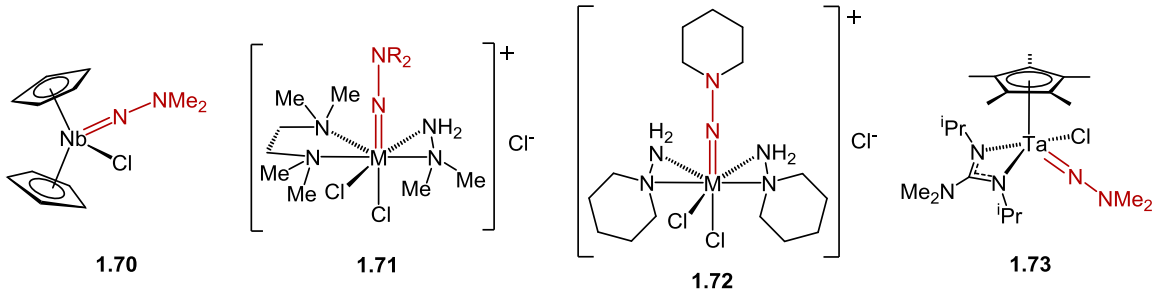
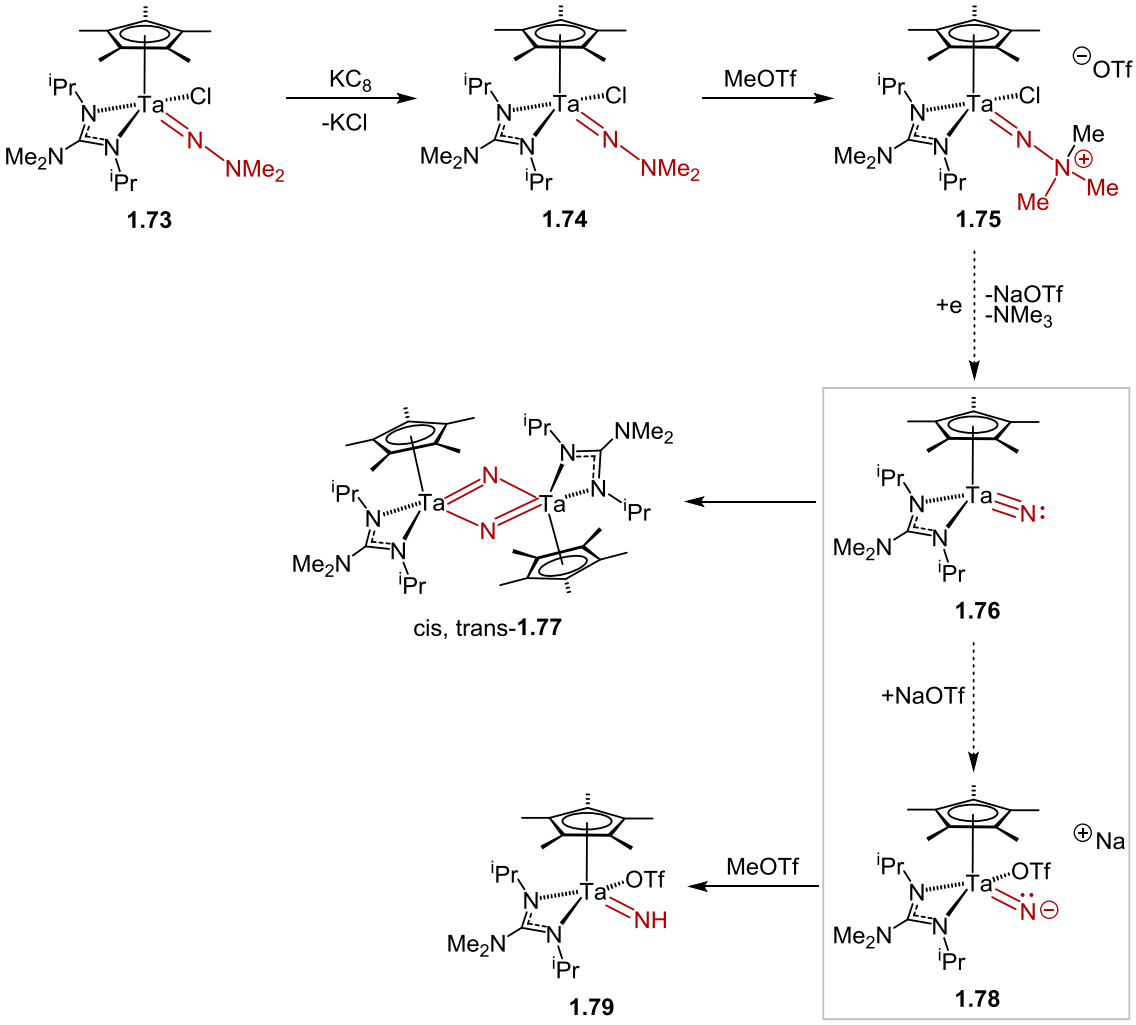


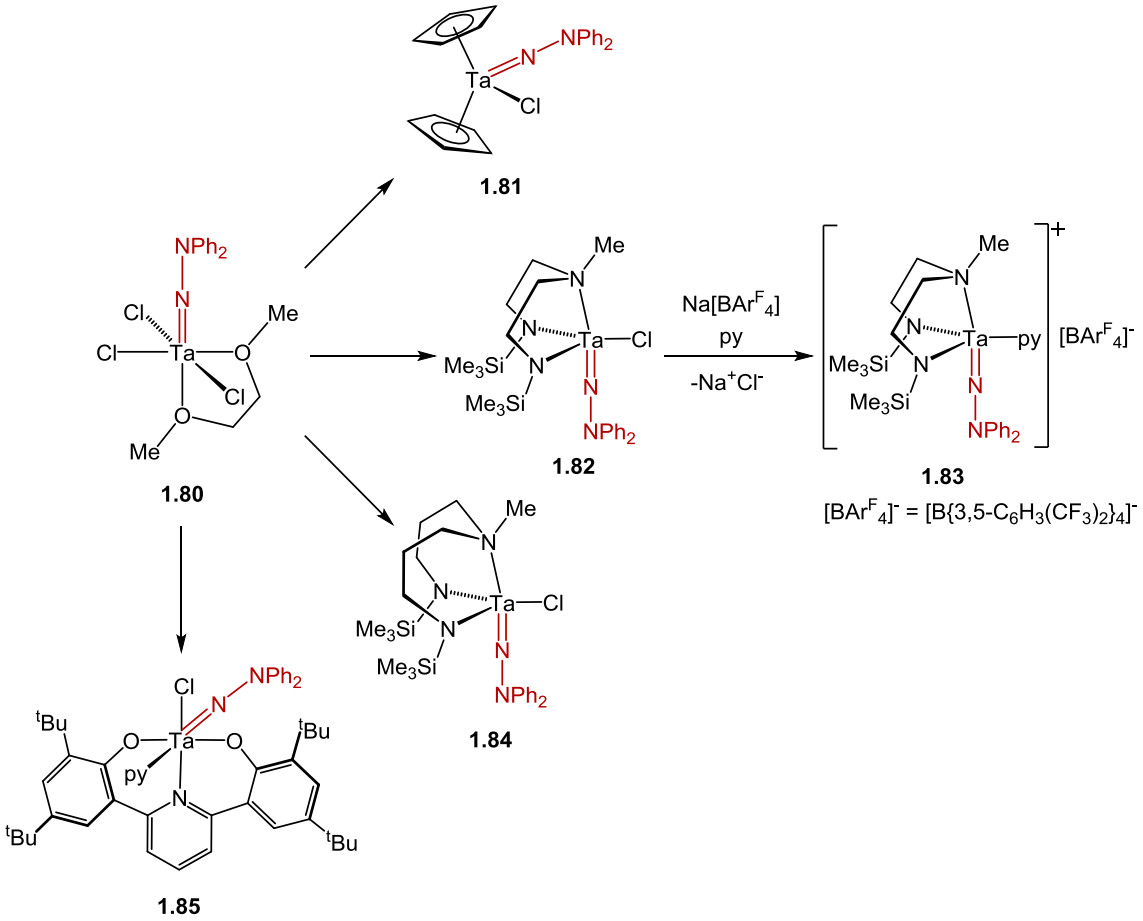
Figure 1.7. Examples of tantalum hydrazido(2-) complexes. [37,39,134]

Moreover, complex **1.73** was reduced to the Ta(IV) hydrazido complex Cp*Ta{N(^{i}Pr)C(NMe$_2$)N(^{i}Pr)}(NNMe$_2$) (**1.74**, Scheme 1.13) with KC$_8$ in THF at -30 ˚C, which was confirmed by X-ray crystallography.[134] This complex proved to be unstable in solution at RT over the course of 3 h, giving a 1:1 mixture of the hydrazido hydride complex and a product from the C-H activation of a Cp* methyl group. Unexpectedly, the hydrazido complex **1.74** was inert to H_2, H_3SiPh and CO.[134] However, the hydrazido complexes **1.73** and **1.74** undergo alkylation at the N_β with MeOTf giving complexes [Cp*Ta{N(^{i}Pr)C(NMe$_2$)N(^{i}Pr)}(NNMe3)(Cl)][OTf] and [Cp*Ta{N(^{i}Pr)C(NMe$_2$)N(^{i}Pr)}(NNMe$_3$)][OTf] (**1.75**, Scheme 1.13). Reductive cleavage of the N_α–N_β bond of complex **1.75** was achieved on reaction with Na/Hg leading to the formation of either the nitrido complex [Cp*Ta{N(^{i}Pr)C(NMe$_2$)N(^{i}Pr)}(μ-N)]$_2$ (**1.77**) or the parent imido compound Cp*Ta{N(^{i}Pr)C(NMe$_2$)N(^{i}Pr)}(NH)(OTf) (**1.79**) depending of the reaction conditions. It is suggested that **1.77** is formed from the transient nitride species **1.76** followed by dimerization, while protonation of the imide anion (**1.78**) forms the imide complex **1.79** (Scheme 1.13).[134] These systems were the subject of a full mechanistic study by Lu and Wang.[135]



Scheme 1.13. Derivative complexes from Cp*Ta{N(^{i}Pr)C(NMe$_2$)N(^{i}Pr)}(NNMe$_2$)Cl (**1.73**).[134]

Other tantalum hydrazido complexes with a strongly-bonded chloride ligand (instead of the labile pyridine ligand observed in the Group 4 analogues) have been reported by Bercaw and co-workers using the hydrazido synthon Ta(NNPh$_2$)Cl$_3$(DME) (**1.80,** DME = dimethoxyethane, Scheme 1.14). Salt metathesis reactions of complex **1.80** with lithiated mono- and dianionic ligands gave, for example, the tantalocene Cp$_2$TaCl(NNPh$_2$) (**1.81**), the tantalum bis(amide)amine-supported Ta(N$_2$N^{SiMe3})(NNPh$_2$)Cl (**1.82**), the propylene-supported Ta{MeN((CH$_2$)$_3$NSiMe$_3$)$_2$}(NNPh$_2$) (**1.84**) and the aryl-linked bis(phenolate) complex Ta(ONO)(NNPh$_2$)Cl(py) (**1.85**, ONO = 2,6-(OC$_6$H$_2$-^{t}Bu$_2$)$_2$-C$_5$H$_3$N)) (Scheme 1.14).[40]



Scheme 1.14. Examples of various tantalum hydrazido complexes synthesised from $Ta(NNPh_2)Cl_3(DME)$ (**1.80**).[40]

Additionally, when the bis(amide)amine complex $Ta(NNPh_2)Cl(N_2N^{Me})$ (**1.82**) was treated with $Na[BAr^F_4]$ ($[BAr^F_4]^- = [B\{3,5\text{-}C_6H_3(CF_3)_2\}_4]^-$) in the presence of pyridine, the cationic chloride-abstracted product $[Ta(NNPh_2)(N_2N^{Me})(py)](BAr^F_4)$ (**1.83**) was generated (Scheme 1.14).[40] Finally, all these complexes showed negligible reactivity in contrast to their Group 4 counterparts, which have exhibited a wide variety of reactions with unsaturated small molecules. Surprisingly, even complex **1.83** was unreactive upon attempts of pyridine substitution and [2+2] reactions with terminal and internal alkynes.[40]

1.5 Summary and objectives

This Chapter has provided a general introduction to tridentate pincer and tripodal ligands, and the chemistry of Group 4 and 5 imido and hydrazido complexes. In general, the chemistry of Group 5 hydrazido compounds is less diverse than the Group 4 counterpart and complexes with mono- and dianionic supporting ligands have shown low reactivity with unsaturated and other small molecules.

The overall aim of these Thesis is to access neutral Group 5 hydrazido complexes with trianionic, tridentate ligands, based on the premise that replacement of the chloride ligand by a labile Lewis-bases will allow the synthesis of reactive $Ta(N_3)(NNPh_2)(L)_x$ species (N_3 = a trianionic, tridentate ligand, L = Lewis base, x = 0 or 1). Furthermore, reactivity studies with unsaturated and other small molecules are targeted.

1.7 References

1. J. Chatt, J. R. Dilworth and R. L. Richards, *Chem. Rev.*, 1978, **78**, 589-625.
2. M. Hidai, *Coord. Chem. Rev.*, 1999, **185-186**, 99-108.
3. R. R. Schrock, *Angew. Chem., Int. Ed.*, 2008, **47**, 5512-5522.
4. H.-P. Jia and E. A. Quadrelli, *Chem. Soc. Rev.*, 2014, **43**, 547-564.
5. R. J. Burford and M. D. Fryzuk, *Nat, Rev. Chem.*, 2017, **1**, 0026.
6. N. Stucke, B. M. Flöser, T. Weyrich and F. Tuczek, *J. Eur. Inorg. Chem.*, 2018, **2018**, 1337-1355.
7. C. H. Winter, P. H. Sheridan, T. S. Lewkebandara, M. J. Heeg and J. W. Proscia, *J. Am. Chem. Soc.*, 1992, **114**, 1095-1097.
8. T. S. Lewkebandara, P. H. Sheridan, M. J. Heeg, A. L. Rheingold and C. H. Winter, *Inorg. Chem.*, 1994, **33**, 5879-5889.
9. J. B. Cross, S. M. Smith and H. B. Schlegel, *Chem. Mater.*, 2001, **13**, 1095-1100.
10. C. J. Carmalt, A. C. Newport, S. A. O'Neill, I. P. Parkin, A. J. P. White and D. J. Williams, *Inorg. Chem.*, 2005, **44**, 615-619.
11. S. D. Cosham, A. L. Johnson, K. C. Molloy and A. J. Kingsley, *Inorg. Chem.*, 2011, **50**, 12053-12063.
12. P. D. Bolton and P. Mountford, *Adv. Synth. Catal.*, 2005, **347**, 355-366.
13. R. A. Collins, A. F. Russell and P. Mountford, *Appl. Petrochem. Res.*, 2015, **5**, 153-171.
14. R. A. Collins, A. F. Russell, R. T. W. Scott, R. Bernardo, G. H. J. van Doremaele, A. Berthoud and P. Mountford, *Organometallics*, 2017, **36**, 2167-2181.
15. Z.-Q. Zhang, J.-T. Qu, S. Zhang, Q.-P. Miao and Y.-X. Wu, *Polym. Chem.*, 2018, **9**, 48-59.
16. S. Banerjee, Y. Shi, C. Cao and A. L. Odom, *J. Organomet. Chem.*, 2005, **690**, 5066-5077.
17. S. Banerjee and A. L. Odom, *Organometallics*, 2006, **25**, 3099-3101.

18. K. Weitershaus, H. Wadepohl and L. H. Gade, *Organometallics*, 2009, **28**, 3381–3389.
19. A. D. Schofield, A. Nova, J. D. Selby, C. D. Manley, A. D. Schwarz, E. Clot and P. Mountford, *J. Am. Chem. Soc.*, 2010, **132**, 10484-10497.
20. A. A. Dissanayake and A. L. Odom, *Chem. Commun.*, 2012, **48**, 440-442.
21. J. D. Selby, C. D. Manley, M. Feliz, A. D. Schwarz, E. Clot and P. Mountford, *Chem. Commun.*, 2007, 4937-4939.
22. A. J. Clulow, J. D. Selby, M. G. Cushion, A. D. Schwarz and P. Mountford, *Inorg. Chem.*, 2008, **47**, 12049-12062.
23. A. D. Schofield, A. Nova, J. D. Selby, A. D. Schwarz, E. Clot and P. Mountford, *Chem. Eur. J.*, 2011, **17**, 265-285.
24. J. D. Selby, M. Feliz, A. D. Schwarz, E. Clot and P. Mountford, *Organometallics*, 2011, **30**, 2295-2307.
25. P. J. Tiong, A. Nova, L. R. Groom, A. D. Schwarz, J. D. Selby, A. D. Schofield, E. Clot and P. Mountford, *Organometallics*, 2011, **30**, 1182-1201.
26. P. J. Tiong, A. Nova, A. D. Schwarz, J. D. Selby, E. Clot and P. Mountford, *Dalton Trans.*, 2012, **41**, 2277-2288.
27. J. Unruangsri, H. Morgan, A. D. Schwarz, A. D. Schofield and P. Mountford, *Organometallics*, 2013, **32**, 3091-3107.
28. L. C. Stevenson, S. Mellino, E. Clot and P. Mountford, *J. Am. Chem. Soc.*, 2015, **137**, 10140-10143.
29. S. Mellino, L. C. Stevenson, E. Clot and P. Mountford, *Organometallics*, 2017, **36**, 3329-3342.
30. M. Veith, *Angew. Chem., Int. Edit.*, 1976, **15**, 387-388.
31. S. C. Davies, D. L. Hughes, Z. Janas, L. Jerzykiewicz, R. L. Richards, J. Roger Sanders and P. Sobota, *Chem. Commun.*, 1997, 1261-1262.
32. S. C. Davies, D. L. Hughes, Z. Janas, L. B. Jerzykiewicz, R. L. Richards, J. R. Sanders, J. E. Silverston and P. Sobota, *Inorg. Chem.*, 2000, **39**, 3485-3498.
33. J. Bultitude, L. F. Larkworthy, D. C. Povey, G. W. Smith, J. R. Dilworth and G. J. Leigh, *J. Chem. Soc., Chem. Commun.*, 1986, 1748-1750.
34. A. A. Danopoulos, R. S. Hay-Motherwell, G. Wilkinson, T. K. N. Sweet and M. B. Hursthouse, *Polyhedron*, 1997, **16**, 1081-1088.
35. S. Banerjee and A. L. Odom, *Dalton Trans.*, 2008, 2005-2008.

36. T. Moriuchi, K. Ikeuchi and T. Hirao, *Dalton Trans.*, 2013, **42**, 11824-11830.
37. M. L. H. Green, J. T. James and A. N. Chernega, *J. Chem. Soc., Dalton Trans.*, 1997, 1719-1726.
38. M. L. H. Green, J. T. James, J. F. Saunders and J. Souter, *J. Chem. Soc., Dalton Trans.*, 1997, 1281-1288.
39. E. Sebe, M. J. Heeg and C. H. Winter, *Polyhedron*, 2006, **25**, 2109-2118.
40. I. A. Tonks and J. E. Bercaw, *Inorg. Chem.*, 2010, **49**, 4648-4656.
41. I. A. Tonks, A. C. Durrell, H. B. Gray and J. E. Bercaw, *J. Am. Chem. Soc.*, 2012, **134**, 7301-7304.
42. G. van Koten, K. Timmer, J. G. Noltes and A. L. Spek, *J. Chem. Soc., Chem. Commun.*, 1978, 250-252.
43. C. J. Moulton and B. L. Shaw, *J. Chem. Soc., Dalton Trans.*, 1976, 1020-1024.
44. M. E. O'Reilly and A. S. Veige, *Chem. Soc. Rev.*, 2014, **43**, 6325-6369.
45. E. Peris and R. H. Crabtree, *Chem. Soc. Rev.*, 2018, **47**, 1959-1968.
46. J. S. Freundlich, R. R. Schrock and W. M. Davis, *Organometallics*, 1996, **15**, 2777-2783.
47. J. S. Freundlich, R. R. Schrock and W. M. Davis, 1996, **118**, 3643-3655.
48. R. R. Schrock and P. Meakin, *J. Am. Chem. Soc.*, 1974, **96**, 5288-5290.
49. R. R. Schrock, J. Lee, L.-C. Liang and W. M. Davis, *Inorg. Chim. Acta*, 1998, **270**, 353-362.
50. J. Koller, S. Sarkar, K. A. Abboud and A. S. Veige, *Organometallics*, 2007, **26**, 5438-5441.
51. A. Cooper, M. Chem. Thesis, University of Oxford, 2014.
52. L. H. Gade and N. Mahr, *J. Chem. Soc. Dalton Trans.*, 1993, **4**, 489-494.
53. A. F. Clifford and C. S. Kobayashi, presented in part at the 130th National Meeting of the American Chemical Society, Atlantic City, N. J., Sept., 1956.
54. A. F. Clifford, C. S. Kobayashi, J. Wuller and T. Moeller, in *Inorganic Syntheses*, ed. E. G. R. (Ed.), 2007, vol. 6, p. 204.
55. T. R. Cundari, *J. Am. Chem. Soc.*, 1992, **114**, 7879-7888.
56. B. A. Clough, D.Phil. Thesis, University of Oxford, 2017.
57. A. A. Danopoulos, G. Wilkinson, T. Sweet and M. B. Hursthouse, *J. Chem. Soc., Chem. Commun.*, 1993, 495-496.

58. G. Parkin, A. Van Asselt, D. J. Leahy, L. Whinnery, N. G. Hua, R. W. Quan, L. M. Henling, W. P. Schaefer, B. D. Santarsiero and J. E. Bercaw, *Inorg. Chem.*, 1992, **31**, 82-85.
59. K. A. Jørgensen, *Inorg. Chem.*, 1993, **32**, 1521-1522.
60. D. C. Bradley and I. M. Thomas, *J. Chem. Soc.*, 1960, 3857-3861.
61. D. C. Bradley and E. G. Torrible, *Can. J. Chem.*, 1963, **41**, 134-138.
62. P. J. Walsh, F. J. Hollander and R. G. Bergman, *J. Am. Chem. Soc.*, 1988, **110**, 8729-8731.
63. M. E. G. Skinner, T. Toupance, D. A. Cowhig, B. R. Tyrrell and P. Mountford, *Organometallics*, 2005, **24**, 5586-5603.
64. S. C. Dunn, A. S. Batsanov and P. Mountford, *J. Chem. Soc., Chem. Comm.*, 1994, 2007-2008.
65. A. J. Blake, P. E. Collier, S. C. Dunn, W.-S. Li, P. Mountford and O. V. Shishkin, *J. Chem. Soc., Dalton Trans.*, 1997, 1549-1558.
66. D. J. Arney, M. A. Bruck, S. R. Huber and D. E. Wigley, *Inorg. Chem.*, 1992, **31**, 3749-3755.
67. S. R. Dubberley, S. Evans, C. L. Boyd and P. Mountford, *Dalton Trans.*, 2005, 1448-1458.
68. P. E. Collier, S. C. Dunn, P. Mountford, O. V. Shishkin and D. Swallow, *J. Chem. Soc., Dalton Trans.*, 1995, 3743-3745.
69. P. Mountford, *Chem. Comm.*, 1997, 2127-2134.
70. N. Hazari and P. Mountford, *Acc. Chem. Res.*, 2005, **38**, 839-849.
71. P. E. Collier, S. M. Pugh, H. S. C. Clark, J. B. Love, A. J. Blake, F. G. N. Cloke and P. Mountford, *Inorg. Chem.*, 2000, **39**, 2001-2005.
72. A. J. Blake, P. E. Collier, L. H. Gade, P. Mountford, J. Lloyd, S. M. Pugh, M. Schubart, M. E. G. Skinner and D. J. M. Trösch, *Inorg. Chem.*, 2001, **40**, 870-877.
73. A. J. Blake, P. E. Collier, L. H. Gade, M. McPartlin, P. Mountford, M. Schubart and I. J. Scowen, *Chem. Commun.*, 1997, 1555-1556.
74. A. P. Duncan and R. G. Bergman, *Chem. Record*, 2002, **2**, 431-445.
75. S. A. Blum, V. A. Rivera, R. T. Ruck, F. E. Michael and R. G. Bergman, *Organometallics*, 2005, **24**, 1647-1659.

76. A. Bashall, P. E. Collier, L. H. Gade, M. McPartlin, P. Mountford, S. M. Pugh, S. Radojevic, M. Schubart, I. J. Scowen and D. J. M. Trösch, *Organometallics*, 2000, **19**, 4784-4794.
77. L. H. Gade and P. Mountford, *Coord. Chem. Rev.*, 2001, **216-217**, 68-97.
78. B. D. Ward, A. Maisse-Francois, P. Mountford and L. H. Gade, *Chem. Commun.*, 2004, 704-705.
79. K. E. Meyer, P. J. Walsh and R. G. Bergman, *J. Am. Chem. Soc.*, 1995, **117**, 974-985.
80. S. A. Blum, P. J. Walsh and R. G. Bergman, *J. Am. Chem. Soc.*, 2003, **125**, 14276-14277.
81. D. J. M. Trösch, P. E. Collier, A. Bashall, L. H. Gade, M. McPartlin, P. Mountford and S. Radojevic, *Organometallics*, 2001, **20**, 3308-3313.
82. A. Bashall, M. McPartlin, P. E. Collier, P. Mountford, L. H. Gade and D. J. M. Trösch, *Chem. Commun.*, 1998, 2555-2556.
83. S. M. Pugh, D. J. M. Trösch, D. J. Wilson, A. Bashall, F. G. N. Cloke, L. H. Gade, P. B. Hitchcock, M. McPartlin, J. F. Nixon and P. Mountford, *Organometallics*, 2000, **19**, 3205-3210.
84. D. Swallow, J. M. McInnes and P. Mountford, *J. Chem. Soc., Dalton Trans.*, 1998, 2253-2260.
85. S. R. Dubberley, A. Friedrich, D. A. Willman, P. Mountford and U. Radius, *Chem. Eur. J.*, 2003, **9**, 3634-3654.
86. C. L. Boyd, T. Toupance, B. R. Tyrrell, B. D. Ward, C. R. Wilson, A. R. Cowley and P. Mountford, *Organometallics*, 2005, **24**, 309-330.
87. A. E. Guiducci, A. R. Cowley, M. E. G. Skinner and P. Mountford, *J. Chem. Soc., Dalton Trans.*, 2001, 1392-1394.
88. A. E. Guiducci, C. L. Boyd and P. Mountford, *Organometallics*, 2006, **25**, 1167-1187.
89. D. C. Bradley and I. M. Thomas, *Can. J. Chem.*, 1962, **40**, 1355-1360.
90. W. A. Nugent and R. L. Harlow, *J. Chem. Soc., Chem. Commun.*, 1978, 579-580.
91. R. E. Blake, D. M. Antonelli, L. M. Henling, W. P. Schaefer, K. I. Hardcastle and J. E. Bercaw, *Organometallics*, 1998, **17**, 718-725.

92. M. J. Humphries, M. L. H. Green, M. A. Leech, V. C. Gibson, M. Jolly, D. N. Williams, M. R. J. Elsegood and W. Clegg, *J. Chem. Soc., Dalton Trans.*, 2000, 4044-4051.
93. T. C. Jones, A. J. Nielson and C. E. F. Rickard, *J. Chem. Soc., Chem. Commun.*, 1984, 205-206.
94. P. A. Bates, A. J. Nielson and J. M. Waters, *Polyhedron*, 1985, **4**, 1391-1401.
95. B. L. Yonke, A. J. Keane, P. Y. Zavalij and L. R. Sita, *Organometallics*, 2012, **31**, 345-355.
96. A. Merkoulov, S. Schmidt, K. Harms and J. Sundermeyer, *Z. Anorg. Allg. Chem.*, 2005, **631**, 1810-1812.
97. T. R. Helgert, C. E. Webster, T. K. Hollis, H. U. Valle, P. Hillesheim and A. G. Oliver, *Inorg. Chem. Acta*, 2018, **469**, 164-172.
98. D. M. Antonelli, W. P. Schaefer, G. Parkin and J. E. Bercaw, *J. Organomet. Chem.*, 1993, **462**, 213-220.
99. C. M. Jones, M. E. Lerchen, C. J. Church, B. M. Schomber and N. M. Doherty, *Inorg. Chem.*, 1990, **29**, 1679-1682.
100. H.-T. Chiu, S.-H. Chuang, C.-E. Tsai, G.-H. Lee and S.-M. Peng, *Polyhedron*, 1998, **17**, 2187-2190.
101. M. Galajov, C. Garcia and M. Gomez, *Dalton Trans.*, 2011, **40**, 413-420.
102. M. Gómez, C. Hernández-Prieto, A. Martín, M. Mena and C. Santamaría, *Inorg. Chem.*, 2016, **55**, 3815-3821.
103. J. Sundermeyer, J. Putterlik, M. Fotha, J. S. Fieldb and N. Ramesar, *Chem. Ber.*, 1994, **127**, 1201-1212.
104. F. Preuss, E. Fuchslocher, E. Leber and W. Towae, *Z. Naturforsch. B*, 1989, **44b**, 271—277.
105. Y. W. Chao, P. A. Wexler and D. E. Wigley, *Inorg. Chem.*, 1989, **28**, 3860-3868.
106. D. D. Devore, J. D. Lichtenhan, F. Takusagawa and E. A. Maatta, *J. Am. Chem. Soc.*, 1987, **109**, 7408-7416.
107. S. M. Rocklage and R. R. Schrock, *J. Am. Chem. Soc.*, 1980, **102**, 7808-7809.
108. S. M. Rocklage and R. R. Schrock, *J. Am. Chem. Soc.*, 1982, **104**, 3077-3081.
109. A. J. Nielson, *Polyhedron*, 1988, **7**, 67-75.
110. F. Preuss and W. Towae, *Z. Naturforsch. B*, 1981, **86b**, 1130-1135.

111. F. A. Cotton and G. Wilkinson, *Advanced Inorganic Chemistry*, Wiley-Interscience, U.S.A., 4th edn., 1980, pp. 717-718, 831-844.

112. S. M. Pugh, A. J. Blake, L. H. Gade and P. Mountford, *Inorg. Chem.*, 2001, **40**, 3992-4001.

113. I. A. Tonks, L. M. Henling, M. W. Day and J. E. Bercaw, *Inorg. Chem.*, 2009, **48**, 5096-5105.

114. R. R. Schrock and P. R. Sharp, *J. Am. Chem. Soc.*, 1978, **100**, 2389-2399.

115. A. I. Nguyen, K. J. Blackmore, S. M. Carter, R. A. Zarkesh and A. F. Heyduk, *J. Am. Chem. Soc.*, 2009, **131**, 3307-3316.

116. A. F. Heyduk, R. A. Zarkesh and A. I. Nguyen, *Inorg. Chem.*, 2011, **50**, 9849-9863.

117. M. W. Bishop, J. Chatt, J. R. Dilworth, M. B. Hursthouse and M. Motevalle, *J. Less Common Met.* , 1977, **54**, 487-493.

118. J. Chatt, B. A. L. Crichton, J. R. Dilworth, P. Dahlstrom, R. Gutkoska and J. A. Zubieta, *Transition Met. Chem.* , 1979, **4**, 271-272.

119. J. Chatt, J. R. Dilworth, P. L. Dahlstrom and J. Zubieta, *J. Chem. Soc., Chem. Commun.*, 1980, 786-787.

120. Y. Li, Y. Shi and A. L. Odom, *J. Am. Chem. Soc.*, 2004, **126**, 1794-1803.

121. N. Wiberg, H.-W. Häring, G. Huttner and P. Friedrich, *Chem. Ber.*, 1978, **111**, 2708-2715.

122. P. J. Walsh, M. J. Carney and R. G. Bergman, *J. Am. Chem. Soc.*, 1991, **113**, 6343-6345.

123. J. D. Selby, C. D. Manley, A. D. Schwarz, E. Clot and P. Mountford, *Organometallics*, 2008, **27**, 6479-6494.

124. A. J. Blake, J. M. McInnes, P. Mountford, G. I. Nikonov, D. Swallow and D. J. Watkin, *J. Chem. Soc., Dalton Trans.*, 1999, 379-392.

125. J. D. Selby, C. Schulten, A. D. Schwarz, A. Stasch, E. Clot, C. Jones and P. Mountford, *Chem. Commun.*, 2008, 5101-5103.

126. K. Weitershaus, J. Lloret Fillol, H. Wadepohl and L. H. Gade, *Organometallics*, 2009, **28**, 4747-4757.

127. T. Gehrmann, G. T. Plundrich, H. Wadepohl and L. H. Gade, *Organometallics*, 2012, **31**, 3346-3354.

128. H. Herrmann, J. Lloret Fillol, T. Gehrmann, M. Enders, H. Wadepohl and L. H. Gade, *Chem. Eur. J.*, 2008, **14**, 8131-8146.
129. H. Herrmann, J. Lloret Fillol, H. Wadepohl and L. H. Gade, *Angew. Chem. Int. Ed.*, 2007, **46**, 8426-8430.
130. T. Gehrmann, J. Lloret Fillol, H. Herrmann, H. Wadepohl and L. H. Gade, *Organometallics*, 2013, **32**, 3877-3889.
131. G. Thorsten, S. S. A., F. J. Lloret, W. Hubert and G. L. H., *Chem. Eur. J.*, 2012, **18**, 3925-3941.
132. D. J. Mindiola, *Angew. Chem., Int. Ed.*, 2008, **47**, 1557-1559.
133. B. A. Clough, S. Mellino, A. V. Protchenko, M. Slusarczyk, L. C. Stevenson, M. P. Blake, B. Xie, E. Clot and P. Mountford, *Inorg. Chem.*, 2017, **56**, 10794-10814.
134. A. J. Keane, P. Y. Zavalij and L. R. Sita, *J. Am. Chem. Soc.*, 2013, **135**, 9580-9583.
135. N. Lu and H. Wang, *J. Struct. Chem.*, 2016, **57**, 47-53.

Chapter Two

Routes towards the synthesis of tantalum hydrazido complexes with tridentate, trianionic ligands: synthesis, structure and bonding of dialkyl, bis(amido) and alkyl-amido precursors

2.1 Overview

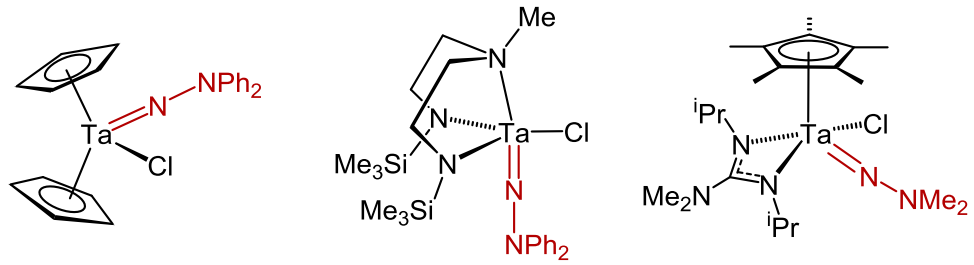
This chapter will describe three different synthetic routes towards tantalum hydrazido complexes with tridentate, trianionic ligands. Firstly, the synthesis and characterisation of the lithium salts of two new tridentate, trianionic pincer ligands, $Li_3(NN_2^{Me})$ (**1**) and $Li_3(NN_2^{iPr})$ (**2**), will be presented. Additionally, the synthesis of the precursor dichloride species $Ta(NN_2^{SiMe3})Cl_2$ (**3**), which is used as a starting material for two of the synthetic routes, will also be described. Subsequently, the three synthetic routes towards the synthesis of tantalum hydrazido complexes with these ligands will be studied. Route A: *via* bis(amido) and dimethyl precursors with $Li_3(NN_2^{SiMe3})$ (**1.1**) or in a one-step synthesis by reacting the dichloride species **3** with hydrazines or their lithiated salts. Route B: *via* the tantalum hydrazide precursor, $Ta(NNPh_2)Cl_3(DME)$ (**1.80**), in a salt metathesis reaction with $Li_3(NNN^R)$ (R = ^{i}Pr (**1.8**) or $SiMe_3$ (**1.9**)). Route C is a multistep route *via* dialkyl precursors with the NN_2^{SiMe3} ligand. Subsequently, the reaction of alkyl-amido $Ta(NN_2^{SiMe3})(NH^tBu)R$ complexes with Lewis bases towards the formation of the Ta=N multiple bond will be explored. DFT calculations will also be presented giving a bonding analysis of dialkyl and alkyl-amido model systems.

2.2 Introduction

As discussed in Chapter One of this Thesis, the chemistry of metal-nitrogen bonds is an ongoing area of extensive interest, wherein the study of hydrazido complexes of Group 4 and 6 metals are well established and various applications have been reported, such as catalytic reduction of dinitrogen, MOCVD (Metal-organic Chemical Vapour Deposition) and olefin polymerisation.[1-30] One particular area of interest within our research group has been the synthesis of titanium hydrazides of the type $(L)Ti{=}NNR_2$ (R = alkyl, aryl; L = ancillary ligand set), which can formally be described as a metal-nitrogen triple bond ($\sigma^2\pi^4$), with a wide variety of auxiliary ligand sets. More recently, the reactivity of these complexes has been explored and a range of reactions with unsaturated substrates was found.[2-5,7-11,31]

Interesting chemistry of Group 4 hydrazido chemistry has been developed for compounds of the type $Ti(N_2N^{Me})(NNPh_2)(py)$ (N_2N^{Me} = $MeN(CH_2CH_2NSiMe_3)_2$) [31] and their analogues with other dianionic N_3-donor ligands and/or with zirconium or hafnium.[1,2,8,17] In these cases dissociation of pyridine forms a reactive $Ti(N_2N^{Me})(NNPh_2)$ intermediate which undergoes cycloaddition reactions, for example with internal alkynes.[11] Group 5

counterparts with strongly-bonded chloride ligand instead of the labile pyridine ligand have been recently reported by Bercaw *et al.* and Sita *et al.* (Figure 2.1). The first example of that kind ($Cp_2TaCl(NNPh_2)$ (**1.81**)) was produced through the reaction of $Ta(NNPh_2)Cl_3(DME)$ (**1.80**, DME = dimethoxyethane) and 2 equiv. of NaCp. A second example was prepared through reaction of the same precursor material (**1.80**) with $Li_2\{MeN((CH_2)_2NSiMe_3)\}_2$, producing the corresponding bis(amide)amine complex, $Ta(N_2N^{Me})(NNPh_2)Cl$ (**1.82**).[32] A third example, was prepared through the reaction of $Cp^*Ta\{N(^iPr)C(NMe_2)N(^iPr)\}Cl_3$ with 2 equiv. of lithium 1,1-dimethylhydrazide ($LiNHNMe_2$) yielding the complex $Cp^*Ta\{N(^iPr)C(NMe_2)N(^iPr)\}(NNMe_2)(Cl)$ (**1.73**).[33]

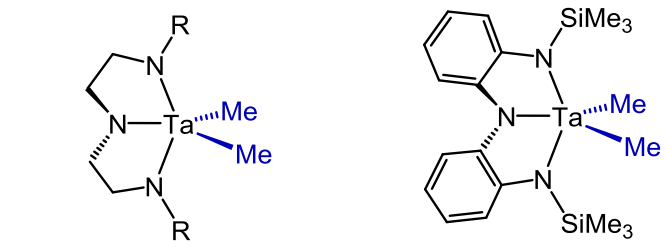


1.81 **1.82** **1.73**

Figure 2.1. Examples of tantalum hydrazido(2-) complexes.[32,33]

These complexes showed negligible reactivity in contrast to their Group 4 counterparts. For this reason, analogous Group 5 complexes with trianionic, N_3-donor pincer ligands in place of the dianionic N_2N^R type were targeted in this work. Following this, the displacement of the chloride ligand for labile Lewis-bases will allow access to reactive $Ta(N_3)(NNPh_2)(L)_x$ species (N_3 = a trianionic, tridentate ligand, L = Lewis base, x = 0 or 1).

The electronic stabilization provided by the anionic charge of the tridentate pincer ligand makes these well-suited to study with high-valent metal ions (M^{n+}; $n \geq 3$).[34] Several $H_3(NNN)$ trianionic ligands have been metalated using $TaMe_5$[35] to give, for example, $Ta\{(Me_3SiNCH_2CH_2)_2N\}Me_2$ (**1.3**), the relatively unstable $Ta\{(C_6F_5NCH_2CH_2)_2NH\}Me_3$, which evolves one equiv. of methane to give $Ta\{N_3(C_6F_5)\}Me_2$ (**1.4**), and $Ta\{(Me_3SiN\text{-}o\text{-}C_6H_4)_2N\}Me_2$ (**1.5**) (Figure 2.2).[36]



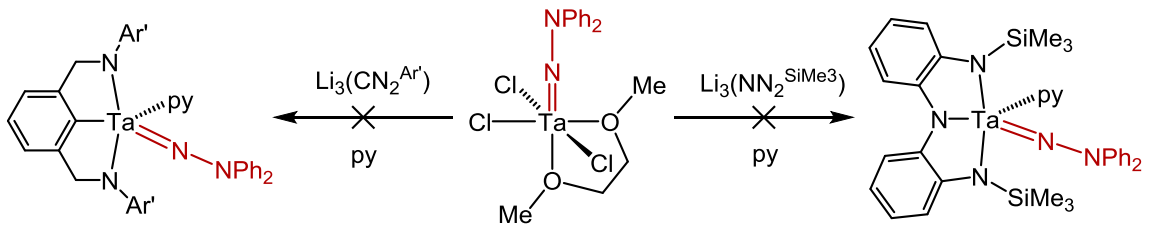
R = $SiMe_3$ (**1.3**) or C_6F_5 (**1.4**) **1.5**

Figure 2.2. Dimethyl tantalum complexes with tridentate, trianionic ligands.[36]

In this Chapter, the synthesis of two new lithiated tridentate, trianionic ligands $Li_3(NN_2^{Me})$ (**1**) and $Li_3(NN_2^{iPr})$ (**2**), and the dichloride tantalum precursor $Ta(NN_2^{SiMe3})Cl_2$ (**3**) will be described and used latter as starting material for two out of three routes towards the synthesis of tantalum hydrazido complexes. **3** can also be used to access bis(amido), dialkyl and alkyl-amido compounds. The synthesis and characterisation of all these compounds will be presented and discussed.

2.3 Selection and synthesis of tridentate, trianionic pincer ligands

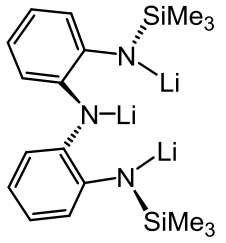
Lithiation of 1,3-$C_6H_4(CH_2N^{Ar'})_2$ ($H_3CN_2^{Ar'}$, Ar' = 2,6-$C_6H_3{}^iPr_2$) with 3.5 equiv. of methyllithium was successfully achieved yielding the trilithiated salt $Li_3(CN_2^{Ar'})$ (**1.6**).[34,37,38] Similarly, the reaction of $H_3\{N(SiMe_3N\text{-}o\text{-}C_6H_4)_2\}$ with 3.5 equiv. of *n*-butyllithium produced $Li_3(NN_2^{SiMe3})$ (**1.7**).[39] Reactions of both lithiated ligands were attempted with the synthon **1.80**[32] to give the corresponding hydrazide as shown in Scheme 2.1. However, this route was found to be unsuccessful as complex mixtures were formed under various conditions.



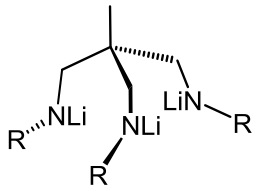
1.80

Scheme 2.1. Attempted synthesis of tantalum hydrazide complexes with $Li_3(CN_2^{Ar'})$ (**1.6**) (Ar' = 2,6-$C_6H_3{}^iPr_2$) and $Li_3(NN_2^{SiMe3})$ (**1.7**) pincer ligands.[32,36,38]

Inspired by Schrock and co-workers' research on tantalum dimethyl complexes such as $Ta\{(Me_3SiN\text{-}o\text{-}C_6H_4)_2N\}Me_2$ (**1.5**)[36], the investigation of this more robust ligand $Li_3(NN_2^{SiMe3})$ (**1.7**)[39] (Figure 2.3, left) was continued. Also one more ligand was included in these studies, the lithiated face-capping ligand $Li_3(NNN^R)$ (R = ^{i}Pr (**1.8**) or $SiMe_3$ (**1.9**)) obtained by reaction of $MeC(CH_2NHR)_3$ (Figure 2.3, right).with 3 equiv. of *n*-butyllithium which was introduced by Gade in 1993.[40,41]



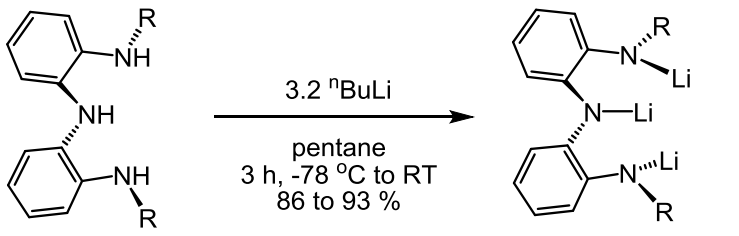
1.7



R = ^{i}Pr (**1.8**) or $SiMe_3$ (**1.9**)

Figure 2.3. Selected tridentate pincer ligands.[36,39-42]

Lithiation of the bis(2-methylaminophenyl)amine ($H_3NN_2^{Me}$) and the analogous bis(2-isopropylaminophenyl)amine ($H_3NN_2^{iPr}$)[42] were carried out in pentane under cold conditions (-78 ˚C) adding 3.2 equiv. of ^{n}BuLi. The pure products $Li_3(NN_2^{Me})$ (**1**) and $Li_3NN_2^{iPr}$ (**2**) were isolated after several extractions with pentane (Equation 2.1). The ^{1}H NMR spectra display resonances for C_{2v} symmetric species on the NMR timescale in solution although the solid state structures are likely to be more complex. The resonances attributed to the four aromatic proton environments can be observed as two doublets and two triplets (overlapping in case of **1**), along with a broad singlet at 2.59 ppm corresponding to the methyl groups in the case of **1,** and a septet and a doublet (3.08 and 0.76 ppm, respectively) for the isopropyl methine and the homotopic isopropyl methyl groups in **2**.

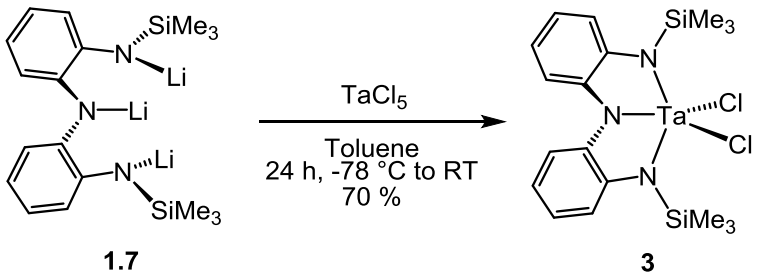


R = Me (**1**) or iPr (**2**)

Equation 2.1.

2.4 Synthesis of $Ta(NN_2^{SiMe3})Cl_2$ (3)

After the unsuccessful reaction of the hydrazide synthon **1.2** with the lithiated ligand **1.7** (Scheme 2.1), an alternative strategy focussed on the corresponding dichloride complex $Ta(NN_2^{SiMe3})Cl_2$ (**3**). Salt metathesis reaction of $TaCl_5$ with the trilithiated ligand **1.7** produced dichloride complex **3** (Equation 2.2). The product was obtained in high yield after several diethyl ether extractions. The ^1H (Figure 2.4) and ^{13}C NMR spectra of **3** indicate a C_{2v} symmetric structure on the NMR timescale in solution. Four resonances corresponding to the aromatic protons can be observed (two overlapping for the protons *meta* and *para* to the central nitrogen atom) along with a singlet at 0.43 ppm (18H) for the equivalent $SiMe_3$ groups.



1.7 **3**

Equation 2.2.

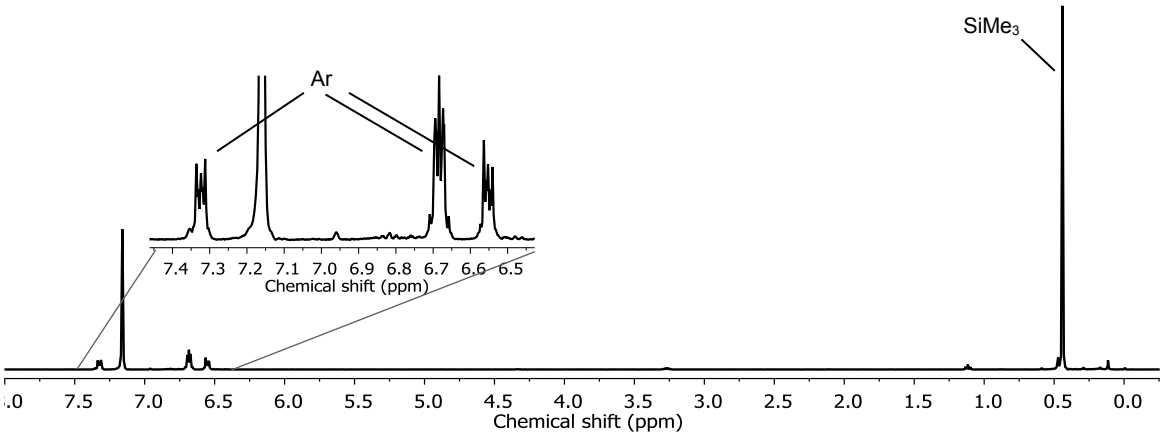


Figure 2.4. ^1H NMR spectra (400.1 MHz) of $Ta(NN_2^{SiMe3})Cl_2$ (**3**) in C_6D_6 at 298 K.

Diffraction-quality crystals of **3** were grown by the slow evaporation of a pentane solution. The molecular structure is shown in Figure 2.5 and selected bond lengths and angles are given in Table 2.1.

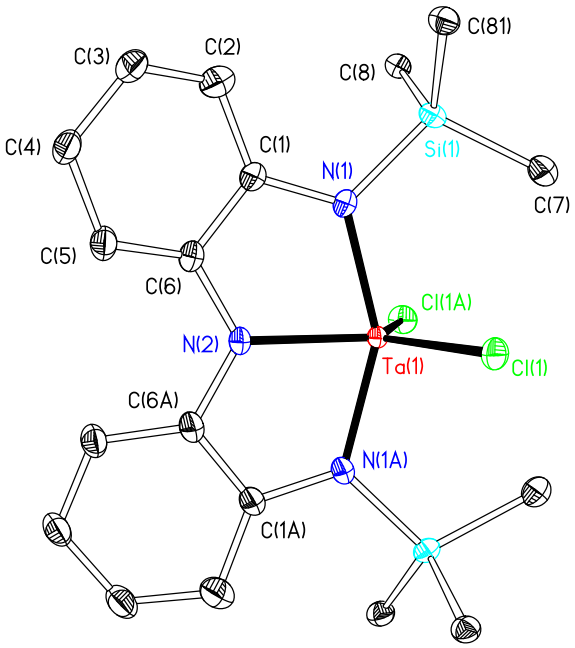


Figure 2.5. Displacement ellipsoid plot (20% probability) of $Ta(NN_2^{SiMe3})Cl_2$ (**3**). H atoms are omitted for clarity. Atoms carrying the suffix 'A' are related to their counterparts by the symmetry operator [-x, y, ½ -z].

Table 2.1. Selected bond distances (Å) and angles (°) for $Ta(NN_2^{SiMe3})Cl_2$ (**3**).

Ta(1)–N(1)	1.993(8)	N(1)–Ta(1)–N(1A)	150.8(5)
Ta(1)–N(2)	2.026(11)	N(1)–Ta(1)–N(2)	75.4(2)
Ta(1)–Cl(1)	2.316(2)	N(1)–Ta(1)–Cl(1)	96.44(10)
N(1)–Si(1)	1.795(9)	N(2)–Ta(1)–Cl(1)	116.45(7)
		N(2)–Ta(1)–Cl(1A)	116.45(7)
		Cl(1)–Ta(1)–Cl(1A)	127.10(13)
		Ta(1)–N(1)–Si(1)	119.4(4)

The molecular solid state structure of **3** has a distorted pentacoordinate geometry. The geometry index or structural parameter (τ) for five-coordinate compounds follows the equation $(\beta - \alpha)/60$, where $\beta \geq \alpha$ are the two greatest L–M–L angles in the complex. Defined by Addison and co-workers, the τ value for a perfect square-based and a perfect trigonal bipyramid are zero and one, respectively and therefore τ allows to describe the geometry when the molecular structure is distorted.[43] In this case, the distortion in the

geometry of **3** is observed in the axial ligand N(1)–Ta–N(1A) due to steric constrains form the NN_2^{SiMe3} ligand with an angle of 150.8(5) °. Therefore, the τ value is equal to 0.40, which defines the geometry of **3** as 40% along the range from square-based pyramidal and trigonal bipyramidal geometries. Mascharak and co-workers found that calculation of τ is not feasible when α and β values are comparable or when the β value is particularly low (~160 °) as a result of out-of-plane distortions and the ligand strain.[44] Following this, τ values will generally not be given for the following five-coordinated complexes with the NN_2^{SiMe3} ligand as the distortion in the geometry is comparable to **3**.

In dichloride complex **3**, the NN_2^{SiMe3} ligand is coordinated in a meridional fashion and slightly twisted out of planarity. This is attributed to the steric interaction of the two C−H protons adjacent to the central nitrogen atom with each other.[36] The equatorial plane contains an N_{aryl} atom and two chloride ligands. The N_{SiMe3} atoms residing 2.023(11) and 1.993(4) Å from the Ta metal centre are within the expected ranges for Ta(V) complexes with NNN^{3-} ligands like the analogue $Ta(NN_2^{SiMe3})Me_2$ (**1.5**).[36] The Ta-Cl bond lengths at 2.316(2) Å are also consistent with the *para*-substituted analogues reported with variations between 2.31 and 2.33 Å.[45,46]

2.5 Electronic structure analysis of $Ta(NN_2^{SiR3})Me_2$

At first sight, $Ta(NN_2^{SiMe3})Cl_2$ (**3**) and its homologues $Ta(NN_2^{R})X_2$ (X = one-electron donor such as Cl or alkyl; R represents the amide ligand substituents) are 16 valence electron compounds, assuming that the lone pairs of the three sp^2 hybridised amide nitrogens of N_2N^R are all able to be donated to the metal centre. However, it is well recognised that in transition metal compounds with π-donor ligands (including 5-coordinate polyamide systems[47-49] related to $Ta(NN_2^{R})X_2$) that symmetry or other restrictions can reduce the extent of π-donation to the metal centre, reducing the formal valence electron count below that otherwise anticipated. To clarify the position for $Ta(NN_2^{R})X_2$, DFT calculations at the B3PW91 level were performed by Philip Mountford on a series of experimental and model systems.

The compounds $Ta(NN_2^{R})X_2$ are based on an approximately trigonal bipyramidal (TBP) geometry which serves as a starting point for discussion. The molecular orbitals (MOs) of TBP systems are well known.[50,51] Figure 2.6 (left) shows the metal (5d based) frontier MOs of a hypothetical σ-only, d^0 TBP compound ML_5, along with the conventional coordinate system. Although a homoleptic TBP ML_5 compound has local D_{3h} symmetry,

the symmetry labels in Figure 2.6 are given for consistency in the approximate C_{2v} symmetry of $Ta(NN_2^R)X_2$ (ignoring the small twisting in the non-planar $N(o\text{-}C_6H_4)_2$ backbone which was discussed above). The $2a_1$ MO of ML_5 (mainly d_{z2} character) is strongly σ* antibonding and does not engage in additional metal-ligand π interactions. The $1a_1$ and $1b_1$ levels (based mainly on d_{x2-y2} and d_{xy}) are slightly metal-ligand σ* antibonding and higher in energy than the strictly σ non-bonding $1b_2$ (d_{xz}) and $1a_2$ (d_{yz}) levels. These four orbitals are all available for metal-ligand π bonding interactions with correctly oriented amide 2p(π) donor orbitals. The $1b_2$ and $1a_2$ levels are the d(π) acceptor orbitals with the best energy match with amide nitrogen 2p lone pairs; on the other hand, *n*d/(*n*+1)p mixing in $1a_1$ and $1b_1$ helps polarise these orbitals favourably towards π-donors in the equatorial sites.

The σ-only MOs of $Ta(NN_2^R)X_2$ will differ from those of idealised D_{3h} ML_5. The chelating nature of NN_2^R decreases the L_{ax}–M–L_{ax} angle so that $1b_2$ will become slightly M–L σ^* antibonding in character and destabilised relative to $1a_2$. In addition, in the case where L_{eq} is a better σ-donor than L'_{eq}, $1b_1$ will become less stable (more σ* antibonding) than $1a_1$, decreasing the former's π-acceptor ability due to a less good energy match with any amide 2p lone pair at the L'_{eq} site. This would be the case for $Ta(NN_2^R)X_2$ where X = alkyl, for example. Nonetheless, the basic metal-based MO ordering ($1b_2$, $1a_2$) < ($1a_1$, $1b_1$) << $2a_1$ remains. Calculations on model compounds including C_{2v}–$TaMe_5$ (Me_{ax}–Ta–Me_{ax} = 150 °) and C_{2v}–$TaMe_4(NH_2)$ confirmed these qualitative conclusions.

Figure 2.6 (right) depicts the representative model compound $Ta(NN_2^{SiH3})Me_2$ (**1.5q**) which is based on Schrock's $Ta(NN_2^{SiMe3})Me_2$ (**1.5**), with $SiMe_3$ replaced by SiH_3 for simplicity. Its three amide lone pairs transform as $b_1 + b_1 + a_2$; these symmetry adapted linear combinations (SALCs) are schematically illustrated in the Figure. The two b_1 SALCs can mix further but are shown separately in Figure 2.6 for clarity.

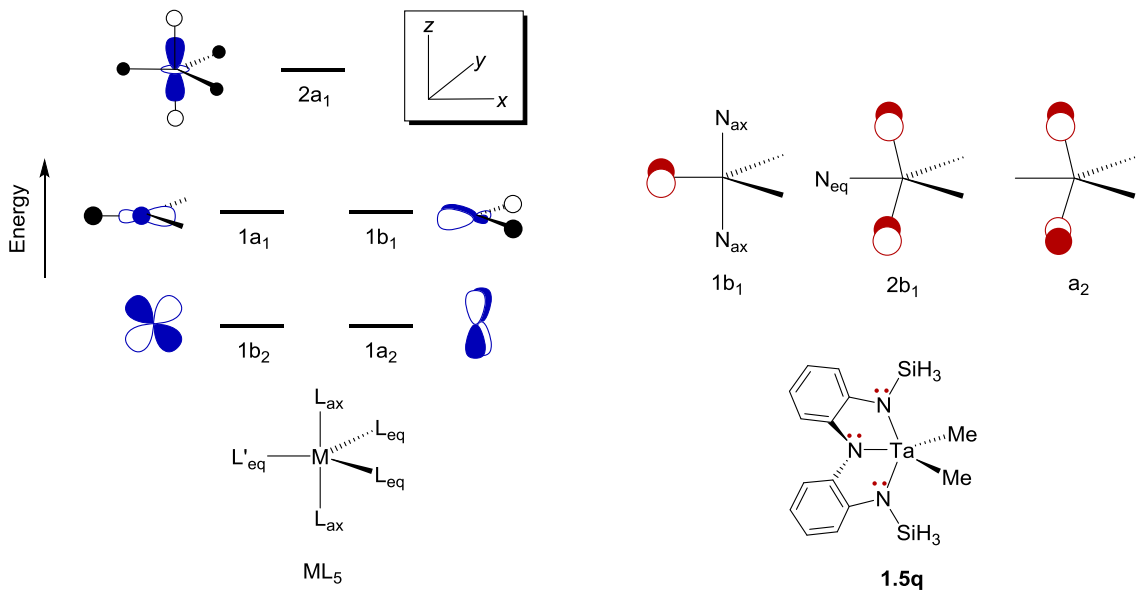


Figure 2.6. Left: the σ-only frontier MOs (d orbitals only, arbitrary energies) for a hypothetical ML_5 system. Right: representation of the model compound $Ta(NN_2^{SiH3})Me_2$ (**1.5q**) emphasising the 2p(π) lone pairs for the equatorial (N_{eq}) and axial (N_{ax}) amide nitrogens.

Figure 2.6 shows that, on symmetry grounds alone, one would therefore expect $Ta(NN_2^{R})X_2$ (X = σ-only donor) to have a maximum formal valence electron count of 14, even though metal centre has four available π-acceptor orbitals and there are three amide lone pairs. This is because there are *two* b_1 symmetry lone pair SALCs but only *one* b_1 π-symmetry acceptor ($1b_1$, mainly d_{xy} in character and slightly Ta–X σ* antibonding). Of the two b_1 symmetry amide donors, it is $1b_1$ (based on the equatorial nitrogen, N_{eq}) that has the better overlap with the $1b_1$ acceptor orbital (note that in the case of L_{ax}–M–L_{ax} = 180 ^{o} the $2b_1$ amide SALC would be strictly non-bonding with respect to the metal d orbitals). On the other hand, the a_2 amide lone pair SALC has a very good overlap and energy match with the corresponding a_2 symmetry (d_{yz}) acceptor orbital for L_{ax}–M–L_{ax} = 180 ^{o}, although this would be slightly attenuated at L_{ax}–M–L_{ax} = *ca.* 150 ^{o} (the typical angle found in the real compounds $Ta(NN_2^{R})X_2$).

DFT calculations were carried out on geometry-optimised $Ta(NN_2^{SiH3})Me_2$ (**1.5q**). Figure 2.7 shows the three highest occupied molecular orbitals (HOMOs) and the the four lowest unoccupied molecular orbitals (LUMOs, based on tantalum). The results support the qualitative conclusions reached above.

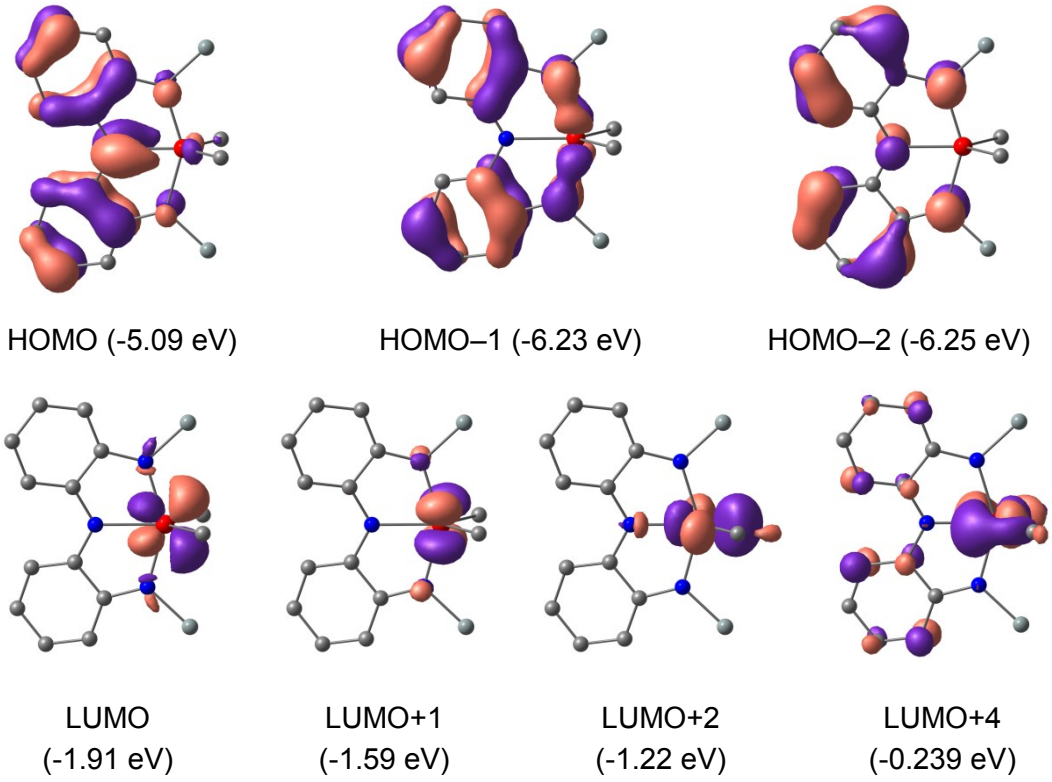


Figure 2.7. DFT computed frontier molecular orbitals of $Ta(NN_2^{SiH3})Me_2$ (**1.5q**). Isosurfaces are drawn at the 0.0432– 0.07465 a.u. contour level. H atoms omitted.

The three highest occupied molecular orbitals of **1.5q** represent the principle contributions from the three amide lone pairs represented in Figure 2.6 (right). It is clear from Figure 2.7 that there is also extensive mixing with the ring π MOs of the two *o*-phenylene groups of NN_2^{SiH3}. The HOMO represents mainly the b_1 symmetry π-interaction between the equatorial amide nitrogen (N_{eq}) and tantalum. The HOMO-1 is the corresponding a_2 symmetry counterpart, and is *ca*. -1.1 eV more stable than the b_1 HOMO for the reasons described above (i.e. is based on donation into the lower energy σ non-bonding a_2 orbital of tantalum). The Wiberg bond indices (measures of relative metal-ligand bond order) for the Ta–N_{eq} and Ta–N_{ax} bonds of **1.5q** are 0.653 and 0.833 (avg.), respectively, consistent with more effective π-donation from the axial amide ligands.

The ligand-based HOMO-2 has no metal character, and effectively represents the non-bonding $2b_1$ SALC illustrated in Figure 2.6 (right), albeit with some mixing with the equatorial amide lone pair as anticipated. Although it seems slightly counter-intuitive that the non-bonding amide lone pair is more stable than the Ta–N π-bonding counterparts,

the latter MOs are raised in energy by more strongly developed N–C_{ipso} antibonding interactions and the contribution from tantalum.

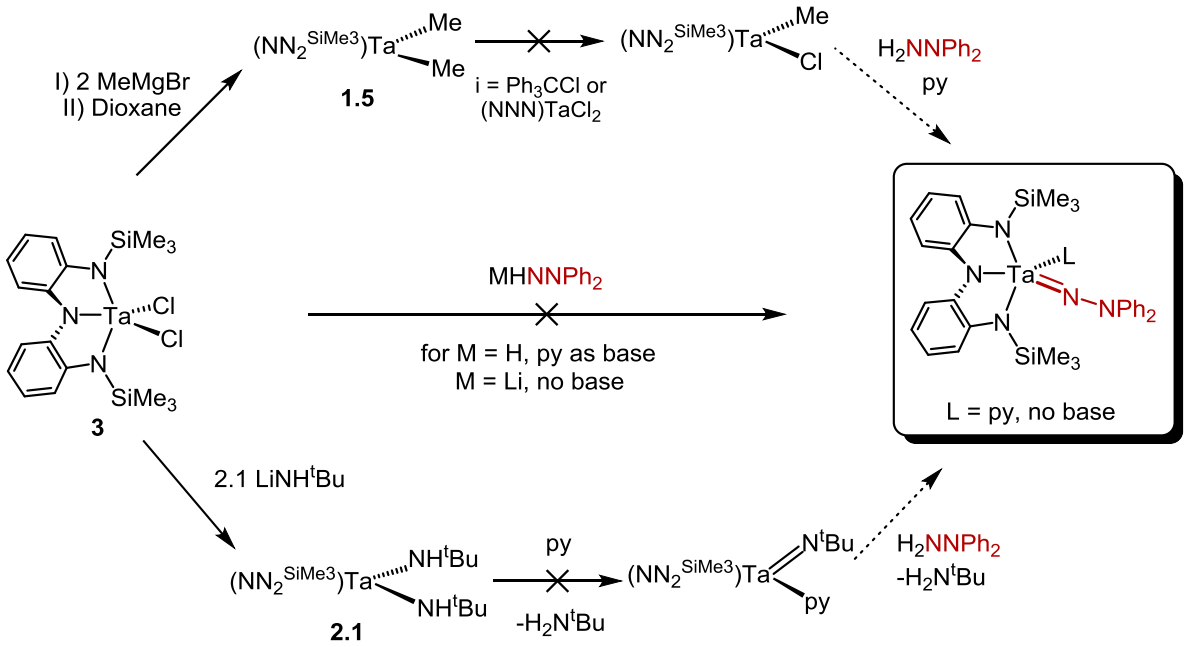
The four metal based LUMOs are consistent with the qualitative picture deveopled above and a formal d^0 (Ta(+5)) metal centre. The LUMO (b_2 symmetry) and LUMO+2 (a_1) are π non-bonding but slightly Ta–N σ antibonding as described above. LUMO+1 (a_2 symmetry) and LUMO+4 (b_1) are the counterparts of the HOMO-1 and HOMO. The LUMO+3 (not shown, -0.32 eV) is ligand-based on the N(*o*-$C_6H_4)_2$ backbone.

In summary, Ta(NN_2^{SiMe3})Cl_2 (**3**) and its homologues Ta(NN_2^R)X_2 are best viewed as 14 valence electron, d^0 compounds with one of the amide lone pair SALCs of NN_2^R being effectively non-bonding due to symmetry restrictions.

2.6 Route A: Reactions of Ta(NN_2^{SiMe3})Cl_2 (3) with hydrazines or *via* bis(amido) and dimethyl precursors

As described in Section 2.2, Sita and co-workers reported the synthesis of Cp*Ta{N(^{i}Pr)C(NMe_2)N(^{i}Pr)}($NNMe_2$)(Cl) (**1.73**) through the reaction of Cp*Ta{N(^{i}Pr)C(NMe_2)N(^{i}Pr)}Cl_3 with 2 equiv. of lithium 1,1-dimethylhydrazide (LiNHNMe_2).[33] In a similar manner, an attempt was made to access the final tantalum hydrazide complex through a one-step synthesis with the reaction of **3** with either 1,1-diphenylhydrazine (H_2NNPh_2, in the presence of pyridine as a donor ligand) or LiNHNPh_2, Scheme 2.2 (middle). Unfortunately, no success was found with either of these cases as complex mixtures of products were observed.

A second attempt involved the salt metathesis reaction of **3** with the slow addition of 2 equiv. of MeMgBr followed by an excess of 1,4-dioxane in toluene at -30 ˚C, proceeding smoothly for 1.5 h at RT. Following work-up, Ta(NN_2^{SiMe3})Me_2 (**1.5**) was isolated in 60 % yield, Scheme 2.2 (top). The complex **1.5** has been previously reported by Schrock and co-workers using a different synthetic route, from $TaMe_5$ with the protio-ligand $H_3NN_2^{SiMe3}$ giving **1.5** in 80 % yield.[36]



Scheme 2.2. Route A: Attempted synthetic pathways towards Ta(NN_2^{SiMe3})($NNPh_2$)(L).

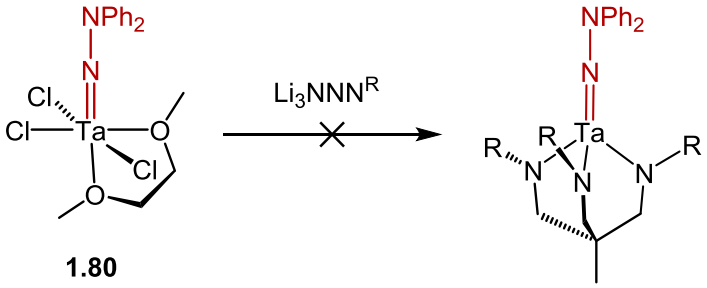
Attempted synthesis of a mono-substituted complex of the type Ta(NN_2^{SiMe3})Cl(Me) by a similar reaction but with just one equivalent of either MeMgBr or MeLi suggest that the second alkylation occurs relatively faster than the first resulting in a mixture of the dichloride **3** and the dimethyl species **1.5** in 1:1 ratio. In 2004, Deck and co-workers reported the halodemethylation of Group 4 dimethyl complexes with trityl chloride (Ph_3CCl),[52] which was here used as an alternative route to form Ta(NN_2^{SiMe3})Cl(Me). However, no reaction occurred at RT and there was no evidence for the formation of either this compound or Ph_3CMe despite forcing reaction conditions that resulted in a mixture of products. As an alternative, the exchange reaction of **3** with dimethyl species **1.5** on the NMR tube scale in C_6D_6 at temperatures between 60 to 80 ˚C for 6 to 8 days, resulted in a mixture of what appears to be the methyl-chloride Ta complex, the dichloride **3** and small amounts of unidentified species, presumably as result of decomposition of remaining **1.5**.

Previous work in this research group demonstrated the preparation of the bis(amide) Ta(NN_2^{SiMe3})(NH^tBu)$_2$ (**2.1**) from reaction of **3** with two equiv. of lithiated amine $LiNH^tBu$.[39,53] Further attempts to form the corresponding imide by reacting **2.1** with an excess of pyridine were not successful, resulting in an apparent equilibrium between complex **2.1**, the tantalum *tert*-butylimide and a mixture of unidentified products (Scheme

2.2, bottom). Furthermore, Chapter 3 (Section 3.4.1) will describe the successful synthesis of Group 5 imido complexes of the type $M(NN_2^R)(N^tBu)(L)$ achieved by a different route.

2.7 Route B: Reaction of the hydrazide precursor $Ta(NNPh_2)Cl_3(DME)$ (\$1.2\$) with the $Li_3(NNN^R)$ ligand

As mentioned in Section 2.3, Bercaw and co-workers reported the synthesis of the $Ta(NNPh_2)Cl_3(DME)$ (**1.80**) synthon which was produced through a Lewis acid-assisted dehydrohalogenation reaction of $TaCl_5$ with H_2NNPh_2 and DME in the presence of pyridine and $ZnCl_2$. This precursor has proved to be a versatile synthon for incorporation of the $Ta{=}NNPh_2$ moiety into complexes bearing mono- and dianionic ligands.[32] In the same way, the precursor **1.80** was reacted with the lithiated face-capping ligands $Li_3(NNN^R)$ (R = ^{i}Pr (**1.8**) or $SiMe_3$ (**1.9**))[40,41] *via* salt metathesis (Equation 2.3). When synthesised on either the NMR tube scale in C_6D_6 or the preparative scale in toluene at low temperature the ^{1}H NMR spectra showed a mixture of products in which the formation of the complexes of the type $Ta(NNN^R)(NNPh_2)$ could be identified. Some of the decomposition products were isolated when attempt to crystallize the hydrazide compounds (Figure 2.8).



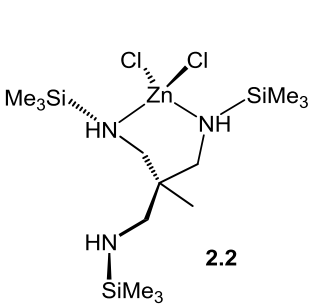
1.80

Equation 2.3.

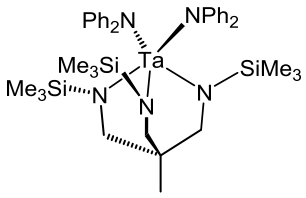
These compounds were shown by X-ray diffraction to be: a zinc dichloride species with the NNN^{SiMe3} ligand (**2.2**), a tantalum bis(diphenylamide) complex $Ta(NNN^{SiMe3})(NPh_2)_2$, (**2.3**) which formed through an N_α-N_β bond cleavage reaction, and the dimeric species $[Ta\{(NCH_2{}^iPr)_3CMe\}(\mu\text{-}N(Li_2)NPh_2)]_2$ (**2.4**). They are shown in Figure 2.8 with selected bond lengths and angles listed in Table 2.2. The zinc dichloride complex $Zn(H_3NNN^{SiMe3})Cl_2$ is a side reaction of the $ZnCl_2$, which was used in the synthesis of the tantalum hydrazide synthon **1.80**, with protio-ligand H_3NNN^{SiMe3}. Various attempts to remove $ZnCl_2$ from complex **1.80** were performed: crystallisation from different solvents

result in either a mixture of navy-blue (**1.80**) and yellow crystals ($ZnCl_2$) or navy-blue crystals coated in a thin yellow film; also repeated extractions with different solvents at low temperature were performed; and attempts to use silica/alumina column chromatography and sublimation also both failed. None of these techniques proved to be useful to obtain a pure product.

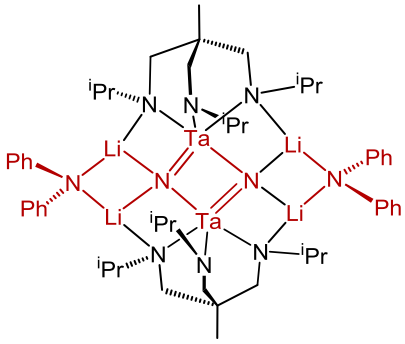
The bis(diphenylamide) $Ta(NNN^{SiMe3})(NPh_2)_2$ (**2.3**) and the dimeric species $[Ta\{(NCH_2{}^iPr)_3CMe\}(\mu\text{-}N(Li_2)NPh_2)]_2$ (**2.4**) are examples of N−N bond cleavage reactions. Detailed experimental[33] and computational[54] studies for these primary N−N bond-cleaving steps for tantalum hydrazide, hydrazidium, and imide intermediates have been recently investigated. Sita and co-workers reported Ta_2N_2 *cis*- and *trans*-four-membered ring complexes[33,55] which are similar to **2.4** compound. The solid state molecular structures of **2.3** and **2.4** obtained from single-crystal X-ray analysis (Figure 2.8) have an approximately trigonal bipyramidal geometry. In the case of **2.4** the four-membered ring adopts a planar geometry with the Ta(1)-N(1) and Ta(1)-N(1A) bond lengths of 1.904(5) and 2.002(5) Å respectively, and the N(1)−Ta(1)−N(1A) angle of 83.4(2) which can be compared with the array of structurally characterised complexes *cis*- and *trans*-$[Cp^*Ta\{N(^iPr)C(NMe_2)N(^iPr)\}(\mu\text{-}N)]_2$,[33] both of which share a similar geometry.



2.2



2.3



2.4

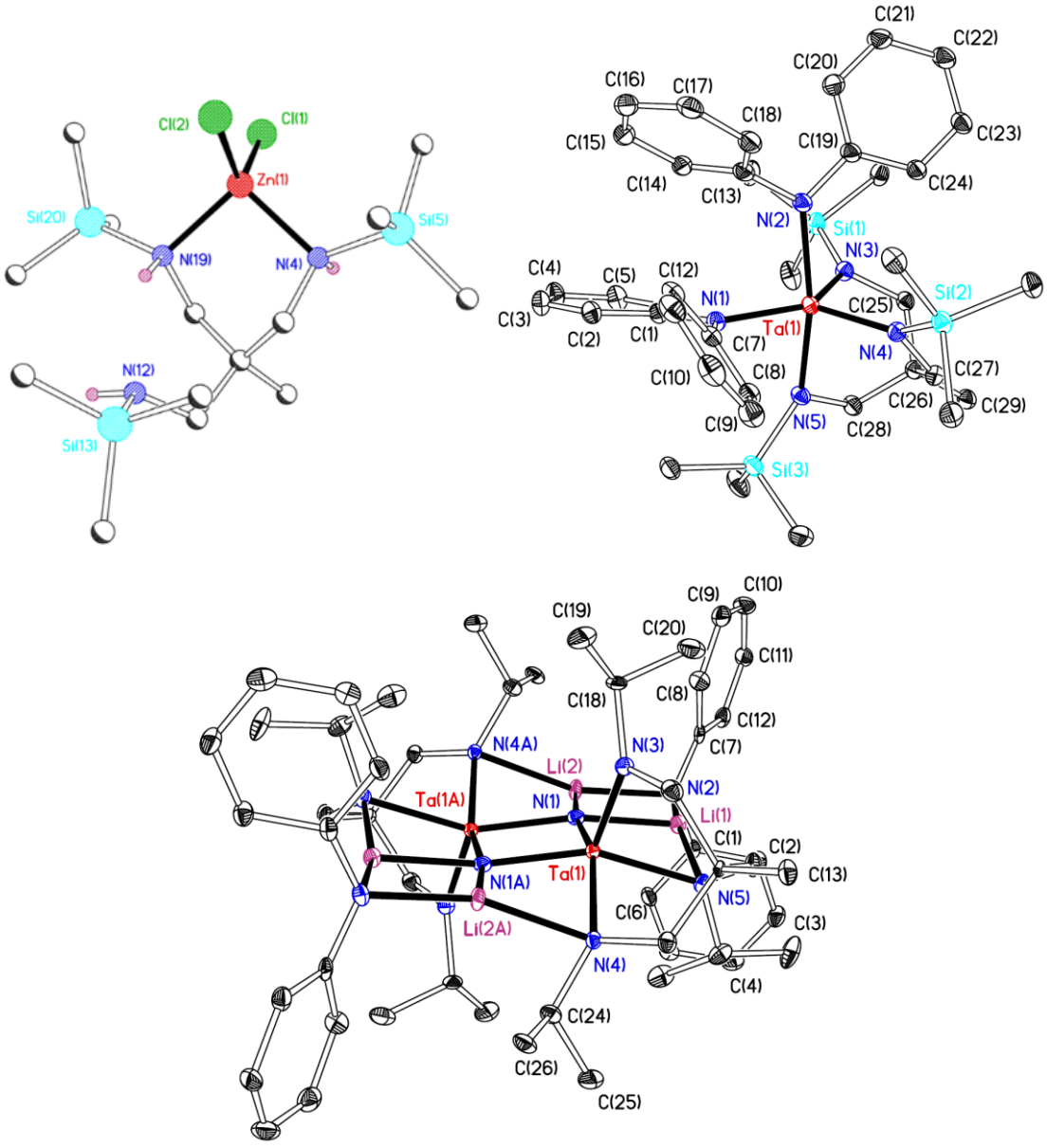


Figure 2.8. By-products in mixture with Ta(NNN^{R})(NNPh$_2$) (R = ^{i}Pr or SiMe$_3$). Displacement ellipsoid plots (20 % probability) of Zn(NNN^{SiMe3})Cl$_2$ (**2.2**, middle left), Ta(NNN^{SiMe3})(NPh$_2$)$_2$ (**2.3**, middle right) and [Ta(NNN^{iPr})(N(Li$_2$)NPh$_2$)]$_2$ (**2.4**, bottom). H atoms are omitted for clarity. H(1) and H(2) are drawn as spheres of an arbitrary radius.

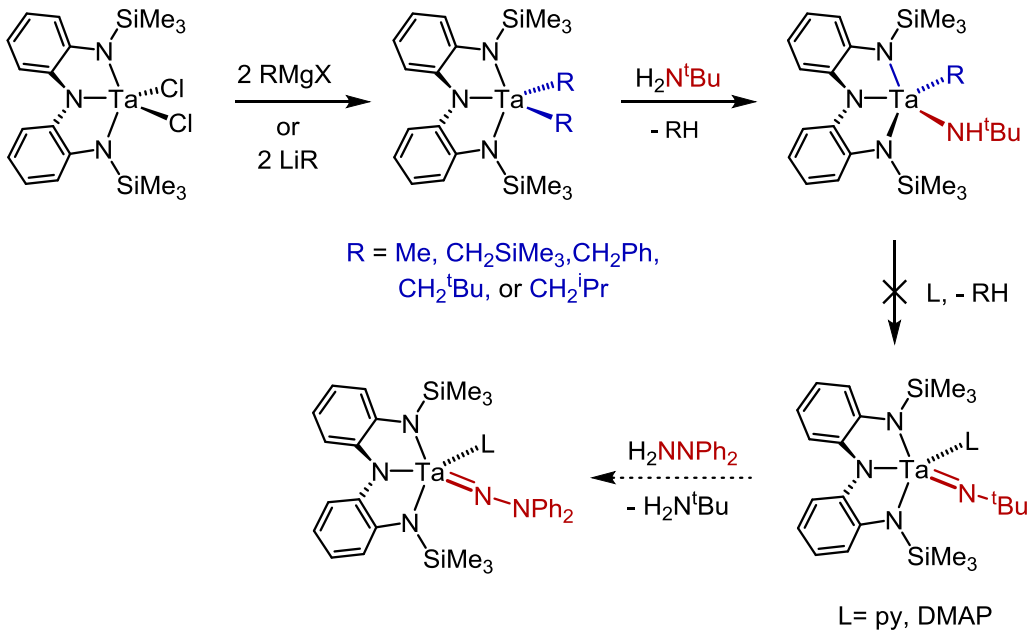
Table 2.2. Selected bond lengths (Å) and angles (°) for $Ta(NNN^{SiMe3})(NPh_2)_2$ (**2.3**) and $[Ta(NNN^{iPr})(N(Li_2)NPh_2)]_2$ (**2.4**).

Parameter	**2.3**	**2.4**
Ta(1)–N(1)	2.063(2)	1.904(5)
Ta(1)–N(2)/N(1A)	2.166(3)	2.002(5)
N(1)–Ta(1)–N(2)/N(1A)	86.44(10)	83.4(2)

With the failure of the attempted purification of **1.80**, focus was next given to an alternative route which involves the synthesis of intermediate dialkyl and alkyl-amido complexes with NN_2^{SiMe3} ligand.

2.8 Route C: Multistep synthetic route *via* dialkyl and alkyl-amido precursors with NN_2^{SiMe3} ligand

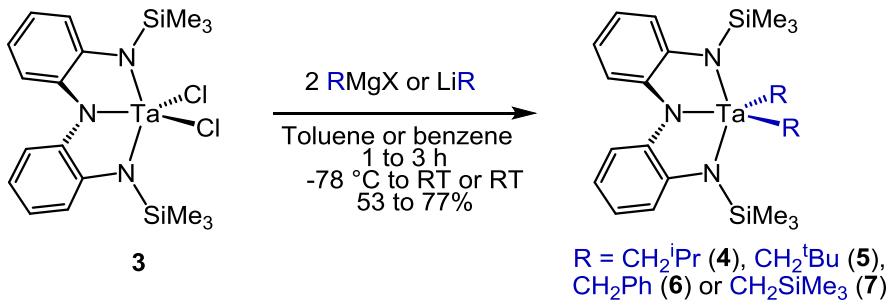
Scheme 1.3 shows a four step route towards tantalum hydrazido complexes. First, tantalum dichloride complex **3** was converted into dialkyl compounds of the type $Ta(NN_2^{SiMe3})R_2$ *via* salt metathesis reactions. This was followed by reaction with *tert*-butylamine to obtain the alkyl-amide complexes of the type $Ta(NNN^{SiMe3})(NH^tBu)R$. In a third step, reactions between the tantalum alkyl-amides and a Lewis base (pyridine or 4-(dimethylamino)pyridine (DMAP)) were attempted to generate the formation of the tantalum imido functionality. However, these reactions proved to be unsuccessful and the final step to obtain the tantalum hydrazide complexes could not be performed. The outcomes of these reactions will be further discussed.



Scheme 1.3. Route C: Attempted multistep synthetic pathway towards $Ta(NN_2^{SiMe3})(NNPh_2)(L)$.

2.8.1 Reactions of $Ta(NN_2^{SiMe3})Cl_2$ (3) with metal alkyls

Salt metathesis and alkane elimination have been used as routes for installation of new ligands in Group 5 complexes.[36,56,57] In a similar manner to the synthesis of **1.5** (described in Section 2.5) a salt metathesis reaction of $Ta(NN_2^{SiMe3})Cl_2$ (**3**) with 2 equiv. of isobutyllithium ($LiCH_2{}^iPr$), neopentyllithium ($LiCH_2{}^tBu$), benzylmagnesium chloride ($PhCH_2MgCl$) or trimethylsilylmethyllithium ($LiCH_2SiMe_3$) produced four dialkyl compounds $Ta(NN_2^{SiMe3})R_2$ (R = $CH_2{}^iPr$ (**4**), $CH_2{}^tBu$ (**5**), CH_2Ph (**6**), CH_2SiMe_3 (**7**)) (Equation 2.4). In preliminary experiments it was found that the substitution of a single chloride ligand through a direct reaction with 1 equiv. of the metal alkyl could not form the monochloride species. Instead a mixture of **3** and the dialkyl complex was observed.



Equation 2.4

Initial characterisation of all four compounds by ^{1}H NMR spectroscopy (Figure $f2.9$) suggested C_{2v}-symmetric structures as only one $NSiMe_3$ resonance and one set of alkyl signals were observed. The trimethylsilyl (18 H) groups corresponding to the NN_2^{SiMe3} ligand display resonances between 0.5 and -0.7 ppm. The ligand aryl proton signals present as three multiplet resonances in the case of **4**, **6** and **7** and two signals in the case of **5**, as two of the multiplets overlapped; these have ^{1}H resonances in the range *ca* 8 - 6 ppm.

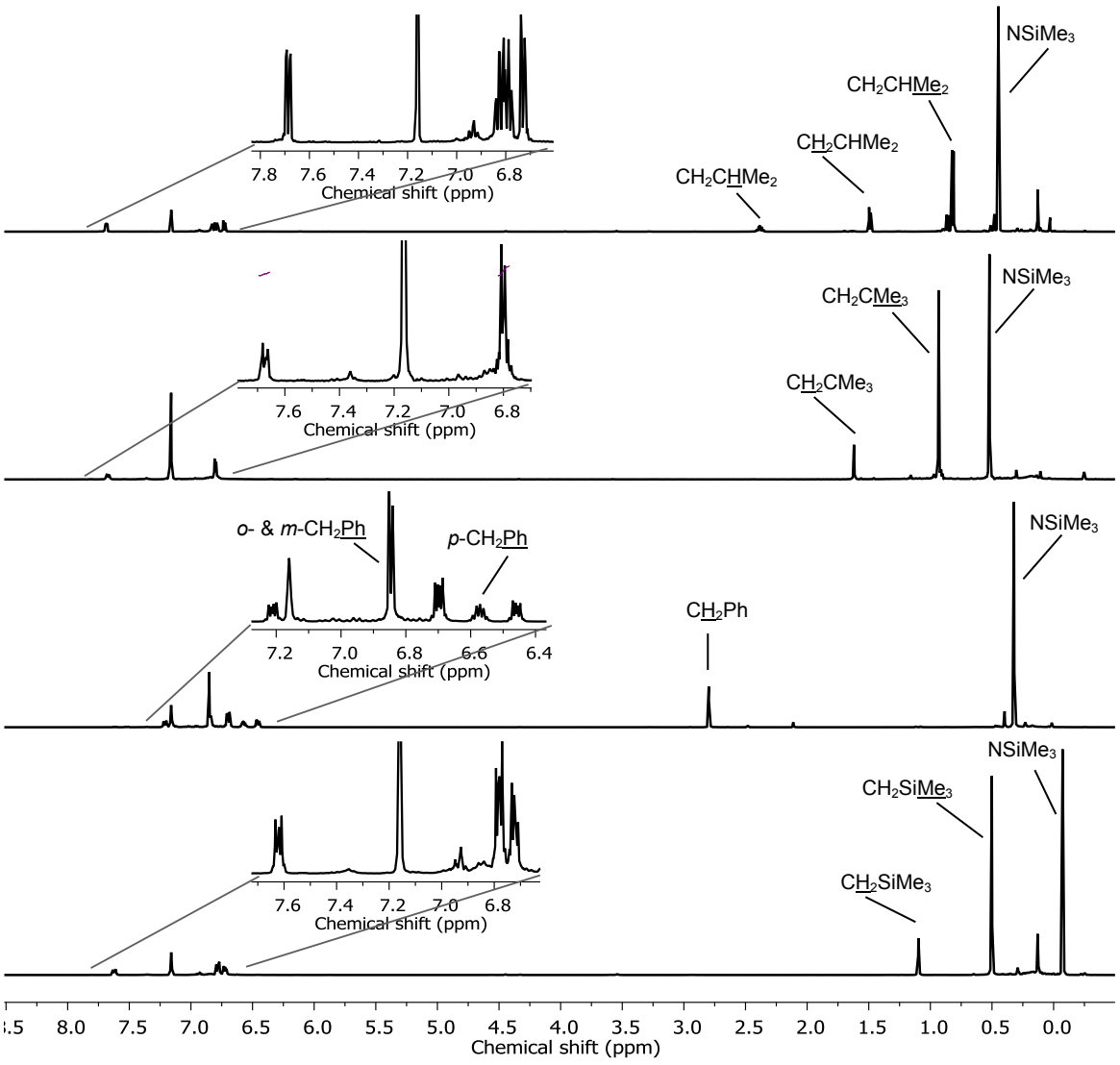


Figure 2.9. ^{1}H NMR spectra (400.1 MHz) of $Ta(NN_2^{SiMe3})R_2$ (R = $CH_2{}^{i}Pr$ (**4**, top), $CH_2{}^{t}Bu$ (**5**, middle top), CH_2Ph (**6**, middle bottom), CH_2SiMe_3 (**7**, bottom)in C_6D_6 at 298 K.

Diffraction-quality crystals of compounds **6** and **7** were grown from saturated hexanes solutions at room temperature giving red block and dark-yellow plate crystals. The molecular solid structures are shown in Figure 2.10 along with selected bond lengths and angles in Table 2.3.

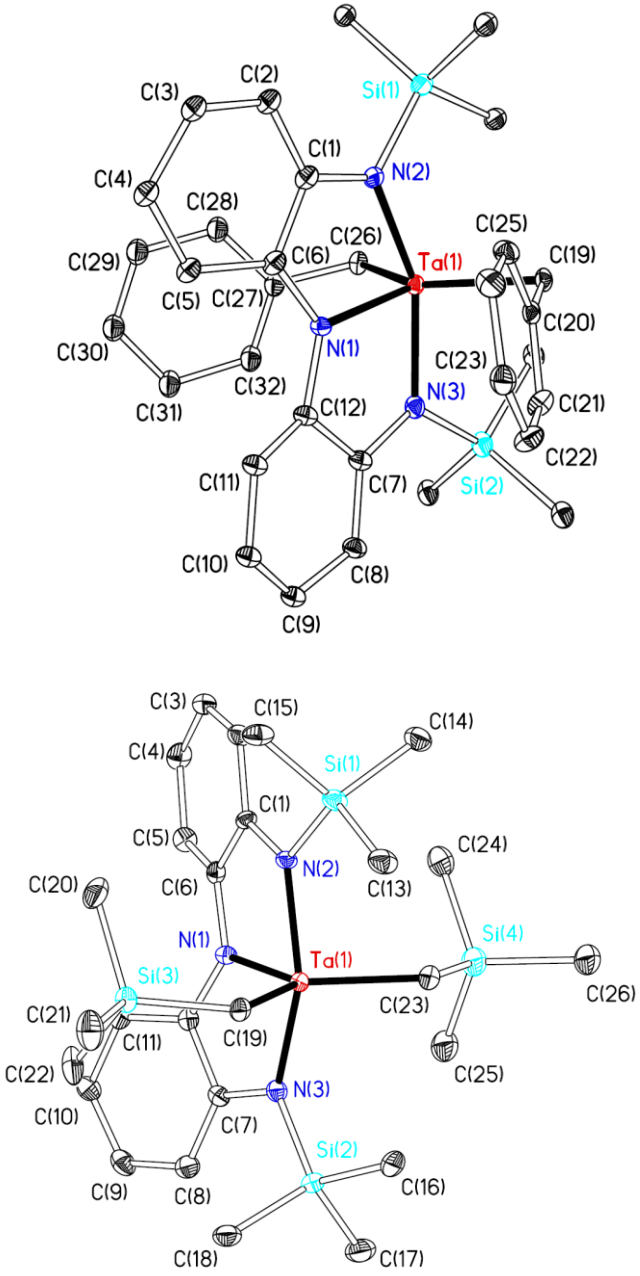


Figure 2.10. Displacement ellipsoid plots (20 % probability) of $Ta(NN_2^{SiMe3})(CH_2R)_2$ (R = Ph (**6**, top) and $SiMe_3$ (**7**, bottom)). H atoms omitted for clarity.

Table 2.3. Selected bond lengths (Å) and angles (°) for $Ta(NN_2^{SiMe3})(CH_2R)_2$ (R = Ph (**6**) or $SiMe_3$ (**7**)).

Parameter	**6**	**7**
Ta(1)–N(1)	2.086(4)	2.064(4)
Ta(1)–N(2)	2.008(5)	2.019(4)
Ta(1)–N(3)	1.982(6)	2.022(4)
Ta(1)–C(19)	2.208(6)	2.153(6)
Ta(1)–C(26)/C(23)	2.217(6)	2.151(5)
N(2)–Si(1)	1.763(6)	1.784(5)
N(3)–Si(2)	1.780(6)	1.785(5)
N(1)–Ta(1)–N(2)	75.3(2)	75.64(17)
N(1)–Ta(1)–N(3)	75.6(2)	75.43(17)
N(2)–Ta(1)–N(3)	150.9(2)	151.07(19)
N(1)–Ta(1)–C(19)	111.6(2)	117.28(18)
N(2)–Ta(1)–C(19)	94.5(2)	97.5(2)
N(3)–Ta(1)–C(19)	94.5(2)	95.8(2)
N(1)–Ta(1)–C(26)/C(23)	108.5(2)	119.3(2)
N(2)–Ta(1)–C(26)/C(23)	96.0(2)	94.30(19)
N(3)–Ta(1)–C(26)/C(23)	94.8(2)	99.6(2)
C(19) –Ta(1)–C(26)/C(23)	139.9(2)	123.4(2)
Ta(1)–N(2)–Si(1)	116.1(3)	121.7(2)
Ta(1)–N(3)–Si(2)	116.5(3)	120.6(2)
Ta(1)–C(19)–C(20)	102.7(4)	-
Ta(1)–C(26)–C(27)	102.4(4)	-
Ta(1)–C(19)–Si(3)	-	117.8(3)
Ta(1)–C(23)–Si(4)	-	119.8(3)

The two complexes have a slightly distorted trigonal bipyramidal geometry, in which the NN_2^{SiMe3} ligand coordinates in a meridional fashion to the tantalum centre and the aryl rings are slightly twisted from each other out of planarity. The angle between the C(3)−C(4)−C(5) plane and the C(9)−C(10)−C(11) plane is *ca* 25.05 °, these atoms were considered as deviation from planarity within the aromatic ring is also observed.[36] The benzyl and trimethylsilylmethyl ligands occupy an equatorial site and are oriented such that the phenyl or trimethylsilyl groups point "backward" towards the *o*-phenylene rings of the NN_2^{SiMe3} ligand. This orientation allows these substituents to avoid unfavourable steric interactions with the NN_2^{SiMe3} ligand $SiMe_3$ substituents which are oriented "forward". The structures of **6** and **7** can also be compared with Schrock's $Ta(NN_2^{SiMe3})Me_2$ (**1.5**) which generally Ta-N and Ta-C distances features that are broadly in-between those of **6** and **7**.[36]

$Ta(NN_2^{SiMe_3})(CH_2R)_2$ (R = Ph (**6**) or $SiMe_3$ (**7**)) complexes also share a largely similar molecular geometry with the previously structurally characterised compounds of the type $(Ar^{Tol_2})Ta(NMe_2)_3R$ (R = Me, Et, ^{n}Pr, ^{n}Bu or $CH_2{}^t$Bu),[58] in which the alkyl ligands are also located in the equatorial sites. Thus, the NMe_2 amide ligands occupy the axial sites showing a similar distortion of the trigonal bipyramidal geometry with τ values within the range 0.342 and 0.729. Complex **7** has a τ value of 0.461 is comparable to those examples reported by Parkin, whereas complex **6** has a smaller τ value of 0.183.[58]

The Ta−CH_2R bond lengths of 2.208(6) and 2.217(6) Å in **6**, and 2.153(6) and 2.151(5) Å in **7** are comparable to those in **1.5** (avg. 2.177(4) Å), and within the range reported for other tantalum or niobium alkyl complexes (avg. M–CH_2 = 2.183 Å, range 2.124(12) – 2.3088(16) Å for nine examples).[56,58-61] The Ta−CH_2−Ph angles (**6**, 102.7(4) and 102.4(4) °)) are considerably smaller than the Ta−CH_2−$SiMe_3$ angles in **7** (117.8(3) and 119.8(3) °). Similarly, the series of dialkyl complexes $(Ar^{Tol_2})Ta(NMe_2)_3R$ (R = Et, ^{n}Pr, ^{n}Bu or $CH_2{}^t$Bu) possess normal Ta−CH_2−R angles (avg. 120.58 °, range 114.87(2) – 130.54(17) °) which are larger than those in **6**.[58] It may also be relevant that the RCH_2–Ta–CH_2R angle for **6** (R = Ph, 139.9(2) °) is significantly larger than those in either **7** (R = $SiMe_3$, 123.4(2) °) or **1.5** (R = H, 130.6(2) °).

Small M–CH_2−Ph angles are often observed for electron-deficient early transition metal compounds, with transfer of π-electron density from the phenyl ring to the metal centre providing some stabilisation.[62] As described above, the compounds $Ta(NN_2^{SiMe_3})(CH_2R)_2$

have formal 14 valence electron counts, and so in principle this electron deficiency could favour a decreased Ta–CH_2–Ph angles in **6** to achieve intramolecular Ta···Ph interactions. In addition, the small Ta–CH_2–Ph angles brings the phenyl rings close (as judged by intramolecular C_{Ph}···C_{ligand} distances in the range *ca.* 3.2 – 3.6 Å) to the quasi-planar and delocalised N(*o*-C_6H_4)$_2$$N_2$ aromatic system, potentially leading to stabilisation through π-π stacking (dispersive) type interactions.[63,64]

Bercaw *et al*. has reported a similar situation for the topologically related bis(phenolate)pyridine compound Ta{($OC_6H_2{}^tBu_2$)$_2$$NC_5H_3$}($CH_2Ph$)$_3$ containing three benzyl ligands.[56] Two of the benzyls have normal Ta–CH_2–Ph linkages with angles of 119 and 120 ° subtended at the methylene carbon. The other has an angle of 97 °, and authors speculated that this could be due to one or more of a number of factors including donation of phenyl ring π-electron density to Ta, and/or π-π interactions between the phenyl ring and the pyridine moiety of the bis(phenolate) supporting ligand.

To help understand the bonding position in **6** additional DFT calculations were carried out both on the full experimental system itself (denoted **6Q**) and a model system, Ta($NN_2^{SiH_3}$)(CH_2Ph)$_2$ (**6q**), with sterically less demanding SiH_3 groups in place of $SiMe_3$ to test for the influence of steric factors on the Ta–CH_2–Ph and $PhCH_2$–Ta–CH_2Ph angles. As was the case for Ta($NN_2^{SiH_3}$)Me_2 (**1.5q**) the geometry optimisations for **6Q** and **6q** were performed using the B3PW91 functional and the def2-svp basis set applied to all atoms. Since it is well known that DFT methods do not represent well (if at all) dispersive interactions (including π–π interactions), additional complementary geometry optimisations (DFT-D3) that included Grimme's empirical d3(bj) dispersion correction[65] were also performed, using the same functional and basis sets. Comparison of the DFT and DFT-D3 results for **6Q** and **6q** therefore give a way to decouple general steric ($SiMe_3$ *vs.* SiH_3), dispersive (π–π) and electronic (orbital-based) contributions to the final geometry and metric parameters for **6**.

The DFT-D3 calculations for **6** reproduced the experimental geometry quite well, giving Ta–CH_2–Ph and $PhCH_2$–Ta–CH_2Ph angles of 97.0 ° (avg.) and 139.7 °, respectively. The average Ta–CH_2Ph distance was 2.230 Å. The corresponding DFT (i.e. without dispersion being taken into account) gave Ta–CH_2–Ph and $PhCH_2$–Ta–CH_2Ph angles of 113.0 ° (avg.) and 122.1 °, respectively, and a shorter average Ta–CH_2Ph distance of 2.212 Å. Calculations for the less sterically crowded **6q** showed the same trend: with

dispersion (DFT-D3) and without (DFT only, in parentheses): average Ta–CH_2–Ph = 95.1 ˚ (110.8 ˚); PhCH_2–Ta–CH_2Ph = 129.8 ˚ (117.8 ˚); average Ta–CH_2Ph = 2.208 Å (2.194 Å). Figure 2.11 shows two views of **6q**: with (left) and without (right) dispersion corrections included in the optimisation.

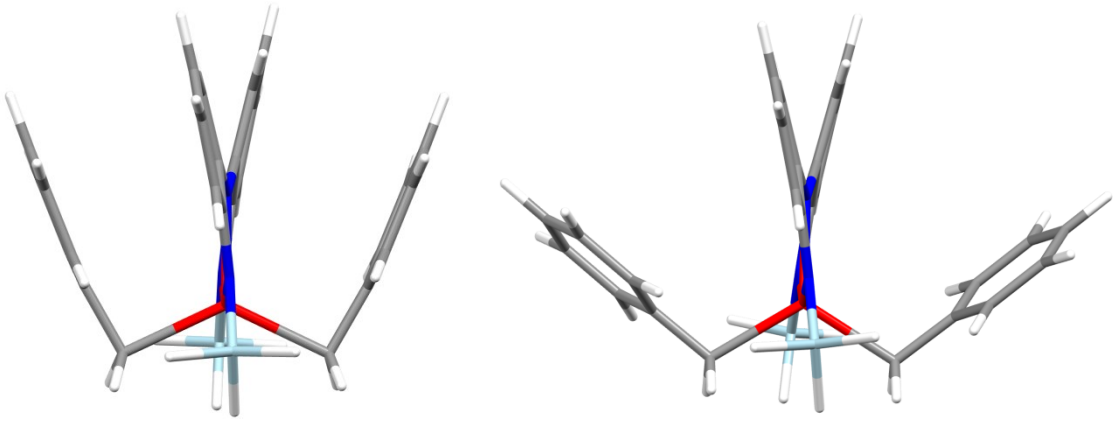


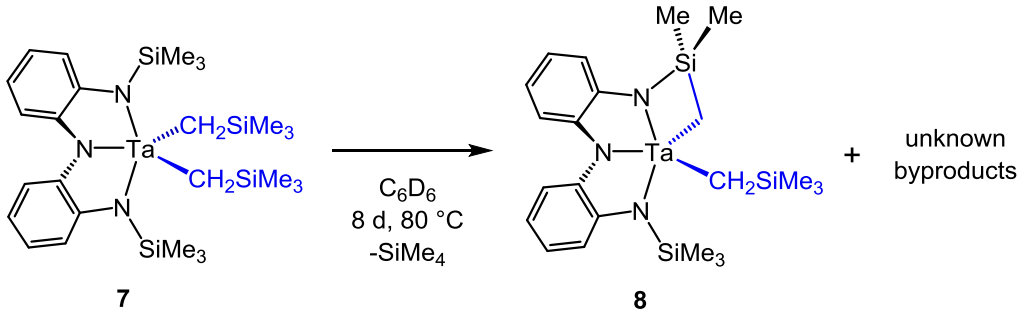
Figure 2.11. Computed geometry of Ta($NN_2^{SiH_3}$)(CH_2Ph)$_2$ (**6q**) viewed perpendicular the the equatorial plane. Left: with dispersion interactions included (avg. Ta–CH_2–Ph = 95.1 ˚). Right: without dispersion interactions included (avg. Ta–CH_2–Ph = 110.8 ˚).

Overall the results for **6Q** and **6q** show that the steric demands of $SiMe_3$ have neglible effect on the parameters associated with the benzyl groups. Dispersive (π–π) interactions are clearly important, and have the effect of contracting the Ta–CH_2–Ph angles. This also opens up the PhCH_2–Ta–CH_2Ph angle, presumably to allow better alignment of the interacting aromatic groups. There is also a lengthening effect on the Ta–CH_2Ph distances. In the absence of dispersion effects, especially for the smaller model **6q** which best separates out steric and electronic factors, there is nonetheless a tendency towards a decreased Ta–CH_2–Ph angle (110.8 ˚) compared to the typical values of *ca*. 120 ˚ for 'normal' benzyl ligands. As a further test of this point, calculations were performed on the sterically reduced model Ta($NN_2^{SiH_3}$)(CH_2SiH_3)$_2$ (**7q**), the analogue of **7**, also without dispersion corrections. In this case an average Ta–CH_2–SiH_3 angle of 116.6 ˚ was found, *ca.* 6 ˚ larger than in **6q** (110.8 ˚).

Overall the DFT and DFT-D3 calculations find contributions from both π–π and orbital-based stabilisation for the geometry of **6**. These interactions require varying degrees of distortion of bond distances and angles both at the benzyl methylene group and at the metal centre itself. Interestingly, as discussed below, replacing one of the benzyl groups in **6** with a strongly π-donating NH^{t}Bu group (giving Ta(NN_2^{SiMe3})(NH^{t}Bu)(CH_2Ph), **12**)

'turns off' any non-classical interaction with the remaining benzyl group, thus indicating a delicate balance of stabilising effects in these electron-deficient systems.

Conversion of the previous tantalum dialkyl complexes **4**, **5**, **6** and **7** to the corresponding alkylidenes *via* intramolecular α-H abstraction was attempted in the presence of pyridine.[56,61,66] However, no evidence of the formation of the alkylidene complex was observed by ^{1}H NMR even under forcing conditions, instead a mixture of starting material and thermal decomposition product was observed for most of them. When this reaction was attempted for Ta(N$_2$N)(CH$_2$SiMe$_3$)$_2$ (**7**) on NMR scale at 80 ˚C for 8 days (Equation 2.5), the resulting ^{1}H NMR spectra showed a new set of resonances which showed to be a product from the intramolecular C−H activation of one of the trimethylsilyl groups (NSiMe$_3$) in the backbone (Figure 2.12).[67]



Equation 2.5.

The ^{1}H (Figure 2.12) and ^{13}C NMR spectra of **8** indicate that the complex has a C_1 symmetric structure in solution. The resonances attributed to the backbone ligand include eight multiplets, integrating to 1H each, between 7.69 and 6.66 ppm for the asymmetric aryls and a singlet (0.45 ppm) for a trimethylsilyl group. The four-membered metallacycle, formed upon elimination of 1 equiv. of tetramethylsilane, displays resonances belonging to two mutually coupled doublets corresponding to the diastereotopic TaC$\underline{H}_2$SiMe$_2$ protons (0.86 and 0.45-0.43 ppm) and two singlets (0.49 and 0.10 ppm) corresponding to the diastereotopic methyl groups in the dimethylsilyl group. Also, resonances attributed to the alkyl moiety include mutually coupled doublets observed at 1.40 and 0.57 ppm which belong to the trimethylsilylmethyl ligand, TaC$\underline{H}_2$SiMe$_3$, and a singlet at 0.13 ppm for the SiMe$_3$ group. When reaction on the preparative scale in benzene solution was carried out, **8** was found to be in a mixture with thermal decomposition products and could not be isolated.

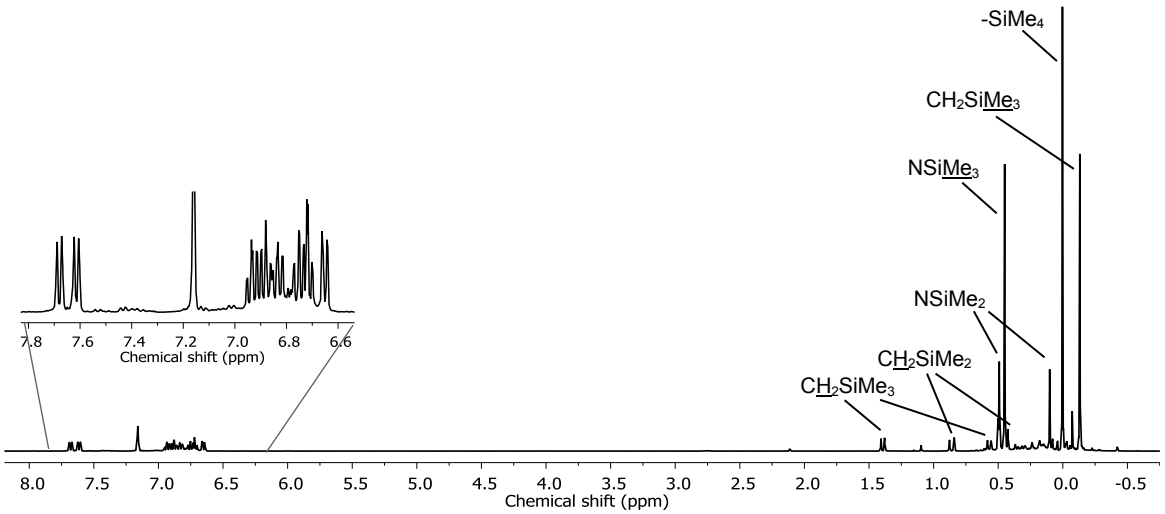


Figure 2.12. ^{1}H NMR spectrum (499.9 MHz) of the crude NMR product of Ta{NN^{SiMe3}N^{SiMe2}(CH$_2$)}(CH$_2$SiMe$_3$) (**8**) in C_6D_6 at 298 K.

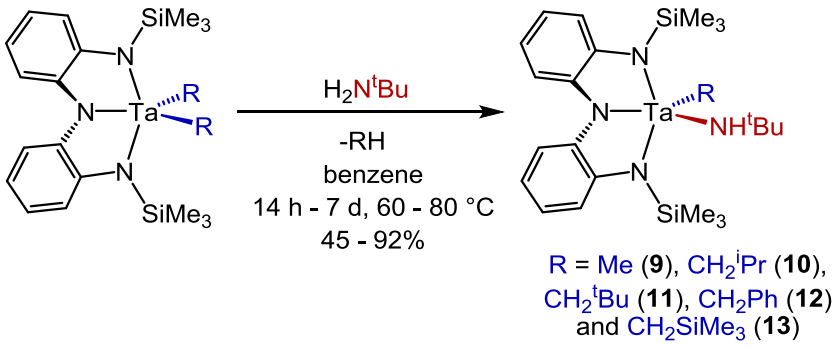
There are some literature examples of cyclometalations using high-valent Ta(V).[56] In 1988, Rothwell reported the preparation of $(ArO)_2TaR_3$ (ArO = 2,6-$C_6H_3{}^{i}Pr_2$, R = Me, Ph) from the salt metathesis reaction of phenoxides and $TaCl_5$ followed by exchange of the remaining chloride ligands with either MeLi or PhLi. Furthermore, the two cyclometalations occurred by elimination of 2 equiv. of alkane upon heating at 150 ˚C followed by the formation of the Ta−C bond from the ^{t}Bu groups in the phenoxides. The monocyclometalated complex is also reported to be obtained at milder conditions (25 ˚C) using the alkylidene precursor photochemically synthesised from $Ta(ArO)_2R_3$.[68] More recently, Bercaw and co-workers found a system capable of C−H/Ta−Me σ-bond metathesis using a potentially trianionic, tridentate ligand bis(phenolate) (OCO = 2,6-$(OC_6H_2$-$^{t}Bu_2)_2C_6H_3$). The coordination of the pincer ligand to the $TaCl_2Me_3$ complex *via* salt metathesis at RT using KBn (Bn = benzyl) followed by σ-bond metathesis affords the cyclometalated complex Ta(OCO)Me$_2$. The C−H bond activation occurring at lower temperature than the examples mentioned above is attributed to a ligand chelation. Alternatively, cyclometalation was induced by direct alkane elimination above 175 ˚C.[69]

Two mechanistic pathways are to be consider for the formation of Ta{NN^{SiMe3}N^{SiMe2}(CH$_2$)}(CH$_2$SiMe$_3$) (**8**). A cyclometalation reaction induced by direct alkane elimination followed by σ-bond metathesis for the C−H bond-activation process. Alternatively, the generation of an alkylidene ligand by α-hydrogen elimination which

simultaneously cleaves the metallacycle.[70] Future deuterium labelling experiments may reveal the mechanistic details of the C−H bond activation in the cyclometallation of **8**.

2.8.2 Reactions of tantalum alkyls with *tert*-butylamine

In Section 2.5, attempts to form the corresponding imide from the bis(amide) $Ta(NN_2^{SiMe3})(NH^tBu)_2$ (**2.1**) were described. With this in mind, the reaction of the tantalum dialkyl complexes $Ta(NN_2^{SiMe3})R_2$ with 1 equiv. of *tert*-butylamine produced five alkyl-amide compounds $Ta(NN_2^{SiMe3})(NH^tBu)R$ (R = Me (**9**), $CH_2{}^iPr$ (**10**), $CH_2{}^tBu$(**11**), CH_2Ph (**12**), CH_2SiMe_3 (**13**)) in yields between 45 and 92 % (Equation 2.5).



Equation 2.5.

The ^1H NMR spectra of the five complexes (Figure 2.13) are indicative of C_s symmetric species on the NMR timescale. The trimethylsilyl (18 H) groups corresponding to the NN_2^{SiMe3} ligand display resonances between 0.51 and 0.43 ppm. The signals observed as multiplets for the ligand aryl protons are a distinctive doublet at 7.78-7.49 ppm and two overlapped multiplets between 6.92 and 6.73 ppm. The resonances for the amide moiety include the characteristic N−H proton signals that shift between 4.72 and 4.43 ppm and the ^{t}Bu groups showed resonances in the range *ca* 0.96-0.93 ppm. A sharp medium intensity ν(N-H) band at 3249 (**9**), 3227 (**10**), 3274 (**11**) and 3248 cm^{-1} (**12**) in the IR spectra is present.

As mentioned in the introduction to this Thesis, there are several examples of tantalum and niobium *tert*-butylamide complexes reported in the literature.[71-77] However, just two examples of tantalum alkyl-amide compounds characterised crystallographically have been reported up to date. The first complex of this type was the imido-amido dialkyl tantalum complex Ta(NAr*)(NHAr*)Me_2 described by Tilley and Gavenonis in 2002.[78] One year later, Mashima and co-workers synthesised Cp*Ta(CH_2Ph)(NHC_6H_4OMe)(η^4-

DMBD) (DMBD = 2,3-dimethyl-1,3-butadiene) which was isolated at low temperature (-10 ˚C) and slowly formed the corresponding imide at RT, achieving full conversion at elevated temperature (60 ˚C).[57]

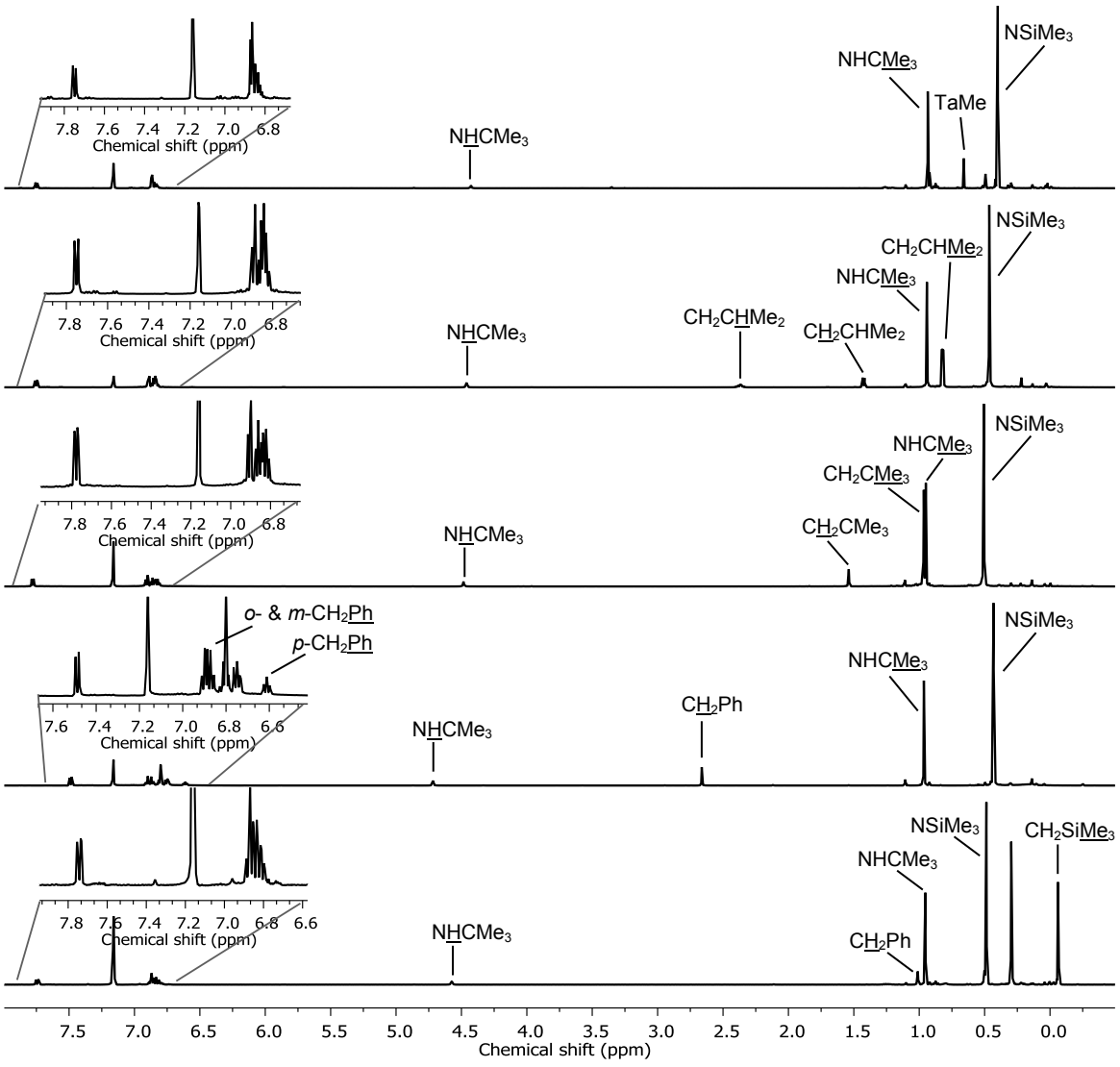


Figure 2.13. ^{1}H NMR spectra (400.1 MHz) of Ta(NN_2^{SiMe3})(NH^tBu)R (R = Me (**9**), $CH_2{}^iPr$ (**10**), $CH_2{}^tBu$(**11**), CH_2Ph (**12**), CH_2SiMe_3 (**13**), from top to bottom) in C_6D_6 at 298 K.

Diffraction-quality crystals of two tantalum alkyl-amides, **9** and **12** were grown from saturated benzene solutions at RT. The solid state structures are shown in Figure 2.14 and selected bond lengths and angles are listed in Table 2.4.

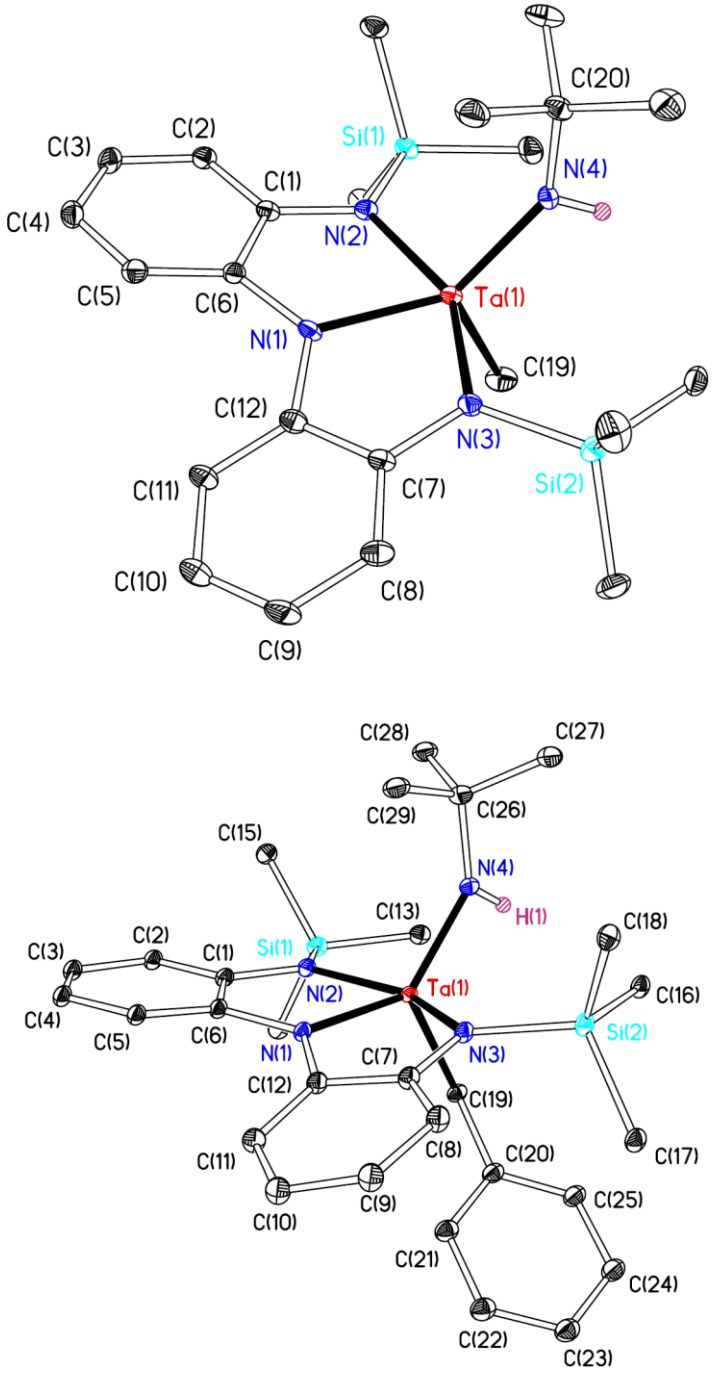


Figure 2.14. Displacement ellipsoid plots (20% probability) of $Ta(NN_2^{SiMe3})(NH^tBu)(R)$ (R = Me (**9**, top) and CH_2Ph (**12**, bottom)). C-bound H atoms omitted for clarity. Other H atoms are drawn as spheres of an arbitrary radius.

Table 2.4. Selected bond lengths (Å) and angles (°) for Ta(NN_2^{SiMe3})(NH^tBu)(R) (R = Me (**9**) or CH_2Ph (**12**)).

Parameter	**9**	**12**
Ta(1)–N(1)	2.065(3)	2.062(5)
Ta(1)–N(2)	2.064(3)	2.061(5)
Ta(1)–N(3)	2.059(3)	2.065(5)
Ta(1)–N(4)	1.954(3)	1.975(6)
Ta(1)–C(19)	2.168(3)	2.164(7)
N(2)–Si(1)	1.774(3)	1.773(6)
N(3)–Si(2)	1.780(3)	1.791(6)
N(4)–H(1)	0.88(4)	0.871(10)
N(1)–Ta(1)–N(2)	75.26(11)	75.1(2)
N(1)–Ta(1)–N(3)	75.28(11)	75.1(2)
N(2)–Ta(1)–N(3)	150.52(11)	149.8(2)
N(1)–Ta(1)–N(4)	134.05(12)	134.5(2)
N(2)–Ta(1)–N(4)	98.84(11)	97.1(2)
N(3)–Ta(1)–N(4)	100.69(12)	100.2(2)
N(1)–Ta(1)–C(19)	113.74(14)	113.2(3)
N(2)–Ta(1)–C(19)	97.19(14)	97.6(2)
N(3)–Ta(1)–C(19)	95.63(14)	98.4(2)
N(4)–Ta(1)–C(19)	112.21(14)	112.3(3)
Ta(1)–N(2)–Si(1)	124.07(15)	122.8(3)
Ta(1)–N(3)–Si(2)	124.12(16)	122.7(3)
Ta(1)–N(4)–C(20)/C(26)	139.0(2)	137.7(5)
Ta(1)–N(4)–H(1)	108(3)	99(7)
Ta(1)–C(19)–C(20)	-	121.8(5)

Both of the complexes have a distorted trigonal bipyramidal geometry. The NN_2^{SiMe3} ligand coordinates in a meridional fashion with the *o*-phenylene rings slightly twisted out of co-planarity. The angle between the C_6H_4 planes is *ca* 27.4 ˚ for **9** and 23.9 ˚ for **12**. The equatorial plane comprises N(1) from the triamide ligand, the alkyl group carbon C(19) and N(4) of the *tert*-butylamide ligand. The Ta(1)−N(4) distances of 1.954(3) and 1.975(6) Å in **9** and **12**, respectively, are equivalent within experimental error and lie within the range of those distances in eight examples of tantalum *tert*-butylamide complexes (range 1.928(7) − 2.019(3) Å). However, the Ta−N_{amide}−C angles of 139.0(2) (**9**) and 137.7(5) ˚ (**12**) are somewhat smaller than the average of the same eight examples (*ca* 147 ˚).[71,73,75-77] The N(4) bound H atoms were located from Fourier difference maps and positionally and isotropically refined. The sums of the angles subtended at N(4) are 360(1) ˚ in each case indicating sp^2 hybridisation.

The Ta(1)−C(19) bond lengths of 2.168(3) and 2.164(7) Å are equivalent within experimental error. In the case of **12** this distance is significantly shorter than in the dibenzyl complex $Ta(N_2N^{SiMe3})(CH_2Ph)_2$ (**6**, avg. 2.213(4) Å) in which the benzyl linkages were significantly distorted (avg. Ta–CH_2–Ph = 102.6(3) ˚). The earlier DFT calculations suggested that this distortion contributed to a lengthening of the Ta–CH_2Ph bond distances and widening of the PhCH_2–Ta–CH_2Ph angle (139.9(2) ˚). In contrast, the benzyl group in **12** is not distorted, having Ta−CH_2−Ph = 121.8(5) ˚. which falls into the normal range for benzyl compounds without additional phenyl-metal interactions.

All of the Ta–N distances to the NN_2^{SiMe3} ligand in **9** and **12** are longer than those to NH^tBu, consistent with the better donor ability of alkylamides compared to arylamides. In addition, the presence of the NH^tBu ligand in **9** and **12** has an effect on the Ta–N distances to the NN_2^{SiMe3} ligand, both relative to each other and in comparison with the dialkyl analogues $Ta(NN_2^{SiMe3})(CH_2R)_2$ (R = H, $SiMe_3$ or Ph). In **9** and **12** the equatorial (Ta(1)–N(1)) distances (avg. 2.064(3) Å) and axial (Ta(1)–N(2,3)) distances (avg. 2.062(2) Å) are equivalent within error. In $Ta(NN_2^{SiMe3})(CH_2R)_2$ the Ta–N_{eq} distances (avg. 2.076(2) Å) are systemmatically longer than Ta–N_{ax} (avg. 2.008(2) Å). Furthermore, the Ta–N_{eq} distances in **9** and **12** tend to be shorter than in the dialkyl counterparts, whereas Ta–N_{ax} are longer.

These geometric variations between the $Ta(NN_2^{SiMe3})(NH^tBu)(CH_2R)$ and $Ta(NN_2^{SiMe3})(CH_2R)_2$ systems can explained by reference to the bonding descriptions

developed earlier for TBP ML_5 in general and $Ta(NN_2^{SiH3})Me_2$ (**1.5q**) (*cf.* Figures 2.6 and 2.7). Replacing one of the alkyl groups of $Ta(NN_2^{SiMe3})(CH_2R)_2$ by NH^tBu (a less good σ-donor) stabilises the $1b_1$ MO of ML_5 (slightly metal-ligand σ* antibonding) allowing for a comparatively better π-interaction with the $1b_1$ π-donor orbital of NN_2^{SiMe3}, accounting for the slightly shorter $Ta–N_{eq}$ bonds in **9** and **12**. On the other hand, the presence of the out-of-plane 2p(π) lone pair on the NH^tBu ligand causes a mixing of the d_{xz} and d_{yz} π-acceptor orbitals (labelled $1b_2$ and $1a_2$ in Figure 2.6) which has a detrimental, knock-on effect on the $Ta–N_{ax}$ π-bonding. The new orbitals obtained from mixing d_{xz} and d_{yz} are oriented approximately along the $Ta–NH^tBu$ and $Ta–CH_2R$ bond vectors of **9** and **12**. This orientation favours π-bonding to NH^tBu but gives a poorer interaction with the a_2 type π-donor SALC of the NN_2^{SiMe3} ligand.

A single point DFT calculation was carried out on $Ta(NN_2^{SiMe3})(NH^tBu)(Me)$ (**9**), and the LUMO and LUMO+2 are shown in Figure 2.15. The LUMO+2 clearly shows the antibonding counterpart of the $Ta–NH^tBu$ π-bond, whereas the LUMO (which is 0.80 eV less stable) corresponds to the antibonding counterpart of the $Ta\text{-}N_{ax}$ π-interaction. The Wiberg bond indices for **9** reflect the variations in the various Ta–N π-interactions: for $Ta–N_{eq}$, WBI = 0.694; for $Ta–N_{ax}$, WBI = 0.760 (avg.); for $Ta–NH^tBu$, WBI = 0.932). Overall, **9** and **12** can be regarded formally as 16 valence electron compounds.

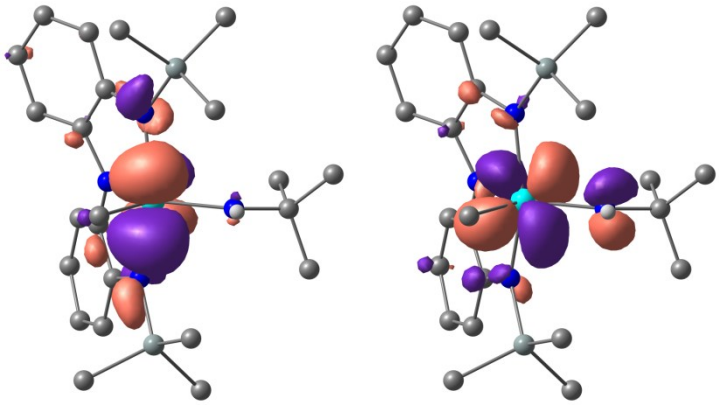


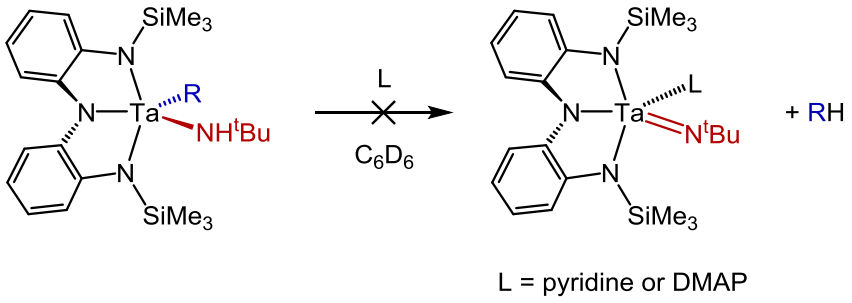
Figure 2.15. Selected MOs of $Ta(NN_2^{SiMe3})(NH^tBu)(Me)$ (**9**). Left: LUMO, energy = -1.35 eV. Right: LUMO+2, energy = -0.55 eV. Isosurfaces are drawn at the 0.0622 a.u. contour level. C-bound H atoms omitted

2.8.3 Reactions of tantalum alkyl-amide complexes with Lewis bases

Over the last 60 years, the chemistry of transition metal complexes containing terminal imido ligands has been extensively studied.[79-84] The use of imido synthons of the type $M(NR)_xCl_y(L)_z$ (M = Groups 4 – 6 transition metals; R = alkyl or aryl substituents; L = Lewis base) of group 4,[85-89] 5[90-97] and 6[98-102] metals have proved to be useful in reactions with a variety of lithiated ligands which have changed the synthesis of imido complexes in the last three decades. In Chapter 3 of this Thesis, salt metathesis reactions between synthons of the type $M(N^tBu)Cl_3(L)$ (M = Group 5 transition metal; L = Lewis base) and tridentate, trianionic ligands will be described.

Synthesis of imido compounds has been also achieved by addition of primary amines. For example, our research group reported the reaction of the dichloride species $Zr(N_2NN')Cl_2$ with $LiCH_2SiMe_3$, H_2N^tBu and pyridine to give the imido complex $Zr(N_2NN')(N^tBu)(py)$ (N_2NN' = $(2\text{-}C_5H_4N)CH_2N(CH_2CH_2NSiMe_3)_2$).[103] Having already synthesised the tantalum alkyl-amide complexes $Ta(NN_2^{SiMe3})(NH^tBu)R$ in this work (discussed in the previous section), attempt to generate the tantalum imido functionality by the addition of a Lewis base (pyridine or 4-(dimethylamino)pyridine (DMAP)) proved to be unsuccessful as product mixtures were obtained (Equation 2.6).

Formation of an imido complex was identified after heating $Ta(NN_2^{SiMe3})(NHSiMe_3)(CH_2Ph)$ (**12**) in the presence of pyridine at 80 ˚C. After 5 days **12** was completely consumed giving a mixture of an unknown product and the imido compound identified by ^1H NMR spectroscopy as $Ta(N^tBu)(NN_2^{SiMe3})(py)_2$ in a 2:1 ratio, yet the tantalum imide compound could not be successfully isolated. Thus, the final step to obtain the tantalum hydrazide complexes from amide compounds in this synthetic route could not be performed.



Equation 2.6

2.9 Conclusions and Outlook

In this Chapter, three different synthetic routes towards the synthesis of tantalum hydrazido complexes with tridentate, trianionic pincer ligands have been described. Additionally, the synthesis and characterisation of two new lithiated pincer ligands, $Li_3(NN_2^{Me})$ (**1**) and $Li_3(NN_2^{iPr})$ (**2**), and the key starting material $Ta(NN_2^{SiMe3})Cl_2$ (**3**), obtained *via* salt metathesis reaction of $TaCl_5$ with the ligand $Li_3(NN_2^{SiMe3})$ (**1.7**), were studied. DFT calculations performed on the model compound $Ta(NN_2^{SiH3})Me_2$ (**1.5q**) gave a better understanding of the bonding interaction in complexes $Ta(NN_2^{R})X_2$ (X = one-electron donor such as Cl or alkyl; R = amide ligand substituents), which due to symmetry restrictions the lone pare of the equatorial amide ligand is effectively non-bonding reducing the formal electron count to 14 valence electron (d^0) complexes.

Route A involved a one-step synthesis by reacting the dichloride species **3** with either H_2NNPh_2 (in presence of pyridine as a base) or $LiNHNPh_2$. Both cases proved to be unsuccessful for the synthesis of the tantalum hydrazide. A second attempt involved the synthesis of the monomethyl-monochloride species which was observed from the exchange reaction of **3** with the dimethyl species $Ta(NN_2^{SiMe3})Me_2$ **1.5**, however this could not be isolated. Finally, the attempt to form the imide complex from $Ta(NN_2^{SiMe3})(NH^tBu)_2$ (**2.1**) in the presence of pyridine was not successful.

Route B described the study of the reactivity of a tantalum hydrazide precursor, $Ta(NNPh_2)Cl_3(DME)$ (**1.80**) with the tripodal pincer ligand $Li_3(NNN^R)$ (R = ^{i}Pr (**1.8**) or $SiMe_3$ (**1.9**)). Evidence of the formation of the hydrazido complexes of the type $Ta(NNN^R)(NNPh_2)$ was observed by ^{1}H NMR spectroscopy, and several byproducts were crystallographically characterised. Unfortunately, the isolation of a single hydrazide complex was not achieved.

In the Route C, a multistep synthesis route was studied. The first step was the synthesis of four new dialkyl compounds $Ta(NN_2^{SiMe3})R_2$ (R = $CH_2{}^iPr$ (**4**), $CH_2{}^tBu$ (**5**), CH_2Ph (**6**), CH_2SiMe_3 (**7**)). The smaller Ta−CH_2−Ph angles in complexes **6** were explored through DFT and DFT-D3 calculations, concluding that both dispersive (π−π) interactions and orbital-based stabilisation geometry are more important than the steric demands of the bulky $SiMe_3$ amide ligand substituents. The second step was the reaction of the dialkyl complexes $Ta(NN_2^{SiMe3})R_2$ with *tert*-butylamine to give the corresponding alkyl-amides $Ta(NNN^{SiMe3})(NH^tBu)R$ (R = Me (**9**), $CH_2{}^iPr$ (**10**), $CH_2{}^tBu$(**11**), CH_2Ph (**12**), CH_2SiMe_3

(**13**)). Molecular structure metrics and DFT calculations on complex **9** showed that replacement of one of the alkyl groups by NH^tBu stabilises these electron-deficient systems (dialkyl complexes) allowing a better π−interaction with the equatorial amide ligand. In addition to the synthesis and characterisation of these complexes, an unexpected product from the intramolecular C−H activation of the trimethylsilyl group ($NSiMe_3$) in the ligand backbone in $Ta(NN_2^{SiMe3})(CH_2SiMe_3)_2$ (**7**) was observed by ^1H NMR spectroscopy. In a third step, the alkyl-amide complexes $Ta(NNN^{SiMe3})(NH^tBu)R$ in the presence of a Lewis base (pyridine or DMAP) formed mixtures of products, possible as a result of forcing conditions (high temperatures) that resulted in decomposition products. Thus, the fourth and final step to obtain the tantalum hydrazide complexes could not be performed.

Looking forward, the chemistry of the synthesised tantalum dialkyl and alkyl-amido complexes could be further explored with donors such as phospines, amines (different to NH_2^tBu), ethers, thioethers, and carbenes towards the formation of tantalum alkylidene complexes with tridentate, trianionic pincer ligands.

2.10 References

1. D. J. Mindiola, *Angew. Chem., Int. Ed.*, 2008, **47**, 1557-1559.
2. A. J. Clulow, J. D. Selby, M. G. Cushion, A. D. Schwarz and P. Mountford, *Inorg. Chem.*, 2008, **47**, 12049-12062.
3. S. Mellino, L. C. Stevenson, E. Clot and P. Mountford, *Organometallics*, 2017, **36**, 3329-3342.
4. L. C. Stevenson, S. Mellino, E. Clot and P. Mountford, *J. Am. Chem. Soc.*, 2015, **137**, 10140-10143.
5. J. Unruangsri, H. Morgan, A. D. Schwarz, A. D. Schofield and P. Mountford, *Organometallics*, 2013, **32**, 3091-3107.
6. P. J. Tiong, L. R. Groom, E. Clot and P. Mountford, *Chem. Eur. J.*, 2013, **19**, 4198-4216.
7. P. J. Tiong, A. Nova, A. D. Schwarz, J. D. Selby, E. Clot and P. Mountford, *Dalton Trans.*, 2012, **41**, 2277-2288.
8. J. D. Selby, M. Feliz, A. D. Schwarz, E. Clot and P. Mountford, *Organometallics*, 2011, **30**, 2295-2307.

9. P. J. Tiong, A. Nova, L. R. Groom, A. D. Schwarz, J. D. Selby, A. D. Schofield, E. Clot and P. Mountford, *Organometallics*, 2011, **30**, 1182-1201.
10. A. D. Schofield, A. Nova, J. D. Selby, A. D. Schwarz, E. Clot and P. Mountford, *Chem. Eur. J.*, 2011, **17**, 265-285.
11. A. D. Schofield, A. Nova, J. D. Selby, C. D. Manley, A. D. Schwarz, E. Clot and P. Mountford, *J. Am. Chem. Soc.*, 2010, **132**, 10484-10497.
12. P. D. Schweizer, H. Wadepohl and L. H. Gade, *Organometallics*, 2013, **32**, 3697-3709.
13. K. Weitershaus, J. Lloret Fillol, H. Wadepohl and L. H. Gade, *Organometallics*, 2009, **28**, 4747-4757.
14. K. Weitershaus, H. Wadepohl and L. H. Gade, *Organometallics*, 2009, **28**, 3381–3389.
15. P. D. Schweizer, H. Wadepohl and L. H. Gade, *Organometallics*, 2014, **33**, 1726-1739.
16. S. A. Scholl, H. Wadepohl and L. H. Gade, *Organometallics*, 2013, **32**, 937-940.
17. T. Gehrmann, G. T. Plundrich, H. Wadepohl and L. H. Gade, *Organometallics*, 2012, **31**, 3346-3354.
18. T. Gehrmann, J. Lloret Fillol, H. Wadepohl and L. H. Gade, *Organometallics*, 2010, **29**, 28-31.
19. I. A. Tonks, A. C. Durrell, H. B. Gray and J. E. Bercaw, *J. Am. Chem. Soc.*, 2012, **134**, 7301-7304.
20. C. Redshaw and M. R. J. Elsegood, *Inorg. Chem.*, 2000, **39**, 5164-5168.
21. M. Hidai, *Coord. Chem. Rev.*, 1999, **185-186**, 99-108.
22. J. D. Niemoth-Anderson, J. R. D. Debord, T. Adrian George, C. R. Ross and J. J. Stezowski, *Polyhedron*, 1996, **15**, 4031-4040.
23. Z. Janas, L. B. Jerzykiewicz, R. L. Richards and P. Sobota, *Inorg. Chem. Acta*, 2003, **350**, 379-386.
24. C. Manzur, D. Carrillo, F. Robert, P. Gouzerh and J.-R. Hamon, *Organometallics*, 1998, **17**, 3728-3732.
25. C. Bustos, C. Manzur, D. Carrillo, F. Robert and P. Gouzerh, *Inorg. Chem.*, 1994, **33**, 1427-1433.
26. C. Bustos, C. Manzur, D. Carrillo, F. Robert and P. Gouzerh, *Inorg. Chem.*, 1994, **33**, 4937-4944.

27. J. Chatt, J. R. Dilworth, P. L. Dahlstrom and J. Zubieta, *J. Chem. Soc., Chem. Commun.*, 1980, 786-787.
28. H. Ishino, S. i. Tokunaga, H. Seino, Y. Ishii and M. Hidai, *Inorg. Chem.*, 1999, **38**, 2489-2496.
29. L. D. Field, N. G. Jones and P. Turner, *Organometallics*, 1998, **17**, 2394-2398.
30. Y. Ishii, S. i. Tokunaga, H. Seino and M. Hidai, *Inorg. Chem.*, 1996, **35**, 5118-5119.
31. J. D. Selby, C. D. Manley, M. Feliz, A. D. Schwarz, E. Clot and P. Mountford, *Chem. Comm.*, 2007, 4937-4939.
32. I. A. Tonks and J. E. Bercaw, *Inorg. Chem.*, 2010, **49**, 4648-4656.
33. A. J. Keane, P. Y. Zavalij and L. R. Sita, *J. Am. Chem. Soc.*, 2013, **135**, 9580-9583.
34. M. E. O'Reilly and A. S. Veige, *Chem. Soc. Rev.*, 2014, **43**, 6325-6369.
35. R. R. Schrock and P. Meakin, *J. Am. Chem. Soc.*, 1974, **96**, 5288-5290.
36. R. R. Schrock, J. Lee, L.-C. Liang and W. M. Davis, *Inorg. Chim. Acta*, 1998, **270**, 353-362.
37. S. Daniele, P. B. Hitchcock, M. F. Lappert, T. A. Nile and C. M. Zdanski, *J. Chem. Soc., Dalton Trans.*, 2002, 3980-3984.
38. J. Koller, S. Sarkar, K. A. Abboud and A. S. Veige, *Organometallics*, 2007, **26**, 5438-5441.
39. A. Cooper, M. Chem. Thesis, University of Oxford, 2014.
40. K. V. Tan, P. A. Pellegrini, B. W. Skelton, C. F. Hogan, I. Greguric and P. J. Barnard, *Inorg. Chem.*, 2014, **53**, 468-477.
41. L. H. Gade and N. Mahr, *J. Chem. Soc. Dalton Trans.*, 1993, **4**, 489-494.
42. P. Ren, O. Vechorkin, K. v. Allmen, R. Scopelliti and X. Hu, *J. Am. Chem. Soc.*, 2011, **133**, 7084-7095.
43. A. W. Addison, T. N. Rao, J. Reedijk, J. van Rijn and G. C. Verschoor, *J. Chem. Soc., Dalton Trans.*, 1984, 1349-1356.
44. D. S. Marlin, M. M. Olmstead and P. K. Mascharak, *Inorg. Chem.*, 2001, **40**, 7003-7008.
45. A. I. Nguyen, K. J. Blackmore, S. M. Carter, R. A. Zarkesh and A. F. Heyduk, *J. Am. Chem. Soc.*, 2009, **131**, 3307-3316.

46. R. F. Munhá, R. A. Zarkesh and A. F. Heyduk, *Inorg. Chem.*, 2013, **52**, 11244-11255.
47. J. D. Selby, C. D. Manley, A. D. Schwarz, E. Clot and P. Mountford, *Organometallics*, 2008, **27**, 6479-6494.
48. B. D. Ward, G. Orde, E. Clot, A. R. Cowley, L. H. Gade and P. Mountford, *Organometallics*, 2005, **24**, 2368-2385.
49. A. J. Blake, P. E. Collier, L. H. Gade, P. Mountford, J. Lloyd, S. M. Pugh, M. Schubart, M. E. G. Skinner and D. J. M. Trösch, *Inorg. Chem.*, 2001, **40**, 870-877.
50. T. A. Albright, J. K. Burdett and M.-H. Whangbo, *Orbital Interactions in Chemistry*, Wiley-Interscience, New York, 1985.
51. A. R. Rossi and R. Hoffmann, *Inorg. Chem.*, 1975, **14**, 365-374.
52. E. J. Hawrelak and P. A. Deck, *Organometallics*, 2004, **23**, 9-11.
53. D. R. Armstrong, A. Carstairs and K. W. Henderson, *Organometallics*, 1999, **18**, 3589-3596.
54. N. Lu and H. Wang, *J. Struct. Chem.*, 2016, **57**, 47-53.
55. M. Hirotsu, P. P. Fontaine, A. Epshteyn and L. R. Sita, *J. Am. Chem. Soc.*, 2007, **129**, 9284-9285.
56. T. Agapie, M. W. Day and J. E. Bercaw, *Organometallics*, 2008, **27**, 6123-6142.
57. K. Mashima, H. Yonekura, T. Yamagata and K. Tani, *Organometallics*, 2003, **22**, 3766-3772.
58. A. Sattler and G. Parkin, *Organometallics*, 2015, **34**, 1828-1843.
59. L. P. H. Lopez, R. R. Schrock and P. J. Bonitatebus, *Inorg. Chim. Acta*, 2006, **359**, 4730-4740.
60. S. VenkatRamani, C. D. Roland, J. G. Zhang, I. Ghiviriga, K. A. Abboud and A. S. Veige, *Organometallics*, 2016, **35**, 2675-2682.
61. J. S. Freundlich, R. R. Schrock and W. M. Davis, *Organometallics*, 1996, **15**, 2777-2783.
62. M. Bochmann, *Organometallics 1*, Oxford University Press, Oxford, U.K., 1994.
63. C. A. Hunter and J. K. M. Sanders, *J. Am. Chem. Soc.*, 1990, **112**, 5525-5534.
64. C. Janiak, *J. Chem. Soc., Dalton Trans.*, 2000, 3885-3896.
65. S. Grimme, J. Antony, S. Ehrlich and H. Krieg, *J. Chem. Phys.*, 2010, **132**, 154104.

66. L. A. Morton, S. Chen, H. Qiu and Z.-L. Xue, *J. Am. Chem. Soc*, 2007, **129**, 7277-7283.
67. A. V. Protchenko, A. D. Schwarz, M. P. Blake, C. Jones, N. Kaltsoyannis, P. Mountford and S. Aldridge, *Angew. Chem. Int. Ed.*, 2013, **52**, 568-571.
68. I. P. Rothwell, *Acc. Chem. Rev.*, 1988, **21**, 153-159.
69. T. Agapie and J. E. Bercaw, *Organometallics*, 2007, **26**, 2957-2959.
70. M. Albrecht, *Chem. Rev.*, 2010, **110**, 576-623.
71. R. E. Blake, D. M. Antonelli, L. M. Henling, W. P. Schaefer, K. I. Hardcastle and J. E. Bercaw, *Organometallics*, 1998, **17**, 718-725.
72. M. J. Humphries, M. L. H. Green, M. A. Leech, V. C. Gibson, M. Jolly, D. N. Williams, M. R. J. Elsegood and W. Clegg, *J. Chem. Soc., Dalton Trans.*, 2000, 4044-4051.
73. T. C. Jones, A. J. Nielson and C. E. F. Rickard, *J. Chem. Soc., Chem. Commun.*, 1984, 205-206.
74. P. A. Bates, A. J. Nielson and J. M. Waters, *Polyhedron*, 1985, **4**, 1391-1401.
75. B. L. Yonke, A. J. Keane, P. Y. Zavalij and L. R. Sita, *Organometallics*, 2012, **31**, 345-355.
76. A. Merkoulov, S. Schmidt, K. Harms and J. Sundermeyer, *Z. Anorg. Allg. Chem.*, 2005, **631**, 1810-1812.
77. T. R. Helgert, C. E. Webster, T. K. Hollis, H. U. Valle, P. Hillesheim and A. G. Oliver, *Inorg. Chem. Acta*, 2018, **469**, 164-172.
78. J. Gavenonis and T. D. Tilley, *Organometallics*, 2002, **21**, 5549-5563.
79. W. A. Nugent and B. L. Haymore, 1980, **31**, 123-175.
80. L. H. Gade and P. Mountford, *Coord. Chem. Rev.*, 2001, **216-217**, 68-97.
81. J. M. Mayer and W. A. Nugent, *Metal-Ligand Multiple Bonds.*, Wiley−Interscience, New York, 1988
82. D. E. Wigley, *Organoimido Complexes of the Transition Metals*, *Progress in Inorganic Chemistry*, ed. K. D. Karlin, Wiley−Interscience, New York, 1994, Vol. 42, pp. 239−482.
83. M. H. Chisholm and I. P. Rothwell, *in Comprehensive Coordination Chemistry*, ed. G. Wilkinson, R. D. Gillard and J. A. McCleverty, Pergamon Press, Oxford, 1987, Vol. 2, pp. 161−184.
84. P. Mountford, *Chem. Comm.*, 1997, 2127-2134.

85. S. C. Dunn, A. S. Batsanov and P. Mountford, *J. Chem. Soc., Chem. Comm.*, 1994, 2007-2008.
86. A. J. Blake, P. E. Collier, S. C. Dunn, W.-S. Li, P. Mountford and O. V. Shishkin, *J. Chem. Soc., Dalton Trans.*, 1997, 1549-1558.
87. D. J. Arney, M. A. Bruck, S. R. Huber and D. E. Wigley, *Inorg. Chem.*, 1992, **31**, 3749-3755.
88. S. R. Dubberley, S. Evans, C. L. Boyd and P. Mountford, *Dalton Trans.*, 2005, 1448-1458.
89. P. E. Collier, S. C. Dunn, P. Mountford, O. V. Shishkin and D. Swallow, *J. Chem. Soc., Dalton Trans.*, 1995, 3743-3745.
90. C. M. Jones, M. E. Lerchen, C. J. Church, B. M. Schomber and N. M. Doherty, *Inorg. Chem.*, 1990, **29**, 1679-1682.
91. H.-T. Chiu, S.-H. Chuang, C.-E. Tsai, G.-H. Lee and S.-M. Peng, *Polyhedron*, 1998, **17**, 2187-2190.
92. M. Galajov, C. Garcia and M. Gomez, *Dalton Trans.*, 2011, **40**, 413-420.
93. M. Gómez, C. Hernández-Prieto, A. Martín, M. Mena and C. Santamaría, *Inorg. Chem.*, 2016, **55**, 3815-3821.
94. J. Sundermeyer, J. Putterlik, M. Fotha, J. S. Fieldb and N. Ramesar, *Chem. Ber.*, 1994, **127**, 1201-1212.
95. F. Preuss, E. Fuchslocher, E. Leber and W. Towae, *Z. Naturforsch. B*, 1989, **44b**, 271—277.
96. Y. W. Chao, P. A. Wexler and D. E. Wigley, *Inorg. Chem.*, 1989, **28**, 3860-3868.
97. D. D. Devore, J. D. Lichtenhan, F. Takusagawa and E. A. Maatta, *J. Am. Chem. Soc.*, 1987, **109**, 7408-7416.
98. J. Sundermeyer, *Chem. Ber.*, 1991, **124**, 1977-1979.
99. D. C. Bradley, M. B. Hursthouse, K. M. A. Malik, A. J. Nielson and R. L. Short, *J. Chem. Soc., Dalton Trans.*, 1983, 2651-2656.
100. L. K. Johnson, R. H. Grubbs and J. W. Ziller, *J. Am. Chem. Soc.*, 1993, **115**, 8130-8145.
101. P. W. Dyer, V. C. Gibson, J. A. K. Howard, B. Whittle and C. Wilson, *Polyhedron*, 1995, **14**, 103-111.
102. H. H. Fox, K. B. Yap, J. Robbins, S. Cai and R. R. Schrock, *Inorg. Chem.*, 1992, **31**, 2287-2289.

103. M. E. G. Skinner, T. Toupance, D. A. Cowhig, B. R. Tyrrell and P. Mountford, *Organometallics*, 2005, **24**, 5586-5603.

Chapter Three

Group 5 imido complexes with tridentate, trianionic ligands: synthesis, structure and reactivity

3.1 Overview

This chapter will describe the synthesis and characterisation of new Group 5 imido complexes with tridentate, trianionic ligands. Firstly, a different synthetic route to form Group 5 imido synthons with 2,2'-bipyridyl (bipy) will be explored along with three new synthons with 4,4'-di-tert-butyl-2,2'-bipyridyl (di-^{t}Bu-bipy). Subsequently, the synthesis and characterisation of Group 5 imido complexes obtained *via* salt metathesis with lithiated ligands of the type $Li_3(NN_2^{R})$ and $Li_3(NNN^{SiMe3})$ will be discussed. Finally, reactivity studies of the imido complex $Nb(NN_2^{iPr})(N^{t}Bu)(py)_2$ with unsaturated small substrates will be explored.

3.2 Introduction

Over the last 60 years, the chemistry of transition metal complexes containing terminal imido ligands has been extensively studied.[1-6] In the last decade, imido synthons of the type $M(NR)_xCl_y(L)_z$ (M = Groups 4 – 6 transition metals; R = alkyl or aryl substituents; L = Lewis base) of Group 4[7-11], 5[12-25] and 6[26-30] metals have been useful for reactions with a variety of lithiated ligands which simplified the synthesis of imido complexes.

In Chapter 2 of this Thesis, an attempt was made to form the imido functionality from tantalum alkyl-amide complexes $Ta(NN_2^{SiMe3})(NH^{t}Bu)R$ (R = Me (**9**), $CH_2{}^{i}Pr$ (**10**), $CH_2{}^{t}Bu$ (**11**), CH_2Ph (**12**), CH_2SiMe_3 (**13**)) by addition of a Lewis base (pyridine or DMAP). As these reactions gave complicated mixtures of products, the alternative use of synthons containing an imido functionality was targeted next to obtain Group 5 metal imido complexes with tridentate, trianionic ligands in a one-step reaction.

The first Group 5 imido synthons of this type were the tantalum and niobium imides $M(NR)Cl_3(THF)_2$ (M = Ta or Nb, R = Ph, Me or ^{t}Bu) reported by Schrock and co-workers in 1980.[12] These complexes were obtained from the reaction of $M(CH_2{}^{t}Bu)Cl_3$ in THF, and RN═CHPh, which yielded *cis*- and *trans*-^{t}BuCH═CHPh and the corresponding imido complexes.[12] Later, these compounds gave access to olefin complexes of the type $Ta(NPh)(olefin)(L)_3Cl$.[31]

Previous studies by Mountford and Gade and their co-workers have shown the convenient access to imido compounds from $M(N^{t}Bu)Cl_3(py)_2$ (M = Ta (**1.41**) or Nb (**1.42**)) with diamido-amine-pyridine and diamido-pyridine ligands, analogues to the previously reported Group 4 imido complexes.[32,33] Incorporating these lithiated ligands by salt

metathesis reactions with the tantalum and niobium precursors resulted in six-coordinated neutral complexes such as the diamido-amine-pyridine-supported complex $Ta(N_2NN')(N^tBu)Cl$ (**1.49**, N_2NN' = $(2\text{-}NC_5H_4)CH_2N(CH_2CH_2NSiMe_3)_2$)[32] and the diamido-pyridine-supported compounds $M(N_2N_{py})(N^tBu)Cl(py)$ (**1.47**, M = Ta or Nb, N_2N_{py} = $MeC(2\text{-}C_5H_4N)(CH_2NSiMe_3)_2$)[33].

In general, the chemical properties of vanadium differ significantly from those of niobium and tantalum, the chemistry of which are dominated by the +5 oxidation state and are more resistant to redox processes than vanadium.[34] The relative stability of lower oxidation states (vanadium (IV), (III) and (II)) makes studies of vanadium (V) more challenging. This was exemplified by Mountford and co-workers, when efforts to obtain vanadium complexes with the diamido-pyridine ligands N_2N^{py} or N'_2N^{py} using the synthon $V(NAr)Cl_3(THF)$ resulted in product mixtures. Nonetheless, the isolation of compound $V(NAr)Cl_2(H_3N'N'N^{py})$ (**1.52**, $H_3N'N'N^{py}$ = $MeC(2\text{-}C_5H_4N)(CH_2NHSiMe_2{}^tBu)(CH_2NH_2)$)[33] was achieved, Figure 3.1.

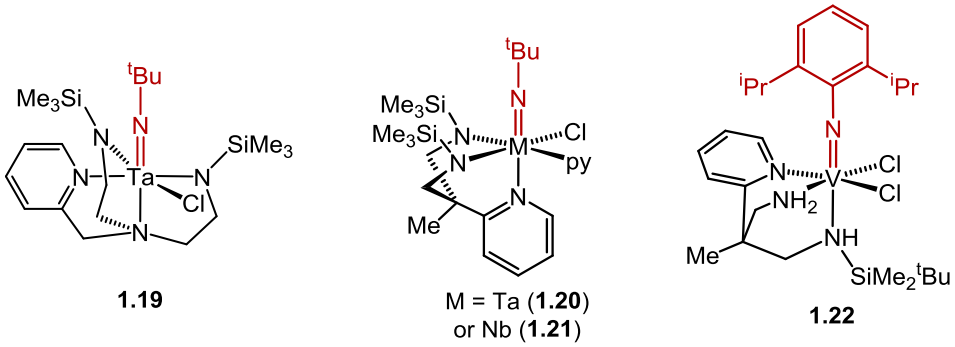


Figure 3.1. Examples of Group 5 imido complexes supported by diamido-amine-pyridine and diamido-pyridine ligands.[32,33]

Ligand exchange reactions of the imido complexes **1.41** and **1.42** showed the formation of aryloxide, amide and benzamidinate derivatives by displacement of the pyridine and the chloride ligands with the respective co-ligand.[35] Reaction of the same two complexes with $MgClCH_2Ph$, LiC_5H_4Me and $LiCHR(SiMe_3)$ (R = H or $SiMe_3$) resulted in the first Group 5 alkyl complexes incorporating both imido and diamido ligands.[35]

There is particular interest on multidentate ligands as they offer a wide variety of symmetries and donor groups, which allows to tailor the properties of the metal complex. Bercaw and co-workers studied a series of tantalum imido and amido compounds supported by the bis(phenolate)pyridine ligand (ONO^{cat}) ($(2,6\text{-}OC_6H_2\text{-}2,4\text{-}{}^tBu_2)_2NC_5H_3$)

that exhibit either C_s- or C_2-symmetric binding which is determined by the degree of Ta−O π-bonding required to complete the 18-electron count. They found that the bis(phenolate)pyridine ligand is not a strong enough π-donor to provide control over the electronic and geometric properties of the complexes.[36] The particular design of the redox-active bis(2-isopropylamino-4-methoxyphenylamine (NNN^{cat}) ligand in contrast to the well-known (ONO^{cat}) first offers three amides acting as strong π-donors towards the metal centre. This allows the ligand to have one- and two-electron oxidations to retain the formal Ta(V) metal centre. Heyduk and co-workers synthesised Ta(NNN^{cat})Cl_2 (**1.53**) by direct coordination of the ligand (NNN^{cat})H_3 with the previously reported $TaCl_2Me_3$.[37] Two-electron oxidation is observed when **1.53** reacts with PhN_3 and *p*-$^tBuC_6H_4N_3$ by releasing N_2 to afford the tantalum imido complexes Ta(NNN^{cat})(NR)Cl_2 (**1.54**, R = Ph or *p*- $^tBuC_6H_4$).[38] Nitrogen transfer to olefins, alkynes, SMe_2, H_2 and PPh_3 cannot be achieved with these imide complexes. However, they can be reduced with hydrazine to form aniline and azobenzene or fully reduced to the dichloride complex **1.53** when reactions are carried out in THF.[39,40]

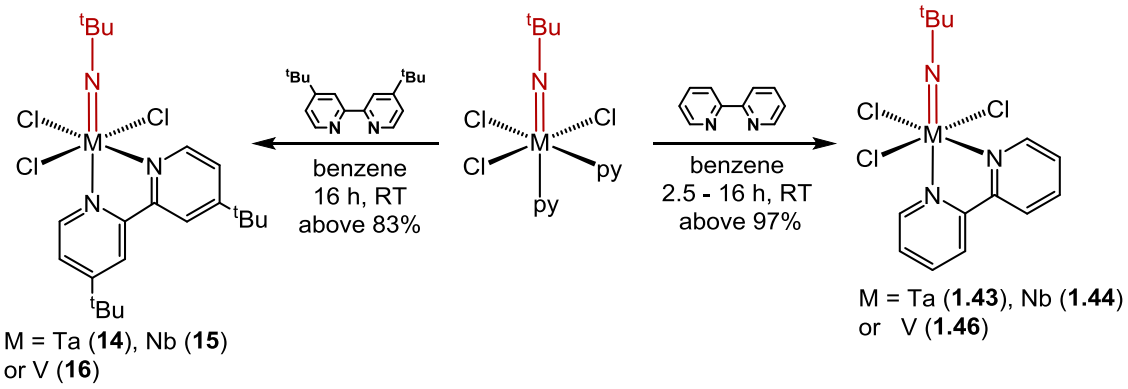
The overall aim is to access Group 5 imido complexes with tridentate, trianionic pincer ligands in order to further synthesise the corresponding hydrazido compounds by hydrazine/*tert*-butylimide exchange reactions. The synthesis and characterisation of imido complexes is presented in this Chapter and further reactions with hydrazines will be discussed in Chapter Four.

3.3 Pyridine substitution reactions of M(N^{t}Bu)$Cl_3(py)_2$ (M = Ta, Nb or V)

The imido complexes M(N^{t}Bu)$Cl_3(py)_2$ (M = Ta (**1.41**) or Nb (**1.42**)) were obtained by the reaction of the metal pentachloride and three equiv. of *tert*-butylamine, followed by the addition of 2 equiv. of pyridine to afford the microcrystalline yellow imido complexes. These compounds were first reported by Sundermeyer and co-workers along with a series of hydridotris(pyrazolyl)borate complexes of Group 5–7 metals.[18] More recently, a slightly different methodology for the synthesis of these two complexes, along with a multinuclear NMR spectroscopy analysis and the investigation of their reactivity with isocyanides and ketones, was published by Gómez and co-workers.[23] The analogous compounds M(N^{t}Bu)Cl_3(bipy) (M = Ta (**1.43**) or Nb (**1.44**), bipy = 2,2'-bipyridyl) were prepared by a similar synthetic route in 1988 by Nielson.[14] Preuss and co-workers synthesised the complexes V(N^{t}Bu)$Cl_3(py)_2$ (**1.45**)[15] and V(N^{t}Bu)Cl_3(bipy) (**1.46**)[41] by

ligand exchange reaction between $VOCl_3$ and $V(N^tBu)(OSiMe_3)_3$ yielding the trichloride complex $V(N^tBu)Cl_3$. Further reaction with either pyridine or bipy formed complexes **1.45** and **1.46**, respectively.

In this Thesis, the imido complexes **1.43**, **1.44** and **1.46** were synthesised by ligand exchange. Additionally, the previously omitted NMR characterisation data for **1.43** and **1.44** (Chapter Five) and solid state characterisation of **1.46** is further provided. The modified methodology consists of a ligand substitution reaction of the bis(pyridyl) complexes of the type $M(N^tBu)Cl_3(py)_2$ with bipy (Scheme 3.1, right).



Scheme 3.1 Synthesis of Group 5 imide synthons of the type $M(N^tBu)Cl_3$(R-bipy) (M = Ta, Nb or V; R = H or ^{t}Bu)

The solubility of the complexes $M(N^tBu)Cl_3(py)_2$ (M = Ta (**1.41**) or Nb (**1.42**)) is very limited, although both complexes are soluble enough to be characterised by NMR spectroscopy in chlorinated solvents. In order to improve the solubility of the final imido complexes, the imido synthons with the di-^{t}Bu-bipy ligand were synthesised following the same methodology described above. This yielded the synthons $M(N^tBu)Cl_3$(di-^{t}Bu-bipy) (M = Ta (**14**), Nb (**15**) or V (**16**)) (Scheme 3.1, left). The ^{1}H and ^{13}C NMR spectra are consistent with a bidentate di-*tert*-butyl-bipyridyl ligand coordinated to one axial and one equatorial position of the metal centre.[14]

Diffraction-quality crystals of **1.46** and **15** were both grown by solvent diffusion in dichloromethane/pentane at RT. The molecular solid state structures are shown in Figure 3.2 along with selected bond lengths and angles in Table 3.1.

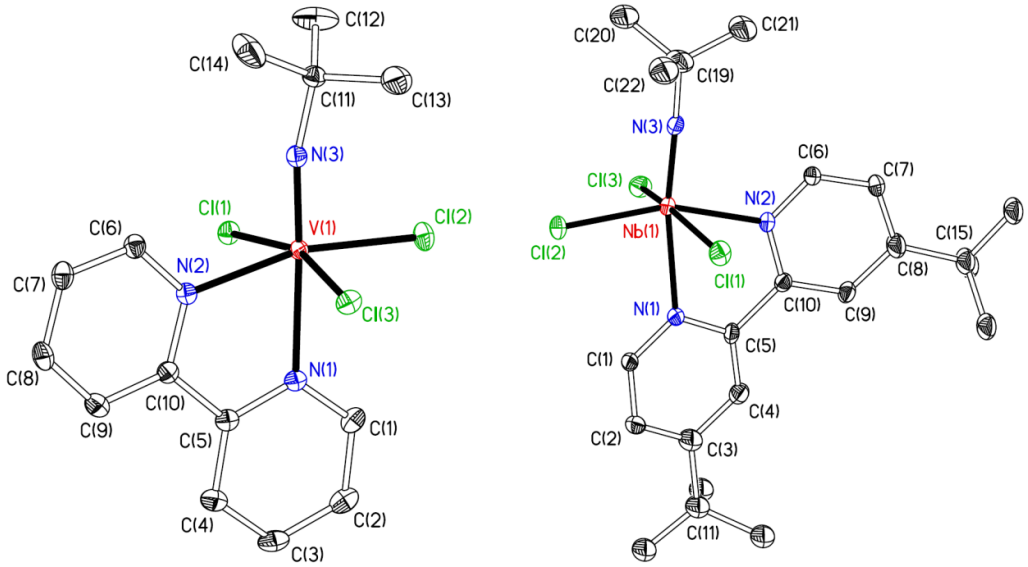


Figure 3.2. Displacement ellipsoid plot (20% probability) of V(N^{t}Bu)Cl$_3$(bipy) (**1.46**, left) and Nb(N^{t}Bu)Cl$_3$(di-^{t}Bu-bipy) (**15**, right). H atoms are omitted for clarity.

Table 3.1. Selected bond distances (Å) and angles (^{o}) for V(N^{t}Bu)Cl$_3$(bipy) (**1.46**) and Nb(N^{t}Bu)Cl$_3$(di-^{t}Bu-bipy) (**15**).

Parameter	**1.46**	**15**
M(1)–N(1)	2.241(2)	2.397(8)
M(1)–N(2)	2.119(2)	2.252(7)
M(1)–N(3)	1.645(2)	1.750(8)
M(1)–Cl(1)	2.3263(7)	2.402(2)
M(1)–Cl(2)	2.2917(7)	2.376(2)
M(1)–Cl(3)	2.3155(7)	2.417(3)
N(3)–C(11/19)	1.446(3)	1.464(15)
N(1)–M(1)–N(2)	74.75(8)	70.6(3)
N(1)–M(1)–N(3)	174.77(9)	170.5(3)
N(2)–M(1)–N(3)	100.75(9)	100.3(3)
N(1)–M(1)–Cl(1)	82.96(6)	81.6(2)
N(2)–M(1)–Cl(1)	83.76(6)	81.9(2)
N(3)–M(1)–Cl(1)	99.33(8)	94.9(3)
N(1)–M(1)–Cl(2)	90.28(6)	89.18(19)

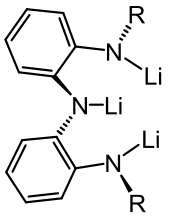
N(2)–M(1)–Cl(2)	165.03(6)	159.7(2)
N(3)–M(1)–Cl(2)	94.22(8)	100.0(3)
Cl(1)–M(1)–Cl(2)	94.11(3)	96.90(10)
N(1)–M(1)–Cl(3)	82.94(6)	81.9(2)
N(2)–M(1)–Cl(3)	84.04(6)	81.1(2)
N(3)–M(1)–Cl(3)	94.03(8)	99.5(3)
Cl(1)–M(1)–Cl(3)	163.36(3)	159.41(10)
Cl(2)–M(1)–Cl(3)	94.75(3)	94.97(10)
M(1)–N(3)–C(11/19)	167.06(19)	171.5(9)

Both complexes have distorted octahedral geometries, in which the two nitrogen atoms of the bipy ligand coordinate to the metal centre occupying an axial and an equatorial position and the three chloro ligands are arranged in a meridional fashion. Therefore, their geometry is entirely analogous to the previously structurally characterised complexes $M(NAr)Cl_3(DME)$ (M = Ta or Nb, Ar = 2,6-diisopropylphenyl, DME = 1,2-dimethoxyethane)[19], $M(NAr)Cl_3(TMEDA)$ (M = Ta or Nb, Ar = 2,6-diisopropylphenyl, TMEDA = tetramethylethylenediamine)[19] and $M(N^tBu)Cl_3(DME)$ (M = Nb[42] or V[25], DME = 1,2-dimethoxyethane). The metal-imide fragment presents the standard characteristics of high-valent metal-imido complexes, in which the angle $M{-}N_{imide}{-}C$ slightly deviates from linearity (V, 167.06(19)˚; Nb, 171.5(9)˚) and the short $M{-}N_{imide}$ bond length of 1.645(2) Å (**1.46**) and 1.750(8) Å (**15**) are consistent with a formal M≡N multiple bond. Within the $MCl_3(L)$ fragment, the most notable feature is the *trans* influence of the imide ligand to the bipyridyl donor in the axial position which has a longer M−N bond length, with values of 2.241(2) (**1.46**) and 2.397(8) Å (**15**), than the *cis*-bonded bipyridyl ring at 2.119(2) (**1.46**) and 2.252(7) Å (**15**).[19]

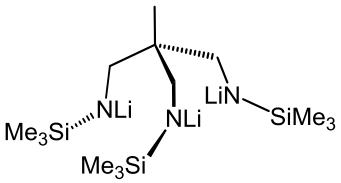
3.4 Installation of tridentate, trianionic supporting ligands

Selection and synthesis of the lithiated tridentate, trianionic pincer ligands $Li_3NN_2^R$ (R = Me (**1**), ^{i}Pr (**2**) or $SiMe_3$ (**1.7**)) and $Li_3(NNN^{SiMe3})$ (**1.9**) were described in Chapter Two of this Thesis (Figure 3.3) along with the synthesis of the tantalum alkyl-amide complexes. Mindful of the failure to generate the imido functionality from the tantalum alkyl-amide

compounds in the presence of a Lewis base, the alternative synthetic route by salt metathesis reaction between the synthons of the type $M(N^tBu)Cl_3(L)$ (M = Group 5 transition metals; L_B = py, bipy or di-^{t}Bu-bipy) and tridentate, trianionic ligands, $Li_3(NN_2^R)$ or $Li_3(NNN^{SiMe3})$, was explored and is described in this section.



R = Me (**1**), iPr (**2**) or $SiMe_3$ (**1.7**)

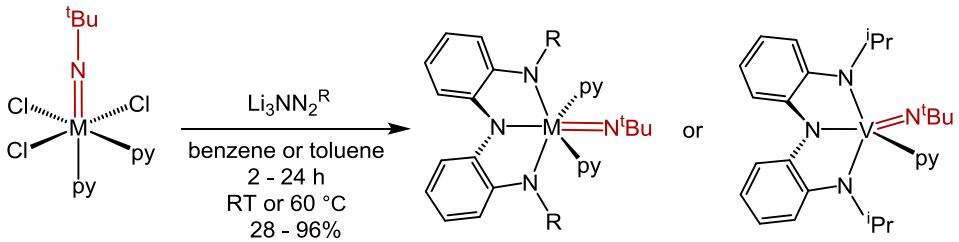


1.4

Figure 3.3. Tridentate, trianionic pincer ligands selected, $Li_3NN_2^R$ (R = Me (**1**), ^{i}Pr (**2**) or $SiMe_3$ (**1.7**)) and $Li_3(NNN^{SiMe3})$ (**1.9**).[43-45]

3.4.1 Installation of NN_2^R supporting ligands

Salt metathesis reactions of the synthons $M(N^tBu)Cl_3(py)_2$ (M = Ta (**1.41**), Nb (**1.42**) or V(**1.45**)) with the respective lithiated ligand $Li_3(NN_2^R)$ (R = Me (**1**), ^{i}Pr (**2**) or $SiMe_3$ (**1.7**)) produced seven imido complexes $M(NN_2^R)(N^tBu)(py)_2$ (M = Ta, R = Me (**17**), ^{i}Pr (**18**) or $SiMe_3$ (**19**); M = Nb, R = Me (**20**), ^{i}Pr (**21**) or $SiMe_3$ (**22**)) and $V(NN_2^{iPr})(N^tBu)Cl_3(py)$ (**23**) as shown in Equation 3.1. The reaction conditions of most of these compounds were similar (rapid at RT), except for **19** and **22** where heating at 60 ˚C for 24 and 16 h was needed. This was attributed to the high steric bulk of the $SiMe_3$ groups. Characterisation of these compounds by ^{1}H (Figure 3.4) and ^{13}C NMR spectroscopy is consistent with C_{2v} symmetric molecules (except for complex **23**) in which two equivalent pyridine ligands and the imido moiety are coordinated to the tantalum or niobium centre.



M = Ta, R = Me (**17**), ^{i}Pr (**18**) or $SiMe_3$ (**19**); M = Nb, R = Me (**20**), ^{i}Pr (**21**) or $SiMe_3$ (**22**)

23

Equation 3.1

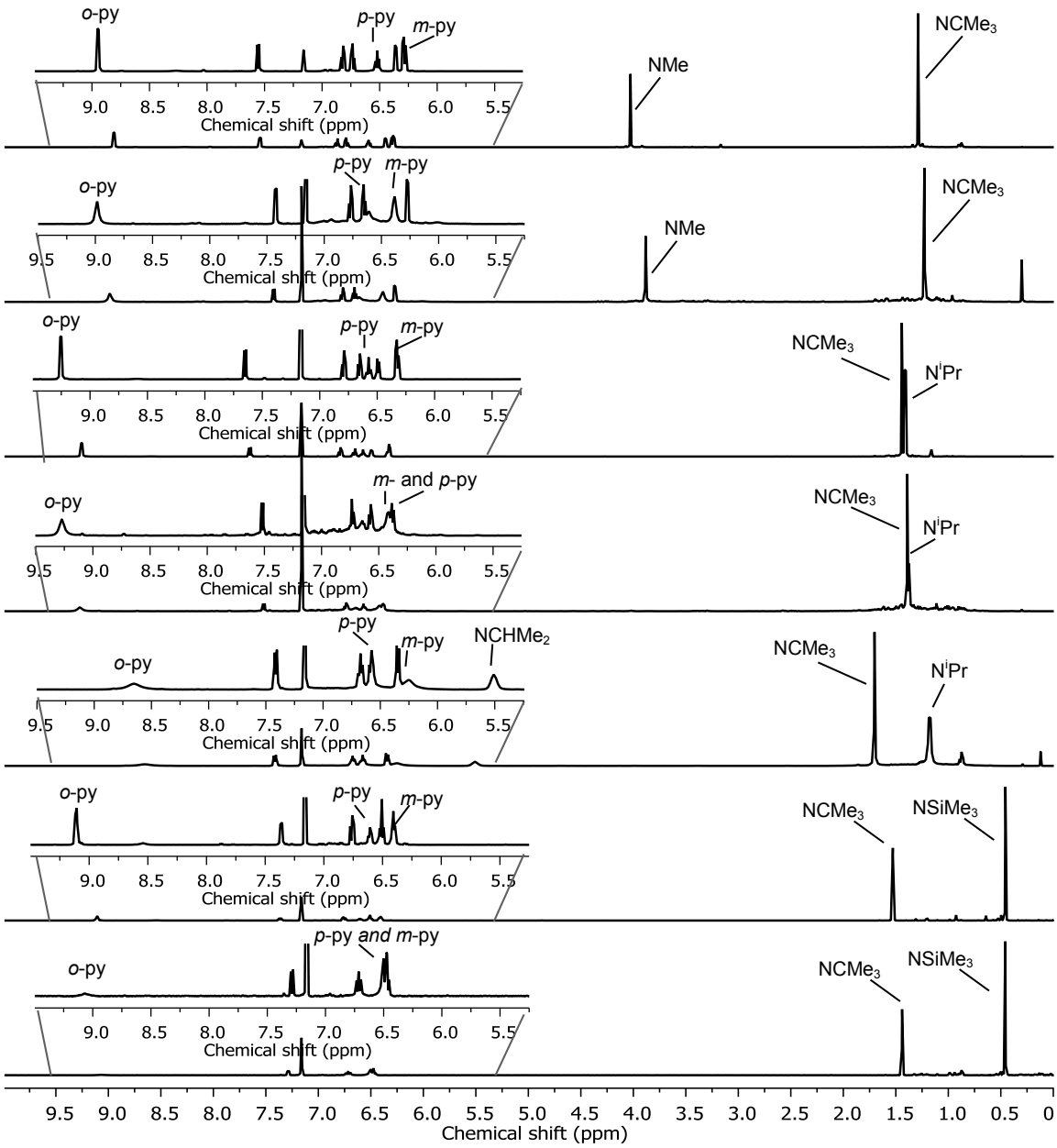


Figure 3.4. ^{1}H NMR spectra (500.3 MHz) of, from top to bottom, Ta(NN_2^{Me})(N^tBu)$(py)_2$ (**17**), Nb(NN_2^{Me})(N^tBu)$(py)_2$ (**20**), Ta(NN_2^{iPr})(N^tBu)$(py)_2$ (**18**), Nb(NN_2^{iPr})(N^tBu)$(py)_2$ (**21**), V(NN_2^{iPr})(N^tBu)(py) (**23**), Ta(NN_2^{SiMe3})(N^tBu)$(py)_2$ (**19**) and Nb(NN_2^{SiMe3})(N^tBu)$(py)_2$ (**22**) in C_6D_6 at 298 K.

The NMR data further suggests the coordination of just one pyridine ligand to the metal centre in the case of vanadium (**23**). In particular, the *tert*-butyl imido moiety can be observed as a singlet between 1.70 to 1.23 ppm. Further, the resonances can be attributed to the tridentate supporting ligand which methyl (singlet in the range 4.00 – 3.88 ppm), isopropyl (doublet in the range *ca* 1.41 – 1.18 ppm, broadened septet at 5.55 ppm for the isopropyl methine was observed only for **23**) or trimethylsilyl groups (singlet at 0.46 ppm

for both complexes **19** and **22**). Finally, the aryl rings displaying four multiplet resonances (in some cases two of these can be overlapped) in the range *ca* 7.65 – 6.27 ppm.

Diffraction–quality crystals of compound **17** were grown from a saturated benzene-d_6 solution at RT and the molecular solid state structure is shown in Figure 3.5 with selected bond lengths and angles in Table 3.2.

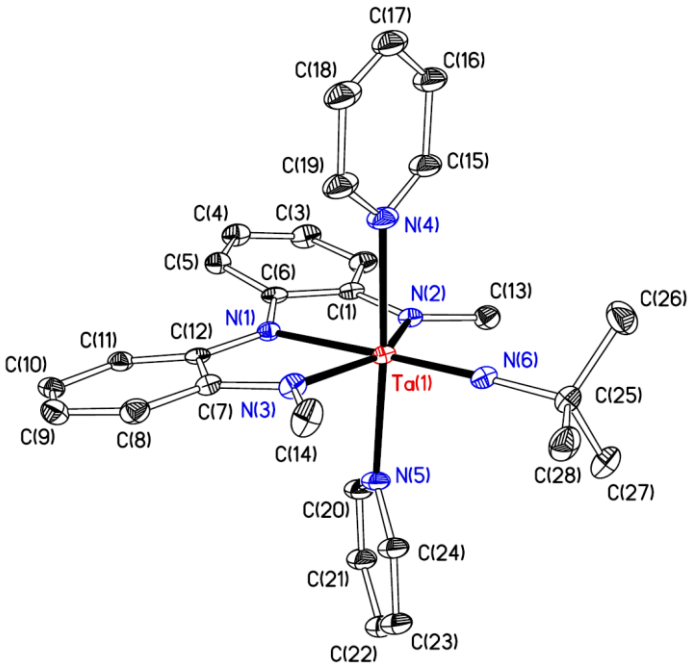


Figure 3.5. Displacement ellipsoid plot (20% probability) of $Ta(NN_2^{Me})(N^tBu)(py)_2$ (**17**). H atoms omitted for clarity.

Table 3.2. Selected bond distances (Å) and angles (°) for $Ta(NN_2^{Me})(N^tBu)(py)_2$ (**17**).

Ta(1)–N(1)	2.186(2)	N(1)–Ta(1)–N(2)	74.89(10)
Ta(1)–N(2)	2.054(2)	N(1)–Ta(1)–N(3)	74.50(10)
Ta(1)–N(3)	2.047(3)	N(2)–Ta(1)–N(3)	149.36(10)
Ta(1)–N(4)	2.277(3)	N(1)–Ta(1)–N(4)	86.96(10)
Ta(1)–N(5)	2.280(3)	N(2)–Ta(1)–N(4)	88.09(12)
Ta(1)–N(6)	1.820(3)	N(3)–Ta(1)–N(4)	91.67(13)
N(2)–C(13)	1.460(4)	N(1)–Ta(1)–N(5)	87.31(10)
N(3)–C(14)	1.455(4)	N(2)–Ta(1)–N(5)	87.43(11)

N(6)–C(25)	1.435(4)	N(3)–Ta(1)–N(5)	89.78(12)
		N(4)–Ta(1)–N(5)	173.49(12)
		N(1)–Ta(1)–N(6)	178.90(10)
		N(2)–Ta(1)–N(6)	105.85(11)
		N(3)–Ta(1)–N(6)	104.74(11)
		N(4)–Ta(1)–N(6)	93.87(12)
		N(5)–Ta(1)–N(6)	91.89(12)
		Ta(1)–N(2)–C(13)	124.9(2)
		Ta(1)–N(3)–C(14)	125.6(2)
		Ta(1)–N(6)–C(25)	176.5(2)

Complex Ta(NN_2^{Me})(N^tBu)$(py)_2$ (**17**) has two pyridine ligands (*trans* to each other) and the imido moiety in the equatorial plane, along with an N_{aryl} atom from the pincer ligand. The angles subtended at the metal between these ligands in the equatorial positions are all close to the ideal 90˚ expected for a regular octahedral geometry. However, a distortion in the geometry is observed in the tridentate ligand NN_2^{Me} which sits along the axial positions and that, due to steric constrains, forms an angle N(2)−Ta(1)−N(3) of 149.36(10)˚ which is consistent with the solid state structures of tantalum complexes when this type of ligand is coordinated (avg. N(2)−Ta(1)−N(3) of 150.6˚, range 149.8(2) – 151.07(19)˚ for five examples previously described in Chapter Two). The aryl rings in the NN_2^{Me} ligand are slightly twisted from each other out of planarity, the angle between the planes being *ca* 18.64˚.[43]

The Ta═N_{imide} distance of 1.820(3) Å is relatively long compared to other tantalum and niobium terminal *tert*-butylimides reported, with examples ranging from 1.61(3) to 1.793(7) Å.[33,46-50] Although, it is similar to the Ta═N_{imide} bond length of the previously reported tantalum arylimide Ta(N_2N^{py})(NAr')Cl(py) (Ar' = 2,6-$C_6H_3{}^iPr_2$) with a value of 1.822(4) Å.[33] Mountford and co-workers attributed a greater M≡N distance partially to the steric crowed coordination environment of the arylimido group, but also more significantly to the *trans* influence of these imido R group.[33,51] Thus, the long bond distance observed in complex **17** is probably due to a stronger *trans* influence of the N_{aryl}

from the pincer ligand. This is also observed in the two further niobium imide complexes as would be expected from the essentially identical covalent radii of Ta and Nb,{Cordero, 2008 #267;Pyykkö, 2009 #266} the solid state structures are reported herein. The Ta−N_{imide}−C(25) angle of 176.5(2)˚ is close to linearity.

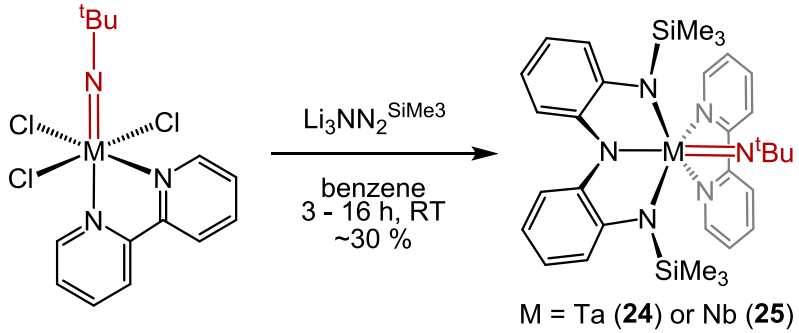
The Ta(1)−N(1) bond length in the imido complex **17** of 2.186(2) Å is longer than in the amide-alkyl complexes (2.065(3) (**9**) and 2.062(5) Å (**12**)) and the dialkyl compounds (2.086(4) (**6**) and 2.062(5) Å (**7**)) described in Chapter Two of this Thesis, consistent with the trans-bond lengthening effect of imido ligands and π-bonding competition in these complexes (*vide infra*).[51] The Ta−N(2) and Ta−N(3) bonds length in **17** (2.054(2) and 2.047(3) Å respectively) are slightly shorter than the alkyl-amides complexes **9** (2.064(3) and 2.059(3)Å) and **12** (2.061(5) and 2.065(5)Å). The two pyridine ligands positioned *trans* to each other have Ta–N bond lengths of 2.277(3) and 2.280(3) Å which are similar to that of the pyridine ligand *cis* to the imide moiety in Ta(N^tBu)$Cl_3(py)_2$ (**1.41**)[20]. These values are significantly shorter than the pyridine ligand in complexes M(N^tBu)Cl(N_2N_{py})(py) (**1.47**, M = Ta or Nb) and Ta(N_2N^{py})(NAr')Cl(py)[33] as lengthening of the Ta−N_{py} bond is observed as a result of the relatively strong *trans* influence of the imido ligand.[51]

Previously, our research group obtained the isolated intermediate Nb(N^tBu)Cl(N_2N^{py}) (**1.48**) by high-vacuum (10^{-6} mbar) sublimation of Nb(N^tBu)Cl(N_2N^{py})(py) in which the imido group is positioned *cis* to the pyridine ligand, although this complex is unstable in solution over 24 h.[33] Attempts to remove the pyridine ligand(s) from the imido complexes presented in this Section (Equation 3.1) at various temperatures under high-vacuum unfortunately resulted in complex mixtures of unidentified products.

At first sight the compounds M(NN_2R)(N^tBu)$(py)_2$ are formally 22 valence electron compounds if all three of the ligand-based lone pairs of NN_2^R (*cf* Chapter Two, Figure 2.6) are able to donate to the metal, and a M≡Nimide triple bond is also formed. A molecular analysis of the bonding in these compounds and their hydrazido counterparts is presented in Chapter Four and find that only one of the three lone pairs SALCS of NN_2^R (the a2 combination in Figure 2.6) is able to donate effectively to the metal centre.

Analogous complexes in which the pyridine ligands are substituted by the bipy ligand were synthesised by salt metathesis reactions of M(N^tBu)Cl_3(bipy) (M = Ta (**1.43**), Nb (**1.44**) or V(**1.46**)) with the lithiated ligands $Li_3(NN_2^R)$ (R = Me (**1**), ^{i}Pr (**2**) or $SiMe_3$

(**1.7**)). The complexes M(NN_2^{SiMe3})(N^tBu)(bipy) (M = Ta (**24**) and Nb (**25**)) were the only ones successfully isolated after several extractions in dichloromethane as they were found to be insoluble in benzene (Equation 3.2). Complex Nb(NN_2^{iPr})(N^tBu)(bipy) (**26**) could not be isolated on a preparative scale. However, some crystals were obtained and the X-ray characterisation is discussed.



Equation 3.2

Characterisation of Ta(NN_2^{SiMe3})(N^tBu)(bipy) (**24**) and Nb(NN_2^{SiMe3})(N^tBu)(bipy) (**25**) by ^1H (Figure 3.5) and ^{13}C NMR spectroscopy at RT is consistent with C_s symmetric molecules as the trimethylsilyl groups remained chemically equivalent to each other. The *tert*-butyl imido moiety can be observed as singlets at 1.25 and 1.30 ppm, in **24** and **25** respectively. The resonances attributed to the tridentate supporting ligand NN_2^{SiMe3} include singlets for the trimethylsilyl groups at -0.14 and -0.13 ppm, respectively, and the aryl rings display four multiplet resonances (two overlapped in the case of **25**) within the range 7.26 – 6.40 ppm. The spectra showed a coordinated monodentate bipyridyl ligand (namely **25a**), which displays one signal for each proton in the range of 10.43 – 6.96 ppm. The proton in the 1-position of the coordinated bipyridyl ring appears at higher chemical shifts: 10.43 and 10.20 ppm in **24a** and **25a**, respectively.

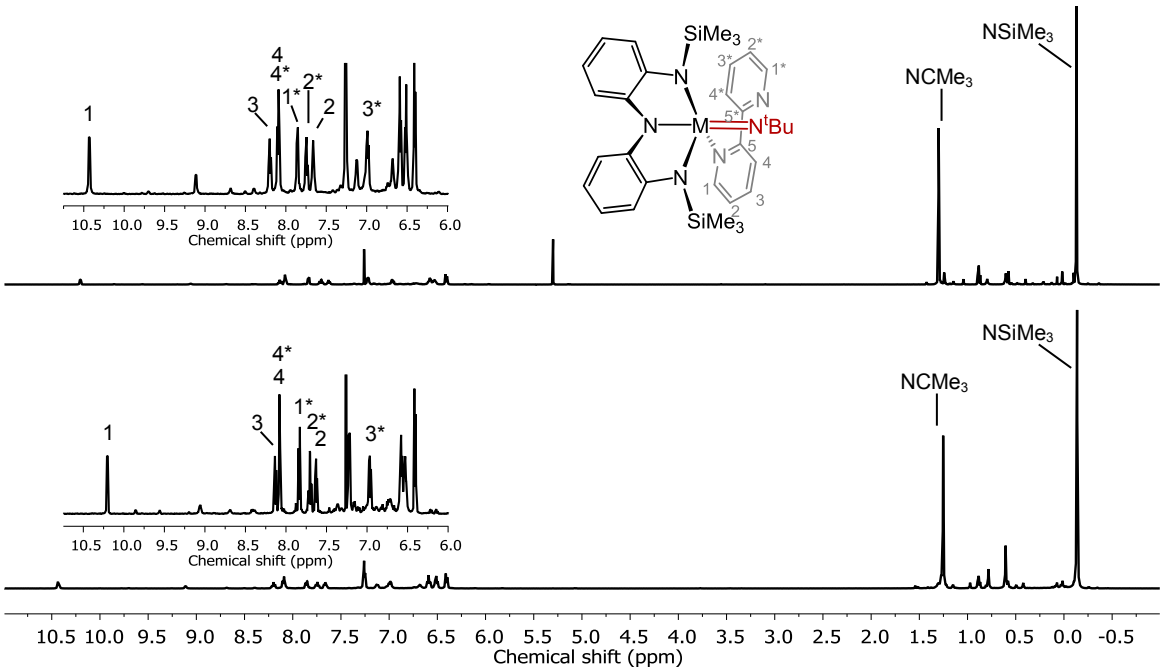
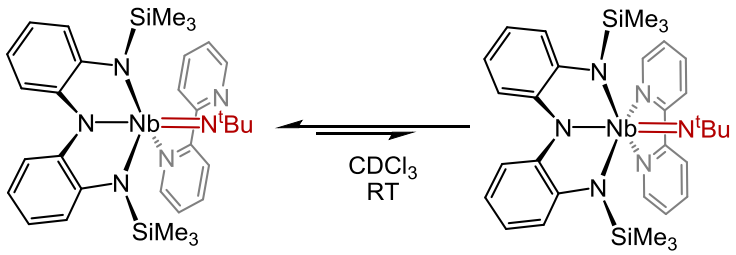


Figure 3.6. ^{1}H NMR spectra (500.3 MHz) of Ta(NN_2^{SiMe3})(N^tBu)(bipy) (**24a**, top) and Nb(NN_2^{SiMe3})(N^tBu)(bipy) (**25a**, bottom) in $CDCl_3$ at 298 K.

Close inspection of the ^{1}H NMR spectrum of **25a** at RT suggests that two small signals between 1.0 and 0.5 ppm correspond to the imido and the $SiMe_3$ groups from the bidentate bipy complex (namely **25b)**. This equilibrium mixture of the monodentate and bidentate bipy complexes is in a ratio of 90:10 by integration of $SiMe_3$ groups at RT (Equation 3.3).



25a 90% **25b** 10%

Equation 3.3

Characterisation of **25b** by ^{1}H and ^{13}C NMR was obtained at 213 K and is in agreement with C_s symmetric molecules and chemically equivalent bipyridyl rings. Analysis of the spectra of variable temperature NMR experiment beetween 298 and 213 K shows a mixture of **25a** and **25b** complexes in a *ca* 1:1 integration ratio for the $SiMe_3$ groups at 213 K (Figure 3.7). At this temperature the resonances corresponding to the imido and the

trimethylsilyl groups can be observed as singlets at 0.65 and 0.55 ppm respectively. As the temperature of the system is lowered the proton signals described as 1, 2 and 3 of the bidentate bipy rings are clearly distinguishable as multiplets integrating to 2H within the range 8.90 to 6.73 ppm at 213 K. The resonance for the protons in position 4 was not identified.

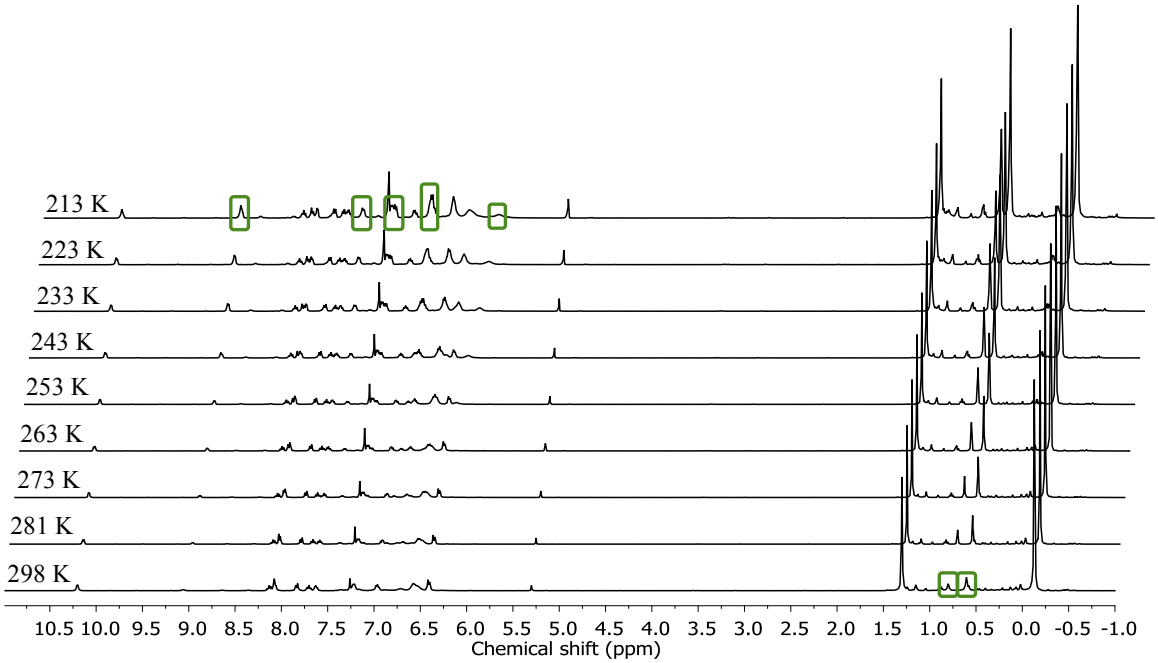


Figure 3.7. Variable temperature NMR experiment for the equilibrium between monodentate and bidentate bipy coordination for the complex Nb(NN_2^{SiMe3})(N^tBu)(bipy) (**25**) in $CDCl_3$ between 298 and 213 K.

^1H–^1H ROESY NMR experiment at 213 K (Figure 3.8) showed correlations of the imido and the trimethylsilyl group resonances with the bipyridyl signals for both mono- and bidentate bipy molecules of **25**. In the case of the monodentate-bipy (subscripts "a"), the signal for the $SiMe_3$ groups correlates with the closest proton in the aryl ring from the NN_2^{SiMe3} ligand (C2), proton 1 from the coordinated bipy ring and proton 4 from the non-coordinated bipy ring. In the case of the bidentate-bipy complex (subscripts "b") the signal for the $SiMe_3$ groups correlates with the closest protons in the aryl rings from the NN_2^{SiMe3} ligand (C2) and protons 1 and 2 from the bipy rings.

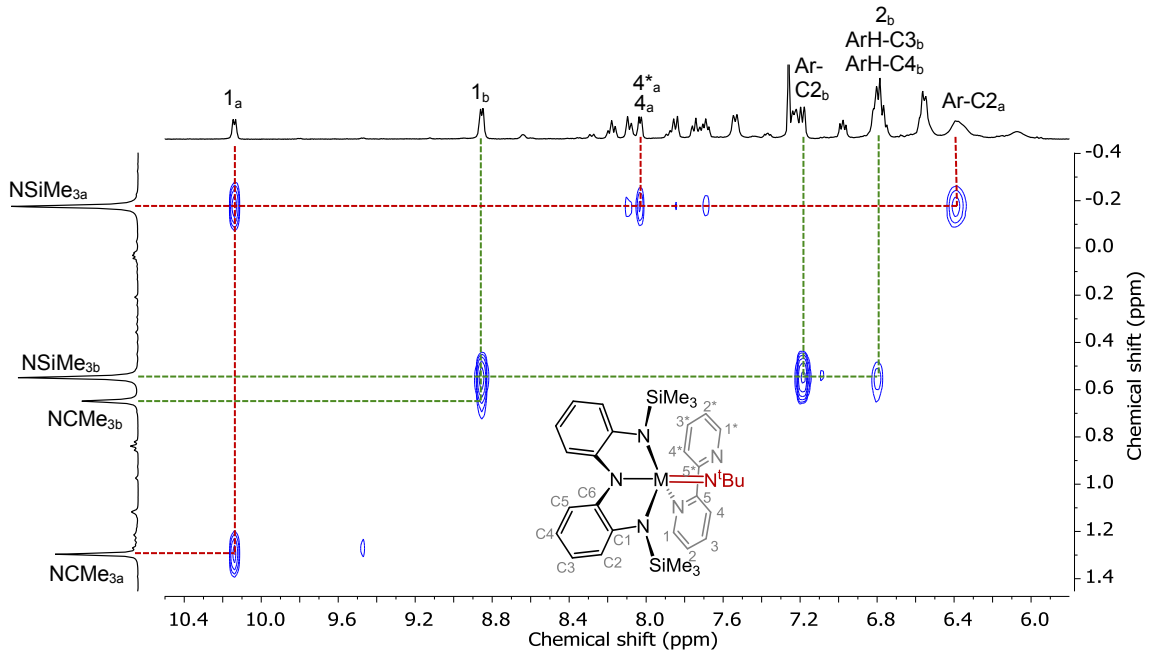


Figure 3.8. ^{1}H–^{1}H ROESY experiment for the equilibrium between monodentate and bidentate bipy coordination (red and green dotted lines respectively) for the complex $Nb(NN_2^{SiMe3})(N^tBu)(bipy)$ (**25**) in $CDCl_3$ at 213 K.

Thermodynamic analysis of the equilibrium between **25a** and **25b** was measured by integration of the protons in 1-position at 10.20 and 8.85 ppm in VT NMR experiments (Figure 3.7) in $CDCl_3$ between 298 and 233 K. The data obtained from this analysis is presented in Table 3.3 and the natural logarithm of the equilibrium constant is calculated and plotted with respect to the inverse of absolute temperature to give a linear relation in a Van't Hoff plot, Figure 3.9, using the equation:

$$\ln K_{eq} = \left(-\frac{\Delta H^{\circ}}{RT}\right) + \frac{\Delta S^{\circ}}{R}$$

And from which the Gibbs free energy can be also obtained:

$$\Delta G^{\circ} = -RT \ln K_{eq}$$

Using this Van't Hoff plot, it is possible to obtained values for ΔH (-3.9(2) kcal mol^{-1}) and ΔS (-17(1) cal mol^{-1} K^{-1}) and the corresponding value of ΔG_{298} = 1.3(5) kcal mol^{-1} (R^2 = 0.984). It is suggested that ΔS is somewhat negative due to loss of some degrees of rotational flexibility and greater ordering in the bidentate bipy example.

Table 3.3. Data obtained by VT NMR experiment for the equilibrium between monodentate and bidentate bipy coordination in **25** in $CDCl_3$ between 298 and 233 K and calculated equilibrium constant.

Integration (**25a**)	Integration (**25b**)	T (K)	In K_{eq}
1	0.21	298	-2.254
1	0.35	281.6	-1.743
1	0.48	273	-1.427
1	0.61	263	-1.187
1	0.81	253	-0.904
1	1.03	243	-0.664
1	1.37	233	-0.378

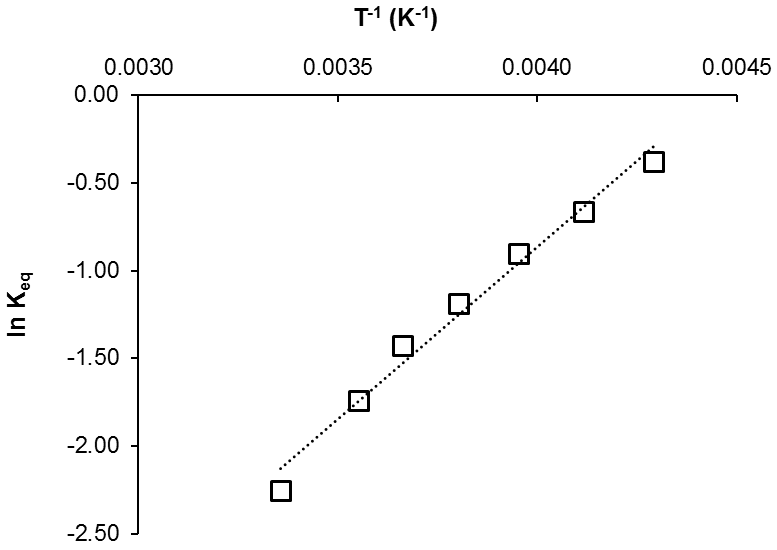


Figure 3.9. Van't Hoff plot for the equilibrium between monodentate and bidentate bipy coordination for complex **25**. ΔG_{298} = 1.3(5) kcal mol^{-1} (R^2 = 0.984), ΔH = -3.9(2) kcal mol^{-1}, ΔS = -17(1) cal mol^{-1} K^{-1}.

Diffraction quality crystals of Nb(NN_2^R)(N^tBu)(bipy) (R = ^{i}Pr (**26**) and $SiMe_3$ (**25**)) were grown from a saturated benzene-d_6 solution at RT. The solid state structures are showed in Figure 3.10 and selected bond lengths and angles are listed in Table 3.4.

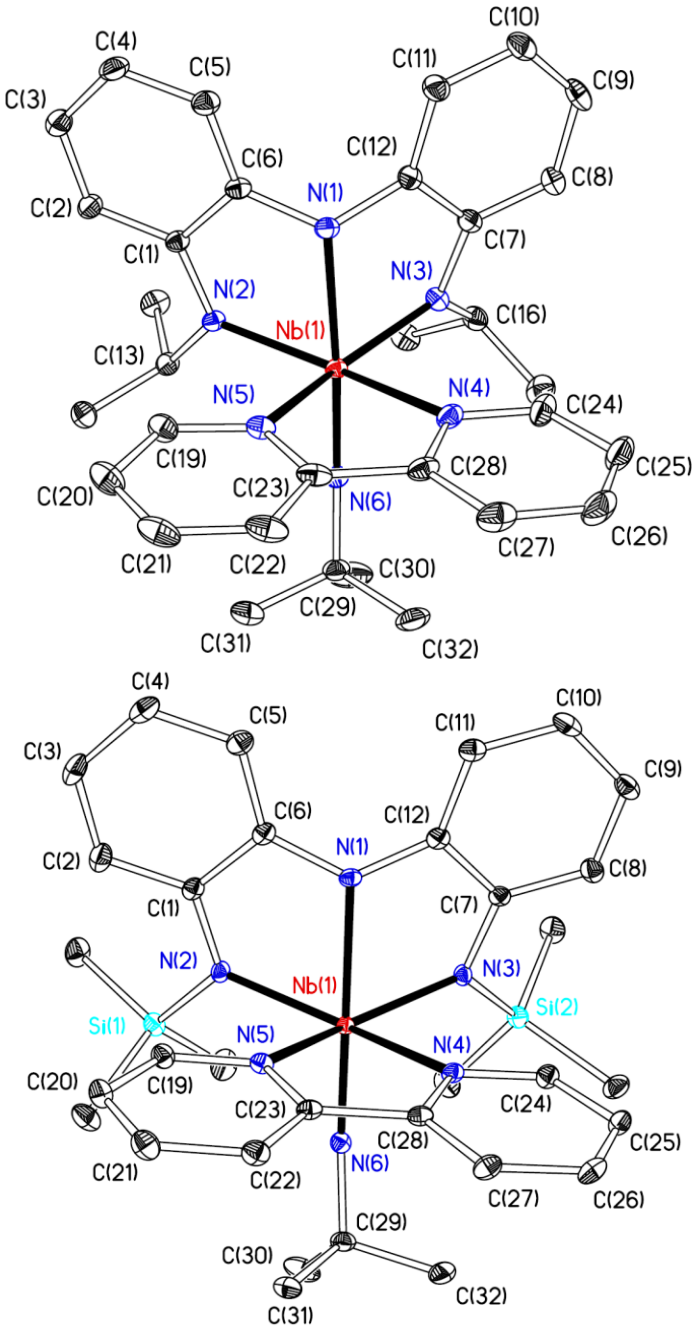


Figure 3.10. Displacement ellipsoid plots (20% probability) of Nb(NN_2^R)(N^tBu)(bipy) (R = ^{i}Pr (**26**, top) and $SiMe_3$ (**25**, bottom)). H atoms omitted for clarity.

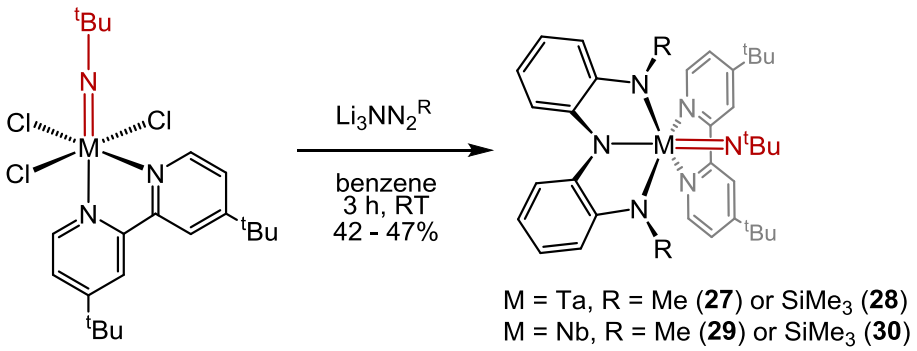
Table 3.4. Selected bond lengths (Å) and angles (°) for Nb(NN_2^R)(N^tBu)(bipy) (R = ^{i}Pr (**26**) and $SiMe_3$ (**25**)).

Parameter	**26**	**25**
Nb(1)–N(1)	2.1798(18)	2.1837(19)
Nb(1)–N(2)	2.0671(18)	2.1097(19)
Nb(1)–N(3)	2.0673(19)	2.114(2)
Nb(1)–N(4)	2.3312(18)	2.3335(18)
Nb(1)–N(5)	2.3192(19)	2.325(2)
Nb(1)–N(6)	1.8030(18)	1.810(2)
N(6)–C(29)	1.456(3)	1.465(3)
N(1)–Nb(1)–N(2)	75.78(7)	74.92(8)
N(1)–Nb(1)–N(3)	76.21(7)	74.77(8)
N(2)–Nb(1)–N(3)	109.59(7)	117.80(8)
N(1)–Nb(1)–N(4)	91.78(6)	93.48(7)
N(2)–Nb(1)–N(4)	155.20(7)	150.89(7)
N(3)–Nb(1)–N(4)	87.49(7)	83.30(7)
N(1)–Nb(1)–N(5)	87.94(7)	90.68(7)
N(2)–Nb(1)–N(5)	88.97(7)	84.59(7)
N(3)–Nb(1)–N(5)	151.25(7)	147.68(7)
N(4)–Nb(1)–N(5)	68.92(7)	68.68(7)
N(1)–Nb(1)–N(6)	175.89(7)	177.80(8)
N(2)–Nb(1)–N(6)	100.19(8)	103.96(8)
N(3)–Nb(1)–N(6)	104.72(8)	104.30(8)
N(4)–Nb(1)–N(6)	92.26(7)	88.38(8)
N(5)–Nb(1)–N(6)	92.81(7)	91.10(8)
Nb(1)–N(6)–C(29)	166.87(17)	164.21(17)

In the solid state the structures of Nb(NN_2^R)(N^tBu)(bipy) (R = ^{i}Pr (**26**) and $SiMe_3$ (**25**)) show the coordination of a bidentate bipy ligand in a pseudo-octahedral geometry. In this case the NN_2^R ligand is κ^3-*fac* coordinated instead of the κ^3-*mer* coordination observed in the previous bis(pyridine) complex Ta(NN_2^{Me})(N^tBu)$(py)_2$ (**17**). This mode of binding has been previously observed in the chemistry of titanium hydrazido complexes developed by Mountford and co-workers.[53,54] The Nb−N_{imide} bond lengths of 1.8030(18) and 1.810(2) Å, and the near linear Nb−N_{imide}−C(29) angles of 166.87(17) and 164.21(17)º for **26** and **25** respectively, are consistent with a formal niobium-nitrogen triple bond for the Nb≡N_{imide} moiety. These Nb−N_{imide} bond lengths for **26** and **25** are relatively close to the one observed in the imido moiety in **17** (1.820(3) Å). As discussed previously these parameters for the Nb− N_{imide} bond are longer than other tantalum and niobium terminal *tert*-butylimide complexes reported in the literature, with examples ranging from 1.61(3) to 1.793(7) Å.[33,46-50] This may be due to a strong *trans* influence of the N_{aryl} from the pincer ligand.[33,51]

The Nb(1)−N(1) bond lengths in complexes **26** and **25** at 2.1798(18) and 2.1837(19)Å respectively, are comparable to the one observed in compound **17** at 2.186(2)Å. Although, this is not the case of the Nb(1)−N(2) and Nb(1)−N(3) bond lengths of complex **25** (2.1097(19) and 2.114(2)Å) which are slightly longer than those for both complex **26** (2.0671(18) and 2.0673(19)Å) and **17** (2.054(2) and 2.047(3)Å). A more significant difference is observed in the angle N(2)−Nb(1)−N(3) at 109.59(7) **26** and 117.80(8)˚ (**25**) when the NN_2^R ligand is *fac*-coordinated *vs* 149.36(10)˚ (**17**) when *mer*-coordination mode is observed. The Nb−N_{bipy} bond lengths for the bipyridyl ligand are on avg. at 2.327 Å forming N(4)−Nb(1)−N(5) angles of 68.92(7) and 68.68(7)˚ for **26** and **25** respectively.

Analogous compounds to Nb(NN_2^R)(N^tBu)(bipy) (R = ^{i}Pr (**26**) and SiMe3 (**25**)) with di-^{t}Bu-bipy were synthesised in a similar manner by salt metathesis reaction of the synthons M(N^tBu)Cl_3(di-^{t}Bu-bipy) (M = Ta (**14**), Nb (**15**) or V(**16**)) with the lithiated ligands $Li_3(NN_2^R)$ (R = Me (**1**), ^{i}Pr (**2**) or $SiMe_3$ (**1.7**)). In this case the complexes M(NN_2^R)(N^tBu)(di-^{t}Bu-bipy) (M = Ta, R = Me (**27**) or $SiMe_3$ (**28**); M = Nb, R = Me (**29**) or $SiMe_3$ (**30**)) were successfully isolated in better yields (42 – 47%) after several extractions with dichloromethane on the preparative scale (Equation 3.4).



Equation 3.4

Characterisation of $M(NN_2^R)(N^tBu)$(di-^{t}Bu-bipy) (M = Ta, R = Me (**27**) or $SiMe_3$ (**28**); M = Nb, R = Me (**29**) or $SiMe_3$ (**30**)) by ^{1}H (Figure 3.11) and ^{13}C NMR spectroscopy at RT is consistent with C_s symmetric molecules as either the methyl or the trimethylsilyl groups are equivalent to each other. The ^{1}H resonances for the *tert*-butyl imido moiety are observed in the range from 1.31 to 1.06 ppm. The proton signals attributed to the tridentate ligand NN_2^R include a singlet for either the Me (at *ca* 4.3 ppm for **27** and **29**) or the $SiMe_3$ groups (at -0.13 and -0.12 ppm for **28** and **30**), and the equivalent aryl rings displayed four multiplets in the range *ca* 7.5 – 6.0 ppm.

The bipy ligand can be observed binding to the metal centre in a bidentate (when N_{aryl}-substituents are Me) or a monodentate mode (when N_{aryl}-substituents are $SiMe_3$) in solution at RT. The bidentate bipy ligand in **27** and **29** showed a singlet for the equivalent *tert*-butyl groups and three multiplets for the equivalent bipy rings (in the range *ca* 8.5 – 7.25 ppm). In contrast, the resonances for the monodentate bipy ligand in **28** and **30** showed two singlets for the inequivalent *tert*-butyl groups and six multiplets for the inequivalent bipy rings with a distinctive multiplet at high field (10.19 and 9.97 ppm for **28** and **30** respectively), in a similar way as **24** and **25**. This may be attributed to the large steric profile of the $SiMe_3$ groups clashing with the bulky bipyridyl ligand, giving a preference for a monodentate coordination mode in solution at RT.

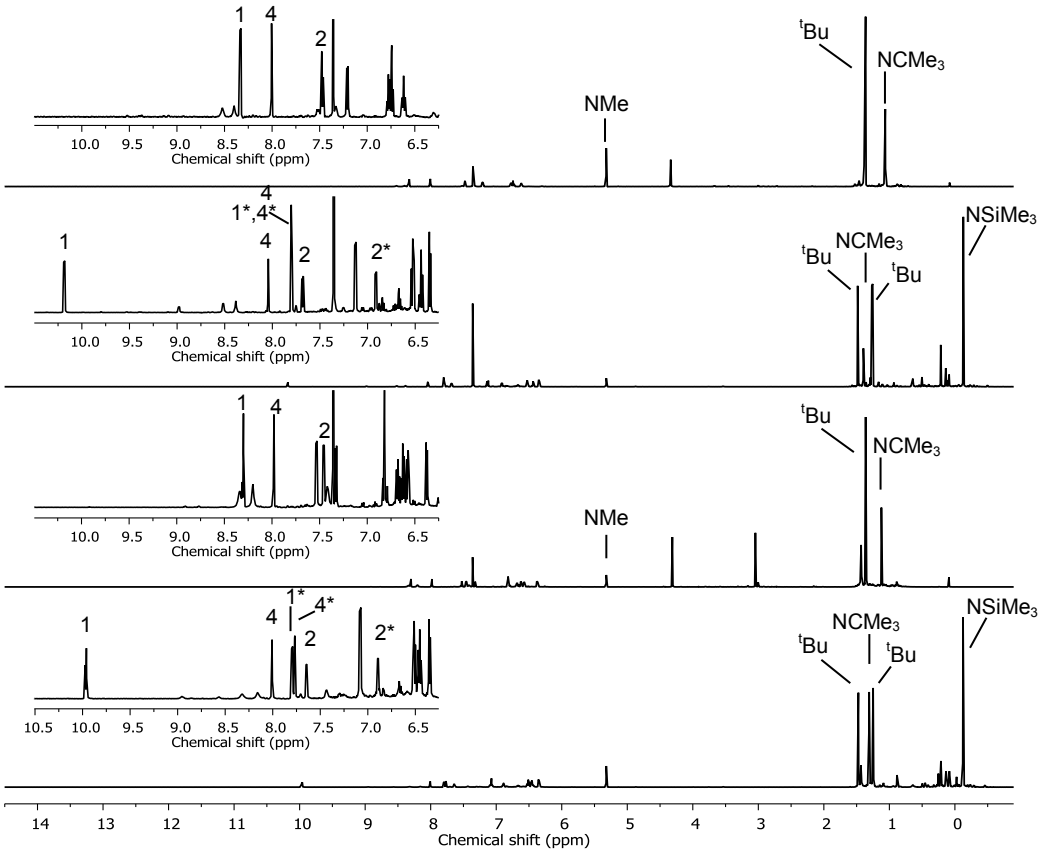
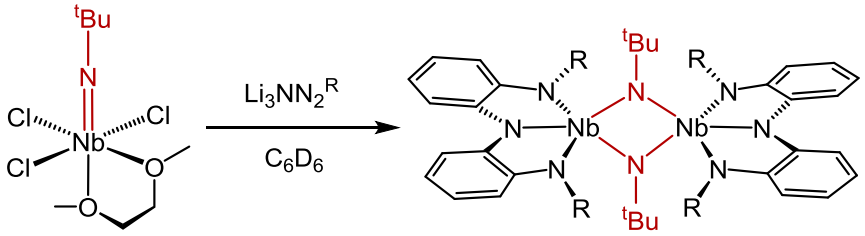


Figure 3.11. ^{1}H NMR spectra (500.3 MHz) of, from top to bottom, M(NN_2^R)(N^tBu)(di-^{t}Bu-bipy) (M = Ta, R = Me (**27**) or $SiMe_3$ (**28**); M = Nb, R = Me (**29**) or $SiMe_3$ (**30**)) in CD_2Cl_2 at 298 K.

Preliminary salt metathesis reactions using the Nb(N^tBu)Cl_3(DME)[42] synthon as an alternative for the bis(pyridine) and bipyridyl analogues with the lithiated ligand of the type $Li_3N_2N^R$ were attempted as shown in Equation 3.5. The NMR scale reactions in C_6D_6 at RT showed product mixtures from which the imide complexes were not identified on the ^{1}H NMR spectra. However, the formation of a dinuclear imido-bridged product [Nb(N_2N^{Me})(N^tBu)]$_2$ was confirmed by X-ray diffraction (Figure 3.12).

Crystals of [Nb(N_2N^{Me})(N^tBu)]$_2$ were grown from a saturated C_6D_6 solution at RT. However, X-ray data were of poor quality. Although they allow to unambiguously determine the connectivity (Figure 3.12) it is not appropriate to discuss details of bond lengths and angles. Nonetheless, the niobium centre is five-coordinated and its geometry is best described as distorted trigonal bipyramidal with N(4) and N(1) in the axial sites and N(2), N(3) and N(4A) in the equatorial positions. The imido ligand is The NN_2^{Me} ligands are κ^3-*fac* coordinated, also observed and discussed previously for complexes **17**, **25** and **26**.



Equation 3.5

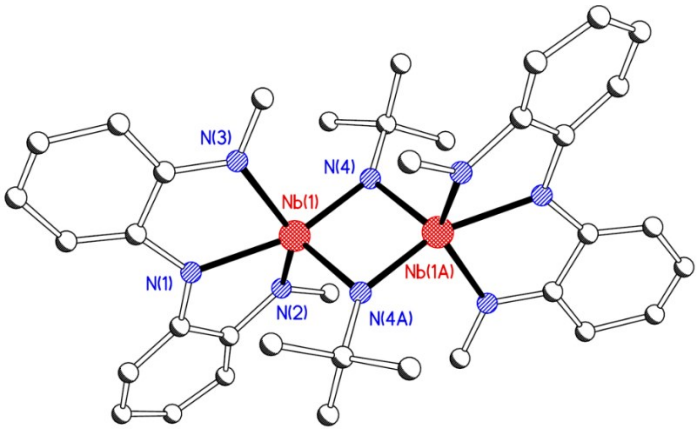


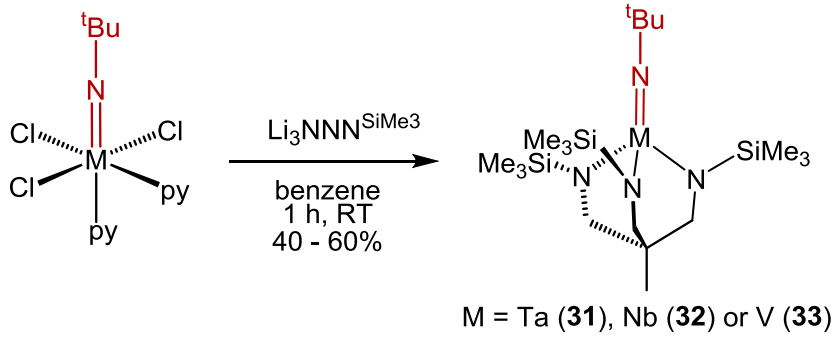
Figure 3.12. Molecular structure of $[Nb(NN_2^{Me})(N^tBu)]_2$.

3.4.2 Installation of NNN^{SiMe3} supporting ligand

In this section, the studies of Group 5 imido complexes will be extended with the synthesis and characterisation of analogous compounds with the face-capping ligand $Li_3(NNN^{SiMe3})$ (**1.9**, NNN^{SiMe3} = $H_3CC(CH_2NSiMe_3)_3$). The triamide tripodal ligand was first introduced by Gade and co-workers in 1993.[55] In the following years, this ligand was used for the synthesis of titanium and zirconium complexes of the type $M(NNN^R)(X)$ (M = Ti, Zr; R = ^{i}Pr, $SiMe_3$; X = Cl, Br) which were also studied with functionalised ligands.[56-61] So far just two examples of Group 5 metal complexes supported by the NNN^{SiMe3} ligand have been reported, the vanadium compound $\{V(TAME)(H_2NO)(NO)(NH_3)\}I$ (TAME = $H_3CC(CH_2NH_2)_3$) and the vanadium dinitrogen complex $N_2\{V(NNN^{SiMe3})\}_2$ (structurally characterised). [62,63]

Salt metathesis reactions of the imide synthons $M(N^tBu)Cl_3(py)_2$ (M = Ta (**1.41**), Nb (**1.42**) or V(**1.45**)) with 0.5 equiv. of the tripodal ligand $Li_3(NNN^{SiMe3})$ (**1.9**) formed the imido complexes $M(NNN^{SiMe3})(N^tBu)$ (M = Ta (**31**), Nb (**32**) or V (**33**)) shown in Equation 3.6. These compounds were isolated as powders after lyophilisation of the oily products (**31** and **32**) or waxy solids (**33**) in yields between 40 and 60%. Characterisation

all three complexes by ^{1}H (Figure 3.13) and ^{13}C NMR spectroscopy is indicative of C_{3v} symmetric molecules with all trimethylsilyl groups equivalent to each other. The *tert*-butyl imido moiety is observed as a singlet at *ca* 1.6 ppm and the resonances attributed to the tridentate supporting ligand include three singlets: one for the $SiMe_3$ groups (in the range 0.4 – 0.2 ppm), a second one for the CH_2 groups (at *ca* 3.5 ppm) and a third one for the Me group (in the range 1.1 – 0.8 ppm). Most importantly, compared to the imido complexes with the robust NN_2^R supporting ligand (see Section 3.4.1) is that the three-dimensional nature of the tripodal-supported ligand in the imido complexes $M(NNN^{SiMe3})(N^tBu)$ (M = Ta (**31**), Nb (**32**) or V (**33**)) block coordination sites for pyridine.[55]



Equation 3.6

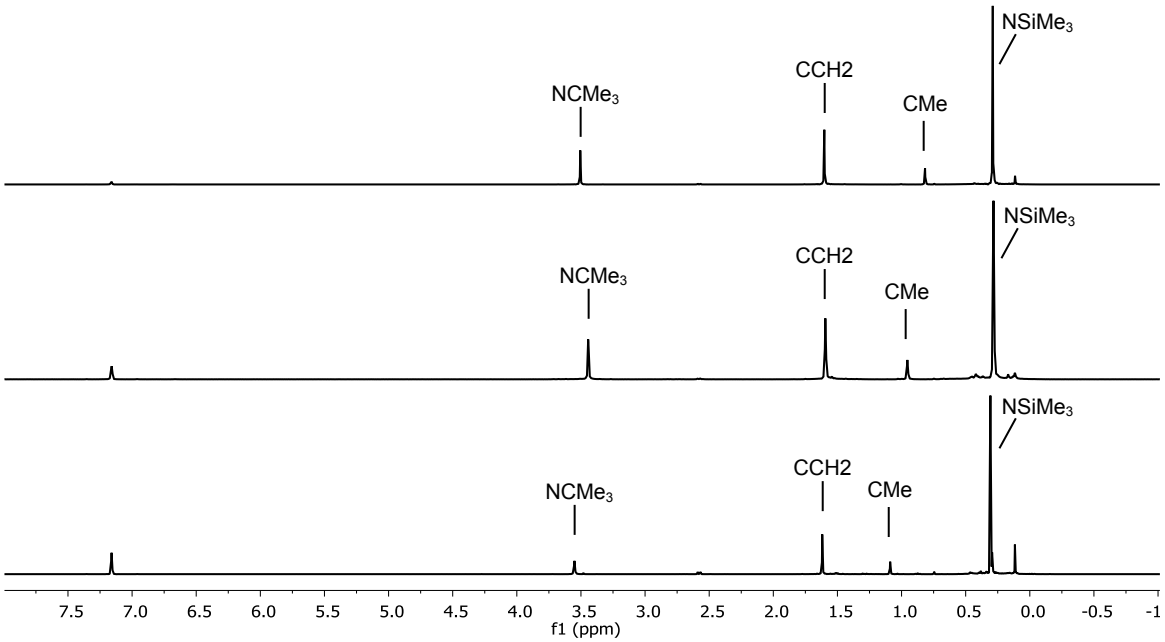


Figure 3.13. ^{1}H NMR spectra (400.1 MHz) of $M(NNN^{SiMe3})(N^tBu)$ (M = Ta (**31**, top), Nb (**32**, middle) or V (**33**, bottom)) in C_6D_6 at 298 K.

Diffraction quality crystals of V(NNN^{SiMe3})(N^{t}Bu) (**33**) were grown from a saturated pentane solution at -80 ˚C. The molecular solid state structure is shown in Figure 3.14 and selected bond lengths and angles are listed in Table 3.5.

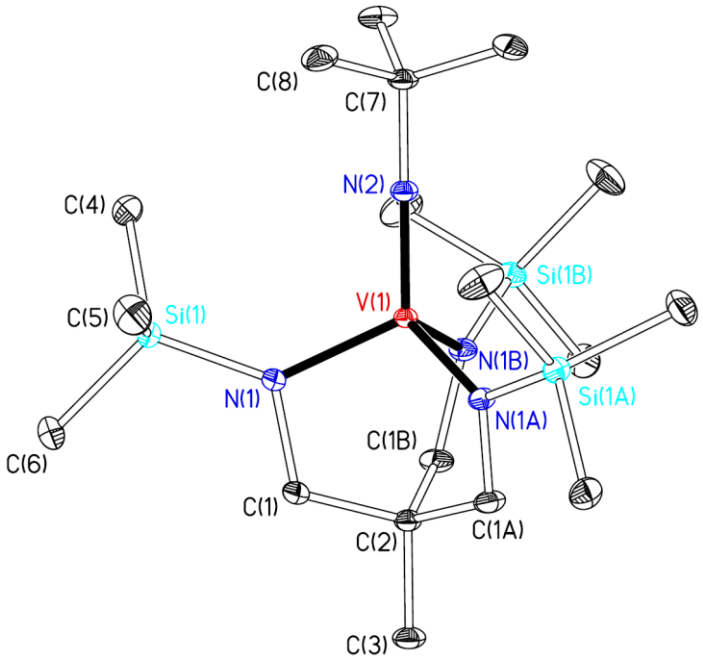


Figure 3.14. Displacement ellipsoid plots (20% probability) of V(NNN^{SiMe3})(N^{t}Bu) (**33**). H atoms omitted for clarity. Atoms carrying the suffix 'A' and 'B' are related to their counterparts by the symmetry operator [1-y,1+x-y, z] and [-x+y,1-x, z].

Table 3.5. Selected bond distances (Å) and angles (°) for V(NNN^{SiMe3})(N^{t}Bu) (**33**).

V(1)–N(1)	1.8636(12)	N(1B)–V(1)–N(1)	104.34(5)
V(1)–N(2)	1.659(3)	N(1)–V(1)–N(2)	114.22(4)
N(1)–Si(1)	1.7252(12)	V(1)–N(1)–Si(1)	133.65(8)
N(2)–C(7)	1.462(4)	V(1)–N(1)–C(1)	104.09(9)
		V(1)–N(2)–C(7)	179.992

The molecular solid state structure of **33** shows a monomeric structure with a tetrahedral geometry. The short V(1)−N(2) distance of 1.659(3) Å and the linear V(1)−N(2)−C(7) angle of 179.992˚ are both consistent with a vanadium-nitrogen triple bond.[64-67] Its

geometry is defined by the three nitrogen of the tripodal amide (N(1B)−V(1)−N(1) angle of 104.34(5)˚) and the nitrogen atom of the imide moiety (N(1)−V(1)−N(2) angle of 114.22(4)˚). The coordination geometry around each amide nitrogen atom in the tripodal ligand is trigonal planar with a C(1)−V(1)−N(1) angle of 104.09(9)˚ and V(1)−N(1) bond length of 1.8636(12) Å comparable to the previously structurally characterised vanadium dinitrogen complex $N_2\{V(NNN^{SiMe3})\}_2$[63].

3.5 Reactivity of $Nb(NN_2^{iPr})(N^tBu)(py)_2$ (21) with unsaturated small molecules

As discussed in Chapter One of this Thesis, many reactivity studies of Group 4 imido compounds (L)M=N−R (R = alkyl or aryl) with small unsaturated molecules have been published in the last decades. Two remarkable examples are the zirconocene imido complex $Cp_2Zr(N^tBu)(THF)$ (**1.12**)[68] and the diamide-amine complex $Ti(N_2N^{py})(N^tBu)(py)$ (**1.20**)[69], both of which showed a rich reaction chemistry.[2,70-79]

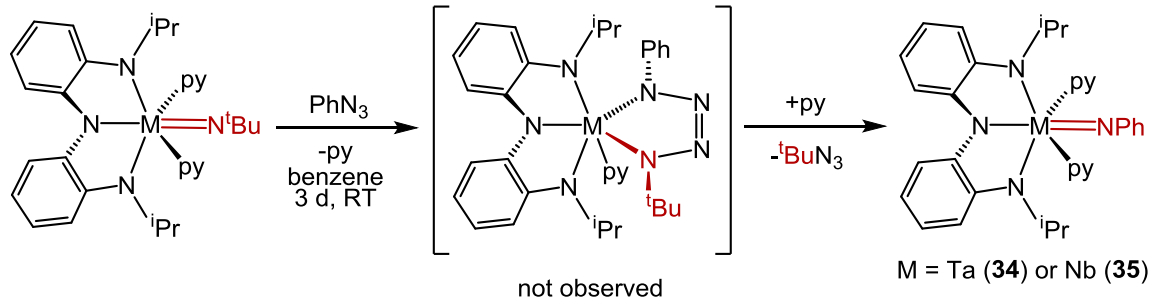
Reactions of **1.12** with both internal and terminal alkynes R'CCR" (R', R" = H, Me or aryl) gave a [2+2] cycloaddition product $Cp_2Zr\{N(^tBu)C(R")C(R')\}$.[80] This behaviour was also observed in reactions with alkenes, such as ethylene and norbornene, in equilibrium with the starting material.[80] Similarly, [2+2] cycloaddition reactions were reported with the diamide-amine-supported complex $Ti(N_2N^{py})(N^tBu)(py)$ (**1.20**) reacting with terminal and internal alkynes or allenes,[76,78,79] and dimerisation reactions with nitriles (MeCN) afforded the complex $[Ti_2\{\mu\text{-}\eta^2\text{-}NC(Me)NBu^t\}_2(L)_2]$.[81] Reactions of the zirconium imide complex $Cp_2Zr(N^tBu)(THF)$ (**1.12**) with organic azides such as *tert*-butyl, phenyl and *p*-tolyl azides are known to proceed through [3+2] cycloaddition reaction resulting in metallatetrazene-type complexes. These complexes proceeded *via* extrusion of *tert*-butyl azide to give $Cp_2Zr(NPh)$ and form tetrazene-type compounds with additional azide.[71]

Mountford and co-workers have observed cycloaddition of CO_2 to the Ti=NR bond in the complexes $Ti(NR)(Me_4taa)$ (Me_4taa = dianion of tetramethyldibenzotetraaza[14]annulene),[82] $Ti(NR)(Me_2calix)$ (Me_2calix = the dianion of 1,3-dimethyl ether *p-tert*-butylcalix[4]-arene),[83] $Ti(NR)(O_2NN')$ (H_2O_2NN' = (2-$C_5H_4N)CH_2N$-(2-HO-3,5-$C_6H_2{}^tBu_2)_2$),[84] and Cp*Ti $(NR)\{MeC\text{-}(N^iPr)_2\}$ (R = ^{t}Bu or Ar)[85] giving a carbamate product of the type $[(L)nTi\{OC(O)N(R)\}]$. Similarly, the cyclopentadienyl-amidinate imido complexes $Cp^*Ti(NR)\{MeC(N^iPr)_2\}$ (R = ^{t}Bu, Ar or Tol) gave cycloaddition-elimination reactions with CS_2 forming the dimeric sulphido-

bridged complexes.[86] More recently, our research group communicated the reactivity of titanium imido and hydrazido complexes with boranes. The imide Cp*Ti(NTol){MeC(N^{i}Pr)$_2$} reacted cleanly with the hydroboranes H_2BTex (Tex = *tert*-hexyl), 9-BBN and $HBAr^{F}_2$ forming the hydride-bridged adducts Cp*Ti{N(Tol)HBRR′}{MeC(N^{i}Pr$_2$)$_2$}.[87]

In this Chapter, NMR scale reactivity studies of the niobium imido complex Nb(NN$_2^{iPr}$)(N^{t}Bu)(py)$_2$ (**21**) were carried out with a number of small unsaturated substrates. It was found to be unreactive with internal alkynes, CS_2, nitriles and epoxides, even upon strong heating. Exposing a solution of **21** in benzene to a CO_2 atmosphere at RT for 2 h gave a complicated mixture in which free pyridine can be observed but none of the other products could be identified. Similarly, a mixture of products is observed with boranes, which are known to form the side product py·HBC_8H_{14} with the pyridine ligands, although none of the other compounds in the mixture were identified.

In the case of organic azides compound **21** was found to be unreactive with Me_3SiN_3. However, when reacted with 1 equiv. of PhN_3 at RT for 3 days, the formation of $^{t}BuN_3$ (confirmed by comparison with an authentic sample) was observed along with the complex Nb(NN$_2^{iPr}$)(NPh)(py)$_2$ (**35**) (Equation 3.7). This is expected to be the result of a [3+2] cycloaddition reaction followed by a retro-cyclisation, although the metallacycle intermediate was not observed.[71,73] Unsymmetrical tetrazene is the least stable metallacycle, the preference for the elimination of $^{t}BuN_3$ is presumably the result of a balance of band energetics for M=NR and RN_3.{Clough, 2017 #217;Meyer, 1995 #172} Complex **35** was identified and characterised by ^{1}H (Figure 3.15) and ^{13}C NMR spectrometry consistent with a C_{2v} symmetric molecule as the ^{i}Pr groups and pyridine ligands are equivalent to each other. The proton ^{1}H resonances for the arylamide are observed at 7.44 (doublet), 7.34 (triplet) and 6.92 ppm (triplet). The proton signals attributed to the pincer ligand NN$_2^{iPr}$ include a doublet for the ^{i}Pr groups at 1.30 ppm (the expected septet for the isopropyl methine was not observed) and the equivalent aryl rings displayed four multiplets in the range *ca* 7.7 – 6.2 ppm. The resonances for the two pyridine ligands coordinated to the metal centre are observed as three multiplets in the range *ca* 9.32 – 6.30 ppm. NMR scale reaction for the analogous Ta(NN$_2^{iPr}$)(NPh)(py)$_2$ (**34**) was also carried out successfully with the same outcome.



Equation 3.7

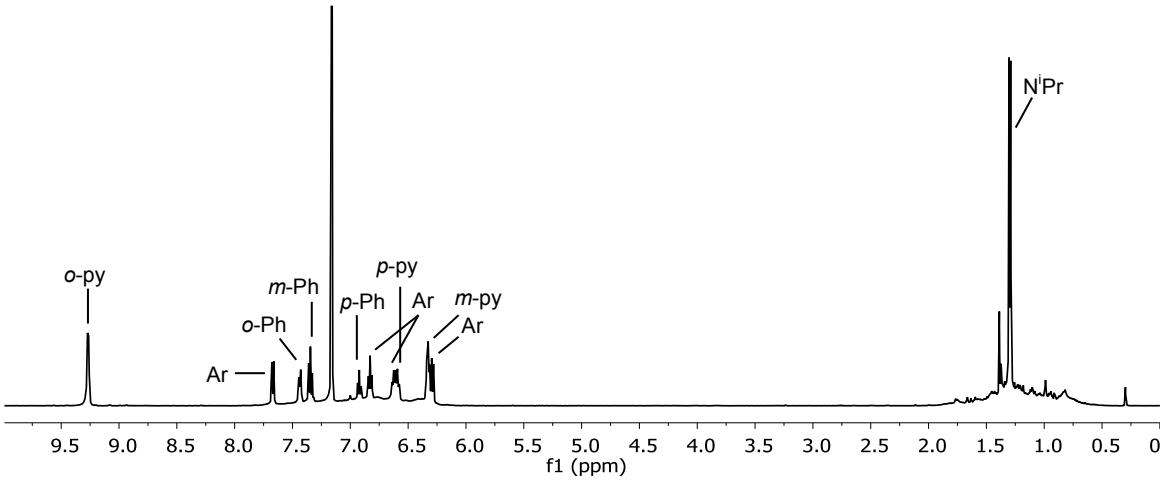


Figure 3.15. ^{1}H NMR spectra (499.9 MHz) of Nb(NN_2^{iPr})(NPh)$(py)_2$ (**35**) in C_6D_6 at 298 K.

3.6 Conclusions and Outlook

In this Chapter, synthesis and characterisation of Group 5 imido complexes with two different tridentate, trianionic ligands have been described. An overview of all new reactions is given in Scheme 3.2.

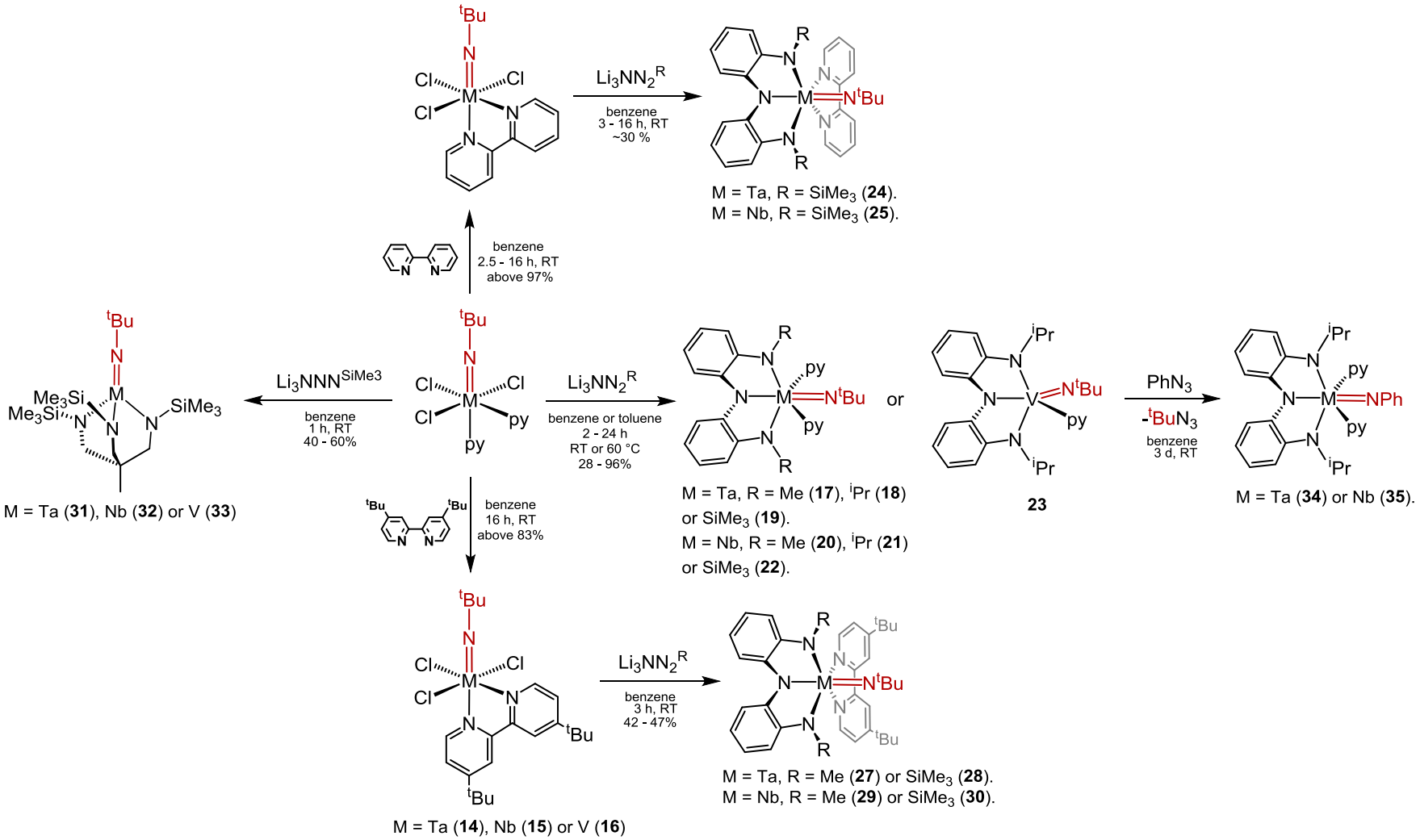
Firstly, a different synthetic route was presented to synthesise the known Group 5 imido synthons of the type M(N^tBu)Cl_3(L) with bipy and the new synthons **14**, **15** and **16** with the di-^{t}Bu-bipy ligand. Subsequently, these synthons were reacted *via* salt metathesis with the lithiated ligand $Li_3(NN_2^R)$ (R = Me (**1**), ^{i}Pr (**2**) or $SiMe_3$ (**1.7**)) yielding the imido complexes M(NN_2^R)(N^tBu)$(py)_2$ (M = Ta, R = Me (**17**), ^{i}Pr (**18**) or $SiMe_3$ (**19**); M = Nb, R = Me (**20**), ^{i}Pr (**21**) or $SiMe_3$ (**22**)) and V(NN_2^{iPr})(N^tBu)Cl_3(py) (**23**). Along with M(NN_2^{SiMe3})(N^tBu)(bipy) (M = Ta (**24**) and Nb (**25**)) and M(NN_2^R)(N^tBu)(di-^{t}Bu-bipy) (M = Ta, R = Me (**27**) or $SiMe_3$ (**28**); M = Nb, R = Me (**29**) or $SiMe_3$ (**30**)). The NMR characterisation at RT of complexes **24**, **25**, **28** and **30** showed the coordination of a

monodentate bipyridyl ligand and the equilibrium between monodentate and bidentate bipy coordination for the complex **25** was studied at low temperatures. The solid state structures of complexes $Ta(NN_2^{Me})(N^tBu)(py)_2$ (**17**) presented a NN_2^R ligand κ^3-*mer* while the compounds $Nb(NN_2^R)(N^tBu)(bipy)$ (R = ^{i}Pr (**26**) and $SiMe_3$ (**25**)) were κ^3-*fac* coordinated.

NMR scale reaction of the $Nb(N^tBu)Cl_3(DME)$ synthon with the $Li_3N_2N^{Me}$ (**1**) ligand formed a dinuclear imido-bridged product $[Nb(N_2N^{Me})(N^tBu)]_2$ (identified by X-ray crystallography). The imido complexes $M(NNN^{SiMe3})(N^tBu)$ (M = Ta (**31**), Nb (**32**) or V (**33**)) were also synthesised *via* salt metathesis by reaction of the imido synthons $M(N^tBu)Cl_3(py)_2$ (M = Ta (**1.41**), Nb (**1.42**) or V(**1.45**)) with the tripodal ligand $Li_3(NNN^{SiMe3})$ (**1.9**).

Finally, reactivity studies with a range of unsaturated small molecules showed that complex **20** is unreactive with alkynes, CS_2 and nitriles, and complicated mixtures of products are formed with CO_2 and boranes. However, reaction with PhN_3 gave the complex $Nb(NN_2^{iPr})(NPh)(py)_2$ (**35**) as a result of a combined [3+2] cycloaddition and cycloreversion reaction. The analogous tantalum complex (**34**) was also prepared.

Looking forward, the reactivity studies with unsaturated small molecules could be extended to the Group 5 imido complexes with bipyridyl and di-^{t}Bu-bipyridyl ligands, and the imido complexes of the type $M(NNN^{SiMe3})(N^tBu)$. Reactions with hydrazines to form the hydrazido complexes will be discussed in Chapter Four of this Thesis.



Scheme 3.2. New reactions discussed in this Chapter.

3.7 References

1. W. A. Nugent and B. L. Haymore, 1980, **31**, 123-175.
2. L. H. Gade and P. Mountford, *Coord. Chem. Rev.*, 2001, **216-217**, 68-97.
3. J. M. Mayer and W. A. Nugent, *Metal-Ligand Multiple Bonds.*, Wiley−Interscience, New York, 1988
4. D. E. Wigley, *Organoimido Complexes of the Transition Metals*, *Progress in Inorganic Chemistry*, ed. K. D. Karlin, Wiley−Interscience, New York, 1994, Vol. 42, pp. 239−482.
5. M. H. Chisholm and I. P. Rothwell, *in Comprehensive Coordination Chemistry*, ed. G. Wilkinson, R. D. Gillard and J. A. McCleverty, Pergamon Press, Oxford, 1987, Vol. 2, pp. 161−184.
6. P. Mountford, *Chem. Comm.*, 1997, 2127-2134.
7. D. J. Arney, M. A. Bruck, S. R. Huber and D. E. Wigley, *Inorg. Chem.*, 1992, **31**, 3749-3755.
8. S. C. Dunn, A. S. Batsanov and P. Mountford, *J. Chem. Soc., Chem. Comm.*, 1994, 2007-2008.
9. P. E. Collier, S. C. Dunn, P. Mountford, O. V. Shishkin and D. Swallow, *J. Chem. Soc., Dalton Trans.*, 1995, 3743-3745.
10. A. J. Blake, P. E. Collier, S. C. Dunn, W.-S. Li, P. Mountford and O. V. Shishkin, *J. Chem. Soc., Dalton Trans.*, 1997, 1549-1558.
11. S. R. Dubberley, S. Evans, C. L. Boyd and P. Mountford, *Dalton Trans.*, 2005, 1448-1458.
12. S. M. Rocklage and R. R. Schrock, *J. Am. Chem. Soc.*, 1980, **102**, 7808-7809.
13. D. D. Devore, J. D. Lichtenhan, F. Takusagawa and E. A. Maatta, *J. Am. Chem. Soc.*, 1987, **109**, 7408-7416.
14. A. J. Nielson, *Polyhedron*, 1988, **7**, 67-75.
15. F. Preuss, E. Fuchslocher, E. Leber and W. Towae, *Z. Naturforsch. B*, 1989, **44b**, 271—277.
16. Y. W. Chao, P. A. Wexler and D. E. Wigley, *Inorg. Chem.*, 1989, **28**, 3860-3868.
17. C. M. Jones, M. E. Lerchen, C. J. Church, B. M. Schomber and N. M. Doherty, *Inorg. Chem.*, 1990, **29**, 1679-1682.
18. J. Sundermeyer, J. Putterlik, M. Fotha, J. S. Fieldb and N. Ramesar, *Chem. Ber.*, 1994, **127**, 1201-1212.

19. K. S. Heinselman, V. M. Miskowski, S. J. Geib, L. C. Wang and M. D. Hopkins, *Inorg. Chem.*, 1997, **36**, 5530-5538.
20. H.-T. Chiu, S.-H. Chuang, C.-E. Tsai, G.-H. Lee and S.-M. Peng, *Polyhedron*, 1998, **17**, 2187-2190.
21. J. M. Benito, E. de Jesús, F. Javier de la Mata, J. C. Flores, R. Gómez and P. Gómez-Sal, *J. Organomet. Chem.*, 2002, **664**, 258-267.
22. A. Neshat, C. L. Seambos, J. F. Beck and J. A. R. Schmidt, *Dalton Trans.*, 2009, 4987-5000.
23. M. Galajov, C. Garcia and M. Gomez, *Dalton Trans.*, 2011, **40**, 413-420.
24. M. Gómez, C. Hernández-Prieto, A. Martín, M. Mena and C. Santamaría, *Inorg. Chem.*, 2016, **55**, 3815-3821.
25. F. Preuss, G. Hornung, W. Frank, G. Reiß and S. Müller-Becker, *Z. anorg.allg. Chem.*, 1995, **621**, 1663-1671.
26. D. C. Bradley, M. B. Hursthouse, K. M. A. Malik, A. J. Nielson and R. L. Short, *J. Chem. Soc., Dalton Trans.*, 1983, 2651-2656.
27. J. Sundermeyer, *Chem. Ber.*, 1991, **124**, 1977-1979.
28. H. H. Fox, K. B. Yap, J. Robbins, S. Cai and R. R. Schrock, *Inorg. Chem.*, 1992, **31**, 2287-2289.
29. L. K. Johnson, R. H. Grubbs and J. W. Ziller, *J. Am. Chem. Soc.*, 1993, **115**, 8130-8145.
30. P. W. Dyer, V. C. Gibson, J. A. K. Howard, B. Whittle and C. Wilson, *Polyhedron*, 1995, **14**, 103-111.
31. S. M. Rocklage and R. R. Schrock, *J. Am. Chem. Soc.*, 1982, **104**, 3077-3081.
32. M. E. G. Skinner, D. A. Cowhig and P. Mountford, *Chem. Commun.*, 2000, 1167-1168.
33. S. M. Pugh, A. J. Blake, L. H. Gade and P. Mountford, *Inorg. Chem.*, 2001, **40**, 3992-4001.
34. F. A. Cotton and G. Wilkinson, *Advanced Inorganic Chemistry*, Wiley-Interscience, U.S.A., 4th edn., 1980, pp. 717-718, 831-844.
35. S. M. Pugh, D. J. M. Trösch, M. E. G. Skinner, L. H. Gade and P. Mountford, *Organometallics*, 2001, **20**, 3531-3542.
36. I. A. Tonks, L. M. Henling, M. W. Day and J. E. Bercaw, *Inorg. Chem.*, 2009, **48**, 5096-5105.

37. R. R. Schrock and P. R. Sharp, *J. Am. Chem. Soc.*, 1978, **100**, 2389-2399.
38. A. I. Nguyen, K. J. Blackmore, S. M. Carter, R. A. Zarkesh and A. F. Heyduk, *J. Am. Chem. Soc.*, 2009, **131**, 3307-3316.
39. A. F. Heyduk, R. A. Zarkesh and A. I. Nguyen, *Inorg. Chem.*, 2011, **50**, 9849-9863.
40. M. E. O'Reilly and A. S. Veige, *Chem. Soc. Rev.*, 2014, **43**, 6325-6369.
41. F. Preuss and W. Towae, *Z. Naturforsch. B*, 1981, **86b**, 1130-1135.
42. A. V. Korolev, A. L. Rheingold and D. S. Williams, *Inorg. Chem.*, 1997, **36**, 2647-2655.
43. R. R. Schrock, J. Lee, L.-C. Liang and W. M. Davis, *Inorg. Chim. Acta*, 1998, **270**, 353-362.
44. A. Cooper, M. Chem. Thesis, University of Oxford, 2014.
45. P. Ren, O. Vechorkin, K. v. Allmen, R. Scopelliti and X. Hu, *J. Am. Chem. Soc.*, 2011, **133**, 7084-7095.
46. N. J. Bailey, J. A. Cooper, H. Gailus, M. L. H. Green, J. Thomas James and M. A. Leech, *J. Chem. Soc., Dalton Trans.*, 1997, 3579-3584.
47. W. A. Nugent and R. L. Harlow, *J. Chem. Soc., Chem. Commun.*, 1978, 579-580.
48. T. C. Jones, A. J. Nielson and C. E. F. Rickard, *J. Chem. Soc., Chem. Commun.*, 1984, 205-206.
49. P. A. Bates, A. J. Nielson and J. M. Waters, *Polyhedron*, 1985, **4**, 1391-1401.
50. L. R. Chamberlain, B. D. Steffey, I. P. Rothwell and J. C. Huffman, *Polyhedron*, 1989, **8**, 341-349.
51. N. Kaltsoyannis and P. Mountford, *J. Chem. Soc., Dalton Trans.*, 1999, 781-790.
52. N. N. Greenwood and A. Earnshaw, *Chemistry of the elements*, Pergamon Press, Oxford, 1994, p. 1141.
53. J. Unruangsri, H. Morgan, A. D. Schwarz, A. D. Schofield and P. Mountford, *Organometallics*, 2013, **32**, 3091-3107.
54. A. D. Schofield, A. Nova, J. D. Selby, C. D. Manley, A. D. Schwarz, E. Clot and P. Mountford, *J. Am. Chem. Soc.*, 2010, **132**, 10484-10497.
55. L. H. Gade and N. Mahr, *J. Chem. Soc. Dalton Trans.*, 1993, **4**, 489-494.
56. S. Friedrich, L. H. Gade, A. J. Edwards and M. McPartlin, *Chem. Ber.*, 1993, **126**, 1797-1805.
57. H. Memmler, L. H. Gade and J. W. Lauher, *Inorg. Chem.*, 1994, **33**, 3064-3071.

58. H. Memmler, K. Walsh, L. H. Gade and J. W. Lauher, *Inorg. Chem.*, 1995, **34**, 4062-4068.
59. M. Schubart, B. Findeis, L. H. Gade, W. S. Li and M. McPartlin, *Chem. Ber.*, 1995, **128**, 329-334.
60. S. Friedrich, L. H. Gade, W. S. Li and M. McPartlin, *Chem. Ber.*, 1996, **129**, 1287-1291.
61. B. Findeis, M. Schubart, L. H. Gade, F. Moller, I. Scowen and M. McPartlin, *J. Chem. Soc., Dalton Trans.*, 1996, 125-132.
62. K. Wieghardt and U. Quilitzsch, *Z. anog. allg. Chem.*, 1979, **457**, 75-83.
63. N. Desmangles, H. Jenkins, K. B. Ruppa and S. Gambarotta, *Inorg. Chim. Acta*, 1996, **250**, 1-4.
64. S. Jae-Inh and G. Sandro, *Chem. Eur. J.*, 1996, **2**, 1258-1263.
65. P. L. Hill, G. P. A. Yap, A. L. Rheingold and E. A. Maatta, *J. Chem. Soc., Chem. Commun.*, 1995, 737-738.
66. W. H. Harman, M. F. Lichterman, N. A. Piro and C. J. Chang, *Inorg. Chem.*, 2012, **51**, 10037-10042.
67. U. Piarulli, E. Solari, C. Floriani, A. Chiesi-Villa and C. Rizzoli, *J. Am. Chem. Soc.*, 1996, **118**, 3634-3642.
68. P. J. Walsh, F. J. Hollander and R. G. Bergman, *J. Am. Chem. Soc.*, 1988, **110**, 8729-8731.
69. A. J. Blake, P. E. Collier, L. H. Gade, M. McPartlin, P. Mountford, M. Schubart and I. J. Scowen, *Chem. Commun.*, 1997, 1555-1556.
70. S. Y. Lee and R. G. Bergman, *Tetrahedron*, 1995, **51**, 4255-4276.
71. K. E. Meyer, P. J. Walsh and R. G. Bergman, *J. Am. Chem. Soc.*, 1995, **117**, 974-985.
72. S. Y. Lee and R. G. Bergman, *J. Am. Chem. Soc.*, 1995, **117**, 5877-5878.
73. A. P. Duncan and R. G. Bergman, *Chem. Records*, 2002, **2**, 431-445.
74. S. A. Blum, V. A. Rivera, R. T. Ruck, F. E. Michael and R. G. Bergman, *Organometallics*, 2005, **24**, 1647-1659.
75. N. Hazari and P. Mountford, *Acc. Chem. Res.*, 2005, **38**, 839-849.
76. A. Bashall, M. McPartlin, P. E. Collier, P. Mountford, L. H. Gade and D. J. M. Trösch, *Chem. Commun.*, 1998, 2555-2556.

77. A. Bashall, P. E. Collier, L. H. Gade, M. McPartlin, P. Mountford, S. M. Pugh, S. Radojevic, M. Schubart, I. J. Scowen and D. J. M. Trösch, *Organometallics*, 2000, **19**, 4784-4794.

78. D. J. M. Trösch, P. E. Collier, A. Bashall, L. H. Gade, M. McPartlin, P. Mountford and S. Radojevic, *Organometallics*, 2001, **20**, 3308-3313.

79. B. D. Ward, A. Maisse-Francois, P. Mountford and L. H. Gade, *Chem. Commun.*, 2004, 704-705.

80. P. J. Walsh, F. J. Hollander and R. G. Bergman, *Organometallics*, 1993, **12**, 3705-3723.

81. S. M. Pugh, D. J. M. Trösch, D. J. Wilson, A. Bashall, F. G. N. Cloke, L. H. Gade, P. B. Hitchcock, M. McPartlin, J. F. Nixon and P. Mountford, *Organometallics*, 2000, **19**, 3205-3210.

82. D. Swallow, J. M. McInnes and P. Mountford, *J. Chem. Soc., Dalton Trans.*, 1998, 2253-2260.

83. S. R. Dubberley, A. Friedrich, D. A. Willman, P. Mountford and U. Radius, *Chem. Eur. J.*, 2003, **9**, 3634-3654.

84. C. L. Boyd, T. Toupance, B. R. Tyrrell, B. D. Ward, C. R. Wilson, A. R. Cowley and P. Mountford, *Organometallics*, 2005, **24**, 309-330.

85. A. E. Guiducci, A. R. Cowley, M. E. G. Skinner and P. Mountford, *J. Chem. Soc., Dalton Trans.*, 2001, 1392-1394.

86. A. E. Guiducci, C. L. Boyd and P. Mountford, *Organometallics*, 2006, **25**, 1167-1187.

87. S. Mellino, L. C. Stevenson, E. Clot and P. Mountford, *Organometallics*, 2017, **36**, 3329-3342.

88. B. A. Clough, S. Mellino, A. V. Protchenko, M. Slusarczyk, L. C. Stevenson, M. P. Blake, B. Xie, E. Clot and P. Mountford, *Inorg. Chem.*, 2017, **56**, 10794-10814.

Chapter Four

Group 5 hydrazido complexes with tridentate, trianionic ligands: synthesis, structure, bonding and reactivity

4.1 Overview

This chapter will describe the synthesis and characterisation of new Group 5 hydrazido complexes with tridentate, trianionic ligands. Firstly, hydrazido synthons of the type $M(NNR_x)Cl_3(L)$ with either 2,2'-bipyridyl (bipy) or 4,4'-di-*tert*-butyl-2,2'-bipyridyl (di-^{t}Bu-bipy) will be explored. Secondly, two synthetic routes to obtain Group 5 hydrazido complexes of the type $M(N_2N^R)(NNPh_2)(L)_x$ with tridentate, trianionic ligands will be discussed, alongside DFT calculations giving a bonding analysis of imido compounds $M(NN_2^R)(N^tBu)(py)_2$ and their hydrazido analogues $M(NN_2^R)(NNPh_2)(py)_2$ (as well as the corresponding bipyridyl counterparts). Finally, the reactivity studies of the hydrazido complex $Nb(NN_2^{iPr})(NNPh_2)(py)_2$ with unsaturated and other small substrates will be described.

4.2 Introduction

Since imido and hydrazido functional groups (M=NH, $M=NNH_2$) were proposed as intermediates in the Chatt-type[1] cycle of N_2 reduction, the chemistry of transition metal–ligand multiple bonding has been an active area of investigation. Much of the early work focussed on Group 6 metal compounds with a wide range of molybdenum and tungsten hydrazido complexes prepared.[2-5] Many other nitrogen-containing products from the reactions of $M{=}NNR_2$ moieties have also been studied in detail. For instance, Group 4 hydrazido complexes exhibit a rich reactivity with small molecules at the $M{=}N_\alpha$ multiple bond *via* [2+2] cycloaddition reaction,[6-15] $N_\alpha{-}N_\beta$ bond cleavage[7,12,16-22] and catalytic hydrohydrazination[11,20,23-25].

Although there exist examples of vanadium hydrazido(2-) complexes[26-32], the number of niobium and tantalum compounds is comparatively smaller. The complex $CpNb(NNMe_2)Cl_2$ was the first niobium hydrazido complex reported by Green in 1997.[33] The solid state structure of this complex showed it to be a dimer with two hydrazido ligands with different coordination modes: η^1 and an unusual μ-η^2 bonding. Reaction of compound $CpNb(NNMe_2)Cl_2$ with LiCp gave the niobocene hydrazido complex $Cp_2Nb(NNMe_2)Cl$ (**1.70**) and the solid state structure of the analogous compound $Cp'_2Nb(NNMe_2)Cl$ proved to be monomeric.[34]

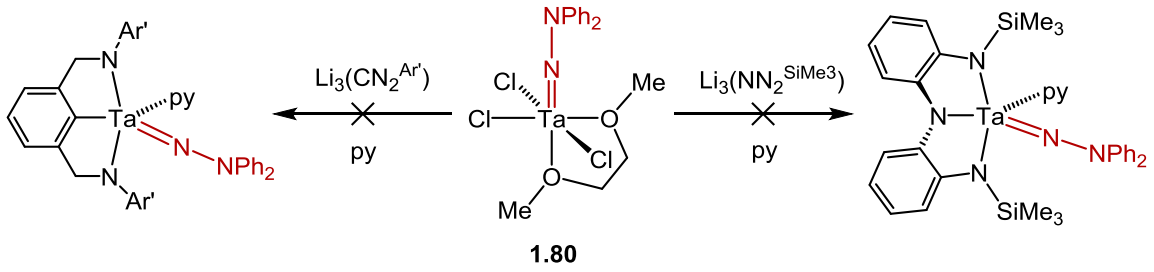
In the case of tantalum hydrazide chemistry, Wilkinson and co-workers reported in 1997 the anionic complex $[Ta\{NN(2,6\text{-}C_5H_6Me_2)\}_2Cl_4]^-$ alongside the niobium analogue.[30]

Metric data for the two hydrazido moieties suggested a weak π-bond interaction between the ligand and the metal; this resonance form is better described as isodiazene(0) rather than hydrazido(2-). A decade later, Winter and co-workers synthesised tantalum and niobium cationic complexes of the formula $[M(NNR_2)Cl_2(NH_2NR_2)(TMEDA)]Cl$ (**1.71**) and $[M\{NN(CH_2)_5\}Cl_2\{NH_2N(CH_2)_5\}]Cl$ (**1.72**) in which different hydrazido ligand coordination modes are present, with η^1 and η^2 bonding.[35] More recently, Bercaw and co-workers reported the diphenyl hydrazido synthons $M(NNPh_2)Cl_3(DME)$ (M = Ta (**1.80**) or Nb, DME = 1,2-dimethoxyethane).[36,37] Complex **1.80** was used for the synthesis of a range of tantalum hydrazido complexes supported by mono- and dianionic ligands *via* salt metathesis reactions. For example, when the bis(amide)amine complex $Ta(NNPh_2)Cl(C_2\text{-}N_2N^{Me})$ was treated with $Na[BAr^F]$ ($[BAr^F]^- = [B(3,5\text{-}C_6H_3(CF_3)_2)_4]^-$) in the presence of pyridine, the cationic chloride-abstracted product $[Ta(NNPh_2)(N_2N^{Me})(py)][BAr^F]$ was generated. However, this compound was unreactive when attempts were made of pyridine substitution and [2+2] reactions with terminal and internal alkynes.[36]

These complexes with chloride substituents showed negligible reactivity in contrast to their Group 4 counterparts. For this reason, analogous neutral Group 5 complexes with trianionic, tridentate ligands in place of the dianionic N_2N^R type were targeted in this work. Following this, the displacement of the chloride ligand for labile Lewis-bases will allow access to reactive $Ta(N_3)(NNPh_2)(L)_x$ species (N_3 = a trianionic, tridentate ligand, L = Lewis base, x = 0 or 1).

4.3 Synthesis of hydrazido synthons

Preliminary reactions of the diphenylhydrazido synthon $Ta(NNPh_2)Cl_3(DME)$ (**1.80**)[36] with the lithiated salts $Li_3(CN_2^{Ar'})$ (**1.6**, $CN_2^{Ar'} = 1,3\text{-}C_6H_4(CH_2N^{Ar'})_2$, $Ar' = 2,6\text{-}C_6H_3{}^iPr_2$[38-40] and $Li_3(NN_2^{SiMe3})$ (**1.7**, $NN_2^{SiMe3} = N(SiMe_3N\text{-}o\text{-}C_6H_4)_2$)[41] were attempted to give the corresponding hydrazido complexes as shown in Scheme 4.1. However, this route was found to be unsuccessful as complex mixtures were formed under various conditions and only protio-ligands were identified by ^1H NMR spectroscopy.



1.80

Scheme 4.1. Attempted synthesis of tantalum hydrazido complexes with $Li_3(CN_2^{Ar'})$ (**1.6**) (Ar' = 2,6-$C_6H_3{}^iPr_2$) and $Li_3(NN_2^{SiMe3})$ (**1.7**) pincer ligands.[36,39,41,42]

Bercaw and co-workers showed that the synthon $Ta(NNPh_2)Cl_3(DME)$ (**1.80**) undergoes ligand substitution with pyridine, tetramethylethylenediamine (TMEDA), bipy and THF in NMR scale reactions, of which the bipy and THF adducts decompose in solution.[36] However, when these reactions were attempted on the preparative scale isolation of the complexes was unsuccessful.

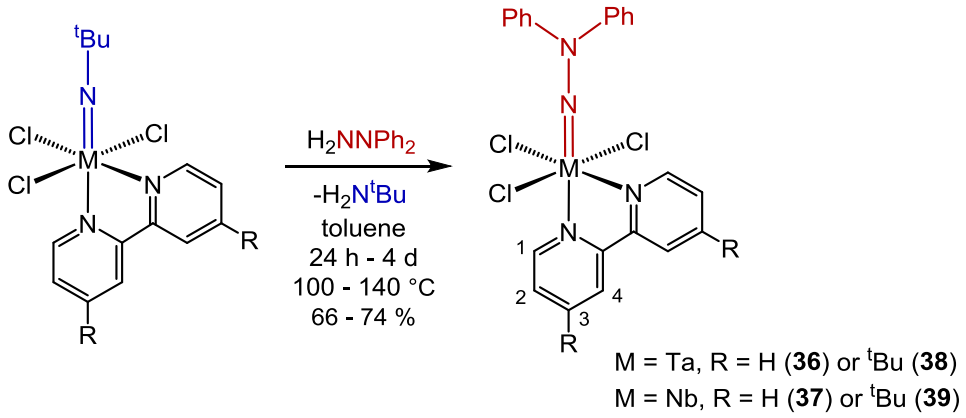
This Chapter will describe two different approaches to the formation of Group 5 hydrazido complexes with tridentate, trianionic ligands. Firstly, the synthesis of hydrazido synthons from the analogous imido synthons by hydrazine/*tert*-butylimide exchange reactions, followed by salt metathesis reaction with the lithiated tridentate ligand will be described. Secondly, the formation of the hydrazido complexes by hydrazine/*tert*-butylimide exchange reactions from the imido complexes with the tridentate ligand already coordinated to the metal centre will be discussed.

4.3.1 Synthesis of $M(NNPh_2)Cl_3(L)$

The hydrazido synthons $M(NNPh_2)Cl_3$(R-bipy) (M = Ta, R = H (**36**) or ^{t}Bu (**38**); M = Nb, R = H (**37**) or ^{t}Bu (**39**)) were synthesised *via* hydrazine/*tert*-butylimide exchange reaction from the imido analogues $M(N^tBu)Cl_3$(R-bipy) in toluene during a long period of time (1 to 4 days) at high temperatures (100 to 140 ˚C). The pure products were dried *in vacuo* at 80 ˚C for 16 h (Equation 4.1). Surprisingly, no reaction was observed in the attempt to synthesise the bis(pyridine) adducts following the same methodology.

The ^{1}H (Figure 4.1) and ^{13}C NMR spectra are consistent with a bidentate bipy or di-^{t}Bu-bipy ligand coordinated to one axial and one equatorial position around the metal centre.The diphenylhydrazido moiety can be observed as three ^{1}H multiplets between 7.65 and 7.04 ppm for all complexes **36**, **37**, **38** and **39** as shown in Figure 4.1 (from top to bottom, respectively). The resonances attributed to the bipy ligand include four (**36** and

37) and three (**38** and **39**) multiplets for the inequivalent aryl rings and two singlets for the ^{t}Bu groups in the di-^{t}Bu-bipy complexes **38** (1.48 and 1.42 ppm) and **39** (1.47 and 1.41 ppm).



Equation 4.1

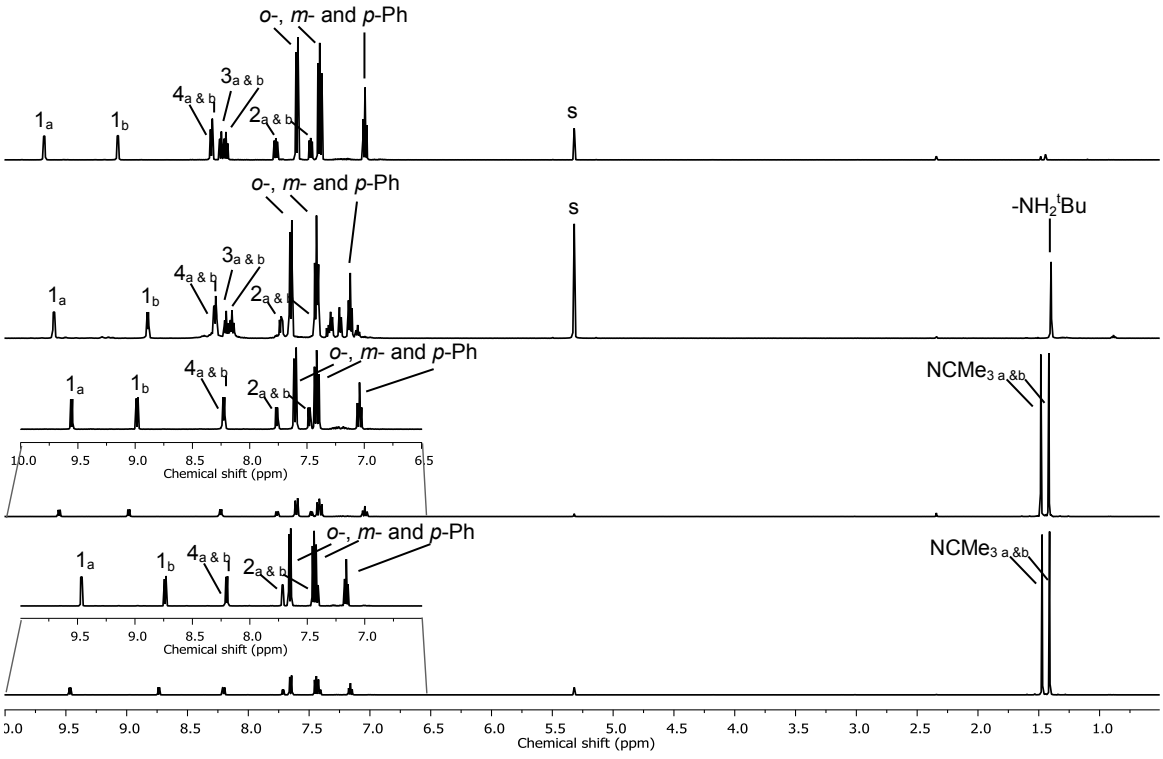


Figure 4.1. ^{1}H NMR spectra (500.3 MHz) of M(NNPh$_2$)Cl$_3$(bipy) (M = Ta (**36**, top) or Nb (**37**, middle top)) and M(NNPh$_2$)Cl$_3$(di-^{t}Bu-bipy) (M = Ta (**38**, middle bottom) or Nb (**39**, bottom)) in CD_2Cl_2 at 298 K. Note: subscripts "a" and "b" refer to inequivalent R-bipy environments and "s" denotes residual protio solvent.

Diffraction-quality crystals of **36**, **38** and **39** were grown by solvent diffusion in dichloromethane/pentane at RT. The molecular solid state structures are shown in Figure 4.2 along with selected bond lengths and angles in Table 4.1.

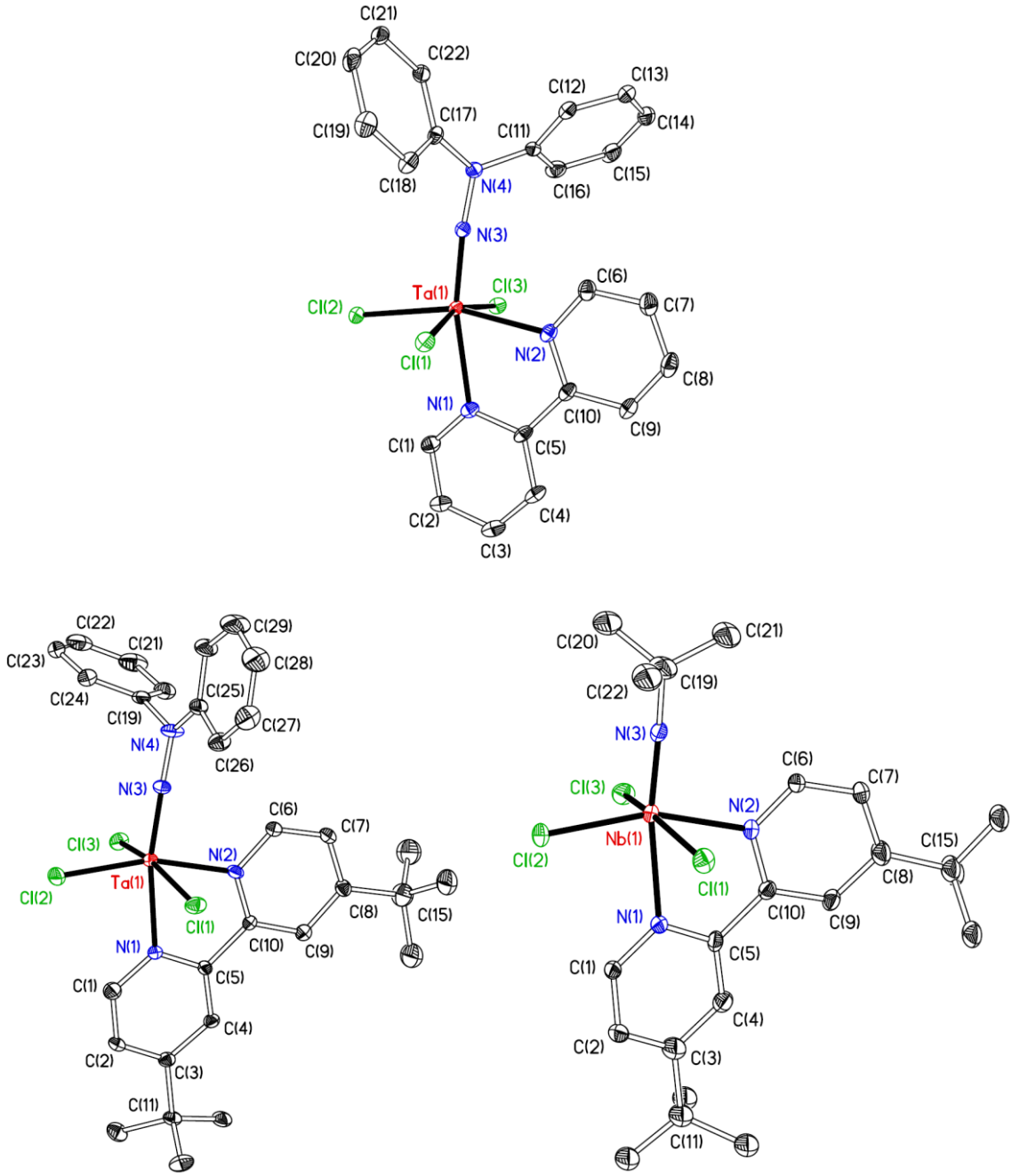


Figure 4.2. Displacement ellipsoid plots (20 % probability) of $M(NNPh_2)Cl_3(R\text{-bipy})$ (M = Ta, R = H (**36**, top) or ^{t}Bu (**38**, bottom left); M = Nb, R = ^{t}Bu (**39**, bottom right)). H atoms are omitted for clarity.

Table 4.1. Selected bond lengths (Å) and angles (°) for $M(NNPh_2)Cl_3$(R-bipy) (M = Ta, R = H (**36**) or ^{t}Bu (**38**); M = Nb, R = ^{t}Bu (**39**)).

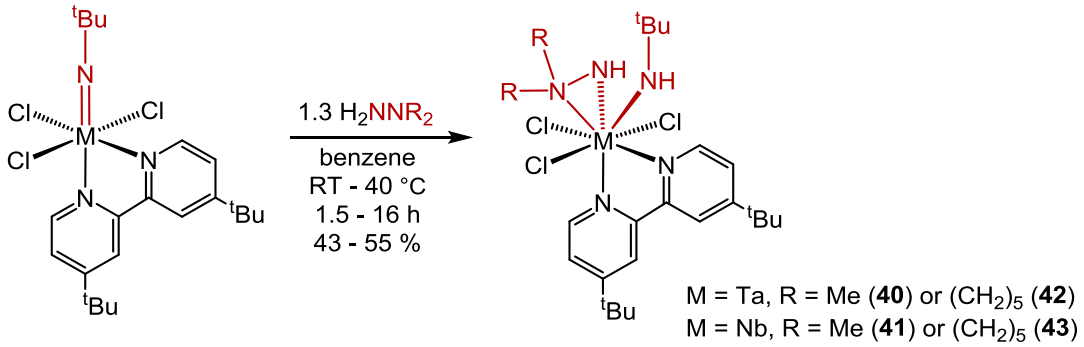
Parameter	**36**	**38**	**39**
M(1)–N(1)	2.3287(19)	2.326(3)	2.339(3)
M(1)–N(2)	2.2362(19)	2.217(3)	2.240(3)
M(1)–N(3)	1.7869(19)	1.784(3)	1.783(3)
M(1)–Cl(1)	2.4175(5)	2.4024(7)	2.4103(8)
M(1)–Cl(2)	2.3839(5)	2.3826(9)	2.3927(8)
M(1)–Cl(3)	2.3660(5)	2.3798(8)	2.3956(8)
N(3)–N(4)	1.348(3)	1.340(4)	1.332(4)
N(1)–M(1)–N(2)	71.51(7)	71.73(9)	71.26(9)
N(1)–M(1)–N(3)	166.63(7)	166.36(11)	166.65(11)
N(2)–M(1)–N(3)	95.24(8)	94.82(11)	95.60(11)
N(1)–M(1)–Cl(1)	82.76(5)	81.40(7)	81.72(7)
N(2)–M(1)–Cl(1)	81.91(5)	82.95(7)	82.49(7)
N(3)–M(1)–Cl(1)	97.39(6)	99.53(9)	99.29(8)
N(1)–M(1)–Cl(2)	91.41(5)	91.52(7)	92.55(7)
N(2)–M(1)–Cl(2)	162.16(5)	163.17(7)	163.74(7)
N(3)–M(1)–Cl(2)	101.95(6)	101.98(9)	100.64(9)
Cl(1)–M(1)–Cl(2)	91.066(19)	93.21(3)	94.07(3)
N(1)–M(1)–Cl(3)	81.29(5)	81.15(7)	81.41(7)
N(2)–M(1)–Cl(3)	86.37(5)	84.50(7)	83.73(7)
N(3)–M(1)–Cl(3)	96.50(6)	95.69(9)	95.10(8)
Cl(1)–M(1)–Cl(3)	162.56(2)	160.99(3)	160.93(3)
Cl(2)–M(1)–Cl(3)	96.330(19)	94.70(3)	95.50(3)
M(1)–N(3)–N(4)	174.52(15)	168.1(3)	168.2(2)

All complexes are monomeric containing an "end-on" (η^1) bound diphenylhydrazido(2-) ligand and have distorted octahedral geometries, in which the two nitrogen atoms of the bipy ligand coordinate to the metal centre occupying an axial and an equatorial position and the three chloride ligands are arranged in a meridional fashion. Therefore, their geometry is analogous to the previously structurally characterised imido complexes $V(N^tBu)Cl_3(bipy)$ (**1.46**) and $Nb(N^tBu)Cl_3(di\text{-}^tBu\text{-}bipy)$ (**15**) discussed in Chapter Three, and the series of tantalum and niobium hydrazido synthons of the type $M(NNR_2)Cl_3(DME)$[36,37].

The $M{-}N_\alpha$ bond lengths of 1.7869(19) (**36**), 1.784(3) (**38**) and 1.783(3) Å (**39**) and the nearly linear $M(1){-}N(3){-}N(4)$ bond angles of 174.52(15), 168.1(3) and 168.2(2) ° respectively, are consistent with a formal M≡N multiple bond. However, the $M{-}N_\alpha$ bond lengths in these complexes are slightly longer compared to those reported for complexes of the type $M(NNR_2)Cl_3(DME)$ (avg. M−N of 1.7673 Å, range 1.7597 – 1.7742 Å for thirteen examples),[37]which is the result of bipy being a stronger donor ligand that DME. Also, *trans* influence from the hydrazide moiety to the bipy ring in the axial position is observed in a longer $M{-}N_{ax}$ bond length, with values of 2.3287(19) (**36**), 2.326(3) (**38**) and 2.339(3) Å (**39**), than the *cis*-bonded bipy ring at 2.2362(19) (**36**), 2.217(3) (**38**) and 2.240(3) Å (**39**).[43,44] The $N_\alpha{-}N_\beta$ bond distances in complexes **36**, **38** and **39** of 1.348(3), 1.340(4) and 1.332(4) Å respectively, are shorter than the one of free diphenylhydrazine (1.418 Å). In general, these complexes are consistent with a hydrazido(2-) ligand mode.[36]

While the exchange reactions with diphenylhydrazine (**36 - 39**) present a hydrazido(2-) ligand coordinated to the metal centre, reactions of the imido synthons with H_2NNMe_2 (N,N-dimethylhydrazine) and $H_2NN(CH_2)_5$ (1-aminopiperidine) did not proceed by *tert*-butylimide exchange. Instead complexes $M(NHNR_2)(NH^tBu)Cl_3(di\text{-}^tBu\text{-}bipy)$ (M = Ta, R = Me (**40**) or $(CH_2)_5$ (**42**); M = Nb, R = Me (**41**) or $(CH_2)_5$ (**43**)) contain the hydrazide ligand coordinated in a η^2-hydrazido(1-) mode and the *tert*-butyl-amide ligand from a proton exchange reaction to the *tert*-butylimido moiety (Equation 4.2).[35] Previous work on imide/hydrazine exchange reactions showed equally thermodynamically favourable but for H_2NNR_2 with R = alkyl the N_β (sp^3) lone pair is more accessible (no delocalisation) than for $N_\beta Ph_2$, thus it will not present η^1 coordination. Also, the $N_\beta Ph_2$ when R = Ph is more sterically crowded than in the case of R= Me or $(CH_2)_5$.[8,45,46] Synthesis of the analogous tantalum and niobium complex with bipy, double insertion of

the hydrazido ligand and installation of tridentate, trianionic ligands may be carried out in the future.

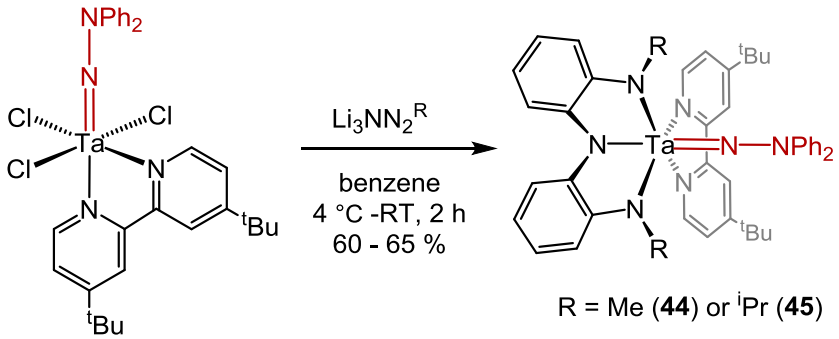


Equation 4.2

4.4. Installation of the tridentate, trianionic supporting ligands NN_2^R

Salt metathesis reactions of $Ta(NNPh_2)Cl_3$(di-^{t}Bu-bipy) (**38**) with the lithiated salts $Li_3(NN_2^R)$ (R = Me (**1**), ^{i}Pr (**2**) or $SiMe_3$ (**1.7**)) yielded the hydrazido complexes $Ta(NN_2^R)(NNPh_2)$(di-^{t}Bu-bipy) (R = Me (**44**) and ^{i}Pr (**45**)) on the preparative scale in benzene after 2 h. at RT (Equation 4.3). Characterisation of both complexes by ^{1}H and ^{13}C NMR spectroscopy in C_6D_6 at RT is consistent with C_s symmetric molecules.

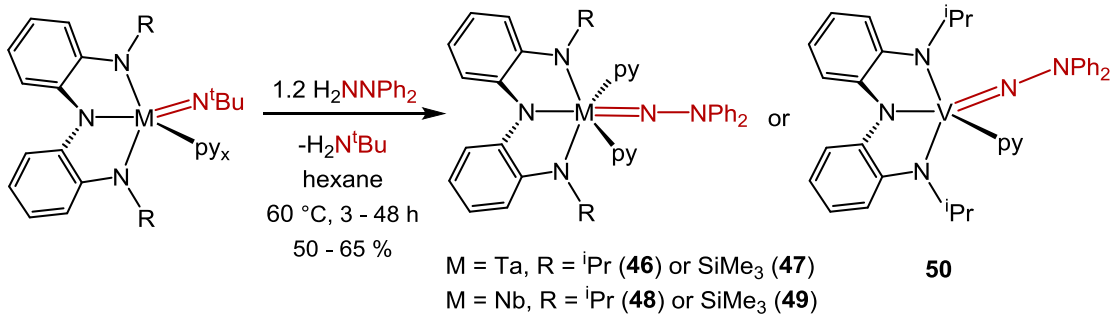
In the ^{1}H NMR spectra the $N_\beta Ph_2$ moiety is observed as three multiplets within the range *ca* 7.0 – 6.7 ppm. The resonances attributed to the tridentate supporting ligand NN_2^R include a singlet for the methyl (4.33 ppm), or two sets of doublets for the diastereotopic methyls of the isopropyl groups (at 1.76 and 1.67 ppm) along with a septet for the isopropyl methine (5.33 ppm), and four multiplets for the aryl rings in the range 7.89 – 6.92 ppm. The spectra showed a coordinated bidentate di-^{t}Bu-bipy ligand, as expected for methyl and isopropyl substituents, which displays three multiplet signals (range 9.28 – 6.54 ppm) and a singlet for the ^{t}Bu groups at 0.77 ppm in both complexes (**44** and **45**).



Equation 4.3

4.5 Synthesis of hydrazido complexes *via* hydrazine/*tert*-butylimide exchange reactions

As discussed throughout this Thesis, several routes towards the formation of Group 5 hydrazido complexes with tridentate, trianionic ligands were attempted. In some of these routes, synthetic pathways *via* hydrazine/*tert*-butylimide exchange reaction were considered from the imido compounds containing the tridentate ligand. The imido complexes $M(NN_2^R)(N^tBu)(py)_2$ (M = Ta, R = Me (**17**), ^{i}Pr (**18**) or $SiMe_3$ (**19**); M = Nb, R = Me (**20**), ^{i}Pr (**21**) or $SiMe_3$ (**22**)) and $V(NN_2^{iPr})(N^tBu)Cl_3(py)$ (**23**) were successfully synthesised *via* salt metathesis reaction of the imido synthons $M(N^tBu)Cl_3(py)_2$ (M = Ta (**1.41**), Nb (**1.42**) or V (**1.45**)) with the respective lithiated tridentate ligand of the type $Li_3(NN_2^R)$ (see Chapter Three). Furthermore, these imido compounds undergo hydrazine/*tert*-butylimide exchange reaction with diphenylhydrazine to yield complexes $M(NN_2^R)(NNPh_2)(py)_2$ (M = Ta, R = ^{i}Pr (**46**) or $SiMe_3$ (**47**); M = Nb, R = ^{i}Pr (**48**) or $SiMe_3$ (**49**)) and $V(NN_2^{iPr})(NNPh_2)(py)$ (**50**) (Equation 4.4).



Equation 4.4

Characterisation of $M(NN_2^R)(NNPh_2)(py)_2$ (M = Ta, R = ^{i}Pr (**46**) or $SiMe_3$ (**47**); M = Nb, R = ^{i}Pr (**48**) or $SiMe_3$ (**49**)) by ^{1}H (Figure 4.3) and ^{13}C NMR spectroscopy in C_6D_6 at RT is consistent with C_{2v} symmetric molecules with two equivalent pyridine ligands and the hydrazido moiety coordinated to the metal centre along with a tridentate ligand in which the isopropyl or trimethylsilyl substituents remain chemically equivalent to each other. In the case of $V(NN_2^{iPr})(NNPh_2)(py)$ (**50**), the ^{1}H NMR (Figure 4.3) characterisation is consistent with a C_s symmetric molecule with just one pyridine ligand coordinated to the vanadium and the tridentate ligand with equivalent isopropyl groups.

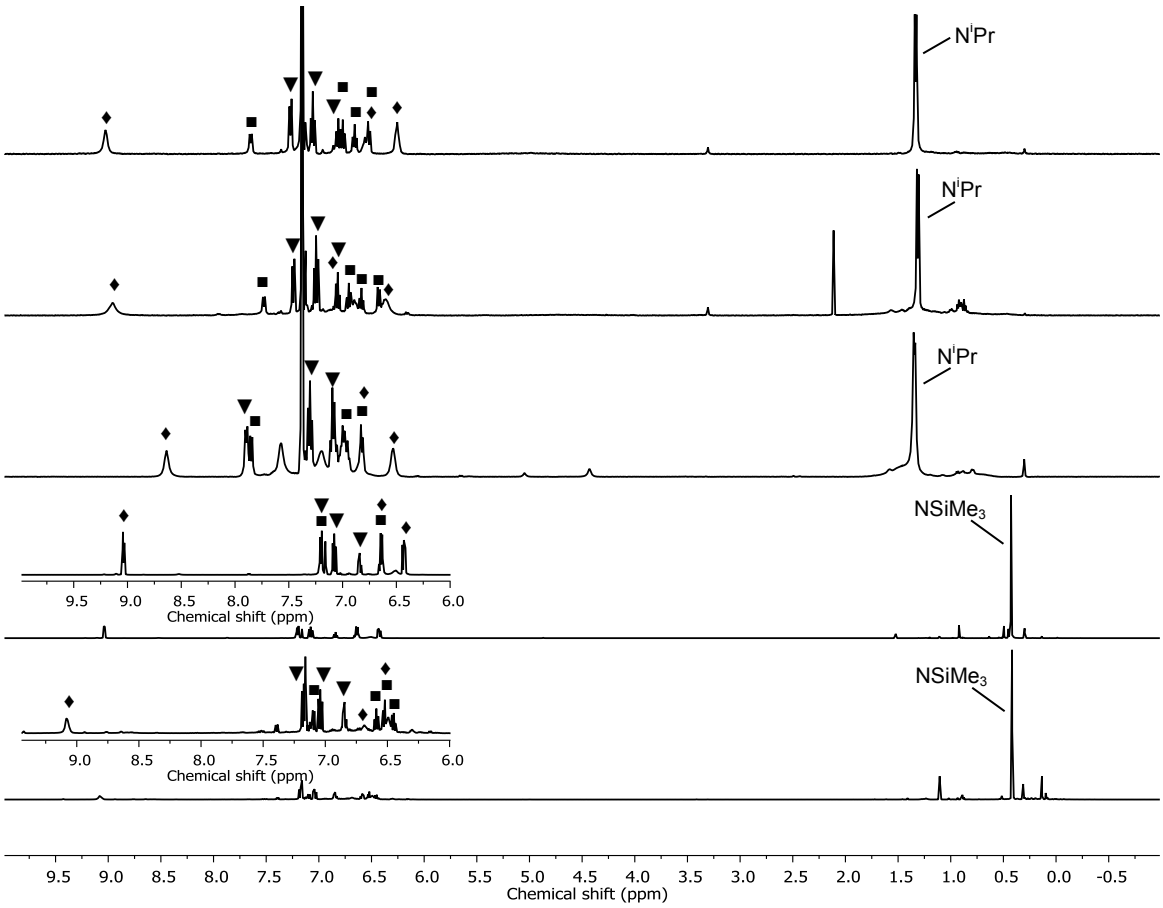


Figure 4.3. ^{1}H NMR spectra (500.3 MHz) of, from top to bottom, M(NN_2^{iPr})($NNPh_2$)(py)$_2$ (M = Ta (**46**) or Nb (**48**)), V(NN_2^{iPr})($NNPh_2$)(py) (**50**) and M(NN_2^{SiMe3})($NNPh_2$)(py)$_2$ (M = Ta (**47**) or Nb (**49**)) in C_6D_6 at 298 K. Note: "▼", "■" and "▼" refer to $N_\beta Ph_2$, NN_2^R and pyridine signals respectively.

The resonances attributed to the $NNPh_2$ ligand are observed as three multiplets within the range 7.7 – 6.75 ppm. Those resonances for the tridentate supporting ligand NN_2^R include a doublet for the methyls of the isopropyl groups (at 1.33 (**46**), 1.31 (**48**) and 1.34 ppm (**50**) (the septet for the isopropyl methine was not observed in any of the three complexes) or a singlet for the trimethylsilyl groups (at 0.43 (**47**) and 0.42 ppm (**49**)); and four multiplets for the aryl rings in the range 7.7 – 6.4 ppm. The ^{1}H NMR spectra showed two chemically equivalent pyridine ligands in complexes **46**, **47**, **48** and **49** and one pyridine ligand in complex **50** coordinated to the metal centre which are observed as three multiplet signals (usually broad signals in the range 9.1 – 6.2 ppm).

Diffraction quality crystals of M(NN_2^R)($NNPh_2$)(py)$_2$ (M = Ta, R = ^{i}Pr (**46**) or $SiMe_3$ (**47**); M = Nb, R = ^{i}Pr (**48**)) were grown from a saturated benzene-d_6 solution at RT. The molecular solid state structures are shown in Figure 4.4 and selected bond lengths and

angles are listed in Table 4.2. All three complexes exist as a single monomer and present pseudo-octahedral geometry. The hydrazido moiety and two pyridine ligands (*trans* to each other) along with an N_{aryl} atom from the tridentate ligand are positioned in the equatorial plane. The angles between these ligands are close to the theoretical 90˚ expected for regular octahedral geometry. A distortion in the geometry is observed along the axial positions occupied by the tridentate ligand NN_2^R as a result of steric constrains forming an angle N(2)−Ta(1)−N(3) of 148.30(12) (**46**), 150.94(4) (**47**) and 147.79(6)˚ (**48**). This distortion observed in the NN_2^R ligand has been described previously in Chapter Two and Three for the solid state structures of tantalum dialkyl, alkyl-amido and imido complexes (avg. N(2)−Ta(1)−N(3) of 149.98˚, range 149.36(10) – 151.07(19)˚ for six examples). Additionally, the aryl rings in the NN_2^R ligand are slightly twisted from each other out of planarity, the angle between the planes being *ca* 29.10, 38.44 and 29.08˚ respectively. The greater angle in **47** might be caused by steric interactions between the trimethylsilyl substituents and the $N_\beta Ph_2$ group.[42]

The hydrazido moiety shows M−N_α bond lengths of 1.856(3) (**46**), 1.8238(12) (**47**) and 1.8496(14) Å (**48**) and nearly linear M−N_α−N_β bond angles of 169.5(3), 178.79(11) and 169.77(12)˚, respectively. The M(1)−N(6) bond lengths in these three complexes are longer than those formal Ta≡N triple bonded hydrazido compounds with mono- and dianionic ligands (avg. Ta−N of 1.7866 Å, range 1.762(3) – 1.7988(1) Å for five examples), approaching an M═N_α double bond as observed in the complex $Cp_2Ta(NNPh_2)Cl$ (Ta−N of 1.8153(16) Å).[36] The lengthening of the M−N bond was also observed in the imido complexes $Ta(NN_2^{Me})(N^tBu)(py)_2$ (**17**) and $Nb(NN_2^R)(N^tBu)(bipy)$ (R = ^{i}Pr (**26**) and $SiMe_3$ (**25**)) and attributed to a stronger *trans* influence of the N_{aryl} from the pincer ligand and π-bonding competition in these complexes (*vide infra*).[43,44] This effect can also be observed in the NN_2^R ligand where the M(1)−N(2) and M(1)−N(3) bonds lengths (avg. 2.076 Å, range 2.063(3) – 2.0903(11) Å) in complexes **46**, **47** and **48** are slightly shorter than the M(1)−N(1) with values of 2.147(3), 2.1365(12) and 2.1617(13) Å respectively.

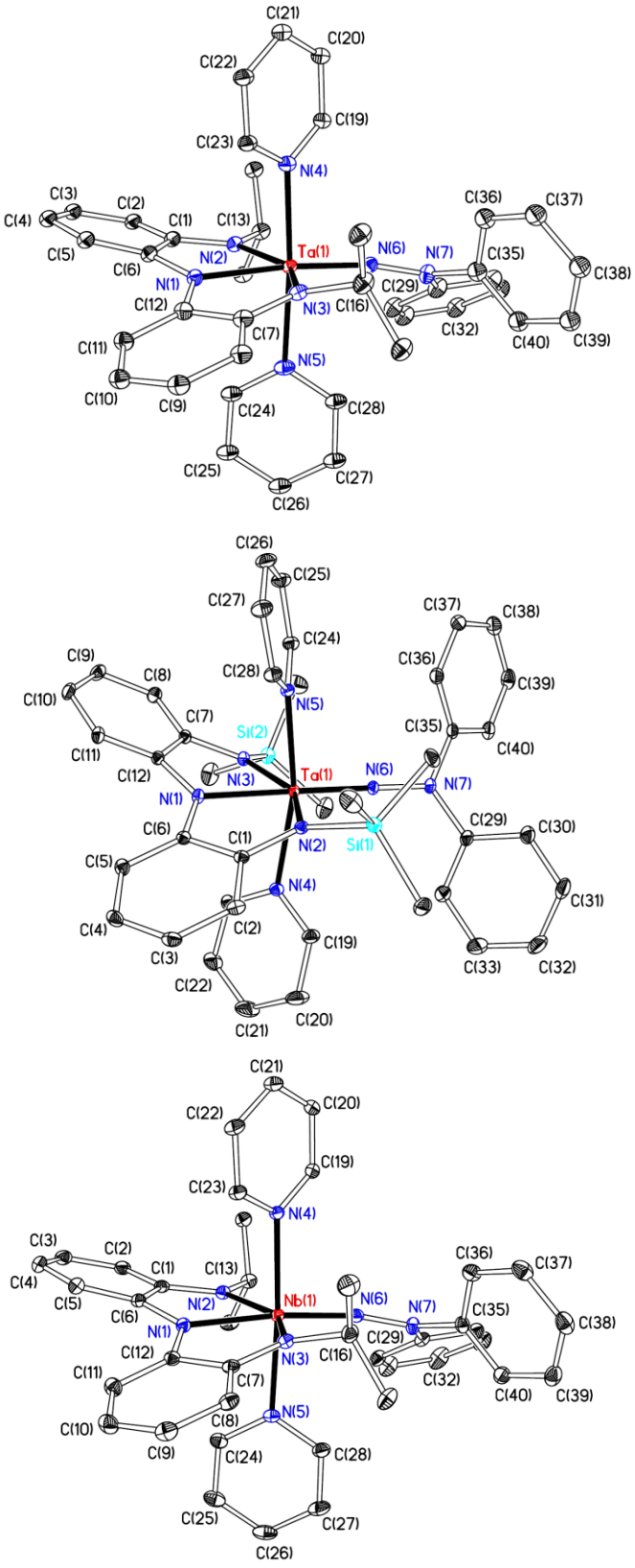
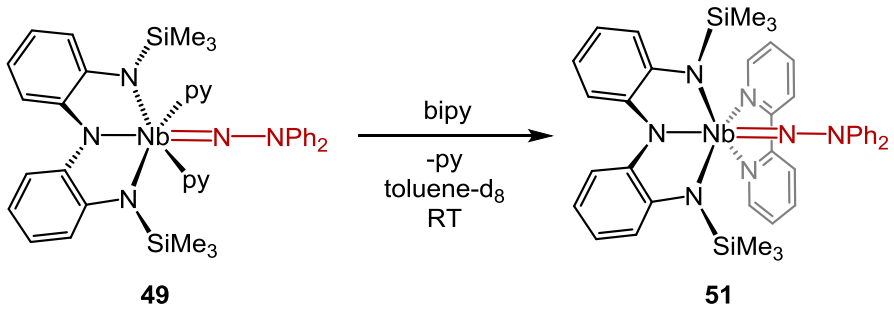


Figure 4.4. Displacement ellipsoid plots (20 % probability) of $M(NN_2^R)(NNPh_2)(py)_2$ (M = Ta, R = ^{i}Pr (**46**, top) or $SiMe_3$ (**47**, middle); M = Nb, R = ^{i}Pr (**48**, bottom)). H atoms omitted for clarity.

Table 4.2. Selected bond lengths (Å) and angles (°) for $M(NN_2^R)(NNPh_2)(py)_2$ (M = Ta, R = ^{i}Pr (**46**) or $SiMe_3$ (**47**); M = Nb, R = ^{i}Pr (**48**)).

Parameter	**46**	**47**	**48**
M(1)–N(1)	2.147(3)	2.1365(12)	2.1617(13)
M(1)–N(2)	2.076(3)	2.0862(11)	2.0784(13)
M(1)–N(3)	2.063(3)	2.0903(11)	2.0641(14)
M(1)–N(4)	2.267(3)	2.2552(12)	2.2938(13)
M(1)–N(5)	2.272(3)	2.2723(12)	2.2968(14)
M(1)–N(6)	1.856(3)	1.8238(12)	1.8496(14)
N(6)–N(7)	1.347(4)	1.3702(17)	1.353(2)
N(1)–M(1)–N(2)	74.93(11)	75.58(5)	74.54(5)
N(1)–M(1)–N(3)	73.48(12)	75.39(5)	73.36(5)
N(2)–M(1)–N(3)	148.30(12)	150.94(4)	147.79(6)
N(1)–M(1)–N(4)	88.75(11)	82.81(5)	88.81(5)
N(2)–M(1)–N(4)	89.40(11)	85.31(4)	89.37(5)
N(3)–M(1)–N(4)	87.32(11)	92.46(4)	87.35(5)
N(1)–M(1)–N(5)	86.03(11)	82.93(5)	86.38(5)
N(2)–M(1)–N(5)	90.80(11)	90.02(4)	91.23(5)
N(3)–M(1)–N(5)	89.64(11)	85.06(4)	89.40(5)
N(4)–M(1)–N(5)	174.53(11)	165.68(5)	174.81(5)
N(1)–M(1)–N(6)	174.38(12)	179.41(4)	173.98(5)
N(2)–M(1)–N(6)	107.97(12)	104.25(5)	108.43(6)
N(3)–M(1)–N(6)	103.73(12)	104.78(5)	103.77(6)
N(4)–M(1)–N(6)	96.04(12)	96.62(5)	96.40(5)
N(5)–M(1)–N(6)	89.10(12)	97.64(5)	88.31(6)
M(1)–N(6)–N(7)	169.5(3)	178.79(11)	169.77(12)

Attempts to access the analogous complexes with a bipy ligand by py/bipy ligand exchange reaction from the already synthesised hydrazido complex $Nb(NN_2^{SiMe3})(NNPh_2)(py)_2$ (**49**) were carried out on the NMR scale in toluene-d_8 at RT (Equation 4.5). The ^1H NMR spectra showed a complex mixture of products, however some crystals were obtained confirming the presence of the bipy compound $Nb(NN_2^{SiMe3})(NNPh_2)(bipy)$ (**51**). Isolation of complex **51** on preparative scale was not successful. The solid state structure of **51** is shown in Figure 4.5 and selected bond lengths and angles are listed in Table 4.3.



49 **51**

Equation 4.5

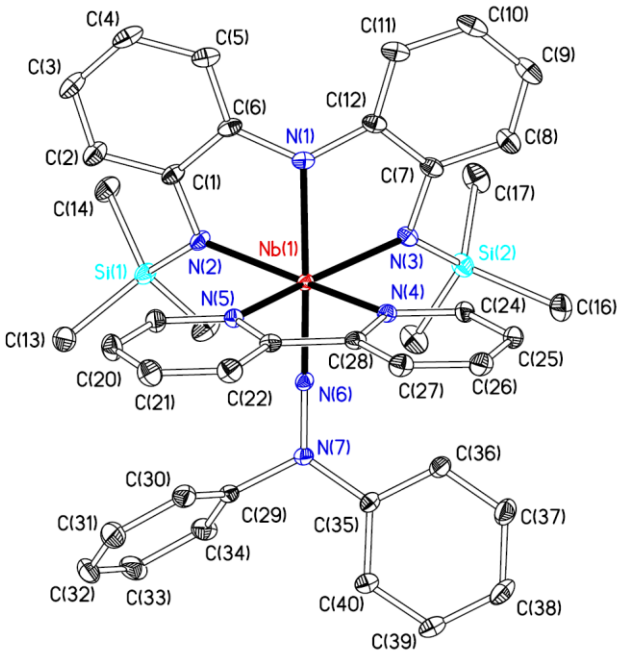


Figure 4.5. Displacement ellipsoid plot (20 % probability) of $Nb(NN_2^{SiMe3})(NNPh_2)(bipy)$ (**51**). H atoms omitted for clarity.

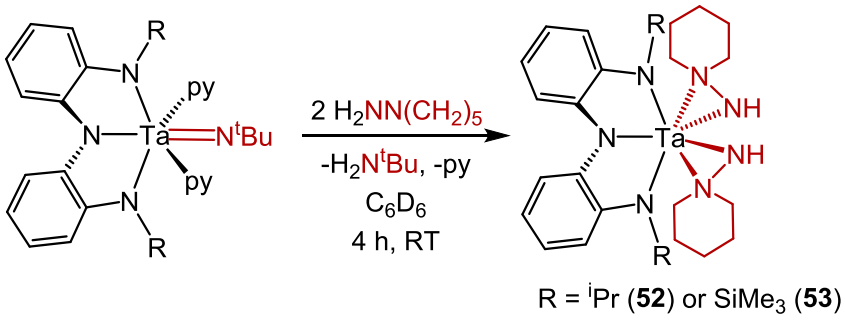
Table 4.3. Selected bond distances (Å) and angles (°) for $Nb(NN_2^{SiMe3})(NNPh_2)(bipy)$ (**51**).

Nb(1)–N(1)	2.175(11)	N(1)–Nb(1)–N(2)	74.98(4)
Nb(1)–N(2)	2.085(11)	N(1)–Nb(1)–N(3)	75.68(4)
Nb(1)–N(3)	2.097(11)	N(2)–Nb(1)–N(3)	117.79(4)
Nb(1)–N(4)	2.337(11)	N(1)–Nb(1)–N(4)	91.69(4)
Nb(1)–N(5)	2.316(11)	N(2)–Nb(1)–N(4)	150.18(4)
Nb(1)–N(6)	1.821(11)	N(3)–Nb(1)–N(4)	83.18(4)
N(6)–N(7)	1.357(15)	N(1)–Nb(1)–N(5)	92.14(4)
		N(2)–Nb(1)–N(5)	84.62(4)
		N(3)–Nb(1)–N(5)	149.46(4)
		N(4)–Nb(1)–N(5)	69.08(4)
		N(1)–Nb(1)–N(6)	174.50(4)
		N(2)–Nb(1)–N(6)	101.29(5)
		N(3)–Nb(1)–N(6)	103.00(5)
		N(4)–Nb(1)–N(6)	93.45(4)
		N(5)–Nb(1)–N(6)	91.51(4)
		Nb(1)–N(6)–N(7)	177.76(9)

The solid state structure of $Nb(NN_2^{SiMe3})(NNPh_2)(bipy)$ (**51**) contains a bidentate bipy ligand in a pseudo-octahedral geometry as it was observed previously in the imido complexes $Nb(NN_2^{R})(N^tBu)(bipy)$ (R = ^{i}Pr (**26**) and $SiMe_3$ (**25**)) (see Chapter 3, Section 3.4). This complex has a C_s-symmetric arrangement where the bipy ligand binds meridionally to the metal centre forcing the tridentate ligand NN_2^R ligand to coordinate in a κ^3-*fac* mode.[15,20] The hydrazido(2-) moiety shows a Ta−N_α bond length of 1.821(11) Å and a near linear M−N_α−N_β bond angle of 177.76(9)º. Similar to the hydrazido complexes **46**, **47** and **48**, the M−N_α bond distance in **51** is longer than those compounds with mono- and dianionic ligands (avg. Ta−N of 1.7866 Å, range 1.762(3) – 1.7988(1) Å for five examples).[36] The N_α−N_β bond length of 1.357(15) Å is also shorter than in the free

diphenylhydrazine (1.418 Å).[37] Bond metrics corresponding to the tridentate ligand NN_2^{SiMe3} are similar to the ones observed in the imido complex $Nb(NN_2^{SiMe3})(N^tBu)(bipy)$ (**25**).

Additionally, formation of the hydrazido functionality *via* hydrazine/*tert*-butylimide exchange was attempted with the imido complexes $Ta(NN_2^R)(N^tBu)(py)_2$ (R = ^{i}Pr (**18**) or $SiMe_3$ (**19**)) and H_2NNMe_2, $H_2NN(Me)Ph$ (1-methyl-1-phenylhydrazine) and $H_2NN(CH_2)_5$ on the NMR scale in C_6D_6 at RT. The ^{1}H NMR spectra of the reactions with H_2NNMe_2 and $H_2NN(Me)Ph$ showed complex mixtures of products, even after long periods of time at RT. However, the reactions of the tantalum imido complexes with $H_2NN(CH_2)_5$ showed the clean formation of a product with two η^2-hydrazido(1-) ligands coordinated, H_2N^tBu and free pyridine after 4 h. at RT (Equation 4.6).



Equation 4.6

The ^{1}H NMR spectra (Figure 4.6) of complexes $Ta(NN_2^R)\{NHN(CH_2)_5\}_2$ (R = ^{i}Pr (**52**) or $SiMe_3$ (**53**)) in C_6D_6 at RT are consistent with C_{2v} symmetric molecules with equivalent isopropyl or trimethylsilyl groups and two hydrazido(1-) ligands. The ^{1}H resonances for the η^2-hydrazido(1-) moiety are observed as multiplets in the range 3.9 – 0.6 ppm along a singlet for the N_α–H at 5.53 (**52**) and 5.41 ppm (**53**). The proton signals attributed to the tridentate ligand NN_2^R include resonances for the ^{i}Pr in complex **52** (doublet at 1.27 ppm for methyls and broadened septet at 3.78 ppm for methine) or the $SiMe_3$ groups in complex **53** (singlet at 0.34 ppm) and the equivalent aryl rings displayed four multiplets in the range 7.9 – 6.2 ppm (in complex **53** two of these multiplets are overlapped).

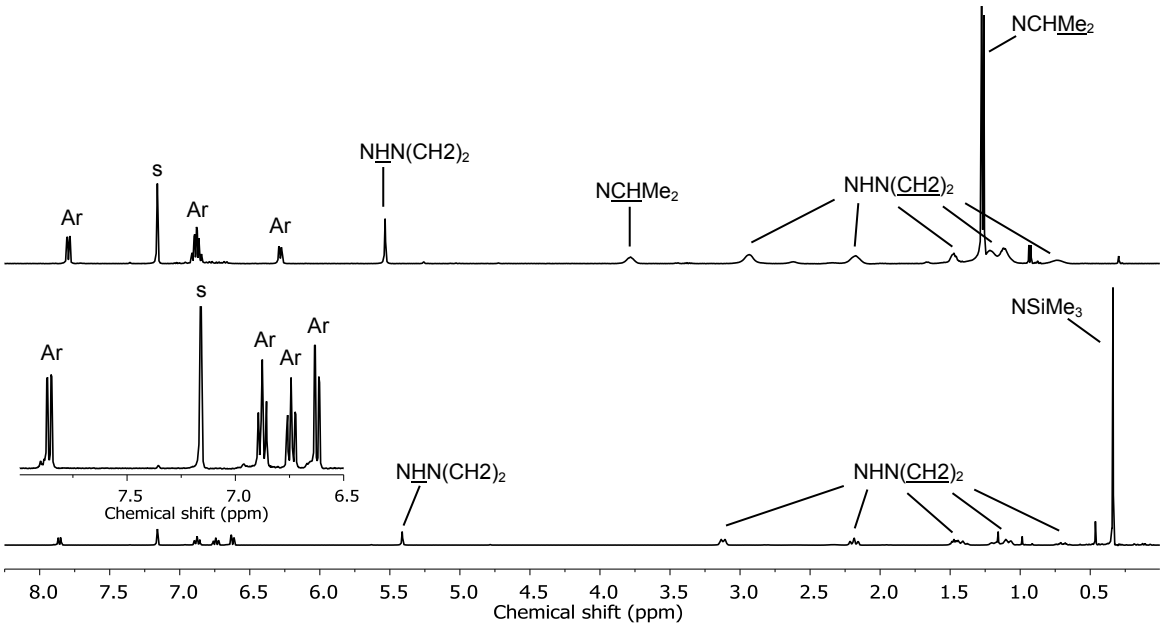


Figure 4.6. ^{1}H NMR spectra (499.9 MHz) of complexes $Ta(NN_2^{R})\{NHN(CH_2)_5\}_2$ (R = ^{i}Pr (**52**, top) or $SiMe_3$ (**53**, bottom)) in C_6D_6 at 298 K. Note: "Ar" refers to the aryl rings in the NN_2^{R} and "s" to the residual protio-solvent.

Diffraction–quality crystals of compound **53** were grown by solvent diffusion in benzene/pentane at RT and the molecular solid state structure is shown in Figure 4.7 with selected bond lengths and angles in Table 4.4.

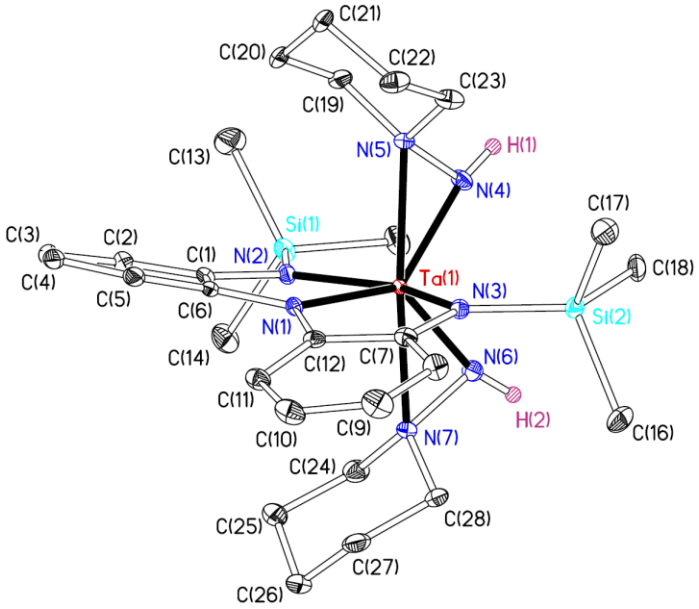


Figure 4.7. Displacement ellipsoid plot (20 % probability) of $Ta(NN_2^{SiMe3})\{NHN(CH_2)_5\}_2$ (**53**). H atoms omitted for clarity. H(1) and H(2) are drawn as spheres of an arbitrary radius.

Table 4.4. Selected bond distances (Å) and angles (°) for $Ta(NN_2^{SiMe3})\{NHN(CH_2)_5\}_2$ (**53**).

Ta(1)–N(1)	2.126(13)	N(1)–Ta(1)–N(2)	75.36(5)
Ta(1)–N(2)	2.089(14)	N(1)–Ta(1)–N(3)	75.27(6)
Ta(1)–N(3)	2.078(14)	N(2)–Ta(1)–N(3)	150.63(6)
Ta(1)–N(4)	1.974(15)	N(1)–Ta(1)–N(4)	131.71(6)
Ta(1)–N(5)	2.259(14)	N(2)–Ta(1)–N(4)	98.84(6)
Ta(1)–N(6)	1.984(16)	N(3)–Ta(1)–N(4)	100.45(6)
Ta(1)–N(7)	2.253(14)	N(1)–Ta(1)–N(5)	93.23(5)
N(4)–N(5)	1.422(2)	N(2)–Ta(1)–N(5)	91.40(5)
N(4)–H(1)	0.797(18)	N(3)–Ta(1)–N(5)	90.07(6)
N(6)–N(7)	1.430(2)	N(4)–Ta(1)–N(5)	38.51(6)
N(6)–H(2)	0.828(18)	N(1)–Ta(1)–N(6)	131.80(6)
		N(2)–Ta(1)–N(6)	103.23(6)
		N(3)–Ta(1)–N(6)	96.39(6)
		N(4)–Ta(1)–N(6)	96.42(6)
		N(5)–Ta(1)–N(6)	134.70(6)
		N(1)–Ta(1)–N(7)	93.42(5)
		N(2)–Ta(1)–N(7)	89.47(5)
		N(3)–Ta(1)–N(7)	92.43(5)
		N(4)–Ta(1)–N(7)	134.81(6)
		N(5)–Ta(1)–N(7)	173.30(5)
		N(6)–Ta(1)–N(7)	38.79(6)
		Ta(1)–N(4)–N(5)	81.68(9)
		Ta(1)–N(4)–H(1)	163(2)
		Ta(1)–N(5)–N(4)	59.81(8)
		Ta(1)–N(6)–N(7)	80.80(9)
		Ta(1)–N(6)–H(2)	164(3)
		Ta(1)–N(7)–N(6)	60.41(8)

The molecular structure of $Ta(NN_2^{SiMe3})\{NHN(CH_2)_5\}_2$ (**53**) is a seven-coordinated monomeric complex with a pseudo pentagonal bipyramidal geometry about the tantalum centre. The tridentate ligand NN_2^R coordinates along the axial positions while the equatorial sites contain an N_{aryl} atom from the tridentate ligand and two η^2-hydrazido(-1) ligands in which the –NH fragments are *syn* to each other within the equatorial plane. Therefore, its geometry is analogous to the previously structurally characterised complexes $Ta(NMe_2)_3(3,5\text{-}^tBu\text{-}C_3HN_2)$[47] and $[Nb\{NN(CH_2)_5\}Cl_2\{NH_2N(CH_2)_5\}_2]Cl$[35].

The η^2-hydrazido(1-) moieties show tantalum–nitrogen bond lengths of 1.974(15) and 1.984(16) Å for the Ta−N_α, and 2.259(14) and 2.253(14) Å for the Ta−N_β, forming Ta−N_α−N_β angles of 81.68(9) and 80.80(9) °. The N_α−N_β bond distances are 1.422(2) and 1.422(2) Å. These metal–nitrogen and nitrogen–nitrogen bond distances are longer compared to complexes **46**, **47** and **48** which contain hydrazido(2-) ligands but within the range when the hydrazide ligands are bound in a η^2-hydrazido(1-) mode.[35,46] The M(1)−N(1) bond length from the NN_2^R ligand in complex **53** (2.126(13) Å) is slightly shorter than the one observed in the hydrazido compounds **46**, **47** and **48** (2.147(3), 2.1365(12) and 2.1617(13) Å), which was attributed to a strong *trans* influence from the hydrazido(2-) moiety. Nonetheless, those M(1)−N(2) and M(1)−N(3) bond distances (2.076(3) and 2.063(3) Å, respectively) for **53** are within the range (2.063(3) – 2.0903(11) Å) observed for **46**, **47** and **48**. The aryl rings in the NN_2^R ligand are slightly twisted from each other out of planarity with an angle between the planes being *ca.* 27.48 °. As expected this is smaller than the angle between planes of 38.44 ° observed in the hydrazido complex $Ta(NN_2^{SiMe3})(NNPh_2)(py)_2$ (**47**) in which there is a steric repulsion between the trimethylsilyl substituents and the $N_\beta Ph_2$ group.

Unexpectedly, the tantalum μ-oxo-bridged dimeric complex $\{Ta(NN_2^{iPr})\{NHN(CH_2)_5\}\}_2(\mu\text{-}O)$ (**54**) was obtained from a concentrated solution of complex $Ta(NN_2^{iPr})\{NHN(CH_2)_5\}_2$ (**52**) in toluene-d_8 at RT that was slowly exposed to air over several months giving a dark-red crystalline product which was identified by X-ray crystallography. Controlled hydrolysis reactions have been previously studied in amidotitanium halides complexes of the type $Ti\{MeC(CH_2N^{SiMe3})_3\}X$ (X = Cl or Br) yielding the corresponding μ-oxo-bridged complex.[48]

The molecular solid state structure of **54** is shown in Figure 4.8 and selected bond lengths and angles are listed in Table 4.5.

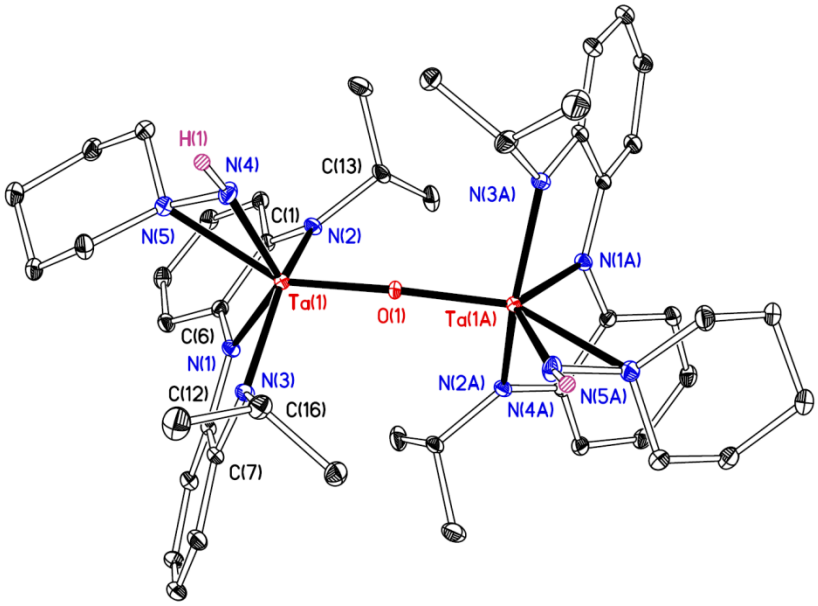


Figure 4.8. Displacement ellipsoid plot (20 % probability) of $\{Ta(NN_2^{iPr})\{NHN(CH_2)_5\}\}_2(\mu\text{-}O)$ (**54**). H atoms omitted for clarity. H(1) and H(2) are drawn as spheres of an arbitrary radius. Atoms carrying the suffix 'A' are related to their counterparts by the symmetry operator [1-x, -y, ½-z].

Table 4.5. Selected bond distances (Å) and angles (°) for $\{Ta(NN_2^{iPr})\{NHN(CH_2)_5\}\}_2(\mu\text{-}O)$ (**54**).

Ta(1)–N(1)	2.086(2)	N(1)–Ta(1)–N(2)	74.49(8)
Ta(1)–N(2)	2.057(2)	N(1)–Ta(1)–N(3)	73.86(9)
Ta(1)–N(3)	2.036(2)	N(2)–Ta(1)–N(3)	145.68(9)
Ta(1)–N(4)	1.981(2)	N(1)–Ta(1)–N(4)	128.87(9)
Ta(1)–N(5)	2.246(2)	N(2)–Ta(1)–N(4)	106.70(10)
Ta(1)–O(1)	1.9206(5)	N(3)–Ta(1)–N(4)	103.31(9)
N(4)–N(5)	1.439(3)	N(1)–Ta(1)–N(5)	90.22(8)
N(4)–H(1)	0.961	N(2)–Ta(1)–N(5)	92.19(9)
		N(3)–Ta(1)–N(5)	100.85(8)
		N(4)–Ta(1)–N(5)	39.17(9)

N(1)–Ta(1)–O(1)	126.68(9)
N(2)–Ta(1)–O(1)	94.72(9)
N(3)–Ta(1)–O(1)	93.61(7)
N(4)–Ta(1)–O(1)	104.39(10)
N(5)–Ta(1)–O(1)	142.95(9)
Ta(1)–N(4)–N(5)	80.41(14)
Ta(1)–N(4)–H(1)	161.2
Ta(1)–N(5)–N(4)	60.42(12)
Ta(1)–O(1)–Ta(1A)	159.40(17)

Each tantalum atom is in a distorted octahedral geometry with the NN_2^{iPr} ligand coordinated along the axial positions, and one N_{aryl} from the tridentate ligand, one η^2-hydrazido moiety and a bridging oxo ligand. The Ta(1)−O(1)−Ta(1A) angle of 159.40(17) ° slightly deviates from linearity, which might be to minimise steric interactions between the ligands around each tantalum atom. The linear Ta_2O unit has been observed in the tantalum-amido complex $\{Ta(NMe_2)_2Cl_2(NHMe_2)\}_2(\mu\text{-}O)$ with a Ta−O−Ta angle of 174.3(3)°.[49] The Ta(1)−O(1) bond length in the oxo-bridged hydrazido complex **54** of 1.9206(5) Å is comparable to the Ta−O bond distance of 1.928(6) Å found in the amido complex $\{Ta(NMe_2)_2Cl_2(NHMe_2)\}_2(\mu\text{-}O)$[49].

The Ta−N_α (1.981(2) and 2.246(2) Å) and N_α−N_β (1.439(3) Å) bond lengths corresponding to the η^2-hydrazido moiety in the tantalum oxo-bridged compound **54** are similar to those in the monomeric bis(hydrazide) complex $Ta(NN_2SiMe_3)\{NHN(CH_2)_5\}_2$ (**53**, Ta−N_α of 1.974(15) and 2.259(14) Å, N_α−N_β of 1.422(2) Å). However, the tantalum–nitrogen bond lengths from the NN_2^{iPr} ligand in complex **54** (Ta(1)−N(1) of 2.086(2), Ta(1)−N(2) of 2.057(2) and Ta(1)−N(3) of 2.036(2) Å) are smaller compared to those in complexes **53** and other hydrazido complexes reported in this Chapter (**46**, **47** and **48**). As one of the hydrazido ligands is replaced by oxygen in the tantalum oxo-bridged dimer complex **54**, metal-ligand π bonding interactions is less crowded allowing a better interaction with the N_{amide} ligands.

4.6 Bonding in $Ta(NN_2^R)(NNPh_2)(py)_2$

As mentioned in Chapter Three, at first sight the imido compounds $M(NN_2^R)(N^tBu)(py)_2$ and their hydrazido analogues $M(NN_2^R)(NNPh_2)(py)_2$ (as well as the corresponding bipyridyl counterparts) are formally 22 valence electron compounds if all three of the ligand-based lone pairs of NN_2^R (*cf* Chapter Two, Figure 2.6) are able to donate to the metal, and a M≡NR (R = ^{t}Bu or $NNPh_2$) triple bond is also formed. In addition, whereas the solid state structures of the less sterically crowded hydrazides $M(NN_2^{iPr})(NNPh_2)(py)_2$ (M = Ta (**46**) or Nb (**48**), Figure 4.4)) have the $NN(C_{ipso})_2$ moiety oriented coplanar with the nitrogens of the NN_2^{iPr} ligand, in the more sterically crowded $Ta(NN_2^{SiMe3})(NNPh_2)(py)_2$ (**47**) this moiety is oriented in the orthogonal direction. This would suggest an electronic preference for the orientation of the hydrazide substituents, and more specifically its different π-donor orbitals.

In order to clarify the bonding situation in these π-loaded complexes as series of DFT calculations were carried out by Prof. Philip Mountford on model complexes of the type $Ta(NN_2^R)(NR')(py)_2$ (R = Me or SiH_3; R' = Me or NMe_2 (constrained to be planar at N_β)) which all pointed towards a common bonding situation. The results for $Ta(NN_2^{SiH3})(NNMe_2)(py)_2$ are discussed in detail here. The sterically reduced NN_2^{SiH3} ligand used in this case is the same as in the DFT calculations in Chapter Two. The 2p(π) lone pairs for the equatorial (N_{eq}, $1b_1$ symmetry) and axial (N_{ax}, $b_1 + a_2$ symmetry) amide nitrogens for NN_2^{SiH3} have been given in Figure 2.6 of Chapter Two and their symmetry labels and nature are the same in the imido and hydrazido complexes. Figure 4.9 represents various model systems studied. The species **47q** and **47q_rot** are isomers of $Ta(NN_2^{SiH3})(NNMe_2)(py)_2$, differing in the orientation of the β-NMe_2 group. In **47q** the NMe_2 group is oriented perpendicular to the approximate plane of NN_2^{SiH3} (as in the real compound $Ta(NN_2^{SiMe3})(NNPh_2)(py)_2$ (**47**, Figure 4.4)), whereas in **47q_rot** the β-NMe_2 lies in the plane of NN_2^{SiH3} (as in the real compounds $M(NN_2^{iPr})(NNPh_2)(py)_2$, **46** and **48**). The models test the electronic preference of the β-NMe_2 (or β-NPh_2 in the real compounds) orientation. Geometry optimisation of **47q** and **47q_rot** was carried out subject to constraining the desired orientation of the β-NMe_2 group, and maintaining a planar β-N atom as in **46** – **48**. The rotamer **47q_rot** was found to be 1.2 kcal mol^{-1} more stable than **47q**. Analogous calculations for the systems $Ta(NN_2^{Me})(NNMe_2)(py)_2$ (with a NN_2^{Me} ligand, models of **46**) found a slightly larger preference (3.8 kcal mol^{-1}) for the

analogue of **47q_rot**. These relative DFT energies are consistent with the experimental geometric preferences of the less sterically crowded compounds $M(NN_2^{iPr})(NNPh_2)(py)_2$, **46** and **48**).

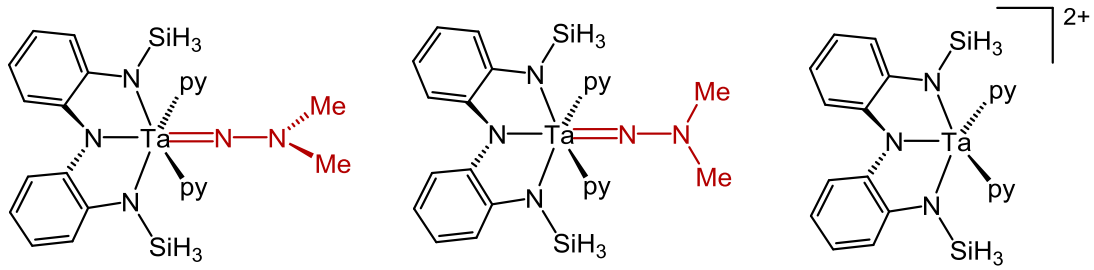


Figure 4.9. DFT optimised model systems $Ta(NN_2^{SiH3})(NNMe_2)(py)_2$ (**47q** and **47q_rot**) and the frozen dicationic fragment $[Ta(NN_2^{SiH3})(py)_2]^{2+}$ (**47q_frag**).

Figure 4.10 compares the optimised geometries and selected bond distances for $Ta(NN_2^{SiH3})(NNMe_2)(py)_2$ (**47q** and **47q_rot**), along with the corresponding Wiberg Bond Indices (WBIs). The orientation of the β-NMe_2 affects the Ta–N distances to both the NN_2^{SiH3} supporting ligand and to the $NNMe_2$ group itself. In **47q** the Ta–N_α and Ta–N_{eq} distances are shorter than in **47q_rot**, whereas the Ta–N_{ax} distances in **47q** are longer, despite this being the most sterically favoured arrangement of the β-NMe_2 and –$NSiH_3$ groups. These trends for **47q** and **47q_rot** mirror those found in the structures of **47** and **46**, respectively, although the magnitudes of the differences differ, as would be expected given the additional steric factors operating on top of underlying electronic ones.

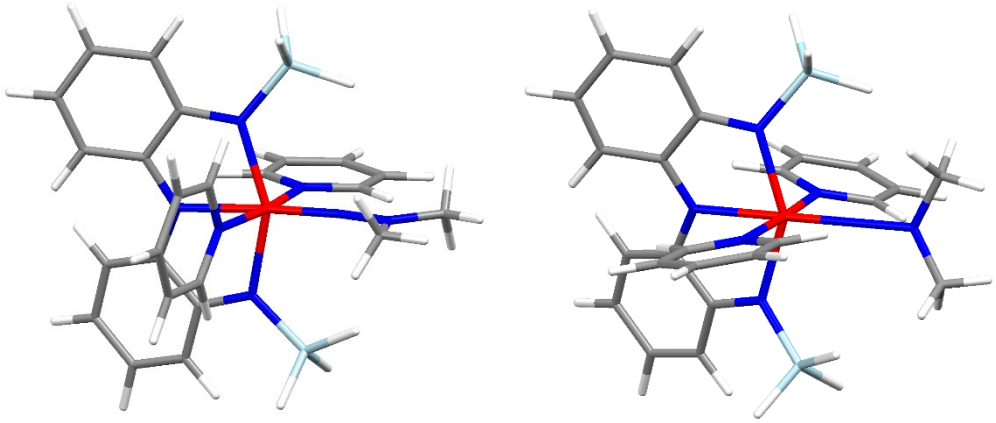


Figure 4.10. Optimised geometries for $Ta(NN_2^{SiH3})(NNMe_2)(py)_2$ (**47q** (left) and **47q_rot** (right)). Selected bond lengths (Å) for **47q** with the values for **47q_rot** in parentheses: Ta–N_α 1.842 (1.847), Ta–N_{eq} 2.174 (2.214), Ta–N_{ax} (av.) 2.101 (2.094). Selected Wiberg Bond Indices (WBIs) for **47q** with the values for **47q_rot** in parentheses: Ta–N_α 0.353 (0.348), Ta–N_{eq} 0.397 (0.347), Ta–N_{ax} (av.) 0.668 (0.695).

The variations in Ta–N bond distances in the two geometries **47q** and **47q_rot**, as well as the overall electronic structure, can be understood with reference to the π-donor competition between NN_2^{SiH3} (*cf.* Figure 2.6 in Chapter Two) and the $NNMe_2$ ligand, and the electronic structure of octahedral complexes in general and the dicationic fragment $[Ta(NN_2^{SiH3})(py)_2]^{2+}$ (**47q_frag**, Figure 4.9).

Figure 4.11 (left) shows the well-known[50] d-orbital based MOs of a hypothetical octahedral complex ML_6 with labels appropriate for the approximate C_{2v} symmetry of **47q** and **47q_rot**. The $1a_1$ and $2a_2$ MOs (the e_g pair in O_h symmetry) are σ* antibonding and do not participate in further M–L π-interactions. The $1a_2$, $1b_1$ and $1b_2$ levels (the t_{2g} set in O_h symmetry) are available for π-interactions. Figure 4.11 (right) shows schematically the four highest occupied MOs of a planar, dianionic $[NNR_2]^{2-}$ ligand based on previous Extended Hückel and DFT calculations.[45,51-54] The lowest energy MO shown is suitable for M–N_α σ bonding, the next MO is N_α-N_β π bonding and would not be expected to interact to any significant extent with a metal centre.[45,51] The π_h (horizontal with respect to the β-R groups) is N_α–N_β non-bonding and would form one of the Ta–N_α π bonds. Finally π_v is the HOMO of $[NNR_2]^{2-}$ and lies significantly higher in energy (≥ 1 eV[45,51]) than π_h because of its N_α–N_β π* anti-bonding nature. Of these two MOs (π_v and π_h), the former is the better π donor due to its better energy match with the metal acceptor orbitals. Previous experimental and computational studies of d^0 hydrazido

complexes[46,54] have rationalised the orientation of the β-NR_2 substituents, and variations in bond distances of the resultant complexes, based on the preferential overlap of the π_v MO. The bonding situation in the imido compound Ta(NN_2^{Me})(N^tBu)$(py)_2$ (**17**) is slightly simpler because both π_v and π_h are based on degenerate N_{imide} 2p atomic orbitals.

In qualitative terms, the basic π-bonding position in **47q** and **47q_rot** can now be rationalised. The $1a_2$ 5d orbital (d_{yz}) of ML_6 interacts with the a_2 N_{ax} lone pair SALC of NN_2^{SiH3} (*cf.* Figure 2.6) and in principle the $1b_1$ metal orbital (d_{xy}) can interact with the N_{eq} $1b_1$ lone pair of NN_2^{SiH3}. The $2b_1$ N_{ax} lone pair SALC is incorrectly orientated, as in the case of Ta(NN_2^{SiH3})Me_2 (**1.5q**, discussed in Chapter Two). Depending on the orientation of the β-NMe_2 group, π_v and π_h transform as either b_1 and b_2 in C_{2v} symmetry or as b_2 and b_1. Either way, the $1b_2$ 5d orbital (d_{xz}) will find a symmetry match with a donor orbital of $NNMe_2$ without competition from NN_2^{SiH3}. In contrast the b_1 π-donor of $NNMe_2$ (either π_h or π_v) will compete with the $1b_1$ N_{eq} amide lone pair for the metal $1b_1$ (d_{yz}) acceptor orbital reducing one or both of the Ta–N_{eq} and Ta–N_α bond orders from their maximum values of 2 (σ+π donation) and 3 (σ+2π donation), respectively.

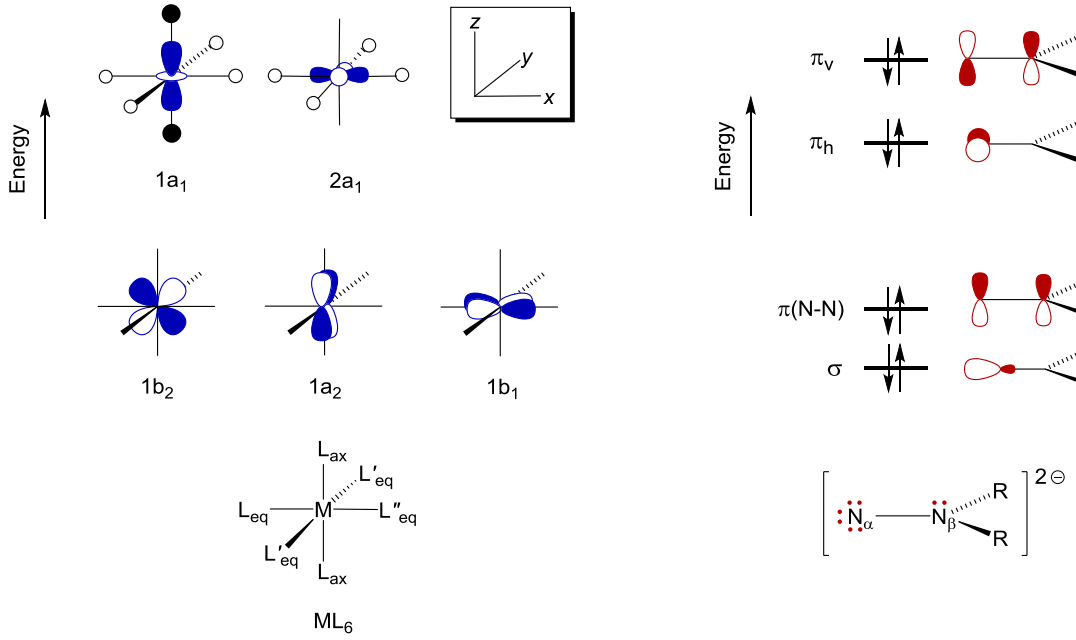
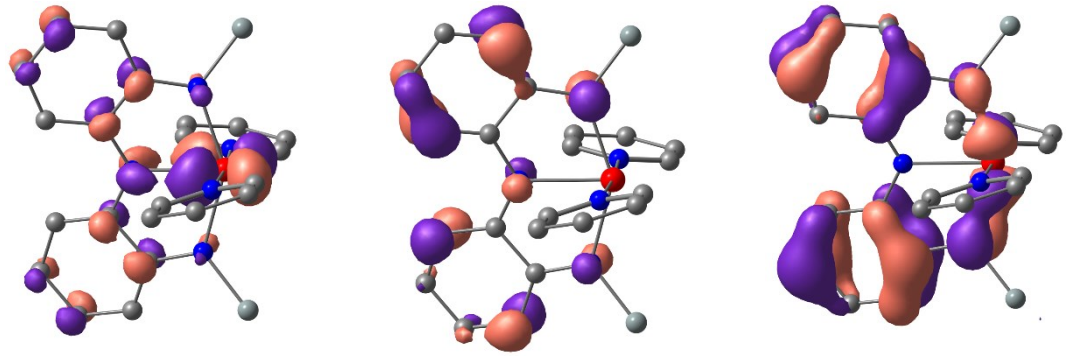


Figure 4.11. Left: the σ-only frontier MOs (d orbitals only, arbitrary energies) for a hypothetical ML_6 system. In the model systems **47q** and **47q_rot** the L_{eq} and L_{ax} sites are occupied by NN_2^{SiH3}, L'_{eq} by the py ligands, and L''_{eq} by $NNMe_2$. Right: the four highest occupied MOs of a C_{2v} symmetric dianion $[NNR_2]^{2-}$.

Figure 4.11 shows the DFT computed frontier molecular orbitals of $[Ta(NN_2^{SiH3})(py)_2]^{2+}$ (**47q_frag**) as an aid to understanding further the bonding and geometric trends in **47q** and **47q_rot** and the corresponding real compounds. The orbitals of $[Ta(NN_2^{SiH3})(py)_2]^{2+}$ were computed in both the optimised geometry of either **47q** or **47q_rot** with the $[NNMe_2]^{2-}$ anion removed and no further geometry optimisation performed. Negligible difference was found between the two fragments; the orbitals and energies given in Figure 4.12 were obtained from **47q_rot**.



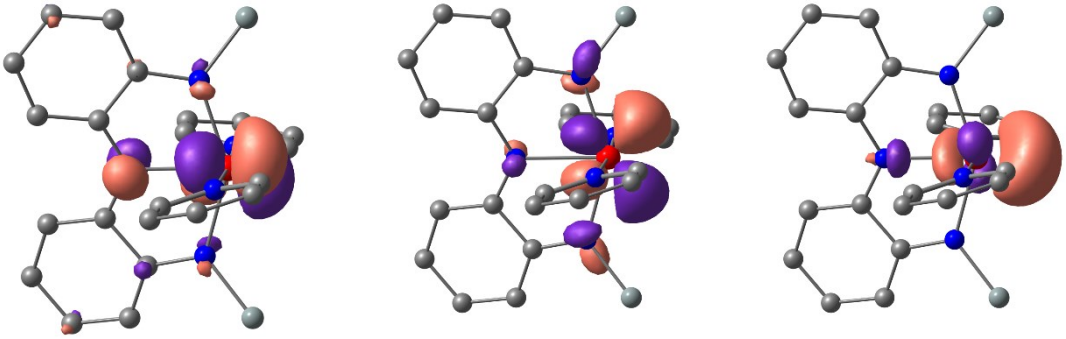


Figure 4.12. DFT computed frontier molecular orbitals of $[Ta(NN_2^{SiH3})(py)_2]^{2+}$ (**47q_frag**). Isosurfaces are drawn at the 0.0432– 0.07465 a.u. contour level. H atoms omitted.

$[Ta(NN_2^{SiH3})(py)_2]^{2+}$ (**47q_frag**) is isoelectronic with $Ta(NN_2^{SiH3})Me_2$ (**1.5q**) (albeit with a geometry closer to square base pyramidal than TBP) discussed in Chapter Two, and the HOMO, HOMO-1 and HOMO-2 of **47q_frag** resemble those of **1.5q** (Figure 2.7). Thus **47q_frag** is formally a 14 valence electron dication with HOMO-1 representing a non-bonding ligand based orbital (nominally the $2b_1$ SALC of NN_2^{SiH3}) and the HOMO and HOMO-2 are Ta–N_{amide} π-bonding interactions (b_1 and a_2, respectively). The LUMO+2

of **47q_frag** is a σ-acceptor MO derived from the $2a_1$ (d_{x2-y2}) orbital of ML_6 and the LUMO+3 (not shown) in the antibonding counterpart of the Ta–N_{ax} π-bonding (a_2) interaction found in HOMO-2. Therefore the LUMO and LUMO+1 of **47q_frag** are the acceptor orbitals to interact with the π_v (HOMO) and π_h donor MOs of $[NNMe_2]^{2-}$. These metal-based orbitals correspond to the $1b_1$ and $1b_2$ AOs of the idealised σ-only model ML_6 shown in Figure 4.11 but differ in an important way. They are not isoenergetic because the LUMO of **47q_frag** is Ta–N_{eq} π*-antibonding, and although the LUMO+1 is π-non-bonding, it is somewhat Ta–N_{ax} σ*-antibonding because of the decreased N_{ax}–Ta–N_{ax} angle (147.5 °) imposed by the pincer ligand. Thus LUMO+1 is the least stable of the two π-acceptor orbitals of **47q_frag** (albeit slightly polarised through 5d-6p orbital mixing towards the incoming $NNMe_2$ ligand) and would have a less good energy match with the HOMO (π_v) of $NNMe_2$.

As stated above, the most stable isomer of Ta(NN_2^{SiH3})($NNMe_2$)$(py)_2$ on electronic grounds is **47q_rot** which permits donation from the π_v of $NNMe_2$ to the lowest energy d-based π-acceptor MO of $[Ta(NN_2^{SiH3})(py)_2]^{2+}$. However, this isomer is close in energy to **47q**, which is also the more sterically favoured isomer according to the experimental data. π-donation into either the LUMO or LUMO+1 of $[Ta(NN_2^{SiH3})(py)_2]^{2+}$ has detrimental effects on the bonding of NN_2^{SiH3} to tantalum. Donation into the LUMO disrupts the Ta–N_{eq} (b_1) π-bonding interaction. Donation into LUMO+1 would, on the other hand, disrupt the Ta–N_{ax} σ-bonding. Referring back the DFT metric data (caption to Figure 4.10) and experimental data (Table 4.2), the longer Ta–N_{eq} (and shorter Ta–N_{ax}) bonds in **47q_rot** and **46** (compared to **47q** and **47**) can be accounted for by consideration of the π-donation effects from the HOMO (π_v) of the NNR_2 ligand.

Figure 4.13 shows the DFT computed frontier molecular orbitals of Ta(NN_2^{SiH3})($NNMe_2$)$(py)_2$ (**47q_rot**). HOMO-1 and HOMO-5 represent the two Ta–N_α π-bonding components of the Ta≡N_α triple bond with negligible contribution of N_{eq} to HOMO-1 (*ca*. 2%). The HOMO-2 represents the only significant Ta–N_{amide} π-bonding interaction between tantalum and NN_2^{SiH3} and is the π-donation from the a_2 lone pair SALC of NN_2^{SiH3} to the $5d_{yz}$ orbital. The HOMO and HOMO-3 of **47q_rot** are ligand-based MOs (mainly the $1b_1$ and $2b_1$ SALCs of NN_2^{SiH3}) and having less than 2% tantalum contribution. It is notable that the π_v of $NNMe_2$ makes a *ca*. 18% contribution to the non-

bonding HOMO which may account for the slightly longer Ta–N_α bond distance in **47q_rot** compared to **47q** (and the corresponding distances in **46** and **47**). The overall orbital description of the model compounds **47q** and **47q_rot** and the real imides and hydrazides $M(NN_2^R)(NR')(py)_2$ (and their bipy analogues) indicates these are 18 valence electron, π-loaded compounds with M–N_α bond orders close to three ($\sigma^2\pi^4$ configuration and net 5 electron donor NN_2^R ligands with both of the b_1 lone pair SALCs being effectively non-bonding.

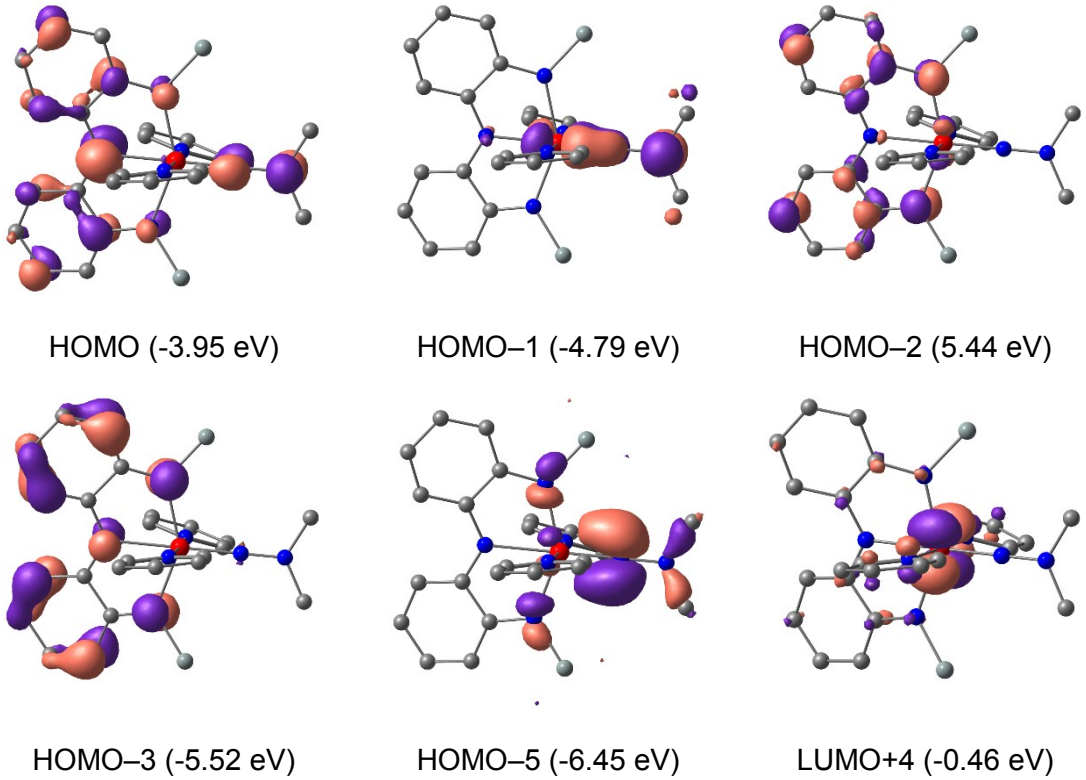
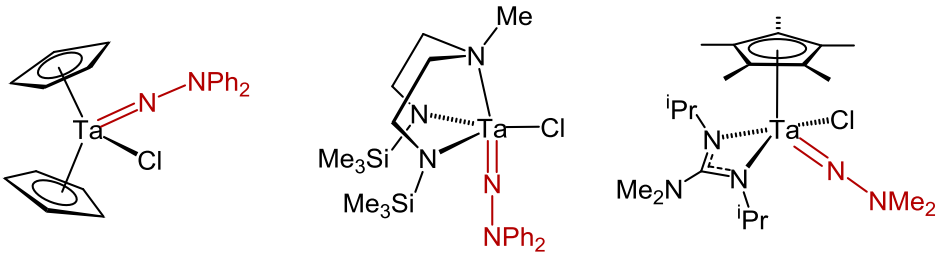


Figure 4.13. DFT computed frontier molecular orbitals of $Ta(NN_2^{SiH3})(NNMe_2)(py)_2$ (**47q_rot**). Isosurfaces are drawn at the 0.0432– 0.07465 a.u. contour level. H atoms omitted.

4.7 Reactivity of $Nb(NN_2^{iPr})(NNPh_2)(py)_2$ (48) with unsaturated small molecules

Recently, tantalum hydrazido complexes with mono- and dianionic ligands have been reported by Bercaw *et al.* and Sita *et al.* in which the presence of a strongly-bonded chloride ligand blocks the coordination site for incoming substrates (examples in Figure 4.14). When the bis(amide)amine complex $Ta(N_2N^{Me})(NNPh_2)Cl$ (**1.82**) was treated with $Na[BAr^F]$ ($[BAr^F]^-$ = $[B(3,5\text{-}C_6H_3(CF_3)_2)_4]^-$) in the presence of pyridine, the cationic chloride-abstracted product $[Ta(N_2N^{Me})(NNPh_2)(py)][BAr^F]$ was generated. However,

this compound was unreactive upon attempts of pyridine substitution and [2+2] reactions with terminal and internal alkynes.[36]



1.81 **1.82** **1.73**

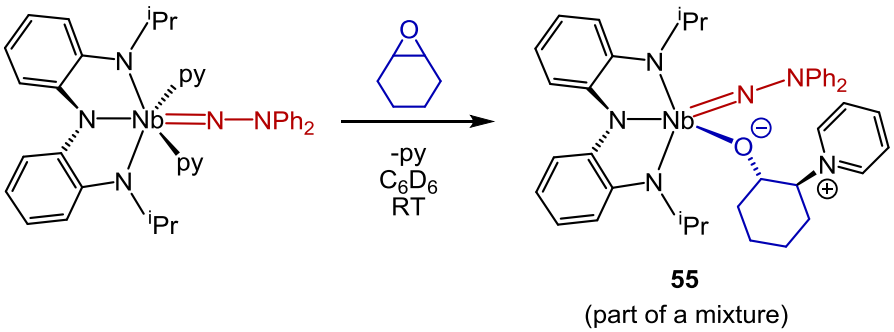
Figure 4.14. Examples of tantalum hydrazido(2-) complexes.[36,55]

These complexes with chloride or pyridine (cationic complex) substituents showed negligible reactivity in contrast to their Group 4 counterparts, which have exhibited a wide variety of reactions with unsaturated small molecules. For example, the titanium hydrazido complexes Cp*Ti{MeC(N^{i}Pr)$_2$}(NNR$_2$) (**1.64**, R = Me or Ph) undergo [2+2] cycloaddition, cycloaddition−insertion or cycloaddition−elimination reaction at the Ti−N$_\alpha$ multiple bond with CO_2, CS_2, and isocyanates depending on the N$_\beta$ substituents.[8] Another example of a [2+2] cycloaddition reaction reported by Mountford and co-workers is the complex Ti(N$_2$N^{py})(NNPh$_2$)(py) (**1.58**) with terminal and internal alkynes.[20] Reaction of the same titanium hydrazido complex with nitriles (MeCN) produced a dimeric product but a cycloaddition intermediate is proposed.[12] Reductive N$_\alpha$−N$_\beta$ bond cleavage is an interesting reaction that can be observed with hydrazido complexes induced by CO_2,[18] isonitriles[12], alkynes [18,20] or as a rearrangement of [2+2] cycloaddition products when heated.[10]

Analogous neutral Group 5 complexes with trianionic, N$_3$-donor pincer ligands were synthesised and presented in this Thesis suggesting that the displacement of the chloride ligand for labile Lewis-bases will allow access to reactive Ta(N$_3$)(NNPh$_2$)(L)$_x$ species (N$_3$ = a trianionic, tridentate ligand, L = Lewis base, x = 0 or 1). NMR scale reactions of the niobium hydrazido complex Nb(NN$_2^{iPr}$)(N^{t}Bu)(py)$_2$ (**48**) were carried out with a number of small unsaturated substrates. It was found to be unreactive with internal alkynes and nitriles, even upon strong heating. Exposing a solution of **48** in C_6D_6 to a CO_2 atmosphere at RT for 2 h gave a complicated mixture in which free-pyridine can be observed but none of the other products could be identified. Similarly, a mixture of products is observed in the reaction with CS_2 when heated up to 80 ˚C. Reaction of **48** with boranes

(9-BBN or H_2BTex (Tex = *tert*-hexyl)) gave a mixture of products from which the already known side product py·HBC_8H_{14} or any other compound were not identified.

Finally, the NMR scale reaction of the niobium hydrazido complex $Nb(NN_2^{iPr})(N^tBu)(py)_2$ (**48**) with cyclohexene oxide (CHO) in C_6D_6 at RT (Equation 4.7) showed a complicated mixture in the ^1H NMR spectra. However, black crystals were obtained from this solution at RT and the product was identified by X-ray crystallography as $Nb(NN_2^{iPr})(NNPh_2)(OC_6H_{10}$-2-py) (**55**). It is proposed that the mechanism for the formation of **55** involves coordination of the epoxide oxygen to niobium first releasing the pyridine ligand, followed by nucleophilic attack of the epoxide by the "non-coordinated" pyridine which results in the ring-opening.



55
(part of a mixture)

Equation 4.7

A similar intermediate compound has been proposed by Kozak and co-workers during studies of copolymerization of CO_2/cyclohexene oxide catalysed by amine-bis(phenolate) chromium (III) chloride complexes with DMAP as co-catalyst.[56] However, the solid state structure of these intermediate is currently unknown. Bergman and co-workers have investigated reactions of the zirconium imido complex $Cp_2Zr(N^tBu)(THF)$ (**1.12**) with epoxides where coordination of either styrene oxide, stilbene oxide or *exo*-norbornene oxide to the metal centre occurred, but in these cases proceeded with ring-opening promoted by the imido moiety followed by the formation of the metallacycle complexes.[57]

The molecular solid state structure of $Nb(NN_2^{iPr})(NNPh_2)(OC_6H_{10}$-2-py) (**55**) is shown in Figure 4.15 and selected bond lengths and angles are listed in Table 4.6. Complex **55** has a distorted pentacoordinate geometry with a τ value of 0.03 defining the geometry as 3 % along the range from square-based pyramidal and trigonal-bipyramidal geometries.[58,59] The N_{aryl} from the NN_2^{iPr} ligand, the $NNPh_2$ and the OC_6H_{10}-2-py moieties occupy

equatorial sites, and the NN_2^{iPr} ligand sits on the axial positions. The diphenylhydrazido ligand shows Nb−N_α and N_α−N_β bond lengths of 1.803(3) and 1.360(4) Å, similar to those in the bis(pyridine) hydrazido complex $Nb(NN_2^{iPr})(NNPh_2)(py)_2$ (**48**, 1.8496(14) and 1.353(2) Å respectively). The Nb−N_α−N_β angle of 163.1(2)˚ in **55** is smaller than the one in **48** (169.77(12)˚), which might be to minimise steric interactions between the comparatively large diphenylhydrazido ligand and the cyclohexene ring (closest non-bonded H−H contact between the $N_\beta Ph_2$ group and the CHO ring is 2.676 Å).

The Nb−O bond distance of 1.963(2) Å falls in the range 1.791(4) – 1.965(5) Å for those linkages of aryloxides known in the literature (avg. 1.877 Å for eleven examples)[60-63]. Most importantly, the small Nb−O−C(31) angle of 130.3(2) Å (avg. 175.2˚, range 139.3(4) – 177.6(6)˚ for the eleven examples mentioned above) results in the pyridine coordinated to the cyclohexene being in close proximity to one of the aromatic rings from the NN_2^{iPr}-supported ligand indicating the possibility of π-π stacking type interactions (intramolecular $C_{py}\cdots C_{ligand}$ distances in the range ca 3.2 – 4.2 Å).[64,65] Finally, the Nb(1)−N(1) bond length is shorter (by 0.0517 Å) while Nb(1)−N(2) and Nb(1)−N(3) bonds distances are longer (by 0.0486 and 0.0349 Å) relative to those in the analogous bis(pyridine) hydrazido compound **48**.

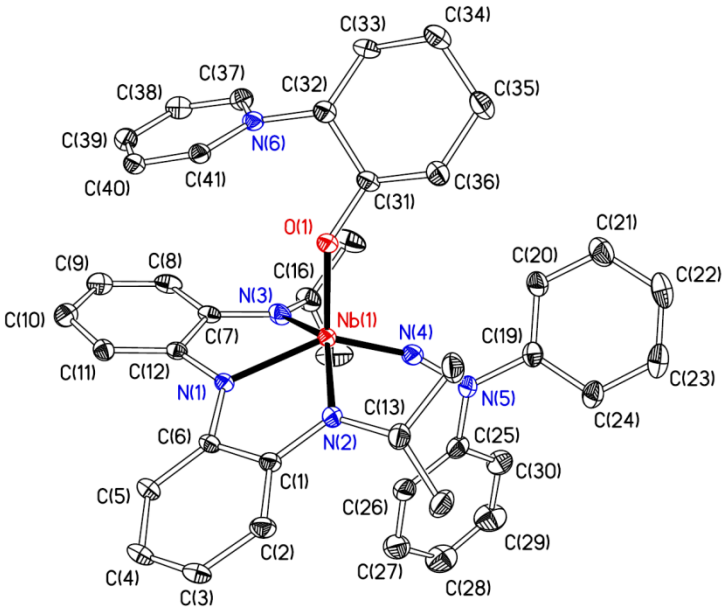


Figure 4.15. Displacement ellipsoid plot (20 % probability) of $Nb(NN_2^{iPr})(NNPh_2)(OC_6H_{10}$-2-py) (**55**). H atoms omitted for clarity.

Table 4.6. Selected bond distances (Å) and angles (°) for $Nb(NN_2^{iPr})(NNPh_2)(OC_6H_{10}$-2-py) (**55**).

Nb(1)–N(1)	2.110(2)	N(1)–Nb(1)–N(2)	73.70(9)
Nb(1)–N(2)	2.127(3)	N(1)–Nb(1)–N(3)	74.97(10)
Nb(1)–N(3)	2.099(3)	N(2)–Nb(1)–N(3)	143.91(10)
Nb(1)–N(4)	1.803(3)	N(1)–Nb(1)–N(4)	141.65(11)
Nb(1)–O(1)	1.963(2)	N(2)–Nb(1)–N(4)	95.65(11)
N(4)–N(5)	1.360(4)	N(3)–Nb(1)–N(4)	97.88(12)
N(6)–C(32)	1.507(4)	N(1)–Nb(1)–O(1)	108.99(9)
		N(2)–Nb(1)–O(1)	103.89(10)
		N(3)–Nb(1)–O(1)	102.86(11)
		N(4)–Nb(1)–O(1)	109.34(11)
		Nb(1)–N(4)–N(5)	163.1(2)
		Nb(1)–O(1)–C(31)	130.3(2)

4.8 Conclusions and Outlook

In this Chapter two different synthetic routes for the synthesis of Group 5 hydrazido complexes supported by the tridentate, trianionic ligands NN_2^R have been explored. An overview of all new reactions is given in Scheme 4.2.

Firstly, the new tantalum and niobium hydrazido synthons $M(NNPh_2)Cl_3$(R-bipy) (M = Ta, R = H (**36**) or ^{t}Bu (**38**); M = Nb, R = H (**37**) or ^{t}Bu (**39**)) were synthesised from the analogous imido synthons *via* hydrazine/*tert*-butylimide exchange reactions. This methodology proved to be a viable alternative to obtain pure hydrazido compounds, however no reaction was observed in attempt to synthesise the bis(pyridine) adduct. While complexes of the type $M(NNPh_2)Cl_3$(R-bipy) present a hydrazido(2-) ligand coordinated to the metal centre, reactions of the imido synthons with dimethylhydrazine or aminopiperidine yielded the complexes $M(NNR_2)(NH^tBu)Cl_3$(di-^{t}Bu-bipy) (M = Ta, R = Me (**40**) or $(CH_2)_5$ (**42**); M = Nb, R = Me (**41**) or $(CH_2)_5$ (**43**)) containing both an η^2-

hydrazido(1-) ligand and a *tert*-butylamide ligand coordinated to the metal centre. Further reaction of the hydrazido synthon $Ta(NNPh_2)Cl_3(di\text{-}^tBu\text{-}bipy)$ (**38**) with the lithiated salts $Li_3(NN_2^R)$ (R = Me (**1**), ^{i}Pr (**2**) or $SiMe_3$ (**1.7**)) yielded the hydrazido complexes $Ta(NN_2^R)(NNPh_2)(di\text{-}^tBu\text{-}bipy)$ (R = Me (**44**) and ^{i}Pr (**45**)) on a preparative scale.

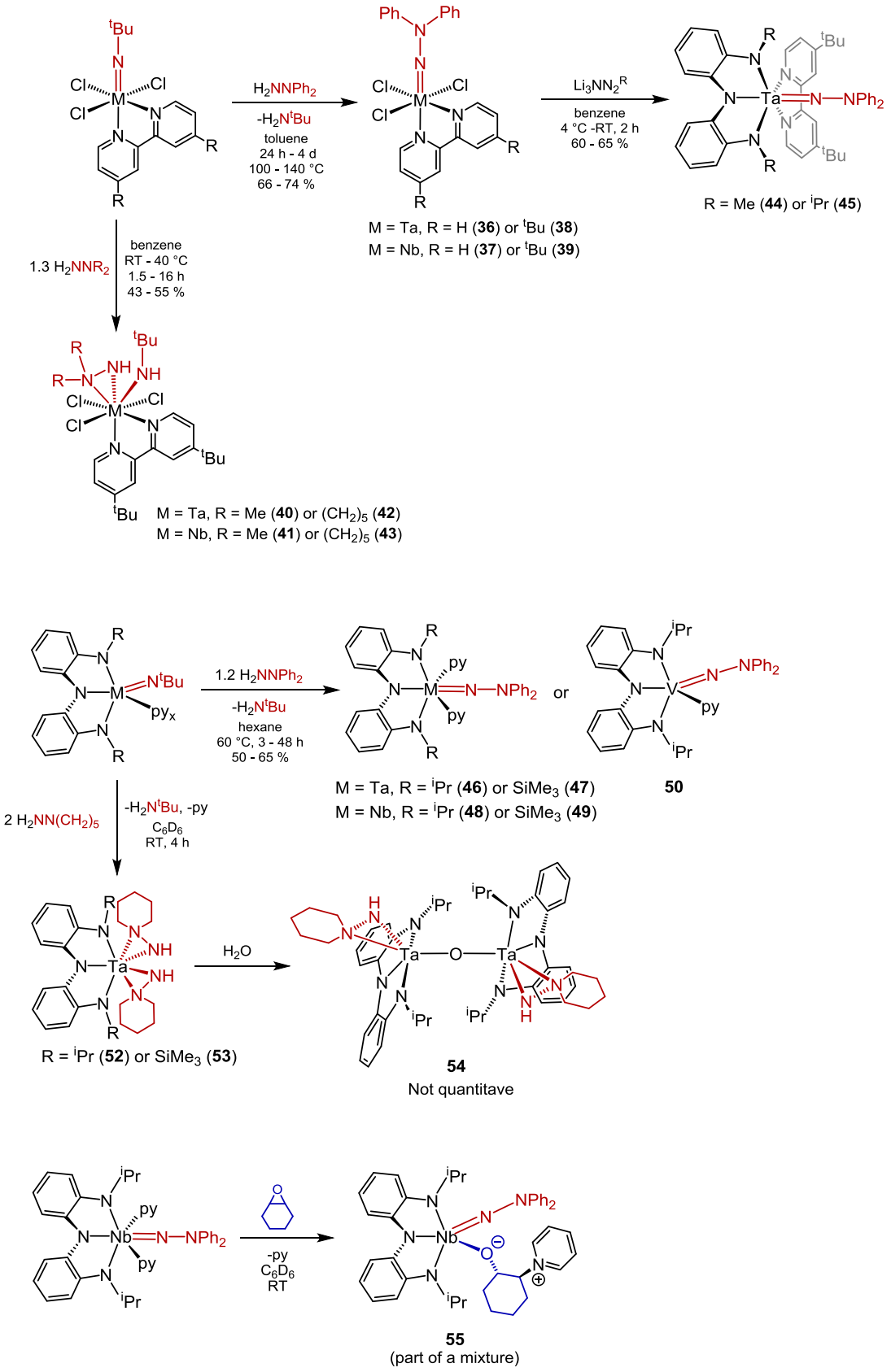
As an alternative for the synthesis of hydrazido complexes with pyridine adducts, hydrazine/*tert*-butylimide exchange reactions were performed with the imido compounds with coordinated tridentate ligands. Reaction of Group 5 imido compounds of the type $M(NN_2^R)(N^tBu)(py)_x$ (R = Me, ^{i}Pr or $SiMe_3$; x = 1 or 2) with H_2NNPh_2 yielded the complexes $M(NN_2^R)(NNPh_2)(py)_2$ (M = Ta, R = ^{i}Pr (**46**) or $SiMe_3$ (**47**); M = Nb, R = ^{i}Pr (**48**) or $SiMe_3$ (**49**)) and $V(NN_2^{iPr})(NNPh_2)(py)$ (**50**). An attempt to access the analogous complex with a bipy ligand by py/bipy ligand exchange reaction from the previously synthesised hydrazido complex $Nb(NN_2^{SiMe3})(NNPh_2)(py)_2$ (**49**) was performed on the NMR scale showing a complex mixture of products. However, the presence of the compound $Nb(NN_2^{SiMe3})(NNPh_2)(bipy)$ (**51**) was confirmed by crystallographic characterisation.

Additionally, formation of the hydrazido functionality with H_2NNMe_2, $H_2NN(Me)Ph$ and $H_2NN(CH_2)_5$ was attempted from the imido complexes $Ta(NN_2^R)(N^tBu)(py)_2$ (R = ^{i}Pr (**18**) or $SiMe_3$ (**19**)) on the NMR scale. Those reactions with H_2NNMe_2 and $H_2NN(Me)Ph$ gave mixtures of products, however reactions with $H_2NN(CH_2)_5$ showed the clean formation of complexes $Ta(NN_2^R)\{NHN(CH_2)_5\}_2$ (R = ^{i}Pr (**52**) or $SiMe_3$ (**53**)) which contain two η^2-hydrazido(1-) ligands coordinated to the metal centre. A tantalum oxo-bridged dimeric complex $\{Ta(NN_2^{iPr})\{NHN(CH_2)_5\}\}_2(\mu\text{-}O)$ (**54**) from the slow hydrolysis of compound **52** was confirmed by crystallographic characterisation.

DFT calculations performed on the model complexes of the type $Ta(NN_2^R)(NR')(py)_2$ (R = Me or SiH_3; R' = Me or NMe_2 (constrained to be planar at N_β)) which all pointed towards a common bonding situation, gave a better understanding of the bonding interaction of the imido complex $Ta(NN_2^{Me})(N^tBu)(py)_2$ (**17**, Chapter Three) and their hydrazido analogues $M(NN_2^R)(NNPh_2)(py)_2$ (as well as the corresponding bipyridyl counterparts) described in this Chapter. It was found that these π-loaded compounds with a formal $M{\equiv}N_\alpha$ triple bond ($\sigma^2\pi^4$) have a NN_2^R ligand acting as a 5 electron donor as both of the b_1 lone pair SALCs are effectively non-bonding, reducing the formal electron count to 18 valence electron complexes.

Finally, NMR scale reactions of the niobium hydrazido complex $Nb(NN_2^{iPr})(N^tBu)(py)_2$ (**48**) were carried out with a number of small unsaturated substrates. It was found to be unreactive with internal alkynes and nitriles, which was unexpected considering that the ligands stabilising the molecule are weakly bound (pyridine). Exposure to a CO_2 atmosphere or reaction with CS_2 or boranes gave a complicated mixture of unidentified products. Surprisingly, the product from the NMR scale reaction of **48** with CHO in C_6D_6 at RT was identified by X-ray crystallography as $Nb(NN_2^{iPr})(NNPh_2)(OC_6H_{10}$-2-py) (**55**). The mechanism for the formation of **55** involves coordination of the epoxide oxygen to niobium releasing the pyridine ligand, followed by nucleophilic attack from the "non-coordinated" pyridine at the epoxide resulting in ring-opening of the epoxide.

To summarise, two viable pathways were proposed for the successful synthesis of Group 5 hydrazido complexes with tridentate, trianionic ligands of the type NN_2^R with different coordination modes of the hydrazido moiety depending on the N_β substituents. Further reactivity studies may focus on the tantalum and niobium hydrazido complexes with bipy or di-^{t}Bu-bipy substituents. Also, the synthesis of hydrazido complexes with the tridentate tripodal ligand $Li_3(NNN^R)$ (R = ^{i}Pr (**1.8**) or $SiMe_3$ (**1.9**)) and their reactivity could be further explored.



Scheme 4.2. New reactions discussed in this Chapter.

4.9 References

1. J. Chatt, J. R. Dilworth and R. L. Richards, *Chem. Rev.*, 1978, **78**, 589-625.
2. M. Hidai, *Coord. Chem. Rev.*, 1999, **185-186**, 99-108.
3. M. W. Bishop, J. Chatt, J. R. Dilworth, M. B. Hursthouse and M. Motevalle, *J. Less Common Met.*, 1977, **54**, 487-493.
4. J. Chatt, B. A. L. Crichton, J. R. Dilworth, P. Dahlstrom, R. Gutkoska and J. A. Zubieta, *Transition Met. Chem.*, 1979, **4**, 271-272.
5. J. Chatt, J. R. Dilworth, P. L. Dahlstrom and J. Zubieta, *J. Chem. Soc., Chem. Commun.*, 1980, 786-787.
6. A. J. Blake, J. M. McInnes, P. Mountford, G. I. Nikonov, D. Swallow and D. J. Watkin, *J. Chem. Soc., Dalton Trans.*, 1999, 379-392.
7. J. D. Selby, C. Schulten, A. D. Schwarz, A. Stasch, E. Clot, C. Jones and P. Mountford, *Chem. Commun.*, 2008, 5101-5103.
8. P. J. Tiong, A. Nova, L. R. Groom, A. D. Schwarz, J. D. Selby, A. D. Schofield, E. Clot and P. Mountford, *Organometallics*, 2011, **30**, 1182-1201.
9. K. Weitershaus, J. Lloret Fillol, H. Wadepohl and L. H. Gade, *Organometallics*, 2009, **28**, 4747-4757.
10. T. Gehrmann, G. T. Plundrich, H. Wadepohl and L. H. Gade, *Organometallics*, 2012, **31**, 3346-3354.
11. S. Banerjee and A. L. Odom, *Organometallics*, 2006, **25**, 3099-3101.
12. A. D. Schofield, A. Nova, J. D. Selby, A. D. Schwarz, E. Clot and P. Mountford, *Chem. Eur. J.*, 2011, **17**, 265-285.
13. H. Herrmann, J. Lloret Fillol, T. Gehrmann, M. Enders, H. Wadepohl and L. H. Gade, *Chem. Eur. J.*, 2008, **14**, 8131-8146.
14. P. J. Tiong, A. Nova, A. D. Schwarz, J. D. Selby, E. Clot and P. Mountford, *Dalton Trans.*, 2012, **41**, 2277-2288.
15. J. Unruangsri, H. Morgan, A. D. Schwarz, A. D. Schofield and P. Mountford, *Organometallics*, 2013, **32**, 3091-3107.
16. H. Herrmann, J. Lloret Fillol, H. Wadepohl and L. H. Gade, *Angew. Chem. Int. Ed.*, 2007, **46**, 8426-8430.
17. T. Gehrmann, J. Lloret Fillol, H. Herrmann, H. Wadepohl and L. H. Gade, *Organometallics*, 2013, **32**, 3877-3889.

18. P. J. Walsh, M. J. Carney and R. G. Bergman, *J. Am. Chem. Soc.*, 1991, **113**, 6343-6345.
19. G. Thorsten, S. S. A., F. J. Lloret, W. Hubert and G. L. H., *Chem. Eur. J.*, 2012, **18**, 3925-3941.
20. A. D. Schofield, A. Nova, J. D. Selby, C. D. Manley, A. D. Schwarz, E. Clot and P. Mountford, *J. Am. Chem. Soc.*, 2010, **132**, 10484-10497.
21. L. C. Stevenson, S. Mellino, E. Clot and P. Mountford, *J. Am. Chem. Soc.*, 2015, **137**, 10140-10143.
22. S. Mellino, L. C. Stevenson, E. Clot and P. Mountford, *Organometallics*, 2017, **36**, 3329-3342.
23. K. Weitershaus, H. Wadepohl and L. H. Gade, *Organometallics*, 2009, **28**, 3381–3389.
24. S. Banerjee, Y. Shi, C. Cao and A. L. Odom, *J. Organomet. Chem.*, 2005, **690**, 5066-5077.
25. A. A. Dissanayake and A. L. Odom, *Chem. Commun.*, 2012, **48**, 440-442.
26. M. Veith, *Angew. Chem., Int. Edit.*, 1976, **15**, 387-388.
27. S. C. Davies, D. L. Hughes, Z. Janas, L. Jerzykiewicz, R. L. Richards, J. Roger Sanders and P. Sobota, *Chem. Commun.*, 1997, 1261-1262.
28. S. C. Davies, D. L. Hughes, Z. Janas, L. B. Jerzykiewicz, R. L. Richards, J. R. Sanders, J. E. Silverston and P. Sobota, *Inorg. Chem.*, 2000, **39**, 3485-3498.
29. J. Bultitude, L. F. Larkworthy, D. C. Povey, G. W. Smith, J. R. Dilworth and G. J. Leigh, *J. Chem. Soc., Chem. Commun.*, 1986, 1748-1750.
30. A. A. Danopoulos, R. S. Hay-Motherwell, G. Wilkinson, T. K. N. Sweet and M. B. Hursthouse, *Polyhedron*, 1997, **16**, 1081-1088.
31. S. Banerjee and A. L. Odom, *Dalton Trans.*, 2008, 2005-2008.
32. T. Moriuchi, K. Ikeuchi and T. Hirao, *Dalton Trans.*, 2013, **42**, 11824-11830.
33. M. L. H. Green, J. T. James, J. F. Saunders and J. Souter, *J. Chem. Soc., Dalton Trans.*, 1997, 1281-1288.
34. M. L. H. Green, J. T. James and A. N. Chernega, *J. Chem. Soc., Dalton Trans.*, 1997, 1719-1726.
35. E. Sebe, M. J. Heeg and C. H. Winter, *Polyhedron*, 2006, **25**, 2109-2118.
36. I. A. Tonks and J. E. Bercaw, *Inorg. Chem.*, 2010, **49**, 4648-4656.

37. I. A. Tonks, A. C. Durrell, H. B. Gray and J. E. Bercaw, *J. Am. Chem. Soc.*, 2012, **134**, 7301-7304.
38. S. Daniele, P. B. Hitchcock, M. F. Lappert, T. A. Nile and C. M. Zdanski, *J. Chem. Soc., Dalton Trans.*, 2002, 3980-3984.
39. J. Koller, S. Sarkar, K. A. Abboud and A. S. Veige, *Organometallics*, 2007, **26**, 5438-5441.
40. M. E. O'Reilly and A. S. Veige, *Chem. Soc. Rev.*, 2014, **43**, 6325-6369.
41. A. Cooper, M. Chem. Thesis, University of Oxford, 2014.
42. R. R. Schrock, J. Lee, L.-C. Liang and W. M. Davis, *Inorg. Chim. Acta*, 1998, **270**, 353-362.
43. S. M. Pugh, A. J. Blake, L. H. Gade and P. Mountford, *Inorg. Chem.*, 2001, **40**, 3992-4001.
44. N. Kaltsoyannis and P. Mountford, *J. Chem. Soc., Dalton Trans.*, 1999, 781-790.
45. T. B. Parsons, N. Hazari, A. R. Cowley, J. C. Green and P. Mountford, *Inorg. Chem.*, 2005, **44**, 8442-8458.
46. J. D. Selby, M. Feliz, A. D. Schwarz, E. Clot and P. Mountford, *Organometallics*, 2011, **30**, 2295-2307.
47. I. A. Guzei, G. P. A. Yap and C. H. Winter, *Inorg. Chem.*, 1997, **36**, 1738-1739.
48. S. Friedrich, L. H. Gade, W. S. Li and M. McPartlin, *Chem. Ber.*, 1996, **129**, 1287-1291.
49. M. H. Chisholm, J. C. Huffman and L.-S. Tan, *Inorg. Chem.*, 1981, **20**, 1859-1866.
50. T. A. Albright, J. K. Burdett and M.-H. Whangbo, *Orbital Interactions in Chemistry*, Wiley-Interscience, New York, 1985.
51. S. Kahlal, J.-Y. Saillard, J.-R. Hamon, C. Manzur and D. Carrillo, *J. Chem. Soc., Dalton Trans.*, 1998, 1229-1240.
52. S. Kahlal, J.-Y. Saillard, J.-R. Hamon, C. Manzur and D. Carrillo, *New J. Chem.*, 2001, **25**, 231-242.
53. N. Lehnert and F. Tuczek, *Inorg. Chem.*, 1999, **38**, 1671-1682.
54. J. D. Selby, C. D. Manley, A. D. Schwarz, E. Clot and P. Mountford, *Organometallics*, 2008, **27**, 6479-6494.
55. A. J. Keane, P. Y. Zavalij and L. R. Sita, *J. Am. Chem. Soc.*, 2013, **135**, 9580-9583.

56. C. M. Kozak, A. M. Woods, C. S. Bottaro, K. Devaine-Pressing and K. Ni, *Faraday Discuss.*, 2015, **183**, 31-46.
57. S. A. Blum, P. J. Walsh and R. G. Bergman, *J. Am. Chem. Soc.*, 2003, **125**, 14276-14277.
58. A. W. Addison, T. N. Rao, J. Reedijk, J. van Rijn and G. C. Verschoor, *J. Chem. Soc., Dalton Trans.*, 1984, 1349-1356.
59. D. S. Marlin, M. M. Olmstead and P. K. Mascharak, *Inorg. Chem.*, 2001, **40**, 7003-7008.
60. R. W. Chesnut, P. E. Fanwick and I. P. Rothwell, *Inorg. Chem.*, 1988, **27**, 752-754.
61. V. M. Visciglio, P. E. Fanwick and I. P. Rothwell, *Inorg. Chim. Acta*, 1993, **211**, 203-209.
62. J. R. Clark, A. L. Pulvirenti, P. E. Fanwick, M. Sigalas, O. Eisenstein and I. P. Rothwell, *Inorg. Chem.*, 1997, **36**, 3623-3631.
63. S. M. Pugh, D. J. M. Trösch, M. E. G. Skinner, L. H. Gade and P. Mountford, *Organometallics*, 2001, **20**, 3531-3542.
64. C. A. Hunter and J. K. M. Sanders, *J. Am. Chem. Soc.*, 1990, **112**, 5525-5534.
65. C. Janiak, *J. Chem. Soc., Dalton Trans.*, 2000, 3885-3896.

Chapter Five

Experimental details and characterising data

5.1 General methods and implementation

All manipulations were carried out using standard Schlenk line or dry-box techniques under an atmosphere of argon or dinitrogen. Solvents were either degassed by sparging with dinitrogen and dried by passing through a column of the appropriate drying agent[1] or refluxed over sodium (toluene), potassium (THF), Na/K alloy (Et_2O) or CaH_2 (pyridine) and distilled. Deuterated solvents were dried over sodium (toluene-d_8), potassium (C_6D_6 and THF-d_8) or P_2O_5 ($CDCl_3$ and CD_2Cl_2), distilled under reduced pressure and stored under argon in Teflon valve ampoules. Unless otherwise stated NMR samples were prepared under dinitrogen in 5 mm Wilmad 507-PP tubes fitted with J. Young Teflon valves. ^{1}H and ^{13}C{^{1}H} spectra were recorded on a Bruker Avance III HD 400 NMR spectrometer, Bruker Avance III 500 NMR spectrometer or on a Bruker Avance III 500 NMR spectrometer fitted with a ^{13}C cryoprobe. Unless otherwise stated, all NMR spectra were recorded at 298 K. ^{1}H and ^{13}C{^{1}H} and spectra were referenced internally to residual protio-solvent (^{1}H) or solvent (^{13}C) resonances, and are reported relative to tetramethylsilane (δ = 0 ppm). Assignments were confirmed as necessary with the use of two dimensional ^{1}H–^{1}H and ^{13}C–^{1}H correlation experiments. Chemical shifts are quoted in δ (ppm) and coupling constants in Hz. IR spectra were recorded on a Thermo Scientific Nicolet iS5 FTIR spectrometer and samples prepared in a dry-box using NaCl plates as a Nujol mull or as a thin film. The data are quoted in wavenumbers (cm^{-1}). Mass spectra were recorded by the mass spectrometry service of Oxford University's Department of Chemistry. Elemental analyses were carried out by the Elemental Analysis Service at the London Metropolitan University.

5.2 Literature preparations

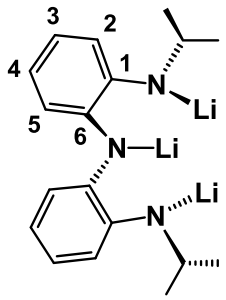
$H_3(NN_2^{Me})$,[1] $H_3(NN_2^{iPr})$,[1] $Li_3(NN_2^{SiMe3})$ (**1.7**),[2] $LiCH_2SiMe_3$,[3] $Li_3(NNN^{SiMe3})$ (**1.9**),[4] $M(N^tBu)Cl_3(py)_2$ (M = Ta (**1.41**),[5] Nb (**1.42**)[5] or V (**1.45**)[6]) were synthesised according to literature procedures. $Li_3(NN_2^{Me})$ (**1**) and $Li_3(NN_2^{iPr})$ (**2**) were prepared in analogy to $Li_3(NN_2^{SiMe3})$ (**1.7**) synthesised by Aidan Cooper,[2] procedure below. $Ta(NN_2^{SiMe3})(NH^tBu)_2$ (**2.1**) were prepared in an analogous manner to that described in a previous Part II Thesis.[2] $Ta(NN_2^{SiMe3})Cl_2$ (**3**)[2], $Ta(NN_2^{SiMe3})Me_2$ (**1.5**)[7] and $M(N^tBu)Cl_3(bipy)$ (M = Ta (**1.43**)[8], Nb (**1.44**)[8] or V (**1.46**)[9]) were synthesised according to a modified published procedure below, the omitted NMR data in the literature for **1.43** and **1.44** is provided in this Thesis, along with the characterisation of **1.46** by X-ray

diffraction, Chapter Three. All other reagents were purchased from commercial suppliers, and (for liquid reagents) degassed before use, unless specified otherwise. H_2N^tBu was dried over CaH_2 and distilled before use.

General procedure for lithiation of $H_3NN_2^R$ (R = Me or ^{i}Pr): Synthesis of $Li_3(NN_2^{Me})$ (1). Inert atmosphere techniques were used throughout. To a stirred solution of $H_3(NN_2^{Me})$ (15.367 g, 67.6 mmol)[1] in pentane (110 mL) at 0 °C was dropwise added ^{n}BuLi (126.75 mL, 202.8 mmol, 1.6 M in hexanes). The mixture was allowed to slowly warm to RT. After stirring for 3 hours, the solution was filtered away and the volatiles were then removed under reduced pressure. The product was washed with pentane (3 × 40 mL) and dried *in vacuo* giving **1** as a bright yellow powder. Yield: 16.46 g (93%).

^{1}H NMR (THF-d_8, 499.9 MHz, 298 K): δ 6.61 (2H, br. s, ArH), 6.25 (2H, t, ^{3}J = 7.1 Hz, ArH), 5.89 (4H, br. s, ArH), 2.59 (6H, br. s, NMe). ^{13}C{^{1}H} NMR (THF-d_8, 125.7 MHz, 298 K): δ 157.15 (*i*-Ar), 115.82 (Ar), 108.5 (Ar), 104.22 (Ar), 36.82 (NMe). IR (NaCl plates, Nujol mull, cm^{-1}): 1532 (m), 1291 (m), 1154 (w), 1101 (m), 1026 (m), 880 (w), 740 (s), 668 (w). EI-MS: m/z = 227 $[H_3NN_2^{Me}]^+$ (100%). A satisfactory elemental analysis of **1** could not be obtained.

Data for **$Li_3(NN_2^{iPr})$ (2)**. Product is a yellow powder. Yield: 9.63 g (81%).



^{1}H NMR (C_6D_6, 499.9 MHz, 298 K): δ 7.33 (2H, dd, ^3J = 8.1, 1.3 Hz, ArH-C5), 7.04 (2H, t, ^{3}J = 6.9 Hz, ArH-C4), 6.87 (2H, d, ^3J = 7.7, 1.3 Hz, ArH-C2), 6.66 (2H, t, ^3J = 8.1 Hz, ArH-C3), 3.08 (2H, sept, ^3J = 6.2, 2.3 Hz, CHMe$_2$), 0.76 (12H, d, ^3J = 5.6 Hz, CHMe$_2$). ^{13}C{^{1}H} NMR (C_6D_6, 125.7 MHz, 298 K): δ 157.1 (*i*-Ar-C1), 136.0 (*i*-Ar-C6), 126.4 (Ar-C4), 124.21 (Ar-C2), 121.0 (Ar-C5), 115.3 (Ar-C3), 47.57 (CHMe$_2$), 21.94 (CHMe$_2$). IR (NaCl plates, Nujol mull, cm^{-1}): 1540 (m), 1523 (m), 1291 (s), 1250 (s), 1171 (m), 1136 (m), 1048 (w), 976 (w), 884 (w), 822 (w), 741 (s), 615 (w). EI-MS: m/z = 283 $[H_3NN_2^{iPr}]^+$ (100 %), 65 $[NH^{iPr}Li]^+$ (20 %). A satisfactory elemental analysis of **2** could not be obtained.

Ta(NN$_2^{SiMe3}$)Cl$_2$ (3). To a stirred solution of **1.7** (3.0 g, 8.30 mmol) in toluene (80 mL) was added dropwise a solution of $TaCl_5$ (2.97 g, 8.3 mmol) in toluene (80 mL), at -78 ^oC. The mixture was allowed to slowly warm to RT. After 24 h, the volatiles were removed under reduced pressure and the product extracted into diethyl ether (4 × 15 mL). The solvent was removed under reduced pressure to afford **3** as a dark brown solid, which was washed with pentane (2 × 10 mL) and dried *in vacuo*. Diffraction-quality crystals were grown from the slow evaporation of a pentane solution in an H-tube apparatus. Yield: 2.65 g (54%).

^{1}H NMR (C_6D_6, 400.2 MHz, 298 K): δ 7.31 (2H, m, Ar<u>H</u>), 6.68 (4H, m, overlapping Ar<u>H</u>), 6.54 (2H, m, Ar<u>H</u>), 0.43 (18H, s, $SiMe_3$). $^{13}C\{^1H\}$ NMR (C_6D_6, 100.6 MHz, 298 K): δ 149.0 (*i*-<u>Ar</u>), 148.2 (*i*-<u>Ar</u>), 122.8 (<u>Ar</u>), 121.8 (<u>Ar</u>), 115.5 (<u>Ar</u>), 114.8 (<u>Ar</u>), 0.8 ($SiMe_3$). IR (NaCl plates, Nujol mull, cm^{-1}): 908 (w), 844 (m), 763 (w). EI-MS: m/z = 591 (77%) $[M]^+$, 556 (2%) $[M\text{-}Cl]^+$, 521 (60%) $[M\text{-}Cl_2]^+$, 73 (80%) $[SiMe_3]^+$. Anal. found (calcd. for $C_{18}H_{26}N_3Si_2Cl_2Ta$): C, 36.58 (36.49); H, 4.61 (4.42); N, 6.85 (7.09).

Ta(NN$_2^{SiMe3}$)Me$_2$ (1.5). To a stirred solution of **3** (0.50 g, 0.84 mmol) in toluene (20 mL) was slowly added a solution of MeMgBr 3.0 M in ether (0.56 mL, 1.68 mmol) and 1,4-dioxane (0.72 mL) in toluene (10 mL), at -30 °C. The mixture was allowed to warm to RT, no colour changes were observed. After 1.5 h, the solution was filtered away and the volatiles were then removed under reduced pressure. The product was washed with pentane (3 × 5 mL) and dried *in vacuo* to afford **1.5** as a light-brown powder. Yield: 0.265 g (60 %).

^{1}H NMR (C_6D_6, 400.2 MHz, 298 K): δ 7.66 (2 H, dd, ^3J = 7.6, 1.8 Hz, ArH), 6.82 (4 H, overlapping 2 × m, ArH), 0.71 (6 H, s, $TaMe_2$), 0.32 (18 H, s, $NSiMe_3$) ppm. $^{13}C\{^1H\}$ NMR (C_6D_6, 100.6 MHz, 298 K): δ 149.89 (*i*-Ar), 146.86 (*i*-Ar), 121.53 and 120.86 (Ar), 115.4 (Ar), 115.20 (Ar), 60.12 ($TaMe_2$), 1.68 ($NSiMe_3$) ppm. IR (NaCl plates, Nujol mull, cm^{-1}): 3058 (w), 1570 (w), 1334 (m), 1254 (s), 1217 (m), 1177 (w), 1161 (w), 1112 (m), 1052 (w), 940 (w), 917 (m), 883 (s), 841 (s), 804 (s), 731 (s), 684 (w), 649 (w), 600 (w). EI-MS: *m*/*z* = 73 $[SiMe_3]^+$ (100%). Anal. found (calcd. for $C_{20}H_{32}N_3Si_2Ta$): C, 40.62 (43.55); H, 5.47 (5.85); N, 7.53 (7.62) %. Repeated attempts to obtain an elemental analysis with satisfactory % C values failed, presumably due to incomplete combustion of the compound.

General procedure for M(N^{t}Bu)Cl$_3$(bipy) (M = Ta (1.43) or Nb (1.44)). Ta(N^{t}Bu)Cl$_3$(bipy) (1.43). A solution of **1.41** (3.0 g, 5.806 mmol) and 2,2'-bipyridyl (bipy, 0.907 g, 5.806 mmol) in benzene (60 mL) was stirred at RT for 2.5 h. After this time the solution was filtered away and the solid washed with pentane (3 × 10 mL) and dried *in vacuo* to afford **1.43** as a pale-yellow powder. Yield: 2.89 g (97 %).

Data for **1.43**, ^{1}H NMR ($CDCl_3$, 499.9 MHz, 298 K): δ 9.64 (1H, ddd, ^3J = 5.3, 1.6, 0.8 Hz, bipy-C1$_a$), 9.54 (1H, ddd, ^3J = 5.5, 1.6, 0.7 Hz, bipy-C1$_b$), 8.29 (1H, d, ^3J = 8.1 Hz, bipy-C4$_b$), 8.24-8.29 (2H, overlapping d and td, bipy-C4$_a$ and bipy-C3$_a$), 8.14 (1H, td, ^3J = 7.9, 1.7 Hz, bipy-C3$_a$), 7.71 (2H, overlapping 2 x m, bipy-C2$_{b,a}$), 1.52 (9H, s, $NCMe_3$). $^{13}C\{^1H\}$ NMR ($CDCl_3$, 125.7 MHz, 298 K): δ 155.37 (bipy-C1$_b$), 152.33 (*i*-bipy-C5$_a$), 151.70 (*i*-bipy-C5$_b$), 150.50 (bipy-C1$_a$), 141.19 (bipy-C3$_b$), 139.84 (bipy-C3$_a$), 127.03 (bipy-C2$_a$), 126.54 (bipy-C2$_b$), 122.91 (bipy-C4$_b$), 122.68 (bipy-C4$_a$), 66.13 (*i*-NCMe3), 32.29 (NCMe3). Note: subscripts "a" and "b" refer to inequivalent bipy rings environments.

Data for **1.44**. Bright-yellow powder. Yield: 2.93 g (98 %). ^{1}H NMR ($CDCl_3$, 499.9 MHz, 298 K): δ 9.59 (1H, ddd, ^3J = 5.2, 1.6, 0.7 Hz, bipy-C1$_a$), 9.29 (1H, ddd, ^3J = 5.4, 1.5, 0.6 Hz, bipy-C1$_b$), 8.25 (1H, d, ^3J = 8.2 Hz, bipy-C4$_b$), 8.20 (1H, d, ^3J = 8.2 Hz, bipy-C4$_a$), 8.15 (1H, td, ^3J = 8.0, 1.7 Hz, bipy-C3$_b$), 8.10 (1H, td, ^3J = 7.9, 1.7 Hz, bipy-C3$_a$), 7.68 (1H, ddd, ^3J = 7.6, 5.2, 1.1 Hz, bipy-C2$_a$), 7.64 (1H, ddd, ^3J = 7.6, 5.5, 1.3 Hz, bipy-C2$_b$), 1.57 (9H, s, $NCMe_3$). $^{13}C\{^1H\}$ NMR ($CDCl_3$, 125.7 MHz, 298 K): δ 154.30 (bipy-C1$_b$), 151.94 (*i*-bipy-C5$_a$), 151.35 (*i*-bipy-C5$_b$), 150.34 (bipy-C1$_a$), 140.90 (bipy-C3$_b$), 139.74 (bipy-C3$_a$), 126.68 (bipy-C2$_a$), 126.21 (bipy-C2$_b$), 122.75 (bipy-C4$_b$), 122.46 (bipy-C4$_a$), 70.52 (*i*-NCMe3), 30.02 (NCMe3). Note: subscripts "a" and "b" refer to inequivalent bipy rings environments.

V(N^{t}Bu)Cl$_3$(bipy) (1.46). A solution of **1.45** (1.0 g, 2.586 mmol) and 2,2'-bipyridyl (bipy, 0.404 g, 2.586 mmol) in pentane (50 mL) was stirred at RT for 16 h. After this time the solvent was filtered away and the solid washed with a mixture of pentane / benzene (3 × 15 mL, 1:1 ratio) and dried *in vacuo* to afford **1.46** as a green powder. Diffraction-quality crystals were grown by solvent diffusion in dichloromethane/pentane at room temperature. Yield: 0.972 g (98 %).

5.3 X-ray data collection and processing parameters

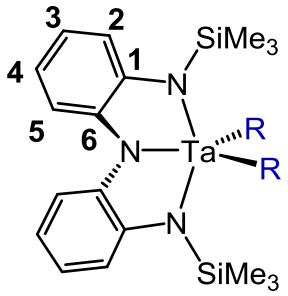
X-ray crystallography data was collected and solved by Dr. Benjamin Clough, Dr. Bowen Xie and Dr. Richard Collins. Molecular structures were refined by the Author with the help and guidance of Dr. Benjamin A. Clough, Dr. Bowen Xie, Dr. Richard Collins, Prof. Philip Mountford and Prof. Richard Cooper. Molecular drawings were produced by Prof. Philip Mountford.

Crystals were mounted on glass fibers using perfluoropolyether oil and cooled rapidly in a stream of cold N_2 using an Oxford Cryosystems Cryostream unit. Diffraction data were measured using either an Enraf-Nonius KappaCCD or Agilent Technologies Supernova diffractometer using Mo-K_α or Cu-K_α radiation, respectively. As appropriate, absorption and decay corrections were applied to the data and equivalent reflections merged.[10] The structures were solved with SIR92[11] or Superflip,[12] and further refinements and all other crystallographic calculations were performed using the CRYSTALS program suite.[13] Other details of the structure solutions and refinements are given in the individual CIFs contained in the CD Appendix.

5.4 Computational details

DFT calculations described in this Thesis were performed by Prof. Philip Mountford at the University of Oxford. Geometry optimisations were performed on model systems as described in the text using the Gaussian09 package (rev. D.01)[14] at the B3PW91 level of hybrid density functional theory,[15,16] and the def2-svp basis set,[17] along with a pseudopotential for tantalum.[18] Additionally, complementary geometry optimisations on full systems as described in the text (DFT-D3) that included Grimme's empirical d3(bj) dispersion correction[19] were also carried out.

5.5 Experimental details and characterising data for Chapter Two



Ta(NN_2^{SiMe3})($CH_2{}^iPr$)$_2$ (4). To a solution of **3** (1.00 g, 1.68 mmol) in benzene (50 mL) was added a solution of isobutyllithium 1.7 M in heptane (1.98 mL, 3.37 mmol). The solution was stirred at RT for 1.5 h, after which time the colour changed to reddish orange. The solution was filtered away and the solvent removed under reduced pressure to give a red oil, which was triturated in pentane (5 mL) and dried *in vacuo* to yield **4** as a reddish brown powder. Yield: 0.585 g (55 %).

^{1}H NMR (C_6D_6, 499.9 MHz, 298 K): δ 7.69 (2 H, dd, ^3J = 7.6, 1.7 Hz, ArH-C5), 6.81 (4H, overlapping 2 × m, ArH-C4 and ArH-C3), 6.73 (2H, dd, ^3J = 7.6, 1.7 Hz ArH-C2), 2.39 (2H, sept, ^3J = 13.0, 6.5 Hz CH_2CHMe_2), 1.49 (4H, d, ^3J = 6.5, CH_2CHMe_2), 0.82 (12H, d, ^3J = 6.5, CH_2CHMe_2), 0.45 (18H, s, $NSiMe_3$). ^{13}C{^{1}H} NMR (C_6D_6, 125.7 MHz, 298 K): δ 149.24 (*i*-Ar-C6), 146.38 (*i*-Ar-C1), 121.43 (Ar-C4), 120.87 (Ar-C3), 115.83 (Ar-C2), 115.03 (Ar-C5), 95.22 (CH_2CHMe_2), 31.85 (CH_2CHMe_2), 28.73 ($CHMe_2$), 2.21 ($NSiMe_3$) ppm. IR (NaCl plates, Nujol mull, cm^{-1}): 3058 (w), 1571 (w), 1334 (m), 1254 (s), 1219 (m), 918 (m), 883 (m), 843 (s), 802 (s), 732 (m). EI-MS: *m*/*z* = 343 [$H_3NN_2^{SiMe3}$]$^+$ (10 %), 73 [$SiMe_3$]$^+$ (100 %). A satisfactory elemental analysis of **4** could not be obtained.

Ta(NN_2^{SiMe3})($CH_2{}^tBu$)$_2$ (5). A solution of **3** (1.00 g, 1.68 mmol) and neopentyllithium (0.263 g, 3.37 mmol) in benzene (50 mL) was stirred at RT for 1 h, after which time the solution was filtered away and the volatiles removed under reduced pressure to give a brown oil, then the product was extracted in pentane (10 mL × 2) at 0 ˚C and dried *in vacuo* to yield **5** as a brown powder. Yield: 0.591 g (53 %).

^{1}H NMR (C_6D_6, 499.9 MHz, 298 K): δ 7.67 (2 H, d, ^3J = 7.7, ArH-C5), 6.79 (6 H, overlapping 3 × m; ArH-C4, ArH-C3 and ArH-C2), 1.62 (4 H, s, $CH_2{}^tBu$), 0.93 (18H, s, $CH_2{}^tBu$), 0.52 (18H, s, $NSiMe_3$). ^{13}C{^{1}H} NMR (C_6D_6, 125.7 MHz, 298 K): δ 148.27 (*i*-Ar-C6), 145.42 (*i*-Ar-C1), 120.61 (Ar-C4), 120.40 (Ar-C3), 115.72 (Ar-C2), 114.56 (Ar-

C5), 101.99 ($\underline{CH_2}^tBu$), 35.09 ($CH_2\underline{^tBu}$), 2.99 ($NSiMe_3$) ppm. IR (NaCl plates, Nujol mull, cm^{-1}): 1570 (w), 1332 (w), 1254 (s), 920 (w), 893 (w), 841 (s), 803 (s), 731 (s). EI-MS: m/z = 663 $[M]^+$ (0.07%), 343 $[(H_3NN_2^{SiMe3})]^+$ (50 %), 73 $[(SiMe_3)]^+$ (98 %). A satisfactory elemental analysis of **5** could not be obtained.

$Ta(NN_2^{SiMe3})(CH_2Ph)_2$ (6). To a solution of **3** (1.00 g, 1.68 mmol) in toluene (50 mL) was added a solution of benzylmagnesium chloride 1.0 M in diethyl ether (3.37 mL, 3.37 mmol) in toluene (10 mL), at -60 ˚C. The solution was slowly warmed up to RT and stirred for 1 h, no colour change was observed. The solution was filtered away and the volatiles removed under reduced pressure to yield **6** as a dark brown powder, which is not soluble in hydrocarbon solvents. Diffraction-quality crystals were grown from a saturated benzene solution at room temperature. Yield: 0.927 g (78 %).

^1H NMR (C_6D_6, 499.9 MHz, 298 K): δ 7.21 (2 H, dd, ^3J = 6.0, 3.4 Hz, Ar$\underline{H}$-C5), 6.85-6.84 (8 H, overlapping *o*- and *m*-$CH_2\underline{Ph}$), 6.70 (4 H, dd, ^3J = 6.0, 3.4 Hz, Ar$\underline{H}$-C4 and Ar$\underline{H}$-C3), 6.57 (2 H, dt, ^3J = 8.5, 4.5 Hz, *p*-$CH_2\underline{Ph}$), 6.46 (2 H, dd, ^3J = 5.9, 3.3 Hz, Ar$\underline{H}$-C2), 2.80 (4 H, s, $\underline{CH_2}Ph$), 0.32 (18H, s, $SiMe_3$). $^{13}C\{^1H\}$ NMR (C_6D_6, 125.7 MHz, 298 K): δ 148.68 (*i*-Ar-C6), 146.38 (*i*-Ar-C1), 142.30 (*i*-$CH_2\underline{Ph}$), 129.07 (*o*-$CH_2\underline{Ph}$), 127.89 (*m*-$CH_2\underline{Ph}$), 123.71 (*p*-$CH_2\underline{Ph}$), 121.18 (Ar-C3), 120.85 (Ar-C4), 114.93 (overlapping ArC5 and ArC2), 85.53 ($\underline{CH_2}Ph$), 0.96 ($NSiMe_3$) ppm. IR (NaCl plates, Nujol mull, cm^{-1}): 1591 (w), 1328 (w), 1278 (m), 1255 (s), 1178 (w), 1114 (w), 911 (m), 835 (s), 804 (s), 743 (m), 729 (s), 692 (m). EI-MS: m/z = 703 $[M]^+$ (4 %), 73 $[(SiMe_3)]^+$ (58 %). Anal. found (calcd. for $C_{32}H_{40}N_3Si_2Ta$): C, 46.63 (54.61); H, 5.59 (5.73); N, 6.26 (5.97) %. Repeated attempts to obtain an elemental analysis with satisfactory % C values failed, presumably due to incomplete combustion of the compound.

$Ta(NN_2^{SiMe3})(CH_2SiMe_3)_2$ (7). To a solution of **3** (3.43 g, 5.77 mmol) in toluene (150 mL) was added a solution of (trimethylsilyl)methyllithium (1.08 g, 11.56 mmol) in toluene (50 mL), at -78 ˚C. The solution was slowly warmed up to RT and stirred for 3 h, after which time the solution was filtered away and the volatiles removed under reduced pressure, then the product was extracted in pentane (3 × 20 mL) and dried *in vacuo* to yield **7** as a light brown powder. Diffraction-quality crystals were grown from a saturated benzene solution at room temperature. Yield: 3.10 g (77 %).

^1H NMR (C_6D_6, 499.9 MHz, 298 K): δ 7.62 (2 H, dd, ^3J = 6.1, 3.3 Hz, Ar$\underline{H}$-C5), 6.78 (4 H, dd, ^3J = 9.4 Hz, Ar$\underline{H}$-C4 and Ar$\underline{H}$-C3), 6.72 (2 H, m, Ar$\underline{H}$-C2), 1.10 (4 H, s,

$\underline{CH_2}SiMe_3$), 0.50 (18H, s, $NSiMe_3$), -0.7 (18H, s, $CH_2\underline{SiMe_3}$). $^{13}C\{^1H\}$ NMR (C_6D_6, 100.6 MHz, 298 K): δ 148.63 (*i*-Ar-C6), 146.24 (*i*-Ar-C1), 121.15 (Ar-C3), 120.80 (Ar-C4), 115.85 (Ar-C2), 115.03 (Ar-C5), 77.76 ($\underline{CH_2}SiMe_3$), 2.73 ($SiMe_3$) ppm. IR (NaCl plates, Nujol mull, cm^{-1}): 1568 (w), 1330 (w), 1244 (s), 1180 (w), 1119 (w), 1059 (w), 921 (s), 896 (s), 840 (s), 805 (m), 729 (s), 681 (m), 599 (m). EI-MS: *m*/*z* = 695 $[M]^+$ (12 %), 521 $[Ta(NN_2^{SiMe3})]^+$ (6 %), 343 $[(H_3NN_2^{SiMe3})]^+$ (50 %), 73 $[SiMe_3]^+$ (100 %). A satisfactory elemental analysis of **7** could not be obtained.

NMR tube scale reaction of thermal decomposition of 7. Synthesis of $Ta\{NN^{SiMe3}N^{SiMe2}(CH_2)\}(CH_2SiMe_3)$ (8). A C_6D_6 solution (0.6 mL) of **7** (50 mg, 0.0719 mmol) was prepared in an NMR tube equipped with a J. Young Teflon valve. The reaction was monitored by ^1H NMR spectroscopy. After 8 days at 80 ˚C, the volatiles were removed under reduced pressure and the resultant orange-brown solid dried *in vacuo* before being redissolved in C_6D_6 (0.6 mL). ^1H NMR showed full conversion of **7** to **8** and small amount of decomposition products. Complex **8** was characterised by ^1H and ^{13}C NMR spectroscopy.

^1H NMR (C_6D_6, 499.9 MHz, 298 K): δ 7.69 (1 H, dd, ^3J = 8.2, 1.2 Hz, $Ar\underline{H_a}$), 7.62 (1 H, dd, ^3J = 8.0, 1.1 Hz, $Ar\underline{H_b}$), 6.94 (1 H, td, ^3J = 7.7, 1.6 Hz, $Ar\underline{H_b}$), 6.89 (1 H, td, ^3J = 7.5, 1.3 Hz, $Ar\underline{H_b}$), 6.84 (1 H, td, ^3J = 8.1, 7.6, 1.5 Hz, $Ar\underline{H_a}$), 6.76 (1 H, td, ^3J = 7.5, 1.2 Hz, $Ar\underline{H_a}$), 6.72 (1 H, dd, ^3J = 7.8, 1.5 Hz, $Ar\underline{H_a}$), 6.66 (1 H, dd, ^3J = 7.5, 1.5 Hz, $Ar\underline{H_b}$), 1.40 (1 H, d, ^2J = 11.3 Hz, $C\underline{H}HSiMe_3$), 0.86 (1 H, d, ^2J = 14.3 Hz, $C\underline{H}HSiMe_2$), 0.57 (1 H, d, ^2J = 11.2 Hz, $CH\underline{H}SiMe_3$), 0.49 (3H, s, $NSi\underline{Me}Me$), 0.45 (9H, s, $NSiMe_3$), 0.45-0.43 (doublet for 1H overlapping singlet at 0.45 ppm, $CH\underline{H}SiMe_2$), 0.10 (3H, s, $NSiMe\underline{Me}$), -0.13 (9H, s, $CH_2Si\underline{Me_3}$). $^{13}C\{^1H\}$ NMR (C_6D_6, 125.7 MHz, 298 K): δ 150.13 (*i*-Ar_b), 148.58 (*i*-Ar_a), 147.78 (*i*-Ar_b), 146.55 (*i*-Ar_a), 121.90 (Ar_a), 121.65 (Ar_b), 120.47 (Ar_b), 119.77 (Ar_a), 116.50 (Ar_b), 116.24 (Ar_a), 116.07 (Ar_b), 113.18 (Ar_a), 75.96 ($\underline{CH_2}SiMe_3$), 62.49 ($\underline{CH_2}SiMe_2$), 2.40 ($Si\underline{Me}Me$), 1.57 ($CH_2Si\underline{Me_3}$), 1.14 ($NSiMe_3$), -2.64 ($SiMe\underline{Me}$) ppm.

$Ta(NN_2^{SiMe3})(NH^tBu)(Me)$ (9). To a solution of **1.5** (0.20 g, 0.362 mmol) in benzene (20 mL) was added $^tBuNH_2$ (0.038 mL, 0.362 mmol). The red solution was stirred for 3 days at 60 ˚C. After which time the solution was concentrated and cooled down, then pentane was added to precipitate the impurities. The red solution was filtered away and the volatiles were removed under reduced pressure to yield **9** as reddish-brown powder.

Diffraction-quality crystals were grown from a saturated benzene solution at room temperature. Yield: 0.10 g (45 %).

^{1}H NMR (C_6D_6, 499.9 MHz, 298 K): δ 7.75 (2 H, d, ^{3}J = 7.1 Hz, Ar<u>H</u>-C5), 6.87-6.82 (6H, overlapping 3 × m; Ar<u>H</u>-C2, Ar<u>H</u>-C4 and Ar<u>H</u>-C3), 4.43 (1H, s, <u>NH</u>CMe$_3$), 0.93 (9H, s, NHC<u>Me$_3$</u>), 0.66 (3H, s, TaMe), 0.40 (18H, s, NSiMe$_3$). ^{13}C{^{1}H} NMR (C_6D_6, 125.7 MHz, 298 K): δ 148.37 (*i*-Ar-C6), 147.41 (*i*-Ar-C1), 120.33 (Ar-C4), 119.45 (Ar-C3), 115.79 (Ar-C2), 114.39 (Ar-C5), 57.19 (*i*-NH<u>C</u>Me$_3$), 54.51 (TaMe), 32.67 (NHC<u>Me$_3$</u>), 2.27 (NSiMe$_3$) ppm. IR (NaCl plates, Nujol mull, cm^{-1}): 3248 (w), 1567 (w), 1331 (m), 1279 (m), 1246 (s), 1205 (m), 1118 (w), 1059 (w), 967 (w), 921 (w), 896 (m), 873 (m), 836 (s), 779 (w), 729 (s), 694 (w), 677 (w), 642 (w), 599 m). EI-MS: *m*/*z* = 608 $[M]^+$ (1%), 73 $[SiMe_3]^+$ (100 %). A satisfactory elemental analysis of **9** could not be obtained.

Ta(NN$_2^{SiMe3}$)(NH^{t}Bu)(CH$_2^i$Pr) (10). To a solution of **4** (0.25 g, 0.393 mmol) in benzene (5 mL) was added ^{t}BuNH$_2$ (0.041 mL, 0.393 mmol), then heated at 80 ˚C and stirred for 16 h, after which the volatiles were removed under reduced pressure, resulting in a reddish-brown oil giving **10** as a brown powder after lyophilisation. Yield: 0.159 g (62 %).

^{1}H NMR (C_6D_6, 499.9 MHz, 298 K): δ 7.75 (2 H, d, ^{3}J = 7.2 Hz, Ar<u>H</u>-C5), 6.91-6.82 (6H, overlapping 3 × m; Ar<u>H</u>-C2, Ar<u>H</u>-C3 and Ar<u>H</u>-C4), 4.46 (1H, s, <u>NH</u>CMe$_3$), 2.37 (1H, sept, ^{3}J = 13.0, 6.5 Hz, CH$_2$<u>CH</u>Me$_2$), 1.42 (2H, d, ^{3}J = 6.5 Hz, <u>CH$_2$</u>CHMe$_2$), 0.94 (9H, s, NHC<u>Me$_3$</u>), 0.82 (6H, d, 6.6 Hz, CH$_2$CH<u>Me$_2$</u>), 0.46 (18H, s, NSiMe$_3$). ^{13}C{^{1}H} NMR (C_6D_6, 125.7 MHz, 298 K): δ 147.81 (*i*-Ar-C6), 147.25 (*i*-Ar-C1), 120.37 (Ar-C3), 119.40 (Ar-C4), 116.04 (Ar-C2), 114.33 (Ar-C5), 89.44 (<u>CH$_2$</u>CHMe$_2$), 57.06 (*i*-NH<u>C</u>Me$_3$), 32.77 (NHC<u>Me$_3$</u>), 30.59 (CH$_2$<u>CH</u>Me$_2$), 27.92 (CH$_2$CH<u>Me$_2$</u>), 2.80 (NSiMe$_3$) ppm. IR (NaCl plates, Nujol mull, cm^{-1}): 3249 (w), 3052 (w), 1567 (m), 1363 (s), 1332 (s), 1309 (w), 1282 (s), 1247 (s), 1204 (s), 1160 (m), 1119 (s), 1059 (m), 1040 (m), 963 (s), 921 (s), 897 (s), 874 (s), 835 (s), 779 (m), 681 (m), 642 (w), 618 (w), 600 (m). EI-MS: *m*/*z* = 75 $[SiMe_3]^+$ (66 %). A satisfactory elemental analysis of **10** could not be obtained.

Ta(NN_2^{SiMe3})(NH^{t}Bu)($CH_2{}^t$Bu) (11). To a solution of **5** (0.50 g, 0.753 mmol) in benzene (10 mL) was added ^{t}BuNH$_2$ (0.079 mL, 0.753 mmol) then heated at 80 ˚C and stirred for 48 h, after which the volatiles were removed under reduced pressure affording **11** as a light-brown powder. Yield: 0.346 g (69 %).

^{1}H NMR (C_6D_6, 499.9 MHz, 298 K): δ 7.78 (2 H, dd, ^3J = 7.8, 1.5 Hz, ArH-C5), 6.91 (2H, dd, ^3J = 7.8, 1.6 Hz, ArH-C2), 6.84 (4H, overlapping 2 x dt, ArH-C3 and ArH-C4), 4.48 (1H, s, NHCMe$_3$), 1.54 (2H, s, CH$_2$CMe$_3$), 0.96 (9H, s, CH$_2$CMe$_3$), 0.95 (9H, s, NHCMe$_3$), 0.51 (18H, s, NSiMe$_3$). ^{13}C{^{1}H} NMR (C_6D_6, 125.7 MHz, 298 K): δ 147.46 (*i*-Ar-C6), 146.89 (*i*-Ar-C1), 120.14 (Ar-C3), 119.04 (Ar-C4), 115.97 (Ar-C2), 114.23 (Ar-C5), 96.24 (CH$_2$CMe$_3$), 57.08 (*i*-NHCMe$_3$), 37.43 (CH$_2$CMe$_3$), 34.80 (CH$_2$CMe$_3$), 32.51 (NHCMe$_3$), 3.29 (NSiMe$_3$) ppm. IR (NaCl plates, Nujol mull, cm^{-1}): 3274 (w), 3053 (w), 1568 (m), 1363 (s), 1324 (s), 1281 (s), 1246 (s), 1201 (s), 1119 (s), 1058 (m), 1041 (w), 960 (s), 921 (s), 895 (s), 872 (s), 836 (s), 776 (s), 728 (s), 681 (s), 642 (w), 599 (m). EI-MS: *m*/*z* = 664 $[M]^+$ (7 %), 593 $[Ta(NN_2^{SiMe3})(NHCMe_3)]^+$ (41 %), 343 $[H_3NN_2^{SiMe3}]^+$ (10 %), 75 $[SiMe_3]^+$ (100 %). A satisfactory elemental analysis of **11** could not be obtained.

Ta(NN_2^{SiMe3})(NH^{t}Bu)(CH_2Ph) (12). To a solution of **6** (1.0 g, 1.42 mmol) in benzene (80 mL) was added ^{t}BuNH$_2$ (0.149 mL, 1.42 mmol) then heated at 60 ˚C and stirred for 14 h, after which the volatiles were removed under reduced pressure. The resulting solid was washed with pentane (3 × 10 mL) and dried *in vacuo* to afford **12** as a light-brown powder. Diffraction-quality crystals were grown from a saturated benzene solution at room temperature. Yield: 0.723 g (74 %).

^{1}H NMR (C_6D_6, 499.9 MHz, 298 K): δ 7.49 (2 H, d, ^3J = 7.5 Hz, ArH-C5), 6.88 (4H, m, overlapping 2 × m, *o*-C_6H_5 and *m*-C_6H_5), 6.81 (4H, overlapping 2 × m, ArH-C3 and ArH-C2), 6.75 (2H, ddd, ^3J = 8.5, 6.1, 2.5 Hz, ArH-C4), 6.61 (1H, t, ^3J = 7.0 Hz, *p*-C_6H_5), 4.72 (1H, s, NHCMe$_3$), 2.66 (2H, s, CH$_2$C$_6$H$_5$), 0.96 (9H, s, NHCMe$_3$), 0.43 (18H, s, NSiMe$_3$). ^{13}C{^{1}H} NMR (C_6D_6, 125.7 MHz, 298 K): δ 147.71 (*i*-Ar-C6), 147.23 (*i*-Ar-C1), 139.98 (*i*-C_6H_5), 128.74 (*o*-C_6H_5), 128.30 (*m*-C_6H_5), 123.59 (*p*-C_6H_5), 120.32 (Ar-C3), 119.29 (Ar-C4), 115.87 (Ar-C2), 114.41 (Ar-C5), 78.46 (CH$_2$C$_6$H$_5$), 57.79 (*i*-NHCMe$_3$), 32.81 (NHCMe$_3$), 2.89 (NSiMe$_3$) ppm. IR (NaCl plates, Nujol mull, cm^{-1}): 3248 (w), 1567 (w), 1372 (m), 1331 (w), 1279 (m), 1246 (s), 1205 (m), 1118 (m), 1059 (w), 967 (m), 921 (m),

896 (s), 873 (m), 836 (s), 779 (w), 729 (s), 694 (w), 677 (w), 642 (w), 599 (m). EI-MS: m/z = 75 $[SiMe_3]^+$ (77 %). A satisfactory elemental analysis of **12** could not be obtained.

Ta(NN_2^{SiMe3})(NH^tBu)(CH_2SiMe_3) (13). To a solution of **7** (0.30 g, 0.4315 mmol) in toluene (20 mL) was added $^tBuNH_2$ (0.068 mL, 0.647 mmol) then heated at 80 ˚C and stirred for 7 d, after which the volatiles were removed under reduced pressure and the product extracted in pentane (3 × 10 mL). The volatiles were removed under reduce pressure and the resulting solid was dried *in vacuo* to afford **13** as a light-brown powder. Yield: 0.270 g (92 %).

^{1}H NMR (C_6D_6, 400.1 MHz, 298 K): δ 7.74 (2 H, dd, ^3J = 7.5, 1.64 Hz, ArH-C5), 6.890 – 6.78 (6H, overlapping 3 × m, ArH-C4, ArH-C3 and ArH-C2), 4.57 (1H, s, $NHCMe_3$), 1.01 (1H, s, CH_2SiMe_3), 0.95 (9H, s, $NHCMe_3$), 0.50 (1H, s, CH_2SiMe_3), 0.49 (18H, s, $NSiMe_3$), -0.06 (9H, s, CH_2SiMe_3) ppm. $^{13}C\{^1H\}$ NMR (C_6D_6, 100.1 MHz, 298 K): δ 147.70 (*i*-Ar-C1), 147.21 (*i*-Ar-C6), 120.27 (Ar-C3), 119.27 (Ar-C4), 115.92 (Ar-C2), 114.43 (Ar-C5), 57.05 (*i*-$NHCMe_3$) 33.55 (CH_2SiMe_3), 32.65 ($NHCMe_3$), 3.09 ($NSiMe_3$), 2.28 (CH_2SiMe_3) ppm.

5.6 Experimental details and characterising data for Chapter Three

General procedure for M(N^tBu)Cl_3(di-^{t}Bu-bipy) (M = Ta (14), Nb (15) or V (16)). Ta(N^tBu)Cl_3(di-^{t}Bu -bipy) (14). A solution of **1.41** (2.0 g, 3.871 mmol) and 4,4'-di-*tert*-butyl-2,2'-bipyridyl (di-^{t}Bu-bipy, 1.039 g, 3.871 mmol) in benzene (80 mL) was stirred at RT for 16 h. After this time the solvent was filtered away and the solid washed with benzene (3 × 15 mL) and dried *in vacuo* to afford **14** as a yellow powder. Yield: 2.43 g (99 %).

Data for **14**, ^{1}H NMR (CD_2Cl_2, 400.2 MHz, 298 K): δ 9.39 (2H, overlapping 2 × d, ^3J = 7.2 Hz, di-^{t}Bu-bipy-C1$_{a,b}$), 8.24 (1H, d, ^3J = 1.8 Hz, di-^{t}Bu-bipy-C4$_b$), 8.21 (1H, d, ^3J = 1.6 Hz, di-^{t}Bu-bipy-C4$_a$), 7.71 (2H, overlapping 2 × m, di-^{t}Bu-bipy-C2$_{a,b}$), 1.48-1.46 (27H, overlapping 3 × s, $NCMe_3$ and di-^{t}Bu-bipy$_{a,b}$). $^{13}C\{^1H\}$ NMR (CD_2Cl_2, 100.6 MHz, 298 K): δ 166.39 (*i*-di-^{t}Bu-bipy-C3$_b$), 164.84 (*i*-di-^{t}Bu-bipy-C3$_a$), 154.78 (di-^{t}Bu-bipy-C1$_b$), 152.13 (*i*-di-^{t}Bu-bipy-C5$_b$), 151.72 (*i*-di-^{t}Bu-bipy-C5$_a$), 149.45 (di-^{t}Bu-bipy-C1$_a$), 124.22 (di-^{t}Bu-bipy-C2$_a$), 123.93 (di-^{t}Bu-bipy-C2$_b$), 119.68 (di-^{t}Bu-bipy-C4$_b$), 119.56 (di-^{t}Bu-bipy-C4$_a$), 65.53 (*i*-$NCMe_3$), 35.87 (*i*-di-^{t}Bu-bipy$_b$), 35.52 (*i*-di-^{t}Bu-bipy$_a$), 31.94 ($NCMe_3$), 29.97 (di-^{t}Bu-bipy$_b$), 29.82 (di-^{t}Bu-bipy$_a$). Note: subscripts "a" and "b" refer to inequivalent di-*tert*-butyl-bipy rings environments. IR (NaCl plates, Nujol mull, cm^{-1}):

1617 (s), 1545 (m), 1411 (s), 1293 (w), 1272 (s), 1217 (w), 1202 (w), 1155 (w), 1124 (w), 1079 (w), 1033 (m), 1021 (m), 929 (w), 900 (m), 891 (m), 858 (m), 850 (m), 740 (w), 697 (s), 676 (w), 605 (s). EI-MS: *m*/*z* = 253 [*di-tert-butyl-bipy*]$^+$ (100 %). Anal. found (calcd. for $C_{22}H_{33}Cl_3N_3Ta$): C, 42.34 (42.16); H, 5.39 (5.31); N, 6.61 (6.70) %.

Data for **15**. Yellow powder. Yield: 2.52 g (99 %). ^{1}H NMR (CD_2Cl_2, 400.2 MHz, 298 K): δ 9.34 (1H, d, ^3J = 5.7 Hz, di-^{t}Bu-bipy-C1$_a$), 9.14 (1H, d, ^3J = 5.9 Hz, di-^{t}Bu-bipy-C1$_b$), 8.22 (1H, d, ^3J = 1.8 Hz, di-^{t}Bu-bipy-C4$_b$), 8.19 (1H, d, ^3J = 1.5 Hz, di-^{t}Bu-bipy-C4$_a$), 7.68 (1H, dd, ^3J = 5.7, 1.8 Hz, di-^{t}Bu-bipy-C2$_a$), 7.65 (1H, dd, ^3J = 5.9, 1.9 Hz, di-^{t}Bu-bipy-C2$_b$), 1.53 (9H, s, NCMe$_3$), 1.46 (18H, overlapping 2 × s, di-^{t}Bu-bipy$_{a,b}$). ^{13}C{^{1}H} NMR (CD_2Cl_2, 100.6 MHz, 298 K): δ 166.39 (*i*-di-^{t}Bu-bipy-C3$_b$), 164.71 (*i*-di-^{t}Bu-bipy-C3$_a$), 153.88 (di-^{t}Bu-bipy-C1$_b$), 151.77 (*i*-di-^{t}Bu-bipy-C5$_a$), 151.46 (*i*-di-^{t}Bu-bipy-C5$_b$), 149.39 (di-^{t}Bu-bipy-C1$_a$), 123.95 (di-^{t}Bu-bipy-C2$_a$), 123.69 (di-^{t}Bu-bipy-C2$_b$), 119.56 (di-^{t}Bu-bipy-C4$_b$), 119.40 (di-^{t}Bu-bipy-C4$_a$), 69.94 (*i*-NCMe$_3$), 35.84 (*i*-di-^{t}Bu-bipy$_b$), 35.54 (*i*-di-^{t}Bu-bipy$_a$), 30.09 (di-^{t}Bu-bipy$_b$), 29.95 (di-^{t}Bu-bipy$_a$), 29.74 (NCMe$_3$). Note: subscripts "a" and "b" refer to inequivalent di- *tert*-butyl-bipy rings environments. IR (NaCl plates, Nujol mull, cm^{-1}): 1615 (s), 1545 (m), 1410 (s), 1364 (s), 1304 (w), 1292 (w), 1242 (s), 1216 (m), 1202 (w), 1122 (w), 1030 (m), 1020 (m), 928 (w), 900 (m), 891 (m), 858 (m), 849 (m), 748 (w), 740 (w), 697 (s), 676 (m), 605 (s), 545 (w). EI-MS: *m*/*z* = 253 [*di-tert-butyl-bipy*]$^+$ (100 %). A satisfactory elemental analysis of **15** could not be obtained.

Data for **16**. Light-green powder. Yield: 2.13 g (83 %). ^{1}H NMR (CD_2Cl_2, 400.2 MHz, 298 K): δ 9.49 (1H, d, ^3J = 5.8 Hz, di-^{t}Bu-bipy-C1$_a$), 8.88 (1H, d, ^3J = 6.0 Hz, di-^{t}Bu-bipy-C1$_b$), 8.18 (2H, overlapping 2 × d, di-^{t}Bu-bipy-C4$_{b,a}$), 7.62 (1H, dd, ^3J = 5.8, 1.8 Hz, di-^{t}Bu-bipy-C2$_a$), 7.57 (1H, dd, ^3J = 6.0, 2.0 Hz, di-^{t}Bu-bipy-C2$_b$), 1.73 (9H, s, NCMe$_3$), 1.46 (18H, overlapping 2 × s, di-^{t}Bu-bipy$_{b,a}$). ^{13}C{^{1}H} NMR (CD_2Cl_2, 100.6 MHz, 298 K): δ 165.37 (*i*-di-^{t}Bu-bipy-C3$_b$), 163.89 (*i*-di-^{t}Bu-bipy-C3$_a$), 152.83 (di-^{t}Bu-bipy-C1$_b$), 151.30 (*i*-di-^{t}Bu-bipy-C5$_b$), 150.86 (*i*-di-^{t}Bu-bipy-C5$_a$), 148.47 (di-^{t}Bu-bipy-C1$_a$), 123.58 (di-^{t}Bu-bipy-C2$_b$), 123.51 (di-^{t}Bu-bipy-C2$_a$), 119.17 (di-^{t}Bu-bipy-C4$_b$), 119.13 (di-^{t}Bu-bipy-C4$_a$), 84.32 (*i*-NCMe$_3$), 35.73 (*i*-di-^{t}Bu-bipy$_b$), 35.40 (*i*-di-^{t}Bu-bipy$_a$), 30.14 (di-^{t}Bu-bipy$_b$), 30.02 (di-^{t}Bu-bipy$_a$), 28.79 (NCMe$_3$). Note: subscripts "a" and "b" refer to inequivalent di- *tert*-butyl-bipy rings environments. IR (NaCl plates, Nujol mull, cm^{-1}): 1614 (m), 1546 (w), 1409 (w), 1302 (w), 1218 (w), 1203 (w), 1155 (w), 1019 (w), 900 (w), 888 (w), 858 (w), 844 (w), 797 (m), 700 (m), 675 (w), 605 (m). EI-MS: *m*/*z* = 390

[*V(N^{t}Bu)(di-tert-butyl-bipy*]$^+$ (0.5 %), 253 [*di-tert-butyl-bipy*]$^+$ (100 %). A satisfactory elemental analysis of **16** could not be obtained.

Ta(NN$_2^{Me}$)(N^{t}Bu)(py)$_2$ (17). A solution of **1.41** (1.5 g, 2.903 mmol) and **1** (0.758 g, 2.903 mmol) in benzene (50 mL) was stirred at RT for 2 h, giving a colour change from greenish yellow to dark brown. The solution was filtered away and concentrated to ~10 mL, then pentane was added (20 mL) forming a dark solid. The solution was filtered away and the solid dried *in vacuo* to yield **17** as a dark-brown powder. Diffraction-quality crystals were grown from a saturated C_6D_6 solution at RT. Yield: 1.3 g (71 %).

^{1}H NMR (C_6D_6, 499.9 MHz, 298 K): δ 8.95 (4H, dd, ^3J = 6.4, 1.5 Hz, *o*-py), 7.56 (2H, dd, ^3J = 7.9, 1.3 Hz, ArH-C2), 6.82 (2H, td, ^3J = 7.6, 1.5 Hz, ArH-C3), 6.74 (2H, td, ^3J = 7.5, 1.3 Hz, ArH-C4), 6.52 (2H, tt, ^3J = 7.8, 1.6 Hz, *p*-py), 6.36 (2H, dd, ^3J = 7.7, 1.5 Hz, ArH-C5), 6.29 (4H, td, ^3J = 6.5, 1.3 Hz, *m*-py), 4.03 (6H, s, NMe), 1.29 (9H, s, NCMe$_3$). ^{13}C{^{1}H} NMR (C_6D_6, 125.7 MHz, 298 K): δ 154.46 (*i*-Ar-C6), 149.78 (*o*-py), 145.53 (*i*-Ar-C1), 137.44 (*p*-py), 124.25 (*m*-py), 120.20 (Ar-C3), 117.86 (Ar-C4), 112.67 (Ar-C2), 108.74 (Ar-C5), 62.91 (*i*-NCMe$_3$), 44.43 (NMe), 33.62 (NC<u>Me$_3$</u>). IR (NaCl plates, Nujol mull, cm^{-1}): 3382 (w), 1602 (w), 1548 (w), 1377 (m), 1351 (m), 1209 (w), 1162 (w), 1105 (w), 1052 (m), 1031 (m), 851 (m), 723 (s), 691 (w), 623 (w). A satisfactory elemental analysis of **17** could not be obtained.

Ta(NN$_2^{iPr}$)(N^{t}Bu)(py)$_2$ (18). To a solution of **1.41** (3.0 g, 5.806 mmol) in toluene (40 mL) was added dropwise a solution of **2** (1.749 g, 5.806 mmol) in toluene (10mL) at -30 ˚C, giving a colour change from greenish yellow to dark green. The solution was slowly warmed up to RT and stirred for 3 h, after which time it was filtered away and concentrated to 10 mL, then pentane was added (20 mL) forming a dark solid. The solution was filtered away and the solid dried *in vacuo* to yield **18** as a dark-green microcrystalline powder. Yield: 1.5 g (38 %).

^{1}H NMR (C_6D_6, 499.9 MHz, 298 K): δ 9.25 (4H, d, ^3J = 5.0 Hz, *o*-py), 7.65 (2H, dd, ^3J = 7.8, 1.2 Hz, ArH-C2), 6.79 (2H, td, ^3J = 7.7, 1.3 Hz, ArH-C3), 6.65 (2H, t, ^3J = 7.6 Hz, ArH-C4), 6.57 (2H, t, ^3J = 7.6 Hz, *p*-py), 6.49 (2H, d, ^3J = 7.7 Hz, ArH-C5), 6.33 (4H, t, ^3J = 7.1 Hz, *m*-py), 1.44 (9H, s, NCMe$_3$), 1.41 (12H, d, ^3J = 6.9 Hz, NCH<u>Me$_2$</u>). ^{13}C{^{1}H} NMR (C_6D_6, 125.7 MHz, 298 K): δ 151.96 (*o*-py), 144.96 (overlapping *i*-Ar-C1 and *i*-Ar-C6), 137.71 (*p*-py), 124.03 (*m*-py), 119.30 (Ar-C3), 118.04 (Ar-C4), 112.95 (Ar-C5), 63.52 (*i*-NCMe$_3$), 34.36 (NC<u>Me$_3$</u>), 22.97 (NCH<u>Me$_2$</u>). The N<u>CH</u>Me$_2$ resonance was not

observed neither by ^{1}H or ^{13}C. IR (NaCl plates, Nujol mull, cm^{-1}): 3062 (w), 1653 (w), 1603 (s), 1571 (w), 1549 (m), 1350 (s), 1283 (s), 1258 (s), 1249 (m), 1231 (s), 1208 (s), 1190 (w), 1147 (w), 1129 (w), 1067 (m), 1058 (m), 1043 (m), 1012 (m), 977 (s), 890 (w), 866 (w), 811 (w), 757 (w), 723 (s), 692 (m), 634 (m), 560 (w). EI-MS: *m*/*z* = 283 $[H_3NN_2^{iPr}]^+$ (18 %), 58 $[N^iPr]^+$ (100 %). A satisfactory elemental analysis of **18** could not be obtained.

Ta(NN$_2^{SiMe3}$)(N^{t}Bu)(py)$_2$ (19). A solution of **1.41** (0.50 g, 0.967 mmol) and **1.7** (0.349 g, 0.967 mmol) in benzene (30 mL) was stirred at 60 ˚C for 24 h, after which time the solution was filtered away and concentrated to ~10 mL, then pentane was added (20 mL) forming a green solid. The solution was filtered away and the solid dried *in vacuo* to yield **19** as a green powder. Yield: 0.510 g (70 %).

^{1}H NMR (C_6D_6, 499.9 MHz, 298 K): δ 9.11 (4H, d, ^{3}J = 5.0 Hz, *o*-py), 7.36 (2H, d, ^{3}J = 7.7 Hz, Ar<u>H</u>-C2), 6.76 (2H, td, ^{3}J = 7.8, 1.8 Hz, Ar<u>H</u>-C3), 6.61 (2H, t, ^{3}J = 7.5 Hz, *p*-py), 6.55-6.48 (4H, overlapping 2 × m, Ar<u>H</u>-C4 and Ar<u>H</u>-C5), 6.41 (4H, t, ^{3}J = 6.7 Hz, *m*-py), 1.53 (9H, s, $NCMe_3$), 0.46 (18H, s, $NSiMe_3$). $^{13}C\{^{1}H\}$ NMR (C_6D_6, 125.7 MHz, 298 K): δ 152.38 (*o*-py), 151.95 (*i*-Ar-C6), 145.60 (*i*-Ar-C1), 137.73 (*p*-py), 123.55 (*m*-py), 120.29 (Ar-C3), 118.80 (Ar-C4), 116.39 (Ar-C5), 111.55 (Ar-C2), 63.69 (*i*-$NCMe_3$), 34.76 ($NC\underline{Me_3}$), 4.95 ($NSiMe_3$). IR (NaCl plates, Nujol mull, cm^{-1}): 1607 (w), 1551 (w), 1219 (w), 1205 (w), 925 (m), 870 (m), 799 (s), 729 (m). EI-MS: *m*/*z* = 343 $[H_3NN_2^{SiMe3}]^+$ (1 %), 520 $[Ta(NN_2^{SiMe3})]^+$ (3 %), 73 $[SiMe_3]^+$ (100 %). Anal. found (calcd. for $C_{32}H_{45}N_6Si_2Ta$): C, 50.46 (51.19); H, 5.83 (6.04); N, 11.33 (11.19)%.

Nb(NN$_2^{Me}$)(N^{t}Bu)(py)$_2$ (20). A solution of **1.42** (1.5 g, 3.50 mmol) and **1** (0.914 g, 3.50 mmol) in benzene (30 mL) was stirred at RT for 2 h, giving a colour change from greenish yellow to dark brown. The solution was filtered away and volatiles removed under reduce pressure. The resulting waxy solid can be either lyophilised or triturated in pentane to afford **20** as a black microcrystalline powder. Yield: 2.0 g (96 %).

^{1}H NMR (C_6D_6, 499.9 MHz, 298 K): δ 8.99 (4H, br. s, *o*-py), 7.42 (2H, dd, ^{3}J = 7.8, 0.9 Hz, Ar<u>H</u>-C2), 6.77 (2H, td, ^{3}J = 7.7, 1.4 Hz, Ar<u>H</u>-C3), 6.66 (2H, td, ^{3}J = 7.6, 1.4 Hz, Ar<u>H</u>-C4), 6.61 (2H, br. s, *p*-py), 6.38 (4H, br. s, *m*-py), 6.27 (2H, dd, ^{3}J = 7.7, 1.4 Hz, Ar<u>H</u>-C5), 3.88 (6H, s, NMe), 1.23 (9H, s, $NCMe_3$). $^{13}C\{^{1}H\}$ NMR (C_6D_6, 125.7 MHz, 298 K): δ 155.13 (*i*-Ar-C6), 150.24 (*o*-py), 146.0 (*i*-Ar-C1), 137.64 (*p*-py), 124.36 (*m*-py), 121.10 (Ar-C3), 117.85 (Ar-C4), 112.41 (Ar-C2), 107.66 (Ar-C5), 63.19 (*i*-$NCMe_3$),

45.27 (NMe), 32.62 (NC<u>Me</u>$_3$). IR (NaCl plates, Nujol mull, cm^{-1}): 1599 (w), 1565 (w), 1377 (m), 1347 (m), 1278 (m), 1237 (m), 1209 (m), 1178 (m), 1158 (m), 1110 (w), 1048 (m), 1030 (m), 847 (w), 723 (s), 692 (m), 627 (m). A satisfactory elemental analysis of **20** could not be obtained.

Nb(NN$_2^{iPr}$)(N^{t}Bu)(py)$_2$ (21). A solution of **1.42** (2.0 g, 4.666 mmol) and **2** (1.405 g, 5.806 mmol) in pentane (60 mL) was stirred at RT for 16 h, giving a colour change from greenish yellow to dark brown. After this time the solution was filtered away and concentrated to 10 mL, then pentane was added (20 mL) forming a solid. The solution was filtered away and volatiles removed under reduced pressure giving **21** as a green powder. Yield: 2.04 g (72 %).

^{1}H NMR (C_6D_6, 499.9 MHz, 298 K): δ 9.27 (4H, br. s, *o*-py), 7.52 (2H, dd, ^3J = 7.9, 1.2 Hz, Ar<u>H</u>-C2), 6.74 (2H, td, ^3J = 7.8, 1.0 Hz, Ar<u>H</u>-C3), 6.64 (2H, m, *p*-py), 6.57 (2H, t, ^3J = 7.2 Hz, Ar<u>H</u>-C4), 6.40 (6H, overlapping 2 × m, *m*-py and Ar<u>H</u>-C5), 1.38 (21 H, overlapping s and d, NCMe$_3$ and NCH<u>Me$_2$</u>), ^{13}C{^{1}H} NMR (C_6D_6, 125.7 MHz, 298 K): δ 152.44 (*i*-Ar-C6), 151.40 (*o*-py), 144.65 (*i*-Ar-C1), 136.99 (*p*-py), 123.29 (*m*-py), 119.39 (Ar-C3), 117.32 (Ar-C4), 111.87 (Ar-C2), 111.42 (Ar-C5), 62.88 (*i*-NCMe$_3$), 32.69 (NC<u>Me$_3$</u>), 22.40 (NCH<u>Me$_2$</u>). The N<u>CH</u>Me$_2$ resonance was not observed either by ^{1}H or ^{13}C. IR (NaCl plates, Nujol mull, cm^{-1}): 1601 (m), 1562 (w), 1545 (w), 1346 (m), 1283 (m), 1226 (m), 1207 (m), 1127 (w), 1067 (w), 1057 (w), 1040 (m), 1011 (w), 973 (s), 890 (w), 861 (w), 806 (w), 754 (w), 723 (s), 692 (m), 631 (m). EI-MS: *m*/*z* = 444 [*Nb(NN$_2^{iPr}$)(N^{t}Bu)*]$^+$ (2 %), 283 [*H$_3$NN$_2^{iPr}$)*]$^+$ (81 %), 58 [*NiPr*] (100 %). A satisfactory elemental analysis of **21** could not be obtained.

Nb(NN$_2^{SiMe3}$)(N^{t}Bu)(py)$_2$ (22). A solution of **1.42** (0.70 g, 1.633 mmol) and **1.7** (0.590 g, 1.633 mmol) in toluene (20 mL) was stirred at 60 ˚C for 16 h, after which time the solution was filtered away and concentrated to ~10 mL, then pentane was added (20 mL) forming a brown solid. The solution was filtered away and the solid dried *in vacuo* to yield **22** as a dark brown powder. Yield: 0.467 g (28 %).

^{1}H NMR (C_6D_6, 499.9 MHz, 298 K): δ 9.07 (4H, br. d, ^3J = 4.9 Hz, *o*-py), 7.29 (2H, dd, ^3J = 7.8, 1.2 Hz, Ar<u>H</u>-C2), 6.72 (4H, td, ^3J = 7.8, 1.6 Hz, Ar<u>H</u>-C3 and Ar<u>H</u>-C4), 6.51-6.44 (overlapping 3 × m, *p*-py, Ar<u>H</u>-C5 and *m*-py), 1.44 (9H, s, NCMe$_3$), 0.46 (18H, s, NSiMe$_3$). ^{13}C{^{1}H} NMR (C_6D_6, 125.7 MHz, 298 K): δ 153.27 (*i*-Ar-C6), 151.63 (*o*-py), 145.90 (*i*-Ar-C1), 137.38 (*p*-py), 123.63 (*m*-py), 123.43 (Ar-C4), 120.75 (Ar-C3), 117.15

(Ar-C5), 111.42 (Ar-C2), 63.74 (*i*-$NCMe_3$), 33.28 ($NC\underline{Me}_3$), 4.81 ($NSiMe_3$). IR (NaCl plates, Nujol mull, cm^{-1}): 1604 (m), 1548 (m), 1362 (s), 1277 (w), 1237 (m), 1215 (s), 1181 (m), 1153 (w), 1106 (m), 1093 (w), 1071 (w), 1042 (m), 1013 (w), 961 (w), 924 (s), 900 (w), 963 (s), 779 (m), 728 (s), 693 (m), 635 (m), 5847 (m). EI-MS: *m*/*z* = 343 $[H_3NN_2^{SiMe3}]^+$ (0.03 %), 73 $[SiMe_3]^+$ (42 %). A satisfactory elemental analysis of **22** could not be obtained.

V(NN_2^{iPr})(N^tBu)(py) (23). A solution of **1.45** (1.0 g, 2.584 mmol) and **2** (0.779 g, 2.584 mmol) in benzene (30 mL) was stirred at RT for 2 h, giving a colour change from greenish yellow to dark red. After this time the solution was filtered away and volatiles removed under reduced pressure. The resulting dark oil was lyophilised to afford **23** as a black powder. Yield: 0.530 g (43 %).

^{1}H NMR (C_6D_6, 400.2 MHz, 298 K): δ 8.65 (2H, br. s, *o*-py), 7.41 (2H, d, ^3J = 7.8 Hz, Ar$\underline{H}$-C2), 6.67 (2H, t, ^3J = 7.3 Hz, Ar$\underline{H}$-C3), 6.58 (3H, br. t, overlapping *p*-py and Ar$\underline{H}$-C4), 6.35 (2H, d, ^3J = 7.9 Hz, Ar$\underline{H}$-C5), 6.25 (2H, br. s, *m*-py), 5.51 (2H, br, sept, ^3J = 6.7 Hz, N$\underline{CH}Me_2$), 1.70 (9H, s, $NCMe_3$), 1.18 (12H, d, ^3J = 6.6 Hz, NCH$\underline{Me}_2$). $^{13}C\{^1H\}$ NMR (C_6D_6, 100.6 MHz, 298 K): δ 154.34 (*i*-Ar-C6), 145.77 (*i*-Ar-C1), 121.41 (Ar-C3), 119.78 (Ar-C4), 113.57 (Ar-C2), 111.35 (Ar-C5), 61.64 (N$\underline{CH}Me_2$), 33.04 ($NC\underline{Me}_3$), 21.09 (NCH$\underline{Me}_2$). The pyridine resonance was observed by ^{1}H, which suggests that just one pyridine is coordinated. However, the correlation ^{1}H-^{1}H or the ^{13}C signals for the pyridine were not observed. IR (NaCl plates, Nujol mull, cm^{-1}): 1599 (w), 1566 (w), 1293 (m), 1293 (m), 1210 (m), 1150 (m), 1128 (w), 975 (m), 904 (w), 846 (w), 726 (s), 692 (m), 642 (w). EI-MS: *m*/*z* = 283 $[H_3NN_2^{iPr})]^+$ (57 %), 58 $[NiPr]^+$ (100 %). A satisfactory elemental analysis of **23** could not be obtained.

General procedure for M(NN_2^{SiMe3})(N^tBu)(bipy) (M = Ta (24) or Nb (25)). Ta(NN_2^{SiMe3})(N^tBu)(bipy) (24). A solution of **1.43** (0.30 g, 0.582 mmol) and **1.7** in benzene (20 mL) was stirred at RT for 16 h, after which time the solvent was removed under reduced pressure. The product was extracted in DCM (3 × 10 mL) and the solution was concentrated to ~5 mL, then pentane was added (15 mL) forming a brown solid. The solution was filtered away and the solid dried *in vacuo* to yield **24** as a brown powder. Yield: 0.130 g (30 %). In the solid state the imido complex has a bidentate bipyridyl ligand but in solution an equilibrium between monodentate and bidentate bipyridyl

complexes is observed and analysed by 1H NMR in a VT and ROESY NMR experiments at temperatures between 298 and 213K (Chapter Three, Section 3.4.1).

Data for **24**. NMR data for **24** monodentate (**24a**): ^{1}H NMR ($CDCl_3$, 499.9 MHz, 298 K): δ 10.43 (1H, d, ^{3}J = 4.7 Hz, $bipy_{coord}$H-C1), 8.20 (1H, t, ^{3}J = 7.8 Hz, $bipy_{coord}$H-C3), 8.09 (2H, overlapping 2 × m, $bipy_{coord}$H-C4 and $bipy_{non\text{-}coord}$H-C4), 7.86 (1H, d, ^{3}J = 7.9 Hz, $bipy_{non\text{-}coord}$H-C1), 7.75 (1H, td, ^{3}J = 7.7, 1.3 Hz, $bipy_{non\text{-}coord}$H-C2), 7.66 (1H, m, $bipy_{coord}$H-C2), 7.26 (overlapping 2H for ArH-C5 and $CHCl_3$ signal), 6.99 (1H, dd, ^{3}J = 7.7, 5.4 Hz, $bipy_{non\text{-}coord}$H-C3), 6.59 (2H, t, ^{3}J = 7.4 Hz, ArH-C4), 6.51 (2H, t, ^{3}J = 7.5 Hz, ArH-C3), 6.40 (2H, dd, ^{3}J = 7.7, 0.9 Hz, ArH-C2), 1.25 (9H, s, $NCMe_3$), -0.14 (18H, s, $NSiMe_3$). $^{13}C\{^{1}H\}$ NMR ($CDCl_3$, 125.7 MHz, 298 K): δ 161.36 ($bipy_{coord}$-C1), 154.39 (*i*-$bipy_{coord}$), 151.21 (*i*-Ar-C1), 150.60 ($bipy_{non\text{-}coord}$-C4), 148.22 (*i*-$bipy_{non\text{-}coord}$), 144.10 (*i*-Ar-C6), 141.10 ($bipy_{coord}$-C3), 138.83 ($bipy_{non\text{-}coord}$-C2), 126.18 ($bipy_{non\text{-}coord}$-C3), 125.00 ($bipy_{coord}$-C2), 122.24 ($bipy_{coord}$-C4), 119.80 ($bipy_{non\text{-}coord}$-C1), 118.97 (Ar-C3), 117.53 (Ar-C2), 116.21 (Ar-C4), 113.48 (Ar-C5), 65.58 (*i*-$NCMe_3$), 34.41 ($NCMe_3$), 2.54 ($NSiMe_3$). Note: subscripts "coord" and "non-coord" refer to the coordinated and the non-coordinated bipy ring, respectively. IR (NaCl plates, Nujol mull, cm^{-1}): 1601 (w), 1560 (w), 1354 (w), 1280 (w), 1245 (m), 1211 (s), 1154 (w), 1116 (m), 1057 (w), 912 (s), 824 (s), 797 (m), 766 (w). EI-MS: *m*/*z* = 748 $[M]^+$ (15 %), 592 $[Ta(NNN^{SiMe})(NtBu)]^+$ (20 %), 343 $[H_3NN_2^{iSiMe3})]^+$ (4 %), 156 $[bipy]^+$ (100 %), 75 $[SiMe_3]^+$ (75 %). A satisfactory elemental analysis of **24** could not be obtained.

Data for **25**. Stirring at RT for 3 h, brown powder. Diffraction-quality crystals were grown from a saturated C_6D_6 solution at RT. Yield: 0.127 g (26 %). NMR data for **25** monodentate (**25a**): ^{1}H NMR ($CDCl_3$, 499.9 MHz, 298 K): δ 10.20 (1H, d, ^{3}J = 5.3 Hz, $bipy_{coord}$H-C1), 8.13 (1H, td, ^{3}J = 7.9, 1.6 Hz, $bipy_{coord}$H-C3), 8.07 (2H, overlapping 2 × m, $bipy_{coord}$H-C4 and $bipy_{non\text{-}coord}$H-C4), 7.84 (1H, d, ^{3}J = 8.0 Hz, $bipy_{non\text{-}coord}$H-C1), 7.70 (1H, td, ^{3}J = 7.8, 1.6 Hz, $bipy_{non\text{-}coord}$H-C2), 7.63 (1H, m, $bipy_{coord}$H-C2), 7.22 (2H, d, ^{3}J = 7.6 Hz, ArH-C5), 6.96 (1H, m, $bipy_{non\text{-}coord}$H-C3), 6.58 (2H, t, ^{3}J = 7.2 Hz, ArH-C4), 6.53 (2H, t, ^{3}J = 6.9 Hz, ArH-C3), 6.41 (2H, d, ^{3}J = 8.6 Hz, ArH-C2), 1.30 (9H, s, $NCMe_3$), -0.13 (18H, s, $NSiMe_3$). $^{13}C\{^{1}H\}$ NMR ($CDCl_3$, 125.7 MHz, 298 K): δ 159.55 ($bipy_{coord}$-C1), 153.87 (*i*-$bipy_{coord}$-C5), 152.51 (*i*-Ar-C1), 150.76 ($bipy_{non\text{-}coord}$-C4), 148.03 (*i*-$bipy_{non\text{-}coord}$-C5), 144.51 (*i*-Ar-C6), 140.68 ($bipy_{coord}$-C3), 138.69 ($bipy_{non\text{-}coord}$-C2), 125.80 ($bipy_{non\text{-}coord}$-C3), 124.67 ($bipy_{coord}$-C2), 122.02 ($bipy_{coord}$-C4), 119.60 (Ar-C3), 119.43 ($bipy_{non\text{-}coord}$-C1), 116.78 (Ar-C2), 116.17 (Ar-C4), 113.13 (Ar-C5), 67.54 (*i*-$NCMe_3$),

32.81 (NC<u>Me</u>$_3$), 2.40 (NSi<u>Me</u>$_3$). Note: subscripts "coord" and "non-coord" refer to the coordinated and the non-coordinated bipy ring, respectively.

NMR data for **25** bidentate (**25b**): ^{1}H NMR ($CDCl_3$, 400.2 MHz, 213 K): δ 8.85 (2H, d, ^3J = 5.0 Hz, bipy<u>H</u>-C1), 7.54 (2H, d, ^3J = 7.8 Hz, bipy<u>H</u>-C3), 7.19 (2H, d, ^3J = 7.5 Hz, Ar<u>H</u>-C2), 6.80-6.77 (6H, overlapping 3 × m, bipy<u>H</u>-C2, Ar<u>H</u>-C3 and Ar<u>H</u>-C4), 6.07 (2H, br., Ar<u>H</u>-C5), 0.65 (9H, s, NC<u>Me</u>$_3$), 0.55 (18H, s, NSi<u>Me</u>$_3$). ^{13}C{^{1}H} NMR ($CDCl_3$, 100.6 MHz, 213 K): δ 149.41 (bipy-C1), 145.94 (*i*-Ar-C1), 144.98 (*i*-Ar-C6), 143.22 (*i*-bipy-C5), 135.58 (Ar-C5), 122.31 (bipy-C2), 118.39 (Ar-C4), 115.63 (Ar-C2), 113.25 (Ar-C3), 112.89 (bipy-C3), 64.34 (*i*-NCMe$_3$), 34.52 (NC<u>Me</u>$_3$), 9.32 (NSi<u>Me</u>$_3$). ^{1}H and ^{13}C signals for bipy-C4 could not be identified for **24** bidentate. IR (NaCl plates, Nujol mull, cm^{-1}): 1601 (m), 1571 (w), 1553 (m), 1357 (s), 1310 (w), 1282 (m), 1245 (w), 1175 (w), 1155 (w), 1118 (m), 1091 (m), 1055 (m), 1020 (m), 924 (s), 910 (s), 862 (s), 797 (m), 756 (m), 725 (m), 669 (w), 651 (w), 631 (w), 595 (w), 579 (w), 563 (w). EI-MS: *m*/*z* = 660 $[M]^+$ (0.3 %), 156 $[bipy]^+$ (100 %), 75 $[SiMe_3]^+$ (62 %). A satisfactory elemental analysis of **25** could not be obtained.

General procedure for M(NN$_2^R$)(N^{t}Bu)(di-^{t}Bu-bipy) (M = Ta, R = Me (27) or SiMe$_3$ (28); M = Nb, R = Me (29) or SiMe$_3$ (30)). Ta(NN$_2^{Me}$)(N^{t}Bu)(di-^{t}Bu-bipy) (27). A solution of **14** (0.50 g, 0.797 mmol) and **1** in benzene (20 mL) was stirred at RT for 3 h, after which time the solution was removed under reduced pressure. The product was extracted in dichloromethane (4 × 5 mL) and the solvent was removed under reduced pressure. The solid was washed with a mixture of pentane/benzene (3 × 10 mL, 3:1 ratio) and dried *in vacuo* to afford **27** as a dark-brown powder. Yield: 0.264 g (44%).

Data for **27** bidentate. ^{1}H NMR ($CDCl_3$, 499.9 MHz, 298 K): δ 8.33 (2H, d, ^3J = 6.0 Hz, bipy<u>H</u>-C1), 8.00 (2H, d, ^3J = 1.8 Hz, bipy<u>H</u>-C4), 7.47 (2H, dd, ^3J = 6.0, 1.9 Hz, bipy<u>H</u>-C2), 7.21 (2H, dd, ^3J = 7.8, 1.04 Hz, Ar<u>H</u>-C5), 6.49-6.73 (4H, overlapping 2 × m, Ar<u>H</u>-C3 and Ar<u>H</u>-C2), 6.62 (2H, td, Ar<u>H</u>-C4), 4.34 (6H, s, NMe), 1.36 (18H, s, CCMe$_3$), 1.06 (9H, s, NCMe$_3$). ^{13}C{^{1}H} NMR ($CDCl_3$, 125.7 MHz, 298 K): δ 164.95 (*i*-bipy-C3), 152.46 (*i*-bipy-C5), 152.35 (*i*-Ar-C1), 151.45 (bipy-C1), 145.66 (*i*-Ar-C5), 123.85 (bipy-C2), 118.37 (bipy-C4), 117.47 (Ar-C3), 116.70 (Ar-C4), 115.87 (Ar-C5), 108.64 (Ar-C2), 61.45 (*i*-N<u>C</u>Me$_3$), 47.90 (NMe), 35.46 (*i*-C<u>C</u>Me$_3$), 33.37 (NC<u>Me</u>$_3$), 29.92 (CC<u>Me</u>$_3$).

Data for **28** monodentate. Yield: 0.042 g (44%). ^{1}H NMR ($CDCl_3$, 499.9 MHz, 298 K): δ 10.19 (1H, d, ^3J = 6.0 Hz, bipy$_{coord}$<u>H</u>-C1), 8.04 (1H, d, ^3J = 1.8 Hz, bipy$_{coord}$<u>H</u>-C4), 7.80

(2H, overlapping 2 × m, bipy$_{\text{non-coord}}$H-C1 and bipy$_{\text{non-coord}}$H-C4), 7.68 (1H, dd, ^{3}J = 6.0, 1.9 Hz, bipy$_{\text{coord}}$H-C2), 7.13 (2H, dd, ^{3}J = 7.8, 1.5 Hz, ArH-C5), 6.91 (1H, dd, ^{3}J = 5.8, 1.6 Hz, bipy$_{\text{non-coord}}$H-C2), 6.53 (2H, td, ^{3}J = 7.5, 1.4 Hz, ArH-C4), 6.44 (2H, td, ^{3}J = 7.6, 1.5 Hz, ArH-C3), 6.34 (2H, dd, ^{3}J = 7.8, 1.3 Hz, ArH-C2), 1.48 (9H, s, CCMe$_{3\text{coord}}$), 1.27 (9H, s, NCMe$_3$), 1.25 (9H, s, CCMe$_{3\text{non-coord}}$), -0.13 (9H, s, NSiMe$_3$). ^{13}C{^{1}H} NMR (CDCl$_3$, 125.7 MHz, 298 K): δ 167.02 (*i*-bipy$_{\text{coord}}$-C3), 164.12 (*i*-bipy$_{\text{non-coord}}$-C3), 160.28 (bipy$_{\text{coord}}$-C1), 154.60 (*i*-bipy$_{\text{non-coord}}$-C5), 151.11 (*i*-Ar-C1), 149.89 (bipy$_{\text{non-coord}}$-C1), 148.99 (*i*- bipy$_{\text{coord}}$-C5), 144.03 (*i*-Ar-C6), 122.95 (bipy$_{\text{non-coord}}$-C2), 122.25 (bipy$_{\text{coord}}$-C2), 119.03 (bipy$_{\text{coord}}$-C4), 118.63 (Ar-C3), 117.25 (Ar-C2), 116.64 (bipy$_{\text{non-coord}}$-C4), 115.82 (Ar-C4), 112.90 (Ar-C5), 65.17 (*i*-NCMe$_3$), 35.94 (*i*-CCMe$_{3\text{coord}}$), 35.25 (*i*-CCMe$_{3\text{non-coord}}$), 34.07 (NCMe$_3$), 29.99 (overlapping CCMe$_{3\text{coord}}$ and CCMe$_{3\text{non-coord}}$), 1.96 (NSiMe$_3$). Note: subscripts "coord" and "non-coord" refer to the coordinated and the non-coordinated ^{t}Bu-bipy ring, respectively.

Data for **29** bidentate. Yield: 0.086 g (47%). ^{1}H NMR (CD_2Cl_2, 499.9 MHz, 298 K): δ 8.31 (2H, d, ^{3}J = 6.0 Hz, bipyH-C1), 7.98 (2H, d, ^{3}J = 1.8 Hz, bipyH-C4), 7.46 (2H, dd, ^{3}J = 6.0, 1.9 Hz, bipyH-C2), 7.33 (2H, dd, ^{3}J = 7.8, 0.9 Hz, ArH-C5), 6.84-6.79 (4H, overlapping 2 × m, ArH-C3 and ArH-C2), 6.68 (2H, ddd, ArH-C4), 4.31 (6H, s, NMe), 1.36 (18H, s, CCMe$_3$), 1.12 (9H, s, NCMe$_3$). ^{13}C{^{1}H} NMR (CDCl$_3$, 125.7 MHz, 298 K): δ 164.79 (*i*-bipy-C3), 152.45 (*i*-bipy-C5), 152.19 (*i*-Ar-C1), 151.48 (bipy-C1), 144.84 (*i*-Ar-C5), 123.58 (bipy-C2), 118.07 (bipy-C4), 117.08 (Ar-C3), 116.66 (Ar-C4), 115.02 (Ar-C5), 107.52 (Ar-C2), 62.27 (*i*-NCMe$_3$), 48.37 (NMe), 35.37 (*i*-CCMe$_3$), 32.06 (NCMe$_3$), 29.95 (CCMe$_3$). IR (NaCl plates, Nujol mull, cm^{-1}): 1607 (m), 1544 (w), 1377 (m), 1280 (m), 1244 (m), 1157 (s), 1111 (w), 1052 (m), 1028 (m), 895 (w), 848 (s), 813 (m), 675 (w). EI-MS: *m*/*z* = 227 $[H_3NN_2^{Me})]^+$ (23 %), 58 $[^{t}Bu]^+$ (36 %). A satisfactory elemental analysis of **29** could not be obtained.

Data for **30** monodentate. Yield: 0.091 g (42%). ^{1}H NMR ($CDCl_3$, 499.9 MHz, 298 K): δ 9.97 (1H, d, ^{3}J = 5.9 Hz, bipy$_{\text{coord}}$H-C1), 8.01 (1H, d, ^{3}J = 1.5 Hz, bipy$_{\text{coord}}$H-C4), 7.80 (1H, d, ^{3}J = 5.6 Hz, bipy$_{\text{non-coord}}$H-C1), 7.77 (1H, br. s, bipy$_{\text{non-coord}}$H-C4), 7.65 (1H, dd, ^{3}J = 5.9, 1.8 Hz, bipy$_{\text{coord}}$H-C2), 7.08 (2H, dd, ^{3}J = 7.8, 1.4 Hz, ArH-C5), 6.89 (1H, dd, ^{3}J = 5.6, 1.6 Hz, bipy$_{\text{non-coord}}$H-C2), 6.51 (2H, m, ArH-C4), 6.45 (2H, td, ^{3}J = 7.7, 1.4 Hz, ArH-C3), 6.35 (2H, dd, ^{3}J = 7.8, 0.8 Hz, ArH-C2), 1.47 (9H, s, CCMe$_{3\text{coord}}$), 1.31 (9H, s, NCMe$_3$), 1.25 (9H, s, CCMe$_{3\text{non-coord}}$), -0.12 (9H, s, NSiMe$_3$). ^{13}C{^{1}H} NMR ($CDCl_3$, 125.7 MHz, 298 K): δ 166.39 (*i*-bipy$_{\text{coord}}$-C3), 163.86 (*i*-bipy$_{\text{non-coord}}$-C3), 158.61

($bipy_{coord}$-C1), 154.07 (*i*-$bipy_{non\text{-}coord}$-C5), 152.29 (*i*-Ar-C1), 150.07 ($bipy_{non\text{-}coord}$-C1), 148.83 (*i*-$bipy_{coord}$-C5), 144.36 (*i*-Ar-C6), 122.59 ($bipy_{non\text{-}coord}$-C2), 121.92 ($bipy_{coord}$-C2), 119.22 ($bipy_{coord}$-C3), 118.82 ($bipy_{coord}$-C4), 116.48 (Ar-C1), 116.28 ($bipy_{non\text{-}coord}$-C4), 115.77 (Ar-C4), 112.46 (Ar-C5), 65.06 (*i*-N<u>C</u>Me_3), 35.75 (*i*-<u>C</u>CMe_{3coord}), 35.14 (*i*-<u>C</u>$CMe_{3non\text{-}coord}$), 32.46 (NC<u>Me</u>$_3$), 30.03 (overlapping CC<u>Me</u>$_{3coord}$ and CC<u>Me</u>$_{3non\text{-}coord}$), 1.81 ($NSiMe_3$). Note: subscripts "coord" and "non-coord" refer to the coordinated and the non-coordinated ^{t}Bu-bipy ring, respectively. IR (NaCl plates, Nujol mull, cm^{-1}): 1614 (w), 1584 (m), 1542 (w), 1408 (w), 1312 (w), 1283 (w), 1257 (w), 1234 (m), 1169 (w), 1150 (w), 1053 (w), 1024 (w), 980 (m), 902 (w), 860 (w), 843 (w), 826 (w), 731 (s), 698 (m), 689 (w), 636 (w), 602 (w).

General procedure for M(NNN^{SiMe3})(N^{t}Bu) (M = Ta (31), Nb (32) or V (33)). Ta(NNN^{SiMe3})(N^{t}Bu) (31). A solution of **1.41** (0.150 g, 0.193 mmol) and **1.9** (0.068 g, 0.193 mmol) in benzene (10 mL) was stirred at RT ˚C for 1 h, after which time the solution was filtered away and volatiles removed under reduced pressure. The resulting light pink oil was lyophilised to afford **31** as a light orange powder. Yield: 0.05 g (44 %).

Data for **31**. ^{1}H NMR (C_6D_6, 499.9 MHz, 298 K): δ 3.51 (6H, s, N<u>C</u>H_2CMe), 1.60 (9H, s, $NCMe_3$), 0.82 (3H, s, NCH_2C<u>Me</u>), 0.29 (27H, s, $NSiMe_3$). $^{13}C\{^1H\}$ NMR (C_6D_6, 101 MHz, 298 K): δ 66.19 (*i*-TaN<u>C</u>Me_3), 58.19 (N<u>C</u>H_2CMe), 36.90 (*i*-NCH_2CMe), 34.98 ($TaNCMe_3$), 28.92 (NCH_2C<u>Me</u>), 1.18 ($NSiMe_3$). EI-MS: *m*/*z* = 582 $[M]^+$ (0.25 %), 567 $[Ta((N^{SiMe3}CH_2)_3C)(N^tBu]^+$ (62 %), 73 $[SiMe_3]^+$ (100 %). A satisfactory elemental analysis of **31** could not be obtained.

Data for **32**. Solution was stirred at RT ˚C for 16 h. Light-yellow oil was lyophilised to afford **32** as a light yellow powder. Yield: 0.06 g (55 %). ^{1}H NMR (C_6D_6, 400.2 MHz, 298 K): δ 3.44 (6H, s, N<u>C</u>H_2CMe), 1.59 (9H, s, $NbNCMe_3$), 0.96 (3H, s, NCH_2C<u>Me</u>), 0.28 (27H, s, $NSiMe_3$). EI-MS: *m*/*z* = 494 $[M]^+$ (0.17 %), 479 $[Nb((N^{SiMe3}CH_2)_3C)(N^tBu]^+$ (14 %), 73 $[SiMe_3]^+$ (100 %). A satisfactory elemental analysis of **32** could not be obtained.

Data for **33**. Solution was stirred at RT ˚C for 3 h. Dark brown waxy solid. Yield: 0.491 g (60 %). ^{1}H NMR (C_6D_6, 400.1 MHz, 298 K): δ 3.55 (6H, s, (N<u>C</u>H_2)$_3$CMe), 1.62 (9H, s, $NCMe_3$), 1.09 (3H, s, $(NCH_2)_3C$<u>Me</u>), 0.30 (27H, s, $NSiMe_3$). $^{13}C\{^1H\}$ NMR (C_6D_6, 101 MHz, 298 K): δ 78.51 (*i*-N<u>C</u>Me_3), 61.68 ((N<u>C</u>H_2)$_3$CMe), 48.62 (*i*-$(NCH_2)_3$<u>C</u>Me), 32.92 ($NCMe_3$), 27.22 ($(NCH_2)_3C$<u>Me</u>), 1.80 ($NSiMe_3$).

General procedure for NMR scale synthesis of M(N_2N^{iPr})(NPh)($py)_2$ (M = Ta (34) or Nb (35)). Ta(N_2N^{iPr})(NPh)($py)_2$ (34). A solution of **18** (0.010 g, 0.014 mmol) in C_6D_6 (0.4 mL) and a solution of PhN_3 (0.0017 g, 0.014 mmol) in C_6D_6 (0.3 mL) were transferred to an NMR tube fitted with a J. Youngs valve, and left at RT for 2 d. After this time, all of **18** had been consumed, giving conversion to **34** and $^tBuN_3$, in addition to an unassigned volatile product.

Data for **34**. ^{1}H NMR (C_6D_6, 499.9 MHz, 298 K): δ 9.23 (4H, d, ^3J = 5.0 Hz, *o*-py), 7.79 (2H, d, ^3J = 8.0 Hz, ArH-C5), 7.46 – 7.38 (4H, overlapping 2 × m, *o*- and *m*-C_6H_5), 6.91 – 6.84 (overlapping 2 × m, *p*-C_6H_5 and ArH-C4), 6.71 (br. d, ^3J = 8.4 Hz, ArH-C3), 6.54 (2H, t, ^3J = 7.6 Hz, *p*-py), 6.39 (2H, d, ^3J = 7.7 Hz, ArH-C2), 6.25 (4H, t, ^3J = 7.7 Hz, *m*-py), 1.3 (12H, d, ^3J = 6.7 Hz, NCHMe_2). $^{13}C\{^1H\}$ NMR (C_6D_6, 125.7 MHz, 298 K): δ 159.49 (*i*-C_6H_5), 153.15 (*i*-Ar-C1), 150.94 (*o*-py), 143.46 (*i*-Ar-C6), 137.66 (*p*-py), 129.10 (*o*-C_6H_5), 126.09 (*m*-C_6H_5), 124.40 (*m*-py), 119.71 (*p*-C_6H_5), 119.46 (Ar-C4), 118.88 (Ar-C3), 118.52 (Ar-C2), 113.02 (Ar-C5), 21.07 (NCHMe_2). Note: ^{1}H or ^{13}C signals for NCHMe_2 were not observed.

Data for **35**. ^{1}H NMR (C_6D_6, 499.9 MHz, 298 K): δ 9.27 (4H, d, ^3J = 4.9 Hz, *o*-py), 7.67 (2H, d, ^3J = 7.7 Hz, ArH-C5), 7.44 (2H, d, ^3J = 7.6 Hz, *o*-C_6H_5), 7.34 (2H, t, ^3J = 7.8 Hz, *m*-C_6H_5), 6.92 (1H, t, ^3J = 7.3 Hz, *p*-C_6H_5), 6.83 (2H, t, ^3J = 7.5 Hz, ArH-C4), 6.63 – 6.61 (4H, overlapping 2 × m, ArH-C3 and *p*-py), 6.33 (4H, t, ^3J = 6.4 Hz, *m*-py), 6.29 (2H, d, ^3J = 7.9 Hz, ArH-C2), 1.3 (12H, d, ^3J = 6.7 Hz, NCHMe_2). $^{13}C\{^1H\}$ NMR (C_6D_6, 125.7 MHz, 298 K): δ 156.65 (*i*-C_6H_5), 153.27 (*i*-Ar-C1), 150.87 (*o*-py), 143.63 (*i*-Ar-C6), 137.37 (*p*-py), 129.06 (*m*-C_6H_5), 124.84 (*o*-C_6H_5), 124.00 (*m*-py), 120.21 (*p*-C_6H_5), 120.01 (Ar-C4), 118.92 (Ar-C3), 112.31 (Ar-C5), 110.15 (Ar-C2), 23.39 (NCHMe_2). Note: ^{1}H or ^{13}C signals for NCHMe_2 were not observed.

5.7 Experimental details and characterising data for Chapter Four

General procedure for M($NNPh_2$)Cl_3(bipy) (M = Ta (36) or Nb (37)). Ta($NNPh_2$)Cl_3(bipy) (36). A solution of **1.43** (0.1 g, 0.194 mmol) and *N,N*-diphenylhydrazine (0.039 g, 0.213 mmol) in toluene (15 mL) was stirred at 100 ˚C for 4 days. After this time the solution was left to cool down slowly and once at RT the solvent was filtered away. The crystalline solid was washed with pentane (3 × 5 mL) and dried *in vacuo* at 80 ˚C for 16 h to afford **36** as an olive-green powder. Yield: 0.08 g (66 %).

Data for **36**. ^{1}H NMR (CD_2Cl_2, 499.9 MHz, 298 K): δ 9.68 (1H, ddd, ^{3}J = 5.4, 1.6, 0.7 Hz, bipy-C1$_a$), 9.07 (1H, ddd, ^{3}J = 5.5, 1.5, 0.6 Hz, bipy-C1$_b$), 8.33 – 8.28 (2H, overlapping 2 × m, bipy-C4$_a$ and bipy-C4$_b$), 8.24 – 8.16 (2H, overlapping 2 × dt, ^{3}J = 18.7, 7.9, 1.7 Hz, bipy-C3$_a$ and bipy-C3$_b$), 7.77 (1H, ddd, ^{3}J = 7.6, 5.4, 1.1 Hz, bipy-C2$_a$), 7.62 – 7.60 (4H, dd, ^{3}J = 8.7, 1.1 Hz, *o*-C_6H_5), 7.51 – 7.46 (1H, m, bipy-C2$_b$), 7.41 (4H, dd, ^{3}J = 8.7, 7.4 Hz, *m*-C_6H_5), 7.04 (2H, tt, ^{3}J = 7.4, 1.1 Hz, *p*-C_6H_5). ^{13}C{^{1}H} NMR (CD_2Cl_2, 125.7 MHz, 298 K): δ 153.05 (bipy-C1$_b$), 151.83 (*i*-C5$_a$), 151.45 (*i*-C5$_b$), 149.95 (bipy-C1$_a$), 143.29 (*i*-C_6H_5), 141.90 (bipy-C3$_b$), 140.61 (bipy-C3$_a$), 128.78 (*m*-C_6H_5), 127.29 (bipy-C2$_a$), 127.05 (bipy-C2$_b$), 124.18 (*p*-C_6H_5), 123.28 (bipy-C4$_a$), 123.16 (bipy-C4$_b$), 120.44 (*o*-C_6H_5). Note: subscripts "a" and "b" refer to inequivalent bipy environments. IR (NaCl plates, Nujol mull, cm^{-1}): 1606 (w), 1594 (s), 1492 (s), 1325 (w), 1315 (m), 1282 (m), 1243 (w), 1186 (w), 1172 (m), 1107 (w), 1046 (w), 1028 (m), 1016 (w), 898 (w), 854 (m), 772 (m), 747 (s), 732 (s), 694 (s), 657 (w), 640 (m). EI-MS: *m*/*z* = 624 $[M]^+$ (0.04 %), 184 $[H_2NNPh_2]^+$ (100 %). Anal. found (calcd. for $C_{22}H_{18}Cl_3N_4Ta$): C, 41.91 (42.23); H, 2.84 (2.90); N, 8.82 (8.95) %.

Data for **37**. Reddish-brown powder. Yield: 0.093 g (74 %). ^{1}H NMR (CD_2Cl_2, 499.9 MHz, 298 K): δ 9.60 (1H, d, ^{3}J = 5.2 Hz, bipy-C1$_a$), 8.83 (1H, d, ^{3}J = 4.6 Hz, bipy-C1$_b$), 8.29 – 8.25 (2H, overlapping 2 × d, bipy-C4$_a$ and bipy-C4$_b$), 8.18 (1H, td, ^{3}J = 8.0, 1.6 Hz, bipy-C3$_a$), 8.13 (1H, td, ^{3}J = 8.0, 1.4 Hz, bipy-C3$_b$), 7.75 – 70.71 (1H, m, bipy-C2$_a$), 7.65 (4H, d, ^{3}J = 7.7 Hz, *o*-C_6H_5), 7.76 – 7.71 (5H, overlapping 2 × m, *m*-C_6H_5 and bipy-C2$_b$), 7.16 (2H, t, ^{3}J = 7.4 Hz, *p*-C_6H_5). ^{13}C{^{1}H} NMR (CD_2Cl_2, 125.7 MHz, 298 K): δ 152.46 (bipy-C1$_b$), 151.52 (*i*-C5$_a$), 151.19 (*i*-C5$_b$), 149.84 (bipy-C1$_a$), 142.12 (*i*-C_6H_5), 141.44 (bipy-C3$_b$), 140.36 (bipy-C3$_a$), 129.15 (*m*-C_6H_5), 126.83 (bipy-C2$_a$), 126.60 (bipy-C2$_b$), 125.22 (*p*-C_6H_5), 122.95 (bipy-C4$_a$), 122.92 (bipy-C4$_b$), 120.49 (*o*-C_6H_5). Note: subscripts "a" and "b" refer to inequivalent bipy environments. IR (NaCl plates, Nujol mull, cm^{-1}): 1594 (m), 1301 (s), 1156 (m), 1026 (m), 844 (w), 771 (m), 722 (s), 693 (w). EI-MS: *m*/*z* = 535 $[M]^+$ (0.014 %), 169 $[NHPh_2]^+$ (100 %). Anal. found (calcd. for $C_{22}H_{18}Cl_3N_4Nb$): C, 46.97 (49.15); H, 4.38 (3.37); N, 10.23 (10.42) %. Elemental analysis with satisfactory % C values failed presumably due to incomplete combustion of the compound.

General procedure for M(NNPh$_2$)Cl$_3$(di-^{t}Bu-bipy) (M = Ta (38) or Nb (39)). Ta(NNPh$_2$)Cl$_3$(di-^{t}Bu-bipy) (38). A solution of **14** (1.5 g, 2.393 mmol) and *N,N*-diphenylhydrazine (0.529 g, 2.871 mmol) in toluene (60 mL) was stirred at 140 ˚C for 37 h. After this time the solution was left to cool down slowly and once at RT the solvent was filtered away. The solid was washed with benzene (3 × 10 mL) and dried *in vacuo* to afford **38** as a green powder. Yield: 1.16 g (66 %).

Data for **38**. ^{1}H NMR (CD_2Cl_2, 400.1 MHz, 298 K): δ 9.55 (1H, d, ^3J = 5.8 Hz, di-^{t}Bu-bipy-C1$_a$), 8.98 (1H, d, ^3J = 6.0 Hz, di-^{t}Bu-bipy-C1$_b$), 8.23 (2H, dd, ^3J = 5.4, 1.7 Hz, di-^{t}Bu-bipy-C4$_a$ and di-^{t}Bu-bipy-C4$_b$), 7.76 (1H, dd, ^3J = 5.8, 1.8 Hz, di-^{t}Bu-bipy-C2$_a$), 7.60 (4H, dd, ^3J = 8.7, 1.1 Hz, *o*-C_6H_5), 7.48 (1H, dd, ^3J = 6.0, 1.9 Hz, di-^{t}Bu-bipy-C2$_b$), 7.41 (4H, m, *m*-C_6H_5), 7.04 (2H, tt, ^3J = 7.6, 1.1 Hz, *p*-C_6H_5), 1.48 (9H, s, di-^{t}Bu-bipy$_a$), 1.42 (9H, s, di-^{t}Bu-bipy$_b$). ^{13}C{^{1}H} NMR (CD_2Cl_2, 125.7 MHz, 298 K): δ 167.20 (*i*-di-^{t}Bu-bipy-C3$_b$), 165.49 (*i*-di-^{t}Bu-bipy-C3$_a$), 152.28 (di-^{t}Bu-bipy-C1$_b$), 151.91 (*i*-di-^{t}Bu-bipy-C5$_b$), 151.52 (*i*-di-^{t}Bu-bipy-C5$_a$), 149.51 (di-^{t}Bu-bipy-C1$_a$), 143.40 (*i*-C_6H_5), 128.74 (*m*-C_6H_5), 124.53 (di-^{t}Bu-bipy-C2$_a$), 124.30 (di-^{t}Bu-bipy-C2$_b$), 124.05 (*p*-C_6H_5), 120.44 (*o*-C_6H_5), 119.86 (di-^{t}Bu-bipy-C4$_a$), 119.71 (di-^{t}Bu-bipy-C4$_b$), 36.00 (*i*-di-^{t}Bu-bipy$_b$), 35.75 (*i*-di-^{t}Bu-bipy$_a$), 30.06 (di-^{t}Bu-bipy$_a$), 29.87 (di-^{t}Bu-bipy$_b$). Note: subscripts "a" and "b" refer to inequivalent di-^{t}Bu-bipy environments. IR (NaCl plates, Nujol mull, cm^{-1}): 1613 (m), 1589 (m), 1544 (m), 1489 (s), 1413 (m), 1356 (m), 1305 (w), 1281 (w), 1203 (w), 1185 (w), 1170 (w), 1034 (w), 931 (w), 902 (w), 893 (w), 857 (m), 763 (w), 742 (s), 697 (m), 689 (w), 636 (m), 606 (w). EI-MS: *m*/*z* = 736 $[M]^+$ (0.04 %), 253 $[di\text{-}^tBu\text{-}bipy]^+$ (100 %), 169 $[NHPh_2]^+$ (30 %). Anal. found (calcd. for $C_{30}H_{34}Cl_3N_4Ta$): C, 48.75 (48.83); H, 4.53 (4.64); N, 7.52 (7.59) %.

Data for **39**. Solution was stirred at 100 ˚C for 24 h. Mustard-yellow powder. Yield: 1.37 g (76 %). ^{1}H NMR (CD_2Cl_2, 499.9 MHz, 298 K): δ 9.47 (1H, d, ^3J = 5.8 Hz, di-^{t}Bu-bipy-C1$_a$), 8.74 (1H, d, ^3J = 5.8 Hz, di-^{t}Bu-bipy-C1$_b$), 8.20 (2H, dd, ^3J = 7.0, 1.8 Hz, di-^{t}Bu-bipy-C4$_a$ and di-^{t}Bu-bipy-C4$_b$), 7.71 (1H, dd, ^3J = 5.8, 1.9 Hz, di-^{t}Bu-bipy-C2$_a$), 7.65 (4H, dd, ^3J = 8.7, 1.1 Hz, *o*-C_6H_5), 7.43 (1H, overlapping 2 × m, *m*-C_6H_5 and di-^{t}Bu-bipy-C2$_b$), 7.16 (2H, tt, ^3J = 7.5, 1.1 Hz, *p*-C_6H_5), 1.47 (9H, s, di-^{t}Bu-bipy$_a$), 1.41 (9H, s, di-^{t}Bu-bipy$_b$). ^{13}C{^{1}H} NMR (CD_2Cl_2, 125.7 MHz, 298 K): δ 166.62 (*i*-di-^{t}Bu-bipy-C3$_b$), 165.16 (*i*-di-^{t}Bu-bipy-C3$_a$), 152.00 (di-^{t}Bu-bipy-C1$_b$), 151.59 (*i*-di-^{t}Bu-bipy-C5$_a$), 151.21 (*i*-di-^{t}Bu-bipy-C5$_b$), 149.38 (di-^{t}Bu-bipy-C1$_a$), 142.23 (*i*-C_6H_5), 129.11 (*m*-C_6H_5), 125.10 (*p*-C_6H_5), 124.07 (di-^{t}Bu-bipy-C2$_a$), 123.84 (di-^{t}Bu-bipy-C2$_b$), 120.50 (*o*-C_6H_5), 119.57 (di-

^{t}Bu-bipy-C4$_a$), 119.49 (di-^{t}Bu-bipy-C4$_b$), 35.85 (*i*-di-^{t}Bu-bipy$_b$), 35.65 (*i*-di-^{t}Bu-bipy$_a$), 30.08 (di-^{t}Bu-bipy$_a$), 29.91 (di-^{t}Bu-bipy$_b$). Note: subscripts "a" and "b" refer to inequivalent di-^{t}Bu-bipy environments. IR (NaCl plates, Nujol mull, cm^{-1}): 1611 (s), 1590 (s), 1545 (m), 1489 (s), 1411 (s), 1344 (m), 1323 (m), 1279 (m), 1202 (w), 1171 (m), 1123 (w), 1072 (w), 1030 (s), 931 (w), 901 (m), 893 (m), 855 (s), 849 (m), 763 (w), 744 (s), 697 (m), 689 (w), 675 (w), 638 (m), 605 (m). EI-MS: *m*/*z* = 648 $[M]^+$ (0.03 %), 253 $[di\text{-}^{t}Bu\text{-}bipy]^+$ (19 %), 169 $[NHPh_2]^+$ (50 %). Anal. found (calcd. for $C_{30}H_{34}Cl_3N_4Nb$): C, 55.35 (55.45); H, 5.19 (5.27); N, 8.70 (8.62) %.

General procedure for M(NHNMe$_2$)(NH^{t}Bu)Cl$_3$(di-^{t}Bu-bipy) (M = Ta (40) or Nb (41)). Ta(NHNMe$_2$)(NH^{t}Bu)Cl$_3$(di-^{t}Bu-bipy) (40). A solution of **14** (0.10 g, 0.159 mmol) and *N,N*-dimethylhydrazine (15.7 μL, 0.207 mmol) in dichloromethane (10 mL) was stirred at 40 ˚C for 16 h. After this time the solvent was removed under reduced pressure and the solid washed with pentane (3 × 5 mL). The product was dried *in vacuo* to afford **40** as a light-orange powder. Yield: 0.060 g (55 %).

Data for **40**. ^{1}H NMR (CD_2Cl_2, 499.9 MHz, 298 K): δ 10.14 (1H, d, ^{3}J = 6.3 Hz, di-^{t}Bu-bipy-C1$_a$), 9.67 (1H, d, ^{3}J = 6.1 Hz, di-^{t}Bu-bipy-C1$_b$), 8.25 (2H, br. s, di-^{t}Bu-bipy-C4$_a$ and di-^{t}Bu-bipy-C4$_b$), 7.84 (1H, dd, ^{3}J = 6.2, 2.0 Hz, di-^{t}Bu-bipy-C2$_b$), 7.71 (1H, dd, ^{3}J = 6.2, 2.0 Hz, di-^{t}Bu-bipy-C2$_a$), 3.77 (3H, s, NMe$_{2a}$), 3.50 (3H, s, NMe$_{2b}$), 1.48-1.47 (18H, overlapping 2 × s, di-^{t}Bu-bipy$_a$ and di-^{t}Bu-bipy$_b$), 0.84 (9H, s, NH^{t}Bu). ^{13}C{^{1}H} NMR (CD_2Cl_2, 125.7 MHz, 298 K): δ 165.77 (*i*-di-^{t}Bu-bipy-C3$_a$), 165.64 (*i*-di-^{t}Bu-bipy-C3$_b$), 153.53 (*i*-di-^{t}Bu-bipy-C5$_b$), 152.73 (di-^{t}Bu-bipy-C1$_a$), 152.22 (*i*-di-^{t}Bu-bipy-C5$_a$), 152.15 (di-^{t}Bu-bipy-C1$_b$), 124.90 (di-^{t}Bu-bipy-C2$_b$), 123.74 (di-^{t}Bu-bipy-C2$_a$), 119.45 (di-^{t}Bu-bipy-C4$_b$), 119.23 (di-^{t}Bu-bipy-C4$_a$), 64.86 (*i*-NHCMe$_3$), 56.73 (NHNMe$_{2a}$), 50.78 (NHNMe$_{2b}$), 35.75 (*i*-di-^{t}Bu-bipy$_b$), 35.67 (*i*-di-^{t}Bu-bipy$_a$), 31.35 (NHCMe$_3$), 30.02 (di-^{t}Bu-bipy$_a$), 29.98 (di-^{t}Bu-bipy$_b$). Note: subscripts "a" and "b" refer to inequivalent di-^{t}Bu-bipy environments. IR (NaCl plates, Nujol mull, cm^{-1}): 1616 (s), 1576 (m), 1544 (m), 1410 (s), 1297 (w), 1263 (s), 1203 (m), 1156 (w), 1079 (w), 1020 (s), 930 (w), 900 (m), 848 (m), 804 (m), 739 (w), 680 (w), 607 (m), 589 (m). EI-MS: *m*/*z* = 612 $[Ta(NNMe_2)Cl_3(di\text{-}^{t}Bu\text{-}bipy)]^+$ (2 %), 253 $[di\text{-}^{t}Bu\text{-}bipy]^+$ (31 %), 344 $[Ta(NHNMe_2)Cl_3]^+$ (2 %), 58 $[NNMe_2]^+$ (9 %). Anal. found (calcd. for $C_{24}H_{41}Cl_3N_5Ta$): C, 41.86 (41.96); H, 5.90 (6.02); N, 10.34 (10.20) %.

Data for **41**. White powder. Yield: 0.05 g (45 %). ^{1}H NMR (CD_2Cl_2, 499.9 MHz, 298 K): δ 10.08 (1H, d, ^{3}J = 6.1 Hz, di-^{t}Bu-bipy-C1$_a$), 9.60 (1H, d, ^{3}J = 6.0 Hz, di-^{t}Bu-bipy-C1$_b$), 8.23 (2H, dd, ^{3}J = 3.7, 2.0 Hz, di-^{t}Bu-bipy-C4$_a$ and di-^{t}Bu-bipy-C4$_b$), 7.80 (1H, dd, ^{3}J = 6.1, 2.0 Hz, di-^{t}Bu-bipy-C2$_b$), 7.68 (1H, dd, ^{3}J = 6.1, 2.0 Hz, di-^{t}Bu-bipy-C2$_a$), 3.63 (3H, s, NMe$_{2a}$), 3.44 (3H, s, NMe$_{2b}$), 1.48-1.47 (18H, overlapping 2 × s, di-^{t}Bu-bipy$_a$ and di-^{t}Bu-bipy$_b$), 0.86 (9H, s, NH^{t}Bu). ^{13}C{^{1}H} NMR (CD_2Cl_2, 125.7 MHz, 298 K): δ 165.53 (*i*-di-^{t}Bu-bipy-C3$_a$), 165.44 (*i*-di-^{t}Bu-bipy-C3$_b$), 153.87 (*i*-di-^{t}Bu-bipy-C5$_b$), 152.80 (*i*-di-^{t}Bu-bipy-C5$_a$), 152.74 (di-^{t}Bu-bipy-C1$_a$), 152.39 (di-^{t}Bu-bipy-C1$_b$), 124.50 (di-^{t}Bu-bipy-C2$_b$), 123.44 (di-^{t}Bu-bipy-C2$_a$), 119.40 (di-^{t}Bu-bipy-C4$_b$), 119.10 (di-^{t}Bu-bipy-C4$_a$), 68.31 (*i*-NHCMe$_3$), 56.35 (NHNMe$_{2a}$), 50.82 (NHNMe$_{2b}$), 35.66 (*i*-di-^{t}Bu-bipy$_b$), 35.59 (*i*-di-^{t}Bu-bipy$_a$), 30.05 (di-^{t}Bu-bipy$_a$), 30.02 (di-^{t}Bu-bipy$_b$), 29.71 (NHCMe$_3$). Note: subscripts "a" and "b" refer to inequivalent di-^{t}Bu-bipy environments. IR (NaCl plates, Nujol mull, cm^{-1}): 1616 (s), 1578 (m), 1544 (w), 1410 (w), 1241 (m), 901 (w), 846 (w). EI-MS: *m*/*z* = 524 [*Nb(NNMe$_2$)Cl$_3$(di-^{t}Bu-bipy)*]$^{+}$ (3 %), 466 [*NbCl$_3$(di-^{t}Bu-bipy)*]$^{+}$ (0.5 %), 253 [*di-^{t}Bu-bipy*]$^{+}$ (36 %), 256 [*Nb(NHNMe$_2$)Cl$_3$*]$^{+}$ (36 %), 58 [*NNMe$_2$*]$^{+}$ (25 %).

General procedure for M{NHN(CH$_2$)$_5$}(NH^{t}Bu)Cl$_3$(di-^{t}Bu-bipy) (M = Ta (42) or Nb (43)). Ta{NHN(CH$_2$)$_5$}(NH^{t}Bu)Cl$_3$(di-^{t}Bu-bipy) (42). A solution of **14** (0.050 g, 0.079 mmol) and 1-aminopiperidine (11.2 μL, 0.103 mmol) in benzene (10 mL) was stirred at 40 ˚C for 2 h. After this time the solvent filtered away and the solid washed with benzene (3 × 5 mL). The product was dried *in vacuo* to afford **42** as a white powder. Yield: 0.025 g (43 %).

Data for **42**. ^{1}H NMR (CD_2Cl_2, 499.9 MHz, 298 K): δ 10.14 (1H, d, ^{3}J = 6.2 Hz, di-^{t}Bu-bipy-C1$_a$), 9.99 (1H, d, ^{3}J = 6.1 Hz, di-^{t}Bu-bipy-C1$_b$), 8.25 (2H, overlapping 2 × m, di-^{t}Bu-bipy-C4$_b$ and di-^{t}Bu-bipy-C4$_a$), 7.83 (1H, dd, ^{3}J = 6.1, 2.0 Hz, di-^{t}Bu-bipy-C2$_b$), 7.70 (1H, dd, ^{3}J = 6.2, 2.0 Hz, di-^{t}Bu-bipy-C2$_a$), 4.02 (1H, m, NC$_5$H$_{10}$), 3.90 (2H, m, NC$_5$H$_{10}$), 3.76 (1H, m, NC$_5$H$_{10}$), 2.57 (1H, m, NC$_5$H$_{10}$), 2.07 (2H, m, NC$_5$H$_{10}$), 1.95 (1H, m, NC$_5$H$_{10}$), 1.82 (1H, m, NC$_5$H$_{10}$), 1.68 (1H, m, NC$_5$H$_{10}$), 1.48 (18H, overlapping 2 × s, CCMe$_{3a}$ and CCMe$_{3b}$), 0.86 (9H, s, NH^{t}Bu). ^{13}C{^{1}H} NMR (CD_2Cl_2, 125.7 MHz, 298 K): δ 165.78 (*i*-di-^{t}Bu-bipy-C3$_a$), 165.61 (*i*-di-^{t}Bu-bipy-C3$_b$), 153.73 (*i*-di-^{t}Bu-bipy-C5$_b$), 152.85 (di-^{t}Bu-bipy-C1$_a$), 152.80 (di-^{t}Bu-bipy-C1$_b$), 152.28 (*i*-di-^{t}Bu-bipy-C5$_a$), 124.79 (di-^{t}Bu-bipy-C2$_b$), 123.61 (di-^{t}Bu-bipy-C2$_a$), 119.41 (di-^{t}Bu-bipy-C4$_b$), 119.20 (di-^{t}Bu-bipy-C4$_a$), 65.13 (NC$_5$H$_{10}$), 64.98 (*i*-NHCMe$_3$), 58.99 (NC$_5$H$_{10}$), 35.73 (*i*-di-^{t}Bu-bipy$_b$), 35.67 (*i*-di-^{t}Bu-bipy$_a$), 31.39 (NHCMe$_3$), 30.01 (di-^{t}Bu-bipy$_a$), 29.97 (di-^{t}Bu-bipy$_b$), 24.31

($N(CH_2)_5$), 23.77 ($N(CH_2)_5$), 22.43 ($N(CH_2)_5$). Note: subscripts "a" and "b" refer to inequivalent di-^{t}Bu-bipy environments. EI-MS: *m*/*z* = 654 [*Ta{NH(CH$_2$)$_5$Cl$_3$(di-^{t}Bu-bipy)*]$^+$ (0.08 %), 253 [*di-^{t}Bu-bipy*]$^+$ (80 %), 85 [*NH(CH$_2$)$_5$*]$^+$ (100 %), 57 [*CMe$_3$*]$^+$ (24 %).

Data for **43**. White powder. ^{1}H NMR (CD_2Cl_2, 499.9 MHz, 298 K): δ 10.08 (1H, d, ^3J = 6.1 Hz, di-^{t}Bu-bipy$_a$-C1), 9.86 (1H, d, ^3J = 6.0 Hz, di-^{t}Bu-bipy$_b$-C1), 8.23 (2H, dd, ^3J = 6.3, 1.7 Hz, di-^{t}Bu-bipy$_a$-C4 and di-^{t}Bu-bipy$_b$-C4), 7.81 (1H, dd, ^3J = 6.1, 1.8 Hz, di-^{t}Bu-bipy$_b$-C2), 7.67 (1H, dd, ^3J = 6.1, 1.69 Hz, di-^{t}Bu-bipy$_a$-C2), 3.91 – 3.71 (4H, m, $N(CH_2)_5$), 2.58 (1H, br. m, $N(CH_2)_5$), 2.01 (3H, br. m, $N(CH_2)_5$), 1.87 (1H, br. m, $N(CH_2)_5$), 1.69 (1H, br. m, $N(CH_2)_5$), 1.47 (18H, s, di-^{t}Bu-bipy), 0.87 (9H, s, NH^{t}Bu). ^{13}C{^{1}H} NMR (CD_2Cl_2, 125.7 MHz, 298 K): δ 165.55 (*i*-di-^{t}Bu-bipy$_a$-C3), 165.42 (*i*-di-^{t}Bu-bipy$_b$-C3), 154.04 (*i*-di-^{t}Bu-bipy$_a$-C5), 153.04 (di-^{t}Bu-bipy$_b$-C1), 152.85 (di-^{t}Bu-bipy$_a$-C1), 152.79 (*i*-di-^{t}Bu-bipy$_b$-C5), 124.42 (di-^{t}Bu-bipy$_b$-C2), 123.36 (di-^{t}Bu-bipy$_a$-C2), 119.40 (di-^{t}Bu-bipy$_a$-C4), 119.09 (di-^{t}Bu-bipy$_b$-C4), 35.65 (*i*-di-^{t}Bu-bipy$_a$), 35.58 (*i*-di-^{t}Bu-bipy$_b$), 30.05 (di-^{t}Bu-bipy$_a$), 30.05 (di-^{t}Bu-bipy$_b$), 29.74 (NH^{t}Bu). Note: subscripts "a" and "b" refer to inequivalent di-^{t}Bu-bipy environments. IR (NaCl plates, Nujol mull, cm^{-1}): 3056 (w), 1615 (s), 1571 (m), 1544 (w), 1409 (s), 1237 (s), 976 (w), 899 (w), 853 (w), 668 (w). EI-MS: *m*/*z* = 564 [*Nb{NH(CH$_2$)$_5$Cl$_3$(di-^{t}Bu-bipy)*]$^+$ (0.03 %), 253 [*di-^{t}Bu-bipy*]$^+$ (100 %), 85 [*NH(CH$_2$)$_5$*]$^+$ (14 %), 57 [*CMe$_3$*]$^+$ (64 %). Anal. found (calcd. for $C_{27}H_{45}Cl_3N_5Ta$): C, 44.52 (50.75); H, 6.68 (7.1); N, 11.39 (10.96) %. Elemental analysis with satisfactory % C values failed presumably due to incomplete combustion of the compound.

General procedure for Ta(NN$_2^R$)(NNPh$_2$)(di-^{t}Bu-bipy) (R = Me (44) or ^{i}Pr (45)). Ta(NN$_2^{Me}$)(NNPh$_2$)(di-^{t}Bu-bipy) (44). A solution of **38** (0.050 g, 0.067 mmol) and **1** (0.023 g, 0.093 mmol) in benzene (10 mL) at 4 ˚C was left to slowly warm up to RT and react for 2 h. After which time it was filtered away and the solvent removed under reduced pressure. The solid was washed with pentane (3 × 5 mL) and dried *in vacuo* to yield **44** as a dark-brown-reddish powder. Yield: 0.035 g (60 %).

Data for **44**.^{1}H NMR (C_6D_6, 499.9 MHz, 298 K): δ 8.43 (2H, d, ^3J = 6.0 Hz, di-^{t}Bu-bipy-C1), 7.89 (2H, dd, ^3J = 7.9, 1.1 Hz, ArH-C5), 7.43(4H, dd, ^3J = 8.6, 1.1 Hz, *o*-C_6H_5), 7.30 (2H, d, ^3J = 1.8 Hz, di-^{t}Bu-bipy-C4), 7.24 (2H, td, ^3J = 7.9, 1.1 Hz, ArH-C3), 7.09 (2H, m, ArH-C1), 7.06-6.97 (6H, overlapping 2 × m, ArH-C4 and *m*-C_6H_5), 6.74 (2H, m, *p*-C_6H_5), 6.54 (2H, dd, ^3J = 6.1, 1.9 Hz, di-^{t}Bu-bipy-C2), 4.33 (6H, s, NMe), 0.77 (18H, s,

CC<u>Me</u>$_3$). ^{13}C{^{1}H} NMR (C_6D_6, 125.7 MHz, 298 K): δ 163.49 (*i*-di-^{t}Bu-<u>bipy</u>-C3), 152.60 (*i*-Ar-C1), 152.02 (di-^{t}Bu-<u>bipy</u>-C1), 151.94 (*i*-di-^{t}Bu-<u>bipy</u>-C5), 145.22 (*i*-Ar-C6), 128.81 (Ar-C2), 128.51 (*m*-C_6H_5), 123.88 (di-^{t}Bu-<u>bipy</u>-C2), 121.36 (*i*-C_6H_5), 119.29 (*o*-C_6H_5), 119.07 (Ar-C3), 117.83 (Ar-C4), 117.08 (di-^{t}Bu-<u>bipy</u>-C4), 116.76 (Ar-C5), 45.54 (NMe), 34.46 (*i*-C<u>C</u>Me$_3$), 29.32 (CC<u>Me</u>$_3$). Note: ^{1}H resonance for Ar-C2 overlaps with protio solvent (benzene at 7.16 ppm). IR (NaCl plates, Nujol mull, cm^{-1}): 15.92 (s), 1543 (w), 1285 (m), 1163 (m), 1056 (w), 691 (w), 668 (w). EI-MS: *m*/*z* = 227 [$H_3NN_2^{Me}$]$^+$ (20 %), 182 [$NNPh_2$]$^+$ (29 %), 253 [*di-^{t}Bu-bipy*]$^+$ (53 %), 169 [$NHPh_2$] $^+$ (100 %), 630 [*Ta(NNPh$_2$)(di-^{t}Bu-bipy)*]$^+$ (0.04 %).

Data for **45**. Dark-brown powder. Yield: 0.040 g (65 %). ^{1}H NMR (C_6D_6, 499.9 MHz, 298 K): δ 9.28 (2H, d, ^3J = 6.1 Hz, di-^{t}Bu-<u>bipy</u>-C1), 7.73 (2H, dd, ^3J = 7.9, 1.2 Hz, Ar<u>H</u>-C5), 7.34 (2H, d, ^3J = 7.9 Hz, Ar<u>H</u>-C1), 7.31 (2H, d, ^3J = 1.8 Hz, di-^{t}Bu-<u>bipy</u>-C4), 7.16 (overlapping m for Ar<u>H</u>-C3 and signal for residual protio solvent), 7.01-6.92 (10H, overlapping 3 × m, *o*-C_6H_5, *m*-C_6H_5 and Ar<u>H</u>-C4), 6.82 (2H, dd, ^3J = 6.1, 1.9 Hz, di-^{t}Bu-<u>bipy</u>-C2), 6.77 (2H, m, *p*-C_6H_5), 5.33 (2H, sept, ^3J = 6.8 Hz, N<u>C</u>HMe$_2$), 1.76 (3H, d, ^3J = 6.8 Hz, NCH<u>Me</u>$_{2a}$), 1.67 (3H, d, ^3J = 6.9 Hz, NCH<u>Me</u>$_{2b}$), 0.77 (18H, s, CC<u>Me</u>$_3$). ^{13}C{^{1}H} NMR (C_6D_6, 125.7 MHz, 298 K): δ 163.33 (*i*-di-^{t}Bu-<u>bipy</u>-C3), 153.49 (di-^{t}Bu-<u>bipy</u>-C1), 152.16 (*i*-di-^{t}Bu-<u>bipy</u>-C5), 150.77 (*i*-Ar-C1), 147.01 (*i*-C_6H_5), 146.45 (*i*-Ar-C6), 128.58 (*m*-C_6H_5), 123.23 (di-^{t}Bu-<u>bipy</u>-C2), 121.08 (*p*-C_6H_5), 118.52 (Ar-C3), 117.94 (Ar-C5), 117.84 (Ar-C4), 117.30 (di-^{t}Bu-<u>bipy</u>-C4), 112.76 (Ar-C1), 56.90 (N<u>C</u>HMe$_2$), 34.48 (*i*-C<u>C</u>Me$_3$), 29.98 (CC<u>Me</u>$_3$), 25.58 (NCH<u>Me</u>$_{2a}$), 22.44 (NCH<u>Me</u>$_{2b}$). Note: subscripts "a" and "b" refer to inequivalent CH<u>Me</u>$_2$ environments. IR (NaCl plates, Nujol mull, cm^{-1}): 1589 (s), 1544 (w), 1365 (m), 1201 (w), 1173 (m), 1154 (w), 978 (w), 872 (m), 846 (m), 836 (m), 739 (s), 691 (m), 669 (w), 605 (w). EI-MS: *m*/*z* = 283 [$H_3NN_2^{iPr}$]$^+$ (1 %), 169 [$NHPh_2$]$^+$ (53 %), 253 [*di-^{t}Bu-bipy*]$^+$ (100 %).

General procedure for M(NN$_2^R$)(NNPh$_2$)(py)$_2$ (M = Ta, R = ^{i}Pr (46) or SiMe$_3$ (47); M = Nb, R = ^{i}Pr (48) or SiMe$_3$ (49)) and V(NN$_2^{iPr}$)(NNPh$_2$)(py) (50). Ta(NN$_2^{iPr}$)(NNPh$_2$)(py)$_2$ (46). A solution of **18** (0.30 g, 0.434 mmol) and *N,N*-diphenylhydrazine (0.088 g, 0.477 mmol) in hexane (10 mL) was stirred at 60 ˚C for 48 h. After which time it was filtered away and the solvent removed under reduced pressure. The product was washed with pentane/benzene (3 × 5 mL, 3:1 ratio) and dried *in vacuo* to yield **46** as a brown powder. Diffraction-quality crystals were grown from a saturated benzene-d_6 solution at room temperature. Yield: 0.225 g (65 %).

Data for **46**. ^{1}H NMR (C_6D_6, 499.9 MHz, 298 K): δ 9.02 (4H, br. s, *o*-py), 7.65 (2H, d, ^{3}J = 7.7 Hz, ArH-C5), 7.27 (4H, d, ^{3}J = 8.0 Hz, *o*-C_6H_5), 7.06 (4H, t, ^{3}J = 7.7 Hz, *m*-C_6H_5), 6.83-6.75 (4H, overlapping 2 × m, *p*-C_6H_5 and ArH-C4), 6.66 (2H, t, ^{3}J = 7.6 Hz, ArH-C3), 6.58-6.51 (4H, overlapping 2 × m, *p*-py and ArH-C2), 6.25 (4H, t, ^{3}J = 7.6 Hz, *m*-py), 1.33 (12H, d, ^{3}J = 6.7 Hz, NCHMe$_2$). ^{13}C{^{1}H} NMR (C_6D_6, 125.7 MHz, 298 K): δ 151.49 (*o*-py), 149.61 (*i*-Ar-C1), 147.15 (*i*-C_6H_5), 140.31 (*i*-Ar-C6), 137.90 (Ar-C2), 129.22 (*m*-C_6H_5), 124.07 (*m*-py), 123.55 (*p*-py), 122.49 (*p*-C_6H_5), 121.89 (*o*-C_6H_5), 119.25 (Ar-C4), 118.36 (Ar-C3), 113.16 (Ar-C5), 23.07 (NCHMe$_2$). Note: ^{1}H or ^{13}C signals for NCHMe$_2$ were not observed. IR (NaCl plates, Nujol mull, cm^{-1}): 3056 (w), 1601 (m), 1592 (m), 1548 (w), 1488 (m), 1338 (w), 1272 (s), 1240 (s), 1210 (m), 1176 (w), 1151 (m), 1126 (m), 1064 (m), 1042 (w), 1010 (w), 978 (s), 871 (w), 816 (m), 762 (w), 742 (w), 725 (s), 693 (s), 634 (m). EI-MS: *m*/*z* = 283 [$H_3NN_2^{iPr}$]$^{+}$ (1 %), 169 [$NH(C_6H_5)_2$]$^{+}$ (96 %), 79 [*py*]$^{+}$ (100 %), 58 [N^iPr]$^{+}$ (44 %). A satisfactory elemental analysis of **46** could not be obtained.

Data for **47**. Solution was stirred at 60 ˚C for 16 h. Brown powder. Diffraction-quality crystals were grown from a saturated benzene-d_6 solution at room temperature. Yield: 0.115 g (50 %). ^{1}H NMR (C_6D_6, 499.9 MHz, 298 K): δ 9.04 (4H, dd, ^{3}J = 6.5, 1.5 Hz, *o*-py), 7.20 (6H, overlapping 2 × m, ArH-C5 and *o*-C_6H_5), 7.08 (4H, m, Hz, *m*-C_6H_5), 6.84 (2H, t, ^{3}J = 7.3 Hz, *p*-C_6H_5), 6.66-6.62 (8H, overlapping 3 × m, ArH-C4, ArH-C3, ArH-C2 and *p*-py), 6.43 (4H, m, *m*-py), 0.43 (18H, s, NSiMe$_3$). ^{13}C{^{1}H} NMR (C_6D_6, 125.7 MHz, 298 K): δ 152.50 (*o*-py), 146.75 (*i*-C_6H_5), 138.23 (*p*-py), 128.84 (*m*-C_6H_5), 123.97 (*m*-py), 122.24 (*p*-C_6H_5), 121.52 (*o*-C_6H_5), 120.97 (Ar-C3 and Ar-C4), 118.98 (Ar-C2), 112.26 (Ar-C5), 3.52 (NSiMe$_3$). Note: the ^{13}C signals for *i*-Ar-C1 and *i*-Ar-C6 were not observed. IR (NaCl plates, Nujol mull, cm^{-1}): 1606 (m), 1584 (m), 1555 (m), 1489 (s), 1356 (m), 1315 (w), 1276 (m), 1240 (w), 1223 (m), 1210 (m), 1183 (m), 1154 (w), 1110 (m), 1067 (w), 1044 (m), 1013 (w), 921 (s), 900 (m), 846 (s), 836 (s), 825 (s), 790 (m), 744 (m), 726 (m), 690 (s), 642 (w), 635 (w), 598 (w), 587 (w). EI-MS: *m*/*z* = 169 [$NH(C_6H_5)_2$]$^{+}$ (100 %), 73 [$SiMe_3$]$^{+}$ (10 %). A satisfactory elemental analysis of **47** could not be obtained.

Data for **48**. Solution was stirred at 60 ˚C for 16 h. Brown powder. Diffraction-quality crystals were grown from a saturated benzene-d_6 solution at room temperature. Yield: 0.320 g (54 %). ^{1}H NMR (C_6D_6, 499.9 MHz, 298 K): δ 8.99 (4H, br. s, *o*-py), 7.52 (2H, d, ^{3}J = 7.7 Hz, ArH-C5), 7.24 (4H, d, ^{3}J = 7.7 Hz, *o*-C_6H_5), 7.03 (4H, t, ^{3}J = 7.9 Hz, *m*-

C_6H_5), 6.87-6.80 (4H, overlapping 2 × m, *p*-py and *p*-C_6H_5) 6.71 (2H, t, ^3J = 7.6 Hz, Ar<u>H</u>-C4), 6.59 (2H, m, Ar<u>H</u>-C3), 6.43 (2H, d, Ar<u>H</u>-C2), 6.34 (4H, br. m, *m*-py), 1.31 (12H, d, ^3J = 6.7 Hz, NCH<u>Me$_2$</u>). $^{13}C\{^1H\}$ NMR (C_6D_6, 125.7 MHz, 298 K): δ 152.77 (*i*-Ar-C1), 148.71 (*o*-py), 146.15 (*i*-C_6H_5), 144.44 (*i*-Ar-C6), 129.18 (*m*-C_6H_5), 123.58 (*m*-py), 123.37 (Ar-C2), 122.57 (*p*-C_6H_5), 121.18 (*o*-C_6H_5), 119.30 (Ar-C4), 118.43 (Ar-C3), 117.83 (*p*-py), 122.06 (Ar-C5), 22.61 (NCH<u>Me$_2$</u>). Note: ^1H or ^{13}C signals for N<u>CH</u>Me$_2$ were not observed. IR (NaCl plates, Nujol mull, cm^{-1}): 1599 (m), 1590 (m), 1545 (w), 1489 (s), 1335 (w), 1272 (m), 1237 (m), 1209 (w), 1174 (w), 1150 (w), 1125 (w), 1064 (w), 1039 (w), 974 (m), 867 (w), 812 (w), 743 (m), 725 (s), 693 (s), 632 (m). EI-MS: *m*/*z* = 283 $[H_3NN_2^{iPr}]^+$ (18 %), 169 $[NH(C_6H_5)_2]^+$ (100 %). A satisfactory elemental analysis of **48** could not be obtained.

Data for **49**. Solution was stirred at 60 ˚C for 16 h. Brown powder. Yield: 0.105 g (60 %). ^1H NMR (C_6D_6, 499.9 MHz, 298 K): δ 9.08 (4H, br. s, *o*-py), 7.18 (4H, dd, ^3J = 8.6, 1.1 Hz, *o*-C_6H_5), 7.09 (2H, dd, ^3J = 7.9, 1.2 Hz, Ar<u>H</u>-C5), 7.04 (4H, m, *m*-C_6H_5), 6.85 (2H, m, *p*-C_6H_5), 6.69 (2H, br. m, *p*-py), 6.59 (2H, td, ^3J = 7.7, 1.4 Hz, Ar<u>H</u>-C4), 6.52 (2H, dd, ^3J = 7.8, 1.4 Hz, Ar<u>H</u>-C2), 6.49 (4H, br. m, *m*-py), 6.45 (2H, td, Ar<u>H</u>-C3), 0.42 (18H, s, $NSiMe_3$). $^{13}C\{^1H\}$ NMR (C_6D_6, 125.7 MHz, 298 K): δ 153.11 (*i*-Ar-C1), 152.30 (*o*-py), 146.07 (*i*-Ar-C6), 145.83 (*i*-C_6H_5), 137.69 (*p*-py), 128.60 (*m*-C_6H_5), 123.41 (*m*-py), 122.40 (*p*-C_6H_5), 121.00 (*o*-C_6H_5), 120.97 (Ar-C4), 117.14 (Ar-C2), 116.89 (Ar-C3), 111.26 (Ar-C5), 3.07 ($NSiMe_3$). IR (NaCl plates, Nujol mull, cm^{-1}): 1603 (w), 1593 (w), 1552 (w), 1278 (2), 1239 (m), 1220 (w), 1210 (w), 1183 (w), 1153 (w), 1110 (w), 1067 (w), 1042 (w), 1011 (w), 921 (m), 895 (w) 858 (w), 836 (s), 725 (s), 691 (m), 668 (w). EI-MS: *m*/*z* = 773 $[M]^+$ (0.2 %), 169 $[NH(C_6H_5)_2]^+$ (100 %), 79 $[py]^+$ (81 %). A satisfactory elemental analysis of **49** could not be obtained.

Data for **50**. Solution was stirred at 60 ˚C for 3 h. Dark-brown powder. Yield: 0.123 g (54 %). ^1H NMR (C_6D_6, 499.9 MHz, 298 K): δ 8.45 (2H, br. s, *o*-py), 7.69 (2H, d, ^3J = 7.6 Hz, *o*-C_6H_{5a}), 7.64 (2H, d, ^3J = 7.6 Hz, Ar<u>H</u>-C5), 7.08 (4H, t, ^3J = 8.0 Hz, *m*-$C_6H_{5a,b}$), 6.86 (4H, overlapping 2 × m, *o*-C_6H_{5a} and *p*-$C_6H_{5a,b}$), 6.79-6.71 (4H, overlapping 2 × m, Ar<u>H</u>-C4 and Ar<u>H</u>-C3), 6.59 (3H, overlapping 2 × m, *p*-py and Ar<u>H</u>-C2), 6.30 (2H, br. s, *m*-py), 1.34 (12H, d, ^3J = 6.0 Hz, NCH<u>Me$_2$</u>). $^{13}C\{^1H\}$ NMR (C_6D_6, 125.7 MHz, 298 K): δ 155.06 (*i*-Ar-C1), 149.32 (*o*-py), 145.82 (*i*-Ar-C6), 144.86 (*i*-C_6H_5), 136.44 (Ar-C2), 129.19 (*m*-C_6H_5), 124.63 (Ar-C4), 124.08 (*p*-C_6H_5), 123.58 (*m*-py), 120.61 (*o*-C_6H_{5a}), 120.18 (Ar-C3), 117.84 (*o*-C_6H_{5b}), 112.38 (Ar-C5). Note: ^1H or ^{13}C signals for N<u>CHMe$_2$</u>

were not observed as well as the ^{13}C signal for *p*-py. IR (NaCl plates, Nujol mull, cm^{-1}): 1591 (s), 1512 (w), 1338 (m), 1294 (m), 1267 (m), 1213 (w), 1170 (m), 1154 (m), 1068 (w), 1046 (w), 1027 (w), 977 (m), 907 (w), 869 (w), 835 (w), 730 (s), 691 (s), 637 (w), 628 (w). EI-MS: *m*/*z* = 169 $[N(C_6H_5)_2]^+$ (100 %), 79 [*py*]+ (12 %). A satisfactory elemental analysis of **50** could not be obtained.

General procedure for NMR scale synthesis of Ta(NN_2^R){$NHN(CH_2)_5$}$_2$ (R = ^{i}Pr (52) or $SiMe_3$ (53)). Ta(NN_2^{iPr}){$NHN(CH_2)_5$}$_2$ (52). A solution of **18** (0.010 g, 0.0144 mmol) in C6D6 (0.6 mL) was transferred to an NMR tube fitted with a J. Youngs valve and 1-aminopiperidine (3 μL, 0.0289 mmol) was added, an immediate colour change from dark green to bright orange was observed. The solution was left at RT for 4 h, after which time the ^1H NMR spectra demonstrated quantitative conversion to Ta(NN_2^{iPr}){$NHN(CH_2)_5$}$_2$ (**52**), H_2N^tBu and free-pyridine. The volatiles were removed under reduced pressure to yield **52** as an orange waxy solid. Diffraction-quality crystals were grown by solvent diffusion in benzene/pentane at RT.

Data for **52**. ^1H NMR (C_6D_6, 499.9 MHz, 298 K): δ 7.79 (2H, dd, ^3J = 7.2, 2.0 Hz, ArH-C5), 6.88 (4H, overlapping 2 × m, ArH-C4 and ArH-C3), 6.28 (2H, br. dd, ArH-C2), 5.53 (2H, s, TaNH), 3.78 (2H, br., $NCHMe_2$), 2.93 (4H, br., $NHN(CH_2)_5$), 2.18 (4H, br., $NHN(CH_2)_5$), 1.47 (2H, br., $NHN(CH_2)_5$), 1.27 (12H, d, ^3J = 6.5 Hz, $NCHMe_2$), 1.22 (4H, br., $NHN(CH_2)_5$), 1.11 (4H, br., $NHN(CH_2)_5$), 0.74 (2H, br., $NHN(CH_2)_5$). $^{13}C\{^1H\}$ NMR (C_6D_6, 125.7 MHz, 298 K): δ 150.38 (*i*-Ar-C1), 145.31 (*i*-Ar-C6), 118.05 (Ar-C4), 117.86 (Ar-C3), 111.32 (Ar-C2), 111.20 (Ar-C5), 62.81 ($NHN(CH_2)_5$), 32.40 ($NCHMe_2$), 24.71 ($NHN(CH_2)_5$), 23.21 ($NHN(CH_2)_5$).

Data for **53**. Dark orange solution. ^1H NMR (C_6D_6, 499.9 MHz, 298 K): δ 7.86 (2H, d, ^3J = 7.9 Hz, Ar<u>H</u>-C5), 6.87 (2H, t, ^3J = 7.2 Hz, Ar<u>H</u>-C4), 6.74 (2H, t, ^3J = 7.1 Hz, Ar<u>H</u>-C3), 6.62 (2H, d, ^3J = 7.7 Hz, Ar<u>H</u>-C2), 5.48 (2H, s, TaNH), 3.13 (4H, d, ^3J = 10.6 Hz, $NHN(\underline{CH_2})_5$), 2.19 (4H, t, ^3J = 11 Hz, $NHN(\underline{CH_2})_5$), 1.43 (4H, m, $NHN(\underline{CH_2})_5$), 1.09 (4H, d, ^3J = 13.7 Hz, $NHN(\underline{CH_2})_5$), 0.74 – 0.66 (4H, m, $NHN(\underline{CH_2})_5$), 0.34 (18H, s, $NSiMe_3$). $^{13}C\{^1H\}$ NMR (C_6D_6, 125.7 MHz, 298 K): δ 148.99 (*i*-Ar-C1), 148.73 (*i*-Ar-C6), 118.64 (Ar-C4), 117.29 (Ar-C3), 116.00 (Ar-C2), 112.77 (Ar-C5), 62.54 (NHN(CH2)5), 32.39 ($NHN(CH_2)_5$), 24.93 ($NHN(CH_2)_5$), 3.48 ($NSiMe_3$).

5.6 References

1. P. Ren, O. Vechorkin, K. v. Allmen, R. Scopelliti and X. Hu, *J. Am. Chem. Soc.*, 2011, **133**, 7084-7095.
2. A. Cooper, M. Chem. Thesis, University of Oxford, 2014.
3. C. Tessier-Youngs, O. T. Beachley, J. P. Oliver and K. Butcher, *Inorganic Syntheses*, ed. J. M. Shreeve, John Wiley & Sons, Inc., Hoboken, N.J., U.S.A., 1986, 24
4. L. H. Gade and N. Mahr, *J. Chem. Soc. Dalton Trans.*, 1993, **4**, 489-494.
5. J. Sundermeyer, J. Putterlik, M. Fotha, J. S. Fieldb and N. Ramesar, *Chem. Ber.*, 1994, **127**, 1201-1212.
6. F. Preuss, E. Fuchslocher, E. Leber and W. Towae, *Z. Naturforsch. B*, 1989, **44b**, 271—277.
7. R. R. Schrock, J. Lee, L.-C. Liang and W. M. Davis, *Inorg. Chim. Acta*, 1998, **270**, 353-362.
8. A. J. Nielson, *Polyhedron*, 1988, **7**, 67-75.
9. F. Preuss and W. Towae, *Z. Naturforsch. B*, 1981, **86b**, 1130-1135.
10. Z. Otwinowski and W. Minor, *Processing of X-ray Diffraction Data Collected in Oscillation Mode*, Academic press, New York, 1997
11. A. Altomare, G. Cascarano, G. Giacovazzo, A. Guagliardi, M. C. Burla, G. Polidori and M. Camalli, *J. Appl. Cryst.*, 1994, **27**, 435.
12. L. Palatinus and G. Chapuis, *J. Appl. Cryst.*, 2007, **40**, 786-790.
13. P. W. Betteridge, J. R. Cooper, R. I. Cooper, K. Prout and D. J. Watkin, *J. Appl. Cryst.*, 2003, **36**, 1487.
14. M. J. Frisch, G. W. Trucks, H. B. Schlegel, G. E. Scuseria, M. A. Robb, J. R. Cheeseman, G. Scalmani, V. Barone, B. Mennucci, G. A. Petersson, H. Nakatsuji, M. Caricato, X. Li, H. P. Hratchian, A. F. Izmaylov, J. Bloino, G. Zheng, J. L. Sonnenberg, M. Hada, M. Ehara, K. Toyota, R. Fukuda, J. Hasegawa, M. Ishida, T. Nakajima, Y. Honda, O. Kitao, H. Nakai, T. Vreven, J. A. M. Jr., J. E. Peralta, F. Ogliaro, M. J. Bearpark, J. Heyd, E. N. Brothers, K. N. Kudin, V. N. Staroverov, R. Kobayashi, J. Normand, K. Raghavachari, A. P. Rendell, J. C. Burant, S. S. Iyengar, J. Tomasi, M. Cossi, N. Rega, N. J. Millam, M. Klene, J. E. Knox, J. B. Cross, V. Bakken, C. Adamo, J. Jaramillo, R. Gomperts, R. E. Stratmann, O. Yazyev, A. J. Austin, R. Cammi, C. Pomelli, J. W. Ochterski, R. L.

Martin, K. Morokuma, V. G. Zakrzewski, G. A. Voth, P. Salvador, J. J. Dannenberg, S. Dapprich, A. D. Daniels, Ö. Farkas, J. B. Foresman, J. V. Ortiz, J. Cioslowski and D. J. Fox, Gaussian 09, Revision D.01 (2009) Gaussian, Inc., Wallingford, CT, USA

15. J. P. Perdew and Y. Wang, *Phys. Rev. B*, 1992, **45**, 13244-13249.
16. A. D. Becke, *J. Chem. Phys.*, 1993, **98**, 5648-5652.
17. F. Weigend and R. Ahlrichs, *Phys. Chem.Chem. Phys.*, 2005, **7**, 3297-3305.
18. D. Andrae, U. Häußermann, M. Dolg, H. Stoll and H. Preuß, *Theor. Chim. Acta*, 1990, **77**, 123-141.
19. S. Grimme, J. Antony, S. Ehrlich and H. Krieg, *J. Chem. Phys.*, 2010, **132**, 154104.